

**Ion Exchange Membranes
Integrated with Electro Chemistry
in the
Kraft Pulping Process**

Carl Haby

A thesis submitted in fulfilment of the requirement for the degree of
Master of Applied Research



Institute for Sustainable Industries &

Liveable Cities

Victoria University

May 2022

Ion Exchange Membranes Integrated with Electro Chemistry in the

Kraft Pulping Process

Abstract

The paper making industry uses sodium hydroxide as a key ingredient to aid the digestion and conversion of cellulose materials from wood-based sources. Sodium hydroxide and sodium sulphide are recovered using the Kraft pulping process. The Kraft pulping process is considered as the global benchmark used to recover the two key chemical compounds that increase the commercial sustainability of paper making. This research investigates an alternative processing technique using ion exchange membranes (IEM) integrated with electrochemistry in the form of a membrane electrolysis cell (MEC) to recover sodium hydroxide.

MEC technology may provide the paper making industry improved specific energy, significant reduction in greenhouse gas emissions, reduced chemical contaminants in the recovered sodium hydroxide stream, and higher sodium hydroxide concentration. A synthesised Green Liquor mixed solute solution was used to assess MEC performance and differentiate between membrane characteristics. Research by Mandal et.al., 2022 reported that a small difference was found between a synthesised Green Liquor solution when compared to a sample collected from a paper making facility. The 5% difference reported by Mandal et.al., 2022 suggests that the synthetic Green Liquor solution was a reasonable facsimile for Green Liquor generated in the paper making industry.

A MEC cell was designed, constructed, and tested at different current densities, temperatures, and feed and product stream concentrations and flows using one IEM. The optimised operating conditions were then used to compare six different membranes supplied by two membrane manufacturers: Selemion in Japan and DuPont in the USA. The capacity for different membrane design and compositions were assessed and the high ion selectivity membranes were shown to deliver enhanced performance across the range of key metrics established as the benchmark for this specific application. Membranes with the high ion selectivity characteristics produced higher sodium hydroxide concentrations at lower specific energy compared to membranes of higher capacity and lower selectivity. The high ion

selectivity membranes provided better operating outcomes than the conventional Kraft pulping process in terms of sodium hydroxide concentration and purity.

MEC operating conditions were improved when a metal mesh support was introduced to the apparatus. The use of the spacer in a 'Zero Gap' configuration allowed current to directly contact the IEM and improved the specific energy and significantly improved process stability from 2 hours to less than 15 minutes. Adopting the 'Zero Gap' configuration proved a step change in MEC performance and improved operating reliability.

The conventional Kraft pulping recovery process recovers sodium hydroxide at a specific energy of 320 kJ/mol, whereas the MEC operated at a specific energy of 312kJ/mol. This represents a modest reduction in specific energy of 2%, however, the associated sodium hydroxide purity of greater than 99% contains no 'deadload' chemical compounds unlike that conventional recovery methods that contain greater than 20% contamination. These contaminants, known as 'deadload', do not add to digestion and reduce the effectiveness of the digestion process.

The concentration of sodium hydroxide achieved was 3.2 M at 1.39kA/m² using the MEC apparatus and was 2.1 times greater than that obtained using the conventional Kraft pulping process, typically 1.5 M. This result represents a significantly better outcome for the pulping process as a similar specific energy provides a much higher mass production of sodium hydroxide and a significant reduction in contaminating chemicals that reduce this crucial operation's effectiveness.

MEC generated 0.09 kg CO₂/kg NaOH which compared favourably to the Kraft pulping process that contributes 0.49kg CO₂/kg NaOH produced. This substantial reduction of 82% in GHG emissions during caustic recovery represents a significant contribution to the environmental sustainability of the Kraft pulping process. MEC employs electrical energy as DC voltage that can be harvested using renewable energy compared to fossil fuels used in conventional Kraft pulping operations. Renewable energy can be harvested using solar photovoltaic cells, wind turbines or utilising steam turbines to convert surplus energy generated through the paper making process. Renewable energy generation coupled with energy storage devices in the form of large-scale batteries have the potential to increase plant availability. Environmental sustainability through reduced GHG emissions is a key challenge for any industry and the ability to achieve a robust reduction in CO₂ emissions coupled with significant improvements

in key recovery metrics illustrates the integrated benefits that MEC can provide to the paper making industry.

The results of this research clearly identified that using IEM integrated with electrochemistry in the form of a membrane electrolysis cell (MEC) can effectively recover sodium hydroxide using a synthesised Green Liquor solution. Using the MEC apparatus identified several issues that should be considered in any scaled-up production facility and included hydraulic distribution, aspect ratio, hydrogen gas production and extraction, optimum sodium hydroxide extraction, operating temperature and most importantly the ion selectivity of the membrane. Optimising these conditions can improve the already significant benefits that MEC can provide the paper making industry over the currently adopted Kraft pulping process.

Acknowledgements

I would like to acknowledge and give my warmest thanks to my supervisors Dr Peter Sancio, Research Fellow, Dr Eddy Ostarcevic, Adjunct Professor and Professor Stephen Gray, Executive Director of the Institute for Sustainable Industries and Liveable Cities at Victoria University, Melbourne.

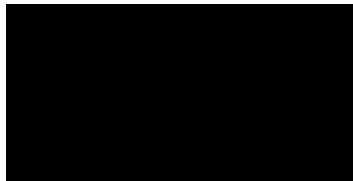
I would like to thank them for the continuous support of my master's study and research, for their patience, motivation, enthusiasm and immense knowledge and experience. Their guidance helped me throughout the time of research, experimentation and writing of this thesis. I could not imagine having a better group of advisors and mentors on the journey to completing this research thesis.

Student Declaration

I, Carl Haby, declare that the Master of Applied Research thesis entitled “Ion Exchange Membranes Integrated with Electro Chemistry in the Kraft Pulping Process” is no more than 60,000 words in length including quotes and exclusive of tables, figures, appendices, bibliography, references, and footnotes. This thesis contains no material that has been submitted previously, in whole or in part, for the award of any other academic degree or diploma. Except where otherwise indicated, this thesis is my own work.

I have conducted my research in alignment with the Australian Code for the Responsible Conduct of Research and Victoria University’s Higher Degree by Research Policy and Procedures.

Signature



Date 24 October, 2022

Table of Contents

Abstract.....	2
Table of Contents.....	6
List of Tables	13
List of Figures	16
Chapter 1 Introduction	21
1.1 Kraft Pulping and Paper Making.....	21
1.2 Opportunities for IEM Processes	22
1.3 Current Research: IEM Processes and Kraft Green Liquor	23
1.4 Gaps in the Current Research	24
1.5 Research Objectives	25
1.6 Thesis Structure.....	26
Chapter 2 Literature Review.....	28
2.1 Kraft Chemical Pulping Process:.....	28
2.1.1 Overview	28
2.1.2 Kraft Process – Digester Chemistry.....	31
2.1.3 Kraft Chemical Recovery – Black Liquor and the Recovery Boiler.....	34
2.1.4 Kraft Chemical Recovery – Reaustization and the Lime Kiln.....	38
2.1.5 Key Metrics – Thermal Energy for NaOH Production – Lime Kiln.....	40
2.1.6 Key Metric of Reausticisation Process - “Deadload Chemicals”	42
2.1.7 Key Metrics of Lime Kiln – CO ₂ Emissions from Fossil Fuel Source	45

2.1.8	Key Metrics of Lime Kiln – Other Emissions.....	45
2.1.9	Summary of Key Metrics Developed for Conventional Reausticisation	47
2.2	Ion Selective Membrane Processes for Recovery of Inorganic Salts in Kraft Green Liquor:	48
2.2.1	Ion Selective Membranes (IEMs) Characterisation	48
2.2.2	Permselectivity – IEM Microstructure and Effect of Process Conditions	56
2.2.3	Permselectivity - IEM Transport Mechanisms	57
2.2.4	IEM Permselectivity and the Influence of Boundary Layers in IEM Systems	59
2.2.5	IEM Leakage and Current Efficiency in an IEM System	60
2.2.6	Summary of IEM Permselectivity Considerations in Context of Green Liquor..	61
2.2.7	Other System Permselectivity Considerations – Ionic Radii and Cell Mobility..	62
2.2.8	Membrane Selection – Fouling, Scaling and Alkali Resistance	63
2.3	IEM Systems – Evaluation in the Context of Kraft Green Liquor	65
2.3.1	IEM Processes – Diffusion Dialysis	65
2.3.2	IEM Process – Electrodialysis	68
2.3.3	Electrodialysis Reversal (EDR)	71
2.3.4	Substitutional Electrodialysis – Metathesis	74
2.3.5	Membrane Electrolysis Cell (MEC).....	79
2.3.6	Kraft Green Liquor Recovery with MEC:	82
2.3.7	Key Operating Metrics of the Membrane Electrolysis Cell.....	90

2.3.8	Summary of Evaluation of best IEM Technologies for Kraft Green Liquor Regeneration.....	95
2.4	Research Objectives Identified from Literature Review	96
Chapter 3	Experimental Methods	97
3.1	Introduction.....	97
3.2	Conceptual Framework - Integration of EMC into the Kraft Cycle	100
3.3	Synthesis of Kraft Green Liquor:	103
3.4	Membrane Electrolysis Cell:.....	104
3.4.1	Membrane Supports:.....	107
3.5	MEC Feed Flow, Concentration and Current Range	109
3.5.1	Design Objective	109
3.5.2	Calculation of Experimental MEC Maximum Current range	110
3.6	Feed Pre-heater.....	114
3.7	Experimental Flowsheet.....	118
3.8	Experimental Measurements.....	120
3.8.1	Electrolysis Cell Voltage and Current.....	120
3.8.2	Electrolysis Cell Temperature	121
3.8.3	NaOH Concentration (MEC Cathode discharge) – Standard Titration	121
3.8.4	NaOH Concentration (MEC Cathode discharge) – Electrical Conductivity	122
3.8.5	Gas-Hydrogen Production Measurement.....	123
3.8.6	MEC feed flow rates (<i>Q_{anode}</i> , <i>Q_{cathode}</i>).....	124

3.8.7	MEC Molar Production of NaOH (<i>NProd</i>).....	125
3.8.8	Current Efficiency (ϵ)	125
3.8.9	Specific Energy for NaOH Production (kJ/mol NaOH)	126
3.8.10	Impact on Green Liquor – MEC Anode Discharge	126
3.9	Start Up and Pre-Trial Performance Verification Procedure:	132
3.9.1	MEC charging and Preheater Start-up.....	133
3.9.2	Standard MEC Integrity Test	133
3.10	Performance of MEC with Na ₂ CO ₃ Feed (Chapter 4)	134
3.10.1	Effect of “Zero Gap” versus “Open Channel” MEC Configuration.....	135
3.10.2	Voltage Stabilisation Time After Current Adjustment.....	136
3.10.3	Production of Strong NaOH Solution by Recirculation of Anode Product	138
3.11	Establishing Operating Parameters Using Synthesized Green Liquor.....	140
3.11.1	MEC NaOH Production Performance Evaluation.....	143
3.11.2	MEC Impact on Kraft Green Liquor (Na ₂ S).....	144
3.12	Comparison of Membrane Performances	144
3.12.1	Ion Exchange Membranes (IEMs) Selection	145
3.12.2	IEM Performance Evaluation	146
Chapter 4	Performance of MEC with Na ₂ CO ₃ Feed.....	147
4.1	Effect of ‘Zero Gap’ and ‘Open Channel’ feed Configurations.....	147
4.1.1	Resistance: Analysis of Effect of Zero Gap versus Open Channel	149
4.1.2	MEC Stabilisation: Analysis of Effect of “Zero Gap” versus “Open Channel” ..	150

4.1.3	Specific Energy (kJ/mol NaOH): Analysis of Effect of “Zero Gap” versus “Open Channel”	151
4.1.4	Comparison to Similar Research with 100 g NaCO ₃ /L Feed	152
4.1.5	“Zero Gap” versus “Open Channel”	153
4.2	Voltage Stabilisation Time after Current Adjustment.....	153
4.2.1	MEC Time to Reach Equilibrium	155
4.2.2	Voltage Stabilisation Time:	157
4.3	Production of Strong NaOH Solution by Recirculation of Anode Product	157
4.3.1	Production of NaOH Solution	159
4.3.2	Discussion – Increase in Catholyte Volume and Implications for Green Liquor Experiments:	161
4.4	Summary of Outcomes.....	162
Chapter 5 ESTABLISHING OPERATING PARAMETERS USING SYNTHESIZED GREEN LIQUOR		
	163	
5.1	Objectives of MEC Green Liquor Trials:	163
5.1.1	Development of Optimum Operating Parameters for NaOH Production	163
5.1.2	Evaluation of MEC Anode Discharge	164
5.1.3	Evaluation of MEC Hydrogen Production Potential with Kraft Green Liquor	165
5.2	Experimental Summary	165
5.3	Experiment Trials.....	166
5.4	Effect of Applied Current Density	168
5.4.1	Current versus Specific Energy and Current Efficiency.....	169

5.4.2	Current Density and Oxidation Reactions at the Anode – Effect on Specific Energy	173
5.4.3	Optimal Current Set Point for Green Liquor Recovery	177
5.5	Effect of Green Liquor Feed Concentration on MEC NaOH Production	179
5.6	Effect of Anode Green Liquor Feed Flow on MEC NaOH Production	182
5.7	Effect of Cathode Feed Concentration on MEC NaOH Production.....	185
5.8	Effect of Preheater Temperature on MEC NaOH Production	187
5.9	Evaluation of MEC Anode Discharge.....	190
5.9.1	Outcomes of MEC Anode Discharge Analysis	197
5.10	MEC Hydrogen Production Results.....	198
5.11	The Way Forward	199
Chapter 6	Membrane Performance	201
6.1	Objectives of Membrane Trials:	202
6.2	Membrane Performance at 40°C.....	205
6.2.1	Current Density vs Voltage at 40°C.....	205
6.2.2	Current Density vs Current Efficiency at 40°C	206
6.2.3	Current Density vs Specific Energy of NaOH Production at 40°C.....	207
6.2.4	Comparison Membrane Performance at 40°C and 5 A (1.39 kA/m ²)	208
6.3	Membrane Performance at 80°C.....	211
6.3.1	Current Density vs Voltage at 80°C.....	211
6.3.2	Current Density vs Current Efficiency at 80°C	212

6.3.3	Current Density vs Specific Energy of NaOH Production at 80°C.....	213
6.3.4	Comparison of CEM Performance at 80°C and 1.39 kA/m ²	215
6.3.5	Comparison of CEM Performance at 80°C at 2.78 kA/m ²	217
6.4	Best Membrane Performance with Optimal Process Parameters.....	219
6.5	Final Evaluation of MEC NaOH Production Metrics vs Kraft Reausticisation.....	220
6.5.1	Metrics 1: NaOH Concentration Required (2.15 M NaOH).....	221
6.5.2	Metrics 2: Specific Energy of MEC	221
6.5.3	Metric 3: Greenhouse Gas (GHG) Emissions	222
6.6	Summary of Outcomes.....	223
Chapter 7	Discussion, Conclusions and Recommendations.....	225
7.1	The Outcome.....	226
7.2	Summary of Thesis and Findings.....	228
7.3	Findings in Context of Current Research.....	233
7.4	Limitations of the Research and Methods	234
7.5	Recommendations for Future Research	235
	Bibliography:.....	238
	Appendix A: Green Liquor Trials 1 to 16: Experimental Results	244
	Appendix B: Trial 16 Repeated – Titration and ICP-OES results	253
	Appendix C: Summary of Na ₂ CO ₃ Pre-Trial Integrity Testing Results.....	255

List of Tables

Table 2.1: Performance Benchmarks for Conventional Kraft Hydroxide Recovery	31
Table 2.2: Typical White Liquor Composition	32
Table 2.3: Typical Composition of Wood Chips and Final Pulp	32
Table 2.4: Typical Black Liquor Inorganic Composition	34
Table 2.5: Points of Chemical Loss in Kraft cycle	36
Table 2.6: Typical Green Liquor Composition	38
Table 2.7: Modelled Typical Lime Kiln Parameters.....	40
Table 2.8: Simulated Energy Balance based on 2.12 Parameters	41
Table 2.9: Summary of Lime Reausticization Thermal Energy Requirements	42
Table 2.10: Lime Kiln Fuel Carbon Emissions (Based on 10 MJ/1kg CaO)	45
Table 2.11: Summary of Key Metrics	47
Table 2.12: Green Liquor Ionic Species, desired separation, and ideal IEM	56
Table 2.13: IEM System Conditions and Possible Impacts on Permselectivity.....	61
Table 2.14: Cation Mobility in Aqueous Solutions: Diffusion Coefficient, D, Stokes Radius, r	62
Table 2.15: Anion Mobility in Aqueous Solutions: Diffusion Coefficient, D, Stokes Radius, r.	63
Table 3.1: Change in Green Liquor Composition with Integration of MEC into Kraft Cycle..	102
Table 3.2: Compositions of Synthesised Kraft Green Liquor	103
Table 3.3: Solubilities of Salts Present in Kraft Green Liquor	104
Table 3.4: MEC Experimental Cell – Na ⁺ Current Limitation (Na ₂ CO ₃ and Na ₂ S).....	112
Table 3.5: ICP-OES Analysed Elements	128

Table 3.6: “Zero Gap” versus “Open Channel” Experiment Settings	135
Table 3.7: Trial 2 Operation Setpoints	137
Table 3.8: Pre-Trial 3 Settings	139
Table 3.9: Stage 1 Experimental Parameters.....	141
Table 3.10: Stage 1 Experimental Trials Operation Settings (5 Current set points per trial)	141
Table 3.11: Standard Schedule for each Experimental Trial.....	143
Table 3.12: Trial Settings.....	144
Table 3.13: Membrane Structural Characteristics (SELEMION(AGC), 2018)	146
Table 4.1: Experiment 1 – NaOH production.....	149
Table 4.2: “Open Channel” versus “Zero Gap” – Specific Energy of NaOH Production	152
Table 4.3: NaOH from Na ₂ CO ₃ Comparison experiment performed by Simon et al., 2014 ..	152
Table 5.1: Green Liquor Experimental List and Operation Settings	166
Table 5.2 – Gas Presentation at the Anode	174
Table 5.3: Comparison of Current (kA/m ²) and MEC Performance – Similar Trials	178
Table 5.4: Average CEM Concentration Gradient for all Trials	179
Table 5.5: Anode Feed Concentration from 100 to 200 g/L all Trials at 1.39 kA/m ² (5 A)....	180
Table 5.6: Comparison of Trial 8 and 16 results at 1.39 kA/m ²	182
Table 5.7: Anode Feed Flow from 175 to 350 mL/hr all Trials at 1.39 kA/m ² (5 A).....	182
Table 5.8: Comparison of Trial 6 and 8 results at 1.39 kA/m ²	184
Table 5.9: Cathode Feed Conc. from 0 to 100 g NaOH/L all Trials at 1.39 kA/m ² (5 A).....	185
Table 5.10: MEC Preheater Temperature from 40 to 80°C all Trials at 1.39 kA/m ² (5 A).....	187

Table 5.11: Comparison of Trial 7 and 8 results at 1.39 kA/m ²	188
Table 5.12: Trial 14 and Trial 16 Process Parameters – Trials Repeated.....	190
Table 5.13: Composition of MEC Anode Discharge Precipitate by SEM – Trial 14 6A.....	197
Table 5.14: Composition of MEC Anode Discharge Precipitate by SEM – Trial 14 8A.....	197
Table 5.15: Composition of MEC Anode Discharge Precipitate by SEM – Trial 14 10A	197
Table 6.1: Cation Exchange Membranes (CEM) Selected for Comparison.....	203
Table 6.2: Comparison Membrane Performance at 40°C and 1.39 kA/m ² (5 A).....	209
Table 6.3: Comparison of CEM Performance at 80°C and 1.39 kA/m ² (5 A)	216
Table 6.4 – Comparison of CEM Performance at 80°C and 2.78 kA/m ² (10 A)	218
Table 6.5 – Membrane Performance at Optimal Parameter Settings.....	220
Table 6.6 – Summary of Key Metrics of Conventional Kraft Caustic Recovery	221
Table 7.1 – Comparison of Key Metrics: Reausticisation vs IEM System.....	227
Table 7.2 – Comparison of Key Metrics: Reausticisation vs IEM System.....	230
Table 7.3 – Comparison of Key Metrics: Reausticisation vs IEM System.....	233
Table 7.4: Anion Mobility in Aqueous Solutions – Diffusion Coefficient, D, Stokes Radius, r 235	
Table A.1: Green Liquor Experimental List and Operation Settings	244
Table C1: Standard Schedule for each Trial	255

List of Figures

Figure 2.1: Flowsheet of the Kraft process	30
Figure 2.2: Lime kiln energy balance and key parameters affecting fuel requirement	40
Figure 2.3: Schematic – Types of Ion Exchange Membrane	49
Figure 2.4: Donnan Equilibrium Across IEM	51
Figure 2.5: Schematic diagram of osmotic pressure (π) at thermodynamic equilibrium.....	52
Figure 2.6: Principle of HCl recovery using Diffusion Dialysis.....	66
Figure 2.7: Hypothetical recovery of Green Liquor feed using counter current CEM DD system. OH ⁻ and S ²⁻ ions more mobile than competing CO ₃ ²⁻	68
Figure 2.8: Example of Conventional Repeating IEM Stack for Desalination	69
Figure 2.9: Electrodialysis Desalination of Green Liquor leaving least mobile ions Na ₂ CO ₃ ...	70
Figure 2.10: Conventional Repeating IEM Stack for Desalination	71
Figure 2.11: EDR Flow Diagram and Schematic	73
Figure 2.12: Example of Metathesis Desalination Process (Tom Davis, 2012)-.....	75
Figure 2.13: Example of NaOH and HCl production using EDM/EDBM.....	76
Figure 2.14: CSIRO In-situ remediation of Bauxite Red Mud.....	78
Figure 2.15: Kraft Green Liquor Regeneration with EDM – Acid and Alkali Generation.....	79
Figure 2.16: Chloro-Alkali Cell Schematic	80
Figure 2.17: Schematic of electrolysis system used by (Simon et al., 2014a)	82
Figure 2.18: Schematic Kraft Green Liquor Electrolysis.....	84
Figure 2.19: Modelled Speciation of S species in Aqueous Solution vs pH.	88

Figure 3.1: Possible Integration of MEC into the Kraft Cycle.....	101
Figure 3.2: Electrolysis Membrane Cell Assembled.....	104
Figure 3.3: Anode Assembly with Flow Plate.....	105
Figure 3.4: Cathode Assembly with Flow Plate.....	105
Figure 3.5: Dismantled Membrane Electrolysis Cell (Anode left, Cathode Right).....	108
Figure 3.6: MMO Titanium Anode (PTFE Gasket removed to show flow plate)	108
Figure 3.7: Assembled Membrane Electrolysis Cell in Insulated Container	109
Figure 3.8: Electrolysis membrane cell feed preheater – Clockwise from top left:	116
Figure 3.9: Experimental flowsheet.....	118
Figure 3.10: Experimental Equipment	119
Figure 3.11: Electrical Conductivity (uS/cm) vs NaOH (wt%).....	122
Figure 3.12: Metrohm 902 Titrand Potentiometric Titrator for endpoint titration	128
Figure 3.13: Example of precipitate formed at bottom of an MEC anode sample	129
Figure 3.14: Trial 14 (Chapter 5) – Example MEC precipitate extracted.	130
Figure 3.15: Thermoscientific Phenom Pharos G2 Desktop FEG-SEM	131
Figure 3.16: Experiment Schematic – Preparation and standardised test.	132
Figure 3.17: Experimental Schematic - “Zero Gap” versus “Open Channel”	136
Figure 3.18 – Experimental Schematic - “Voltage Stabilisation Time”	137
Figure 3.19 – Experimental Schematic - “Production of Strong NaOH Solution”	138
Figure 3.20: Experimental Schematic for trials with Kraft Green Liquor.....	140
Figure 4.1: Flowsheet – Open Channel versus Zero Gap.....	148

Figure 4.2: Zero Gap versus Open Channel configuration – Voltage and NaOH Production	150
Figure 4.3: Flowsheet – Voltage Stabilisation Time	154
Figure 4.4 – Voltage Stabilisation Time after Current Adjustment	155
Figure 4.5: Flowsheet Production of Strong NaOH Solution – Anode Recirculation	158
Figure 4.6: Cell Voltage and NaOH Production over Time	160
Figure 5.1: MEC Experimental Arrangement for trials with Kraft Green Liquor	165
Figure 5.2: Trial 1: Current Efficiency, Voltage and Specific Energy	167
Figure 5.3: Trial 2: Current Efficiency, Voltage and Specific Energy	170
Figure 5.4: Trial 6: Current Efficiency, Voltage and Specific Energy	171
Figure 5.5: Trial 8: Current Efficiency, Voltage and Specific Energy	172
Figure 5.6: Trial 14 (Repeat) MEC Green Liquor Discharge Residual NaOH and Na ₂ CO ₃	175
Figure 5.7: Trial 14: Current Efficiency, Voltage and Specific Energy	176
Figure 5.8: Effect of Increasing Anode Feed Concentration (100 to 200 g/L) on MEC Performance at 1.39 kA/m ² (5 A), arrows indicate effect of increasing temperature.	181
Figure 5.9: Effect of Increasing Anode Feed Flowrate (175 to 350 mL/hr) on MEC Performance at 1.39 kA/m ² (5 A) arrows indicate effect of increasing temperature.	183
Figure 5.10: Effect of Increasing Cathode (NaOH) Feed Concentration (0 to 100 g NaOH/L) on MEC Performance at 1.39 kA/m ² (5 A)	186
Figure 5.11: Effect of Increasing Preheater Temperature (40 to 80°C) on MEC Performance at 1.39 kA/m ² (5 A)	188
Figure 5.12: Trial 14 (Repeated): Titrations (Graph) and Green Liquor Samples (Photo)	192

Figure 5.13: Modelled Speciation of S species in Aqueous Solution vs pH. pKa values obtained from (Dean, 1999).....	193
Figure 5.14: MEC Anode Discharge Trial 14 – Liquid Phase Analysis by ICP-OES.....	194
Figure 5.15: MEC Cathode Discharge Trial 14 – Liquid Phase Analysis by ICP-OES.....	195
Figure 5.16: Trial 14 – Close-up of precipitate formed in MEC Anode Discharge	195
Figure 5.17: SEM Photograph Spot Test Example (Trial 14 – Current Set Point 6A)	196
Figure 5.18: Map Test Example Results (Trial 14: 8 amps) – FW: 26µm, SEM mode: 10 kV.	196
Figure 5.19: Hydrogen Gas Production (mol/hr) versus MEC Current – ALL TRIALS.....	199
Figure 6.1 –Current (A) vs Voltage (V) – All Membranes at 40°C.....	206
Figure 6.2: Current (A) vs Current Efficiency (%) – All Membranes at 40°C.....	207
Figure 6.3: Current (A) vs Specific Energy (kJ/mol NaOH) – All Membranes at 40°C.....	208
Figure 6.4 – Comparison of Membrane Performance at 40°C at 1.39 kA/m ² (5 A)	210
Figure 6.5 – Current (A) vs Voltage (V) – All Membranes at 80°C.....	212
Figure 6.6 – Current (A) vs Current Efficiency (%) – All Membranes at 80°C.....	213
Figure 6.7 – Current (A) vs Specific Energy (kJ/mol NaOH) – All Membranes at 80°C.....	214
Figure 6.8: Comparison of CEM Performance at 80°C and 1.39 kA/m ² (5 A).....	215
Figure 6.9: Comparison of CEM Performance at 80°C at 2.78 kA/m ² (10 A).....	217
Figure 6.10 Comparison of Calculated Carbon Emissions.....	223
Figure 7.1 – Kraft Green Liquor Regeneration cycle with ED and MEC.....	236
Figure A.1: Trial 1 (T = 40°C, AF = 175 mL/H, AC = 200 g/L, CC = 0 g NaOH/L).....	245
Figure A.2: Trial 2 (T = 80°C, AF = 175 mL/H, AC = 200 g/L, CC = 0 g NaOH/L).....	245

Figure A.3: Trial 3 (T = 40°C, AF = 350 mL/H, AC = 200 g/L, CC = 0 g NaOH/L).....	246
Figure A.4: Trial 4 (T = 80°C, AF = 350 mL/H, AC = 200 g/L, CC = 0 g NaOH/L).....	246
Figure A.5: Trial 5 (T = 40°C, AF = 175 mL/H, AC = 200 g/L, CC = 100 g NaOH/L).....	247
Figure A.6: Trial 6 (T = 80°C, AF = 175 mL/H, AC = 200 g/L, CC = 100 g NaOH/L).....	247
Figure A.7: Trial 7 (T = 40°C, AF = 350 mL/H, AC = 200 g/L, CC = 100 g NaOH/L).....	248
Figure A.8: Trial 8 (T = 80°C, AF = 350 mL/H, AC = 200 g/L, CC = 100 g NaOH/L).....	248
Figure A.9: Trial 9 (T = 40°C, AF = 175 mL/H, AC = 100 g/L, CC = 0 g NaOH/L).....	249
Figure A.10: Trial 10 (T = 80°C, AF = 175 mL/H, AC = 100 g/L, CC = 0 g NaOH/L).....	249
Figure A.11: Trial 11 (T = 40°C, AF = 350 mL/H, AC = 100 g/L, CC = 0 g NaOH/L).....	250
Figure A.12: Trial 12 (T = 80°C, AF = 350 mL/H, AC = 100 g/L, CC = 0 g NaOH/L).....	250
Figure A.13: Trial 13 (T = 40°C, AF = 175mL/H, AC = 100 g/L, CC = 100 g NaOH/L).....	251
Figure A.14: Trial 14 (T = 80°C, AF = 175mL/H, AC = 100 g/L, CC = 100 g NaOH/L).....	251
Figure A.15: Trial 15 (T = 40°C, AF = 350mL/H, AC = 100 g/L, CC = 100 g NaOH/L).....	252
Figure A.16: Trial 16 (T = 80°C, AF = 350mL/H, AC = 100 g/L, CC = 100 g NaOH/L).....	252
Figure B.1: Trial 16 Repeated – Titration and ICP-OES results	253
Figure B2: Trial 16 (Repeated):	253
Figure B3: MEC Anode Discharge Trial 16 – Liquid Phase Analysis by ICP-OES.....	254

Chapter 1 Introduction

Development of ion exchange membranes (IEM) integrated with electro chemistry have been adopted by diverse industries and used in a variety of applications that include desalination, acid and alkali recovery, chloralkali production and the manufacture of valuable salts. IEM technology can be extended beyond current applications into the Kraft paper making process where it has the potential to improve resource recovery of key chemical compounds essential to maintain consistent and reliable pulping performance. This improved resource recovery promises to:

- Improve pulping performance efficiency,
- Improve production efficiency,
- Reduce energy consumption, and
- Significantly reduce associated greenhouse gas (GHG) emissions.

1.1 Kraft Pulping and Paper Making

The Australian paper industry is a diverse sector producing a range of paper and paperboard products, including tissue, printing, newsprint, and packaging papers. In 2016, the Australian pulp and paper industry directly employed 12,450 people full time, whilst indirectly creating 60,820 full time jobs (AFPA, 2016). In 2016, the UN Food and Agriculture Organisation reported that of the 1.5 million tons of dry wood pulp for paper and paperboard produced in Australia, over 1.0 million tons was produced using chemical pulping process (UNFAO, 2016). Worldwide (excluding China), in 2016 of the 150 million tons of dry wood pulp produced reported to the UN, 120 million tons was produced using chemical pulping (UNFAO, 2016).

Concentrated sodium hydroxide (NaOH) and sodium sulphide (Na₂S) are pivotal constituents of the Kraft chemical pulping process. They are used to break down woodchips by breaking the lignin macromolecules that bind the woodchips together (Biermann, 1996a). Digestion of wood chips containing lignin produces organic acids and releases resinous compounds that are neutralised by the sodium hydroxide that converts to the weaker alkali salt, sodium carbonate (Na₂CO₃).

The spent liquor after digestion, called Black Liquor, is separated from the pulp, and contains two fractions - organic and inorganic compounds. The Black Liquor is concentrated to reduce

water content and the organic rich solids are fed into a controlled incineration process. The organics entering the incinerator leave with the flue gases. The inorganic fraction is recovered as a smelt of Na_2CO_3 and Na_2S . Water is added to the smelt to become what is called Green Liquor.

The Kraft cycle recovers the weak alkali Na_2CO_3 contained in Green Liquor and converts it into a stronger alkali NaOH solution (60 – 90 g/L), whilst retaining Na_2S (22 – 33 g/L). In the conventional process, hydroxide is returned to the process by the addition of hydrated lime ($\text{Ca}(\text{OH})_2$), which reacts with Na_2CO_3 to form NaOH and a lime mud, CaCO_3 , which is separated by settling. The conversion is limited by the chemistry equilibrium and the process dynamics that dictates a practical conversion of Na_2CO_3 to NaOH between 75% to 85% (GRACE and TRAN, 2009), resulting in a significant load of unreacted Na_2CO_3 that is commonly referred to as deadload since it does not contribute to the conversion of lignin and it reduces the efficiency of the Kraft pulping cycle.

Lime mud (CaCO_3) that is separated from the regenerated liquor is burned in a lime kiln to form quicklime, CaO , for it to be used again. Additional lime is added to make up for losses. The lime kiln requires a thermal specific energy of approximately 7.0 MJ/kg NaOH (280 kJ/mol NaOH) regenerated and, using fossil fuels, emits approximately 0.6 to 1.1 kg CO_2 /kg NaOH regenerated depending on fuel source to the lime kiln. There are additional energy costs associated with deadload Na_2CO_3 remaining in the Kraft cycle, which can add approximately 1.0 MJ/kg NaOH regenerated in the form of additional dilution water requiring more pumping and heating through the Kraft cycle.

1.2 Opportunities for IEM Processes

Ion Exchange Membrane (IEM) processes are an established method used for industrial water desalination and for the recovery of valuable inorganic and organic salts (Ran et al., 2017). IEMs are used in the separation of ions of opposite charge and co-ions of different valences. IEMs integrated with electro chemistry form a suite of technologies that include diffusion dialysis (DD), electrodialysis (ED), electrodialysis reversal (EDR), substitutional electrodialysis metathesis (EDM) and the membrane electrolysis cell (MEC).

IEM systems have revolutionised production in several industries, notably the chloralkali industry, which has gradually moved away from mercury-cell production to the membrane

electrolysis cell process. The motive for this change being concerns over mercury poisoning and pollution, notable occurrences being in Japan (Minamata) and Canada (Matsuyama et al., 2018). In the case of chloralkali processes, membranes replaced mercury as an ion transport medium.

In the context of Kraft Green liquor, IEM has the potential to convert a greater proportion of Na_2CO_3 to NaOH than the conventional lime recovery process that is limited by chemical equilibrium and process dynamics. An IEM system can also selectively target the recovery of useful compounds that include sodium sulphide (Na_2S), whilst rejecting other unwanted deadload ions/compounds that have an adverse impact on the Kraft pulping process. An IEM process has the potential to deliver improved recovery, reduced deadload by eliminating lime addition and provide a smaller environmental footprint with better operational metrics for the paper making industry.

1.3 Current Research: IEM Processes and Kraft Green Liquor

There have been recent investigations into the conversion of Green Liquor into caustic solution using IEM processes including the Membrane Electrolysis Cell (MEC) and Electrodialysis with Bipolar Membranes (BPED).

A MEC process with a cationic exchange membrane (CEM) was used to convert Na_2CO_3 in Kraft Green Liquor to NaOH by (Goel et al., 2021) and (Mandal et al., 2021). In each study the specific energy of NaOH production (kJ/mol NaOH), CEM current density (A/m^2) and final NaOH concentration produced were defining metrics of the MEC operation. Trialling different CEMs (Goel et al., 2021) at a current density of $600 \text{ A}/\text{m}^2$ produced a NaOH solution of 46.8 g/L (1.17 M), at 372 kJ/mol NaOH. Using synthetic and industrial Kraft Green liquor feed solutions delivered to a MEC at a current density of $600 \text{ A}/\text{m}^2$, (Mandal et al., 2022) produced a NaOH solution of 94 g/L (2.35 M) at 454 kJ/mol NaOH.

(Eswaraswamy et al., 2022) used BPED process to convert the Na_2CO_3 in Green Liquor to NaOH, evaluating the role of current density, feed-electrolyte concentration, temperature, and number of cells in the BPED. Using optimal process parameters identified in their research including a current density of $500 \text{ A}/\text{m}^2$, with an industrial Green Liquor feed the BPED produced NaOH solution of 1.2 M (49 g/L) and a specific energy of 31.6 MJ/kg NaOH (790 kJ/mol NaOH)

1.4 Gaps in the Current Research

The conventional Kraft caustic recovery process generates NaOH concentration of approximately 1.5 M NaOH and a specific energy 280 kJ/mol NaOH.

The recent research by (Mandal et al., 2022) has showed that the IEM process they used can convert Na_2CO_3 in Green Liquor into NaOH of concentrations of up to 2.35 M, at a specific energy of 454 kJ/mol NaOH at current density of 600 A/m². Industrial IEMs produced by AGC Selemion LTD and DuPont with their Nafion membrane for NaOH production in the chloralkali industry typically operate at a much higher range of 4,000 to 6,000 A/m² (Selemion, 2019a), so it is important to investigate performance at higher current densities closer to typical industrial systems.

Within the range of IEMs techniques, there is need to explore membranes of varying resistance or selectivity in the context of Kraft Green liquor. This is important because the Kraft pulping process requires concentrations of NaOH greater than 1.5 M and it would be beneficial to produce concentrations higher than 3.0 M to limit chemical storages and transfer volumes within the Kraft process. Higher concentrations of NaOH production in an IEM process present challenges for membrane current efficiencies, which makes it important to evaluate the merits of low and high selectivity IEMs.

Na_2S is critical to the Kraft pulping chemistry. The conventional recovery process converts Na_2CO_3 to NaOH while maintaining the integrity of Na_2S in the Green Liquor. Recent research has focussed on the IEM capacity to convert the Na_2CO_3 in Green Liquor to NaOH, without identifying the impact on the Na_2S leaving the IEM process.

The conducted research aimed to address the issues associated with membrane use in the Kraft pulping process, namely:

- Membrane functionality that may include varying resistivity and ion selectivity,
- NaOH recovery strength,
- Specific energy requirements,
- Fate of important pulping chemical compounds such as Na_2S

These issues were examined as part of the research program aimed at addressing the objectives identified.

1.5 Research Objectives

The overall research objective was to identify whether IEM technologies have the potential to replace conventional NaOH recovery operations using lime in the Kraft pulping process. Understanding the fate of important chemical compounds, such as Na_2S , using MEC enables the membrane technology to be directly compared to the conventional NaOH recovery operation using lime.

The objective of this research was addressed by investigating the following features to determine whether IEM technology has the capacity to deliver improved NaOH recovery as a direct substitute to the conventional NaOH recovery operations. The features identified that assist in developing a view on the research objective include the determination of:

- The chemistry and the key energy and environmental metrics of the conventional Kraft caustic recovery process. Establish these metrics as the benchmark for alternative IEM technologies for a direct comparison to be drawn.
- The most suitable IEM technology for the conversion of Na_2CO_3 to NaOH in Kraft Green Liquor.
- The limit to NaOH recovery that can be delivered by the selected IEM technique. An upper target of 3.0 M (120 g NaOH/L) would provide significant benefits to the paper making industry that requires up to 90 g NaOH/L for woodchip pulping.
- The optimal IEM technology process parameters for the conversion of Na_2CO_3 in Green Liquor to NaOH.
- The impact on Green Liquor solution leaving the IEM system.
- The impact of IEM selectivity on system performance
- IEM System performance at conventional industry settings.
- The specific energy (kJ/mol NaOH) of the IEM process for comparison with the conventional NaOH recovery operation using lime.
- The GHG emissions (kg CO_2 /kg NaOH) of the IEM process for comparison with the conventional Kraft Process.

Understanding the implications of the issues identified will provide a foundation for the research objective to be evaluated.

1.6 Thesis Structure

The outcomes of this research are delivered through a structured thesis report that provides a review of NaOH recovery operations in the Kraft paper-making industry. It also identifies the outcomes of literature research into IEM technology and specific research that relates to the recovery of NaOH. This review of the literature is presented in Chapter 2. This chapter examines the key elements of IEM technology and research that improve the performance of the technology. It also provides a detailed assessment of IEM techniques and distils the information to allow the choice of a technology and the associated benchmarked operational metrics necessary for evaluation against the current conventional method of NaOH recovery. The outcome of Chapter 2 is a pathway towards developing the research methods (Chapter 3) and subsequent experimental investigation of MEC performance with a standard single solute solution (Chapter 4) and with a synthetic Green Liquor (Chapter 5).

Chapter 3 provides the specific details of the equipment, analytical methods, and experiments that were used to deliver the research outcomes. The development of the bench scale IEM pilot equipment is addressed in this chapter and a comprehensive description is provided of the elements used to develop the IEM technique that were used to determine the performance related to the research objectives.

Initial testing of the bench scale IEM apparatus was developed using a single solute solution identified in Chapter 3 to determine whether recent developments in the selected IEM technique can be used to improve performance outcomes and meet the research objectives. The results are presented and discussed in Chapter 4. The response to operating using this single solute solution established the operating protocols that were used in further experiments reported in Chapters 5 and 6. Chapter 4 also provides initial operating experiences with the selected IEM configuration and the apparatus developed for the testing regime in response to the research objective.

Chapter 5 provides details of the developed optimum operating conditions resulting from a comprehensive testing regime using a synthesised Green Liquor solution. These optimum operating conditions are used to benchmark the performance of a variety of commercially available membranes for the selected IEM technique in Chapter 6. Chapter 5 also provides information that directly addresses the research objective of whether the selected IEM

technology can be used as an effective substitute for the current global practice using lime to recover NaOH.

The optimum operating parameters identified in Chapter 5 are used to evaluate the performance of the selected IEM technology using a variety of commercially available IEM membranes of high and low selectivity (Chapter 6). Benchmarking the performance of the membranes under identical operating conditions provides an opportunity to identify membrane(s) with superior performance that can then be directly compared to operational metrics associated with the current NaOH recovery process employed in the Kraft pulping process.

The outcomes of the research are critically examined and compared to the research objectives in Chapter 7. Direct conclusions are drawn to answer the question of whether IEM technology can replace current NaOH recovery methods. This chapter also provides recommendations for further research as a consequence of the findings from the experiments performed. The recommendations proposed may have the potential for further advancements to IEM configuration or applications and advance the application of IEM technologies in Kraft Green Liquor processing.

Chapter 2 Literature Review

The development of ion selective membranes, otherwise known as ion exchange membranes (IEM), integrated with electro chemistry has evolved to incorporate a suite of technologies that include diffusion dialysis (DD), electrodialysis (ED), electrodialysis reversal (EDR), electrodialysis metathesis (EDM) and membrane electrolysis (ME). These technologies are used in a variety of applications that include desalination, acid and alkali recovery, chlor-alkali production, and the manufacture of valuable salts. Ion selective membrane process has the potential to extend beyond current applications and into the Kraft paper making process where they may improve resource recovery thereby improving production efficiency, reducing energy consumption, and lowering associated greenhouse gas (GHG) emissions.

The application of the Kraft process relies on the ability to recover the key pulping chemicals, hydroxide, and sulphide, to promote efficient wood chip digestion to form pulp. The conventional unit operations required to facilitate the recovery of hydroxide and retain sulphide consume energy, generate Green House Gas (GHG) emissions, and retain several compounds that contribute to reduced pulping performance efficiency. Modern membrane technology coupled with electrochemistry provides an alternative method of regenerating hydroxide and retaining sulphide chemicals. Further, the use of membrane-based systems in conjunction with electrochemistry has the potential to significantly reduce energy intensive operations and reduce the GHG production thereby reducing the carbon footprint of a Kraft pulping process.

2.1 Kraft Chemical Pulping Process:

2.1.1 Overview

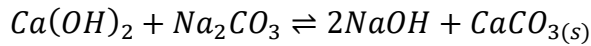
The Australian paper industry is a diverse sector producing a range of paper and paperboard products, including tissue, printing, and writing papers, newsprint, and packaging papers. In 2016, the Australian pulp and paper industry directly employed 12,450 people full time, whilst indirectly creating 60,820 full time jobs (AFPA, 2016). In 2016, the UN Food and Agriculture Organisation reported that of the 1.5 million tons of dry wood pulp for paper and paperboard produced in Australia, over 1.0 million tons was produced using chemical pulping process (UNFAO, 2016). Worldwide (excluding China), in 2016 of the 150 million tons of dry wood

pulp produced reported to the UN, 120 million tons was produced using chemical pulping (UNFAO, 2016).

In the Kraft pulping process wood chips are mixed with a solution of sodium hydroxide and sodium sulphide in a heated vessel to promote the chemical reactions that produce a pulp that is suitable for paper production. The strong alkali sodium hydroxide (NaOH), with sodium sulphide (Na_2S), are pivotal to the Kraft chemical pulping process where it is used to break down woodchips by breaking the lignin macromolecules that bind the woodchips together (Biermann, 1996a). Digestion of wood chips containing lignin produces organic acids and releases resinous compounds that are neutralised by the addition of sodium hydroxide. Sulphide is present to accelerate the cleavage of the oxygen-carbon bond (Biermann, 1996a) and reduces undesirable reactions. Neutralising organic acids generated in the digestion process results in the conversion of sodium hydroxide to a weaker alkali salt, sodium carbonate (Na_2CO_3). Sulphide is not directly consumed in the woodchip digestion, but it can be lost to the process with the separated pulp, through spills and non-condensable gas emissions.

After digestion, the spent liquor is separated from the pulp and contains two fractions, organic and inorganic compounds. The organic fraction in the spent “black” liquor is recovered as an energy source to make the Kraft chemical pulping process economically viable and environmentally compliant (Ellis and Johnson (2011)). After separating the pulp generated in the digestion process, the remaining black liquor that contains organic compounds is concentrated to reduce the water content thereby increasing the solids concentration to between 65% to 75% solids using an evaporative operation. The organic rich solids concentrate is fed into a controlled incineration process known as the Kraft Recovery boiler. The organics entering the boiler leave with the flue gases, and most of the inorganic fraction is recovered as a smelt, predominantly sodium carbonate (Na_2CO_3) and sodium sulphide (Na_2S).

The Na_2CO_3 and Na_2S smelt is mixed with water to become what is called “Kraft Green Liquor”. The Kraft cycle requires the weak alkali Na_2CO_3 to be converted back into the stronger alkali NaOH, in a hydroxide regeneration cycle that is referred to as “Recausticization”. In this process, hydroxide is returned to the process via the addition of hydrated lime ($\text{Ca}(\text{OH})_2$), which reacts with the Na_2CO_3 to form NaOH and lime mud, CaCO_3 .



The lime mud, CaCO_3 , is separated from the regenerated liquor and burned in a lime kiln to form CaO , with carbon dioxide being released to the atmosphere, for it to be used again and some additional lime is added to make up for losses. The regenerated liquor is known as “White Liquor” and is used for woodchip pulping. Calcium is not a direct part of chemical woodchip pulping but is a hydroxide delivery mechanism in the recausticization cycle within the overall Kraft cycle. Figure 2.1 below shows the Kraft cycle flowsheet that illustrates how the hydrated lime is used to recover hydroxide.

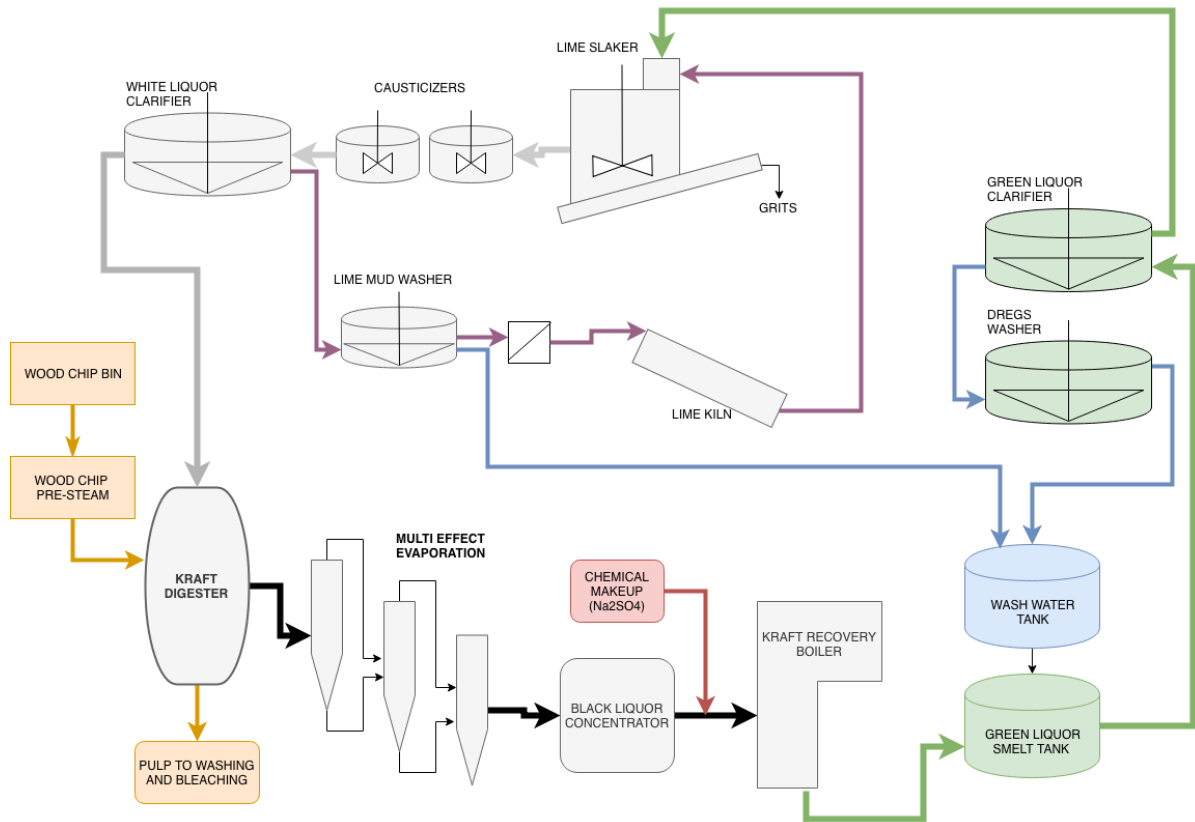


Figure 2.1: Flowsheet of the Kraft process

Recausticization is limited by chemistry equilibrium and process dynamics that dictates a practical conversion of Na_2CO_3 to NaOH of between 75 to 85% (GRACE and TRAN, 2009). This conversion ratio dictates that a significant load of Na_2CO_3 remains in the White Liquor. As Na_2CO_3 is not effective in the digestion of woodchips, it is referred to as a “Deadload”. Deadload imposes significant cost on the Kraft cycle, as liquor concentration controlled at approximately 15% by weight, requires 5.7kg of water for each additional kg of deadload. Heating this volume of water equates to 1780 kJ/kg of deadload or 0.78 GJ per tonne of pulp

produced. The capacity of Kraft plant infrastructure to produce pulp is also reduced with increasing deadload and this can have a substantial impact on the production capacity by imposing internal hurdles that require significant interventions that can adversely affect plant availability.

Thermal energy is applied to limestone, CaCO_3 , to convert it to quick lime, CaO before it is slaked to produce hydrated lime, Ca(OH)_2 in order to recover hydroxide from the sodium carbonate. Recovering the lime based alkali by hydrating lime is a significant energy sink and consumes an average of 1.8 GJ of fuel and emits 300 tons of CO_2 per tonne unbleached pulp (Miner and Upton, 2002). The fuel required for lime burning and fresh makeup lime also introduces contaminants to the Kraft process that cause added plant deadloads, scaling and corrosion. Consequently, the application of conventional Kraft “recausticization” processes include significant capital and operating costs with corresponding operational challenges such as increased deadload chemical accumulation that adversely affects production efficiency. Table 2.1 below details the performance efficiencies achieved by the conventional Kraft Hydroxide Recovery process.

Table 2.1: Performance Benchmarks for Conventional Kraft Hydroxide Recovery

	Recaustization Process Efficiency and Quality of “White Liquor” Product
Na ₂ CO ₃ conversion to NaOH	75 – 85% Limited by reaction equilibrium and process dynamics
Recovery of active sulphide, Na ₂ S	Typical lime kiln chemical losses require that between 1.4 – 4 kg of makeup Na ₂ S is required per tonne of dry pulp produced.
Process Energy Requirement (GJ/tonne dry pulp)	<u>Lime Kiln Fuel Requirement</u> 200 – 300 kg CaO / tonne dry pulp 8 – 10 GJ per tonne of CaO 1.8 – 3.0 GJ per tonne of pulp produced <u>Other Energy Significant Process Equipment</u> Green liquor heaters required for optimal lime mud settling
Greenhouse Gas (ton CO ₂ /ton dry pulp)	<u>Lime Kiln Fuel:</u> 100 kg CO ₂ /tonne dry pulp <u>Lime Kiln – CO₂ from burned CaCO₃</u> 350 – 550 kg of CaCO ₃ per tonne pulp 180 - 250 kg CO ₂ per tonne pulp
Other environmental emissions – NCGs	Lime kiln → 20% of overall process total reduced sulphur emissions because of fuel requirement and entrained sulphur in lime mud.
Overall Deadload	Normally 15 to 25% of lost plant capacity within the Kraft Cycle
Overall energy cost of deadload	0.16 GJ per tonne of pulp

2.1.2 Kraft Process – Digester Chemistry

Kraft pulping is the foremost chemical process in which cellulose fibres are extracted from wood because of its ability to produce high strength pulp, handle almost all species of wood,

and can recover and reuse approximately 97% of process chemicals (Tran and Vakkilainen, 2016).

In the Kraft pulping process debarked wood is chopped into chips (12-25mm long), impregnated with steam, and sent to a digester where they are mixed with White Liquor. The white liquor is a strong alkali solution of predominantly sodium hydroxide (NaOH) and sodium sulphide (Na₂S) (Biermann, 1996b). A typical white liquor composition is in Table 2.2 below:

Table 2.2: Typical White Liquor Composition
(Chandra, 2004, Kevlich et al., 2017)

Chemical component	Formula	Typical White Liquor Composition (%)
Sodium Hydroxide	NaOH	50 - 60
Sodium Sulphide	Na ₂ S	20-25
Sodium Carbonate	Na ₂ CO ₃	10 - 20
Sodium Sulphite	Na ₂ SO ₃	3
Sodium Sulphate	Na ₂ SO ₄	5
Sodium thiosulphate	Na ₂ S ₂ O ₃	3

During digestion woodchips are disintegrated into a fibrous pulp product by breaking the bonds in the lignin macromolecule, dissolving it and allowing them to be separated (JOHNSON, 2011). This digestion process can be summarised as:



The wood is composed of organic compounds: lignin, cellulose, hemi-cellulose, and resins. Hemi-cellulose can be divided into three major organic groups: glucomannan, xylan and other hydrocarbon groups. Table 2.3 below illustrates typically how these elements are present in the wood chips and in the separated fibres after digestion and separation.

Table 2.3: Typical Composition of Wood Chips and Final Pulp
(Lindedahl, 2008)

	Typical Wood Chip – Typical Concentrations (%)	Typical Final Pulp Product (%)
Cellulose	38 - 42	72 – 73
Glucomannan	2 - 20	2 – 10
Xylan	7 – 30	7 – 30
Other hydrocarbons	< 5	< 1
Lignin	20 – 30	2 – 5
Resins	2 – 6	< 1

The process of breaking down the chemical structure of the lignin and rendering it soluble in a liquid is called delignification. Sulphidity, Na₂S, and strong alkali, NaOH, are central to breaking down the lignin (Lindedahl, 2008).

Sulphidity is defined as:

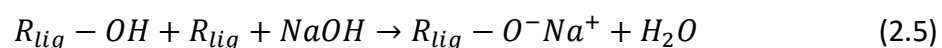
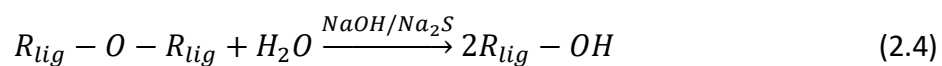
$$\text{Sulphidity} = \frac{100 \times [\text{Na}_2\text{S}]}{[\text{NaOH}] + [\text{Na}_2\text{S}]} \quad (2.1)$$

The sulphide, Na₂S, and hydroxide, NaOH, in the digester are present in the following equilibrium:



The lignin content of timber impacts on the amount of pulping chemicals required to liberate fibres. Fibres are considered liberated when sufficient lignin has been removed from the woodchips and they are soft enough to break apart into fibres with little or no mechanical action (Biermann, 1996b).

Sulphide performs two functions in the digestion process, it promotes and accelerates the cleavage of the ether links in the phenolic units and it reduces undesirable condensation (Saturnino, 2012). The cleavage of ether links is as follows (Holtzapple, 2003):



The digestion process can be designed to operate in either a batch or continuous mode. A mill operating with batch digesters will typically have six to eight pressure vessels, so that as some are in different stages of filling others will be blowing, and others will be offline for maintenance. The digesters can be heated directly with steam, diluting the cooking liquor, or heated indirectly via heat exchange tubing through which steam is passed and condensate recovered (Biermann, 1996b).

A typical digestion sequence involves the following sequence of steps (SOUTAR, 2016):

- Initial filling: Pressure vessel is opened and filled with wood chips, then white liquor and some black liquor.

- Additional woodchip addition: After some initial contact with the liquor, more wood chips are added to the contents of the pressure vessel
- Start of digestion: The digester is closed, and the woodchip mixture is heated and pressurised for about 90 minutes until a cooking temperature of between 130°C to 180°C is achieved.
- Cooking: The temperature is maintained for 20-45 minutes, during which time air and other non-condensable gases are ventilated.

The cooking step is considered complete when the target lignin content of the pulp is achieved. The contents of the digester are transferred to the blow tank. The digester is opened and the sequence repeats.

Reaction with the lignin, neutralisation of organic acids and resins in the wood consumes alkalinity in the digestion fluid. After digestion, the liquor is separated from the pulp and is called “black” liquor. The black liquor contains two fractions: organic and inorganic. The organic fraction is a mixture of lignin, hemicellulose, and other dissolved material from wood, and contains approximately half the mass of the original wood chips. The inorganic fraction is mostly composed of the residual cooking chemicals (Tran and Vakkilainen, 2016).

Table 2.4: Typical Black Liquor Inorganic Composition
(Chandra, 2004, Kevlich et al., 2017)

Chemical component	Formula	White Liquor Composition (%)	Weak Black Liquor Composition (%)
Sodium Hydroxide	NaOH	53	6
Sodium Sulphide	Na ₂ S	21	19
Sodium Carbonate	Na ₂ CO ₃	15	36
Sodium Sulphite	Na ₂ SO ₃	3	9
Sodium Sulphate	Na ₂ SO ₄	5	14
Sodium thiosulphate	Na ₂ S ₂ O ₃	3	16

2.1.3 Kraft Chemical Recovery – Black Liquor and the Recovery Boiler

Approximately 7 tonnes of 15% solids black liquor is produced per tonne of pulp and of the 15% solids in the black liquor, 10% is organic and 5% is inorganic, with a total heat content of 13.5-14.5 MJ/kg solid (Biermann, 1996b).

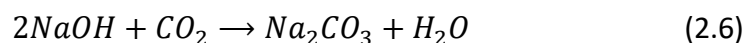
After separation from the pulp, the Black Liquor is passed to what is called the Kraft chemical recovery process, where up to 97% of the inorganic chemicals used in the pulping process are recovered and regenerated for reuse (Tran and Vakkilainen, 2016). The recovery of the inorganic cooking chemicals combined with the generation of large amounts of heat energy by burning the organic materials in the black liquor makes chemical pulping economically feasible (ELLIS and JOHNSON, 2011).

The purpose of the recovery boiler is to recover inorganic chemicals as a smelt (sodium carbonate and sodium sulphide), burn the organic chemicals and recover the heat of combustion in the form of steam (JOHNSON, 2011).

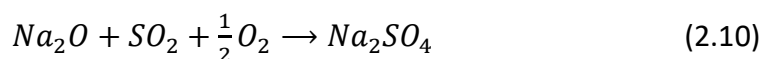
Before being introduced into the recovery boiler furnace, black liquor is concentrated using multi-effect evaporation to approximately 65%-75% solids content. Whilst the viscosity of the black liquor increases drastically, a higher solids concentration in the black liquor will result in higher temperatures in the lower part of the furnace, which increases the rate of smelt reduction, decreasing sulphur emissions (Biermann, 1996b).

The reactions of black liquor incineration are the conversion of sodium salts and the reduction of make-up chemical, Na_2SO_4 . Fly ash is also generated, which is captured, whilst unwanted reactions that can occur in the smelt need to be controlled to avoid odour emissions (Lindedahl, 2008).

Conversion of sodium salts can be summarized as the following reaction:



With the other reactions



Whilst the overall Kraft chemical recovery process regenerates and recirculates most of the sodium and sulphur cooking chemicals, additional chemical must be added to the process to make-up for what is lost from the system. A significant quantity of pulping chemical is lost with the pulp after separation from the black liquor, but also to gas emissions and spills from all process units. Table 2.5 summarises points of chemical loss in the Kraft cycle.

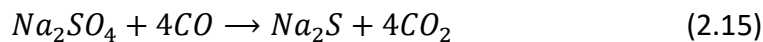
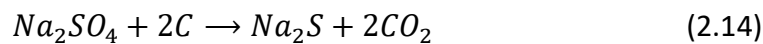
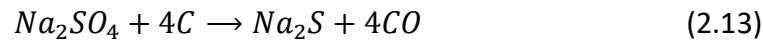
Table 2.5: Points of Chemical Loss in Kraft cycle
(Saturnino, 2012)

UNIT OPERATION	GAS EMISSIONS	LIQUOR EMISSIONS
Digester	NCG/TRS → Furnace (H ₂ S, CH ₃ SH, CH ₃ SCH ₃ , CH ₃ SSCH ₃)	Miscellaneous losses at pumps, leaks in heaters, vapour carry-over
Blow Tank	NCG/ TRS → Furnace (H ₂ S, CH ₃ SH, CH ₃ SCH ₃ , CH ₃ SSCH ₃)	Miscellaneous losses at pumps, leaks in heaters, vapour carry-over
Brown-Stock Washers	NCG/ TRS → Furnace (H ₂ S, CH ₃ SH, CH ₃ SCH ₃ , CH ₃ SSCH ₃)	Black liquor lost in pulp from brown-stock washers. Miscellaneous losses at pumps, leaks in heaters, vapour carry-over.
Multiple Effect Evaporators	NCG/ TRS → Furnace (H ₂ S, CH ₃ SH, CH ₃ SCH ₃ , CH ₃ SSCH ₃)	Miscellaneous losses at pumps, leaks in heaters, vapour carry-over
Recovery Boiler	Losses of volatilized sulphur-containing gases (SO ₂)	
Smelt Dissolving Tank		Miscellaneous losses at pumps, leaks in heaters, vapour carry-over
Causticizing System	Losses of volatilized sulphur-containing gases (SO ₂)	Weak white liquor carried with lime mud and lost in lime kiln.

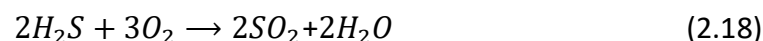
Non-condensable gases, NCGs, which are generated in the Kraft process are corrosive, toxic and odorous gases that contain sulphur compounds (Total Reduced Sulphur – TRS), organic gases such as methanol, water vapour and air. To eliminate harmful environmental emissions, NCGs can be collected to eliminate Kraft plant odour and can be destroyed in the plant lime kiln (Tran and Vakkilainen, 2016).

To make up for lost chemicals, approximately 20-50 kg of Na₂SO₄ per ton dry pulp is typically dissolved in the concentrated black liquor before it is sprayed into the recovery furnace

(Saturnino, 2012). Reduction of make-up chemical Na_2SO_4 occurs in the lower zone of the furnace, where it is deficient in oxygen. This allows the sulphur in the smelt to report as the desired Na_2S and not $\text{Na}_2\text{S}_2\text{O}_3$ or Na_2SO_4 , which are ineffective in the digesting pulp (Biermann, 1996b). The reduction reactions can be summarized as:



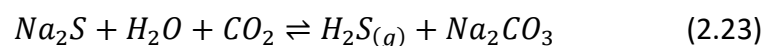
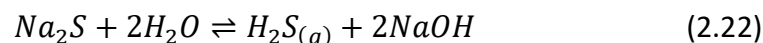
The upper zone of the furnace must be under oxidative conditions to prevent carbon monoxide formation conditions. Fly ash generated by reactions occurring in this zone are drawn away from the recovery boiler at the exit of the electrostatic precipitator with the flue gas. The reactions that occur in the oxidation zone of the furnace are:



The reactions that occur in the fly ash are:



In the smelt, the following unwanted reactions can take place:



The thermal efficiency (heat to steam/heat combustion of black liquor) is typically 60%. Most of the thermal energy lost is via the steam from the black liquor exiting the process with flue gases (Biermann, 1996b).

The sulphur and sodium inorganic materials leave the furnace as a molten slag or smelt, which is directed into the green liquor dissolving tank where they are dissolved in water to create an inorganic aqueous solution called "green liquor". Table 2.6 below summarises the

concentration, temperature, and composition of typical industrial Kraft Green Liquor and compares them to White and Black Liquor process streams.

Table 2.6: Typical Green Liquor Composition
(Chandra, 2004)

Component	Chemical Formula	White Liquor Composition (%)	Thickened Black Liquor Composition (%)	Green Liquor Composition (%)
Sodium Hydroxide	NaOH	53	6	8
Sodium Sulphide	Na ₂ S	21	19	22
Sodium Carbonate	Na ₂ CO ₃	15	36	60
Sodium Sulphite	Na ₂ SO ₃	3	9	2.5
Sodium Sulphate	Na ₂ SO ₄	5	14	5
Sodium thiosulphate	Na ₂ S ₂ O ₃	3	16	2.5
Concentration (g/L)		100-120 g/L	500-700 g/L	100 -150g/L
Temperature		75 to 90°C	80 to 90°C	75 to 90°C

2.1.4 Kraft Chemical Recovery – Reaustization and the Lime Kiln

The green liquor is fed into the clarifier (JOHNSON, 2011) to remove undissolved dregs by sedimentation before the green liquor is recausticized. The insoluble material making up the green liquor dregs is about 0.1% of the liquor and consists of mainly carbon and insoluble metal carbonates, sulphates, sulphides, hydroxides and non-wood fibre silicates, creating a black and bulky material (Biermann, 1996b).

The green liquor clarifier and storage is typically insulated to maintain temperature at 85°C to 95°C. The high temperature is maintained because high temperature lime (CaO) coming directly from the kiln is mixed with the green liquor with a reaction temperature of 99-105°C. A lime mud (CaCO₃) that settles well is formed (Azgomi, 2014), as per the chemical equations below:

Slaking Reaction:



Causticizing Reaction:



Grits are large unreactive lime particles and insoluble impurities formed in lime kiln and enter with the fed lime. Grits, normally less than 2% of the total lime feed, are removed in the lime slaker by the “classifier”, which rakes out larger insoluble particles (Tran, 2008).

In a standard recausticization plant there will be 2-4 continuously stirred reactors, with a retention time of between 2 and 4 hours. The extent of NaOH regeneration is affected by the initial concentration of Na_2CO_3 and the amount of excess lime. Lime is fed in an excess of 1% as much more than this will decrease the filtration rate of the lime mud (Azgomi, 2014). A standard recausticization plant will achieve between 75-85% Na_2CO_3 conversion to NaOH and is normally 3-4% below the equilibrium level in order to avoid “excess liming” (Biermann, 1996b).

Following recausticization, the liquor is clarified in gravity settling tanks to separate the lime mud (CaCO_3) from the white liquor, until the clarified liquid has a turbidity below 100ppm (Tran, 2008). Typically, the white liquor clarifiers will maintain a storage of over 12 hours of white liquor. The settled lime mud will have a solids content above 35% to prevent the loss of NaOH to the lime mud washer. The quality of the settled solids is impacted by the control of excess lime, the concentration of inert contaminants in the lime, or by incomplete lime slaking due to lime kiln capacity or temperature control causing either viscous lime (low temp) or unreactive lime (too high temp) (Azgomi, 2014). Polymer additives are used to aid lime mud settling when required. For further clarification, some plants use pressure filtration, such as tubular membranes to further separate lime mud (Azgomi, 2014).

After leaving the clarifier, usually using sedimentation washing, the lime mud is washed with fresh make-up water to remove any remaining entrained sodium. If Na_2S is present in the lime kiln, it causes slagging and reduced sulphur compounds in kiln emissions as H_2S (Biermann, 1996b). The lime mud is in effect diluted to between 25-30% solids, before it is again thickened in to 60-70% solids in rotary drum filters or centrifuges to limit the running cost of the lime kiln (Tran, 2008).

The thickened lime mud, CaCO_3 , is then passed to the lime kiln to be calcined. The kiln is normally of rotary type, where the lime mud is dried, heated and converted to CaO by gasifying the carbon dioxide, so it can be reused in the recausticization process, as per the following reaction (Lundqvist, 2009):



CaO is required in the ratio of 200-300 kg/t of pulp, or lower depending on the quality and quantity of pulp yields (Biermann, 1996b).

2.1.5 Key Metrics – Thermal Energy for NaOH Production – Lime Kiln

Rotary lime kilns are typically 2.4-4m in diameter and 30-120 m long and can produce 40-400 t/day of CaO (Tran, 2008). The kilns are inclined at about 2-5 degrees and rotate at approximately 1 rpm, moving lime along the length of the kiln. The specific energy consumption of a kiln is the ratio of calcining energy to the CaO production. The temperature of the kiln is around 1200°C, heated by fuel oil or natural gas, which are fed into the kiln counter current to the lime. A rotary kiln calciner will typically require between 7.8 to 10 GJ per tonne of CaO produced, depending on the water content of the lime, the length and the condition of the lime kiln (Biermann, 1996b). (Lundqvist, 2009) performed mass and energy balance across a typical lime kiln with the operation parameters detailed in Table 2.7 below and Figure 2.2.

Table 2.7: Modelled Typical Lime Kiln Parameters
(Lundqvist, 2009)

	Key Parameter	Value
A	Dry content of lime mud	75%
B	Temperature of lime mud	60°C
C	Temperature of flue gases	200°C
D	Temperature of reburned lime	200°C
E	Shell heat losses	12%
F	Excess air	10%

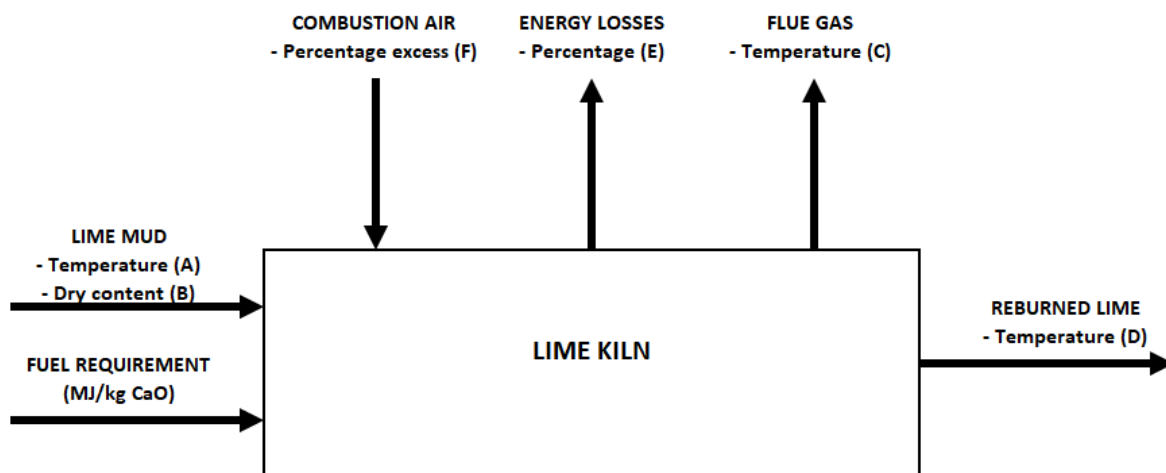


Figure 2.2: Lime kiln energy balance and key parameters affecting fuel requirement

Based on the above parameters (Lundqvist, 2009), the simulated energy balance of the lime kiln was as detailed in Table 2.8 below.

Table 2.8: Simulated Energy Balance based on 2.12 Parameters
(Lundqvist, 2009)

	Heat (Fuel) Requirement (MJ/kg CaO)	Fraction of total Heat Requirement (%)
Energy for calcination	3.18	51
Energy for drying	1.41	23
Energy lost in flue gases	0.96	15
Heat in lime mud (Feed)	-0.22	-4
Heat in reburned lime	0.16	3
Shell heat losses	0.75	12
Total	6.4	100

Using process parameter inputs from Table 2.7 the model (Lundqvist, 2009) determines a total heat requirement of 6.4 MJ/kg CaO, which compared to industry would significantly lower than industry average of approximately 8 to 10 MJ/kg CaO (Tran, 2008).

However, a 10% decrease in the dry content of the lime mud results in a 20% increase in required heat energy. A 100°C increase in the flue gas temperature causes an additional 10% increase in required heat energy. Energy in the CaO product also is a significant contributor to heat losses, if coolers are not employed in the lime kiln, this can leave as high as 900°C contributing another 14% to heat energy requirement. Shell heat losses can also approach 20% which would cause a further 11% increase to heat energy requirements and if excess air is increased to 20%, a further 1% in heat energy is required. These combined efficiency reductions increase the modelled heat energy requirement from 6.4 to 10.8 MJ/kg CaO, which the industry range of 8 – 10 MJ/kg CaO falls within.

Based on the stoichiometric requirement 0.71 kg CaO to produce 1.0 kg of NaOH, allowing for a 1 percent excess supply of CaO, a heat requirement of 10 MJ/kg CaO, the heat requirement to produce 1 kg of NaOH is 7.1 MJ/kg NaOH. However, the value of 7.1MJ/kg NaOH is increased due to other process inefficiencies.

A key inefficiency is that approximately 5% of the produced burnt lime cycle is composed of inert materials, in addition to poor quality and unreactive lime (Tran, 2008). This means that a significant portion of the burnt lime supplied to the recausticization reaction does not take part, requiring additional excess lime to be supplied. The inert materials are mostly magnesium, silica, aluminium, and sodium oxides. The poor quality reburned lime includes large particles that form in the process loop that are neither fully calcined in the lime kiln and are not efficient in the slaking and recausticization process due to insufficient residence time (Biermann, 1996b). A 5% reduction in lime kiln efficiency would increase the fuel requirement to 7.5 MJ/kg.

The calculated specific thermal energy requirements (MJ/kg NaOH) of the lime kiln in the recausticisation process are given in Table 2.9 below.

Table 2.9: Summary of Lime Recausticization Thermal Energy Requirements

	Energy Type	Energy Requirement	
		MJ/kg NaOH	kJ/mol NaOH
Stoichiometric CaO Requirement (0.7 kg CaO/1.0 kg NaOH)	Thermal – Fossil Fuel	7.0	280
+ 1% CaO Excess	Thermal – Fossil Fuel	0.1	4
+ 5% CaO Inert Material	Thermal – Fossil Fuel	0.4	16
Total		7.5	300

2.1.6 Key Metric of Recausticisation Process - “Deadload Chemicals”

“Deadload chemicals” are inorganic chemicals in the white liquor that do not contribute to the pulping reactions in the digester and circulate through the pulping and recovery cycle (THOMAS M. GRACE, 2009). The main deadload elements are sodium carbonate (Na_2CO_3), sodium sulphate (Na_2SO_4), sodium thiosulfate ($\text{Na}_2\text{S}_2\text{O}_3$) and sodium chloride (NaCl) (Saturnino, 2012). Whilst potassium, K, is a soluble element that can also accumulate in the process and typically enters the process with the woodchips, it is not considered a deadload chemical as it is an active alkali pulping agent forming potassium hydroxide (KOH).

There are other non-process elements that enter the system, primarily with the lime, including silica, aluminium, magnesium, phosphorus, and iron. Whilst these are considered “non-process elements”, they do not become part of the recirculated “deadload” as these

elements will precipitate out in the process and are separated (Si, Al) as grits, or as scale on process equipment (Mg, P, Fe).

The Na_2CO_3 deadload is a result of incomplete conversion of causticizing with the lime. This reaction has an equilibrium, and it is not possible to achieve complete conversion in the conventional process. The conversion or “Causticisation efficiency” (THOMAS M. GRACE, 2009) is defined as:

$$CE = \frac{[\text{NaOH}]}{[\text{NaOH}] + [\text{Na}_2\text{CO}_2]} \times 100 \quad (2.27)$$

The consequences of over liming on white liquor clarification, discussed above, mean a typical Kraft pulping recausticization process will achieve a conversion efficiency of between 82-84%.

The amount of deadload sodium carbonate from incomplete causticization is given by:

$$DLC = \frac{106}{62} \times \frac{1-CE}{CE} \times \frac{2(1-S)}{(2-S)Y} \times EA \times 1000 \quad (2.28)$$

Where:

- DLC = amount of Na_2CO_3 deadload, kg per metric ton unbleached pulp
- S = Sulphidity of cooking liquor, %
- EA = Effective Alkali %
- Y = pulp yield, %

A one percent increase in the causticizing efficiency will have a greater proportional impact on the mass of deadload chemical in the white liquor. A Kraft process with 85% causticizing efficiency, will carry approximately 75 kg DL/tonne dry pulp. A 1% increase in causticization efficiency will result in an approximate 6-7 kg/tonne dry pulp decrease in deadload chemical (THOMAS M. GRACE, 2009).

Na_2SO_4 deadload is a result of incomplete reduction in the recovery furnace, the only place where Na_2SO_4 can be reduced to Na_2S the targeted pulping chemical. Sulphate deadload is smaller than the carbonate deadload normally by a factor of 4.

Another source of sulphate deadload is sulphur that can be introduced with the fuel used in the lime kiln. The sulphur in the fuel reacts with the lime mud to generate calcium sulphate,

which reacts with sodium carbonate in the causticization system to form sodium sulphate, adding to the deadload (Biermann, 1996b).

Sodium thiosulphate deadload forms when sulphide in the aqueous green and white liquor systems oxidises in the presence of air. In a typical Kraft plant, it will decompose to molten carbonate in the recovery boiler furnace, minimising the concentration of it in the smelt. The amount of sodium thiosulphate deadload in the white liquor is typically 7-8 kg/ tonne dry pulp.

Chloride deadload in a Kraft mill white liquor can vary greatly from plant-to-plant. Chloride can enter the process via the woodchips, fresh make-up water, make-up chemicals and from effluent from the pulp bleaching plant, where chlorine dioxide can be the generated bleaching agent.

Chloride is highly soluble, and will only leave the process with liquor losses, gas emissions and deliberate purges from the system. Purges will be in the form of dumps of precipitator dust, which has high concentration of NaCl. The NaCl in the precipitator dust can be used to monitor and control the chloride deadload. A 1.5% NaCl concentration in the precipitator dust will correspond to an approximate NaCl deadload of 5-6 kg/ tonne dry pulp. However, this can also be much higher. If the pulping wood supplied has been stored or transported in saltwater, the chloride deadload can be as high as 100 kg/ tonne dry pulp. A NaCl deadload of less than 10 kg/ tonne dry pulp is typical for most plants (THOMAS M. GRACE, 2009).

The greater the deadload, the greater the energy requirement to heat a greater mass of cooking chemical to pulp the same mass of wood chips. The concentration of the white liquor is generally set at the smelt dissolving tank and is normally controlled around 15% by weight. Each additional kilogram of deadload in the smelt requires 5.67 kg of water to balance the process. Heating this additional load equates to 1780 kJ/kg deadload, or 0.16 GJ/ tonne dry pulp.

2.1.7 Key Metrics of Lime Kiln – CO₂ Emissions from Fossil Fuel Source

Lime kilns burn fossil fuel, mainly natural gas, fuel oil or waste oil (Francey et al., 2011). Table 2.10 details the fuel requirement and CO₂ gas emissions per kilogram NaOH produced.

Table 2.10: Lime Kiln Fuel Carbon Emissions (Based on 10 MJ/1kg CaO)

Fuel Type	Energy Density (MJ/kg)	kg fuel per kg CaO	kg CO ₂ per kg fuel*	kg CO ₂ Emissions per kg CaO	kg CO ₂ Emissions per kg NaOH
Diesel	45	0.22	3.18	0.70	0.49
Gasoline	46	0.22	3.29	0.72	0.51
Natural gas	55	0.18	2.25	0.41	0.28

*(Pehl et al., 2017)

The overall CO₂ emitted from the Kraft mill lime kiln is from that released from the CaCO₃, and CO₂ from the burning of fossil fuels, and sometimes pulp mill derived gases (EnvironmentAustralia, 1998). CO₂ is also emitted from the process loop in the conversion of calcium carbonate to calcium oxide in the lime kiln. The carbon in CaCO₃ mud is derived from the woodchips, transported into the calcium loop via the sodium carbonate in the green liquor (Gaudreault et al., 2012).

Stoichiometrically the CO₂ emissions attributable to the conversion of CaCO₃ to CaO are 0.78 kg CO₂/kg CaO, or 0.55 kg CO₂/kg NaOH. Whether or not this is included in a comparison to IEM recovery technology will depend on whether the IEM technology captures this carbon emission.

2.1.8 Key Metrics of Lime Kiln – Other Emissions

The most significant emissions challenge for the lime kiln is that of nitrogen because kilns are operating at high temperature in the presence of excess air (R. Miner a, 2001). The exhaust gases must be treated to remove particle matter, which can be achieved with the use of a venturi scrubber, where water is sprayed to trap particles. Electrostatic precipitators are also used, and offer cleaner emissions, easier control, and lower power costs.

Sulphur oxides are not generally emitted because CaO is a good scavenger of acidic sulphates and sulphites and forms CaSO₃ and CaSO₄. The formation of gypsum, CaSO₄ from these non-condensable gases results in ring formation within the lime kiln, and when severe, expensive

shutdowns are needed for kiln maintenance and ring removal (Tran, 2008). This emphasizes the importance of effective lime mud washing before the kiln.

The process variables around the lime kiln influence fuel requirement and NO_x and SO_x emissions from the process. Emissions from the lime kiln represent 10% of all emissions from the Kraft process (González Suárez et al., 2018).

Sulphur enters the lime cycle in the lime mud and fuel, resulting in to 20% of Kraft process total reduced sulphur (TRS) emissions originate from the lime kiln. Controlling lime mud solids content is a key parameter for reducing the TRS from the lime kiln, by reducing fuel requirement. Efficient mud washing can remove most residual sodium sulphide, therefore improved lime mud dewatering is important for reducing TRS emissions from the lime kiln (Aminvaziri, 2009). The sulphur oxides either flow out of the lime kiln with the flue gas or react with product lime or NaOH present to form Na₂SO₄ or CaSO₄. The formation of CaSO₄ in particular is efficient at cleaning the flue gas of sulphur emissions (Tran, 2008). However, lime kilns can reach a critical level where its capacity to strip sulphur is reached, which results in sudden increases in SO₂ emissions. This can occur when non condensable sulphur gases are introduced to the lime kiln from other parts of the Kraft process (Lundqvist, 2009).

The NO_x emissions from a particular lime kiln will be derived from fuel properties and combustion conditions. Thermal nitrogen oxides (NO_x) are formed in the lime kiln through the reaction of nitrogen and oxygen in the air and is strongly temperature dependent. Fuel NO_x is a result of oxidation of nitrogen in the fuel and can occur at much lower temperatures (Lundqvist, 2009).

2.1.9 Summary of Key Metrics Developed for Conventional Reausticisation

Based on the above literature review of the conventional Kraft process a group of performance metrics have been developed that will be used for comparison to any alternative IEM process technology. Table 2.11 below summarises the metrics found.

Table 2.11: Summary of Key Metrics

Metric 1: NaOH Concentration Requirement	
Minimum required	60 g NaOH/L (1.5 M)
Maximum required	90 g NaOH/L (2.25 M)
Metric 2: Specific Energy Requirements – Thermal Energy Lime Kiln	
CaO Production	10 MJ/kg CaO Produced
NaOH Production	8.0 MJ/kg NaOH Produced
Total Lime Kiln	1.8 – 3.0 GJ/ tonne dry pulp
Metric 3: Greenhouse Gas Emissions – Lime Kiln (kg CO₂/kg NaOH)	
Based on Diesel Fuel	0.49 kg CO ₂ /kg NaOH
Based on Gasoline Fuel	0.51 kg CO ₂ /kg NaOH
Based on Natural Gas Fuel	0.28 kg CO ₂ /kg NaOH
Metric 4: Kraft Cycle Deadload – Attributable Reausticisation Process	
Na₂CO₃ conversion to NaOH	80% (typical range: 75 – 85%) Limited by reaction equilibrium
Na₂CO₃ (Deadload)	15% - 25% 75 kg DL/ tonne dry pulp
Overall Deadload impact (% lost capacity within the Kraft Cycle)	Normally 15 to 25%
Overall energy cost of deadload	0.16 GJ/ tonne dry pulp Approximately 5 – 10% of Lime Kiln energy, or Proportionally 0.3 – 0.6 MJ/kg NaOH
Metric 5: Chemical Losses	
Sodium Sulphide: Na₂S	1 to 2% through lime kiln as S (1.4 to 4 kg/ tonne dry pulp as S required makeup)
Metric 6: Other Key Emissions	
Other environmental emissions – NCGs	Lime kiln → 20% of overall process TRS emissions because of fuel requirement and entrained sulphur in lime mud.

2.2 Ion Selective Membrane Processes for Recovery of Inorganic Salts in Kraft Green Liquor:

Ion exchange membrane (IEM) processes are an established method used for industrial water desalination and for the recovery of valuable inorganic and organic salts (Ran et al., 2017). The mechanics of IEMs and how they can be used in the separation of oppositely charged ions and co-ions of different valences are identified in the context of Kraft Green liquor recovery. The control variables available in an IEM system can be manipulated to affect the recovery of Na and S, the regeneration of alkali (Na_2CO_3 to NaOH) and the rejection of unwanted deadload ions (SO_3^{2-} , SO_4^{2-} , CO_3^- and Cl^-).

2.2.1 Ion Selective Membranes (IEMs) Characterisation

Ion selective membranes (IEMs) are a group of dense polymeric membranes that have a fixed charge in the polymer matrix, so they can selectively permit the passage of oppositely charged ions (Luo et al., 2018). The mechanism of excluding and promoting the passage of targeted ions is referred to as permselectivity (Sata, 2007a). This permselectivity ability of membranes has led to IEM industrial applications, such as Electrodialysis (ED), Diffusion Dialysis (DD) and the Electrolysis Membrane Cell (EMC).

The most widely used IEMs are proton exchange membranes such as the Nafions (E.I. DuPont de Nemours & Co., Inc.), FlemionTM (Asahi Glass, Japan), Neosepta-FTM (Tokuyama, Japan), and Aciplex^{TMs} (Asahi Kasei Chemicals Corporation, Japan) (Bayer et al., 2016).

IEM applications have grown with the development of membranes that have permselectivity between not just counter and co-ions, but also counter-ions of different (monovalent and multivalent) or equal valences. This allows the development of processes that have high membrane permselectivity between counter-ions of different valences (Luo et al., 2018).

IEMs with permselectivity have been developed and used in the electrodialysis of sea water in Japan, for the production of table salt (NaCl) (SELEMION(AGC), 2018). Such systems have membranes with strong transport efficiencies for Na^+ , rather than Mg^{2+} and Ca^{2+} (Ran et al., 2017).

The chlor-alkali process uses alkali resistant IEMs which slow the passage of OH^- ions in the electrolysis of NaCl solution in the production of Cl_2 , NaOH and H_2 (Budiarto et al., 2017).

Referring to Figure 2.3, IEMs are generally classified by their charge and charge distribution of fixed groups, and are generally classified into five groups: Cation Exchange Membranes (CEMs), Anion Exchange Membranes (AEMs), amphoteric IEMs, bipolar membranes and mosaic IEMs (Sata, 2007c).

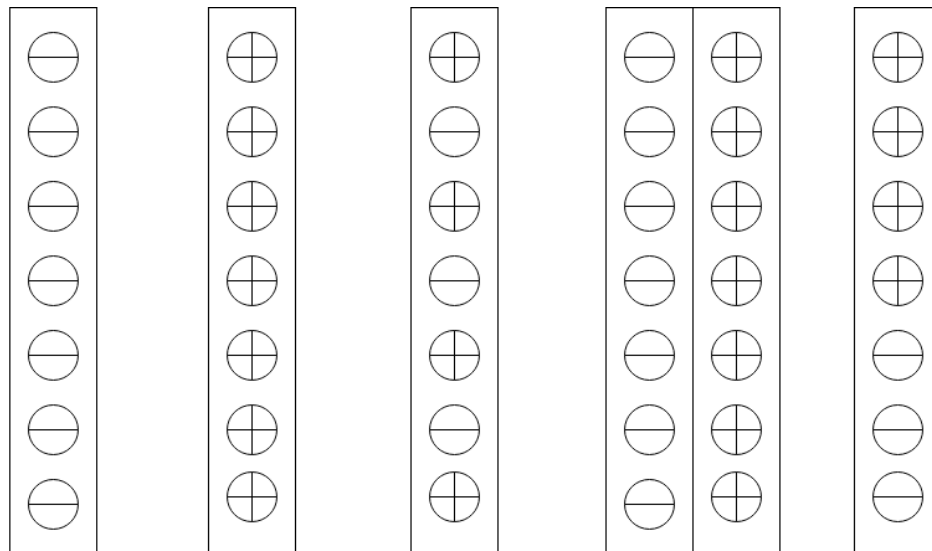


Figure 2.3: Schematic – Types of Ion Exchange Membrane

(Luo et al., 2018). From left to right CEM, AEM, amphoteric IEM, bipolar IEM, and Mosaic IEM.

Most developed applications and current research in ion selective IEMs are in CEMs and AEMs (Luo et al., 2018). The “Donnan potential” is a measure of the thermodynamic membrane equilibrium of the IEM matrix as a “solution” with homogeneously distributed fixed charges (Sata, 2007a), so the potential will uniformly favour the passage of either cations or anions. This permselective ability to accept and exclude co-ions is called the “Donnan Effect”.

To quantify the “Donnan potential” of a semi permeable membrane separating two compartments, it must be differentiated from the “diffusion potential” between two electrolytes. Donnan potential is quantified in an arrangement where permeating ions diffuse through a membrane in the absence of an electrical field owing to concentration gradient, the existing membrane potential continuously electrostatically retards their further migration in both directions until reaching the same exchange rate. A dynamic equilibrium is reached as continuous exchange occurs forward and backwards through the membrane at the same rate, despite the concentration gradient. There is no chemical reaction at the membrane interface between participating chemical species, so a thermodynamic

equilibrium is identified, the Donnan potential. This thermodynamic equilibrium, Donnan Potential, resembles the contact potential at a metal-metal interface or a metal-semiconductor junction in electronic equilibrium (Pyun, 2021).

$$\varphi_{Don} = \varphi^m - \varphi^s = \frac{RT}{z_i F} \ln \frac{a_i^s}{a_i^m} \quad (2.29)$$

The Donnan potential, φ_{Don} , is the potential between the membrane φ^m and solution φ^s potentials; R is the universal gas constant; T is the absolute temperature; F is Faraday constant; z_i , a_i^s , and a_i^m refer to the valance and activity of ion i in the solution and membrane (Luo et al., 2018).

The system Donnan potential is derived for a standard membrane configuration consisting of an α -phase compartment on the left side and a β -phase compartment on the right side, separated by a semipermeable membrane. Figure 2.4 below shows an example of a cell where Na_2CO_3 solution is separated from NaOH . On the left side there are H_2O , Na^+ and CO_3^- which are all able to pass through the membrane, while on the other side there are H_2O , Na^+ , OH^- and R^- where the first three are the diffusible species and R^- is the colloidal macromolecule resin anion that is immobilised in the membrane and hence cannot pass through it. The Donnan Potential for the system is developed below to show how it, and permselectivity, is affected by the non-diffusible charge in the membrane (R^-) and concentration of electrical neutrality and stoichiometry of the α -phase and β -phase compartments.

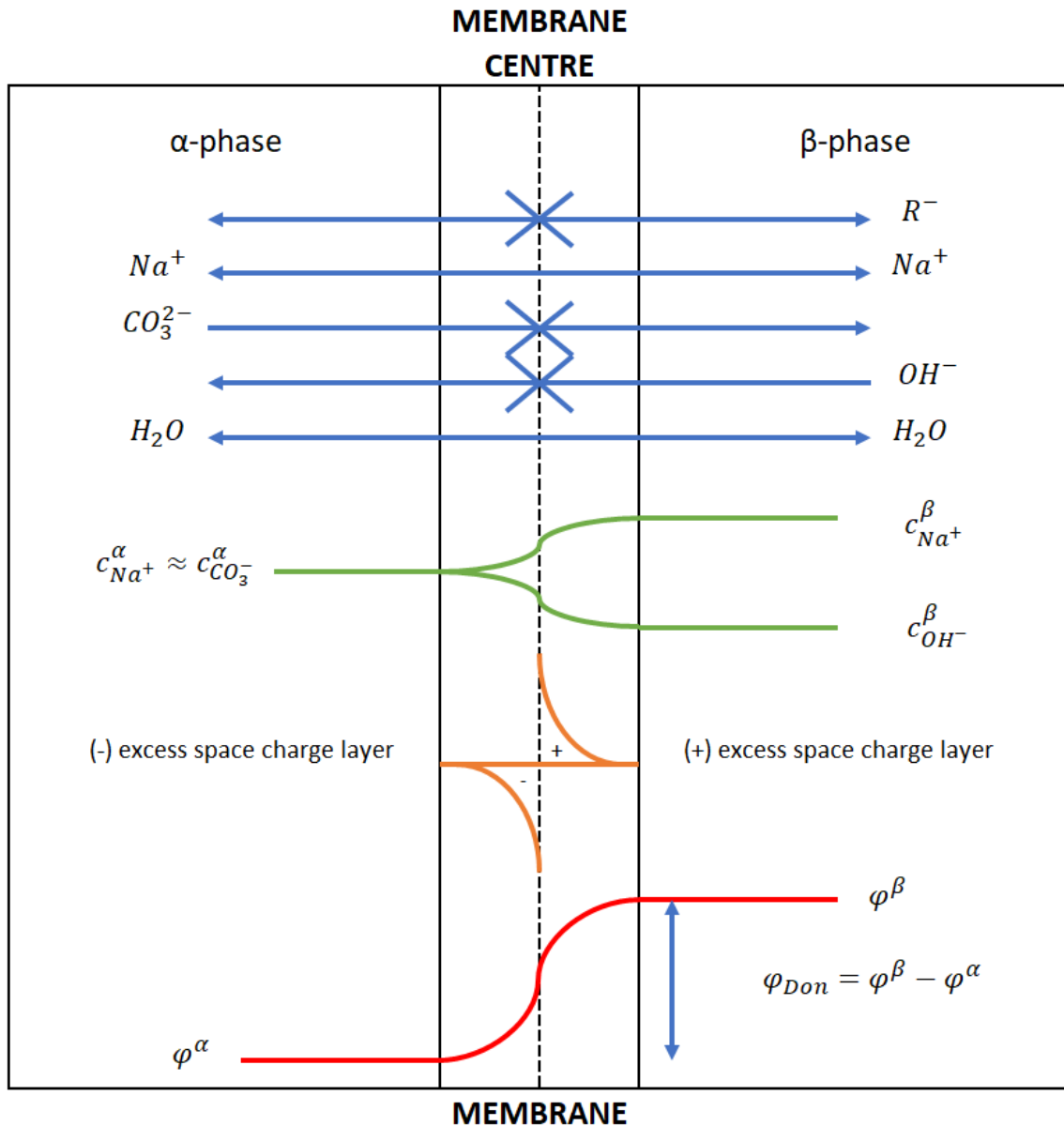


Figure 2.4: Donnan Equilibrium Across IEM

Donnan equilibrium between non-diffusible resin cation R^- free left hand α -phase and Na_2CO_3 electrolytic solution and non-diffusible resin anion R^+ containing right hand β -phase NaOH electrolytic solution, separated by a semipermeable CEM. (Luo et al., 2018, Pyun, 2021)

The system Donnan Potential incorporates the thermodynamic osmotic equilibrium conditions. Figure 2.5 below shows a schematic diagram of the build-up of osmotic pressure at thermodynamic equilibrium to define the osmotic pressure.

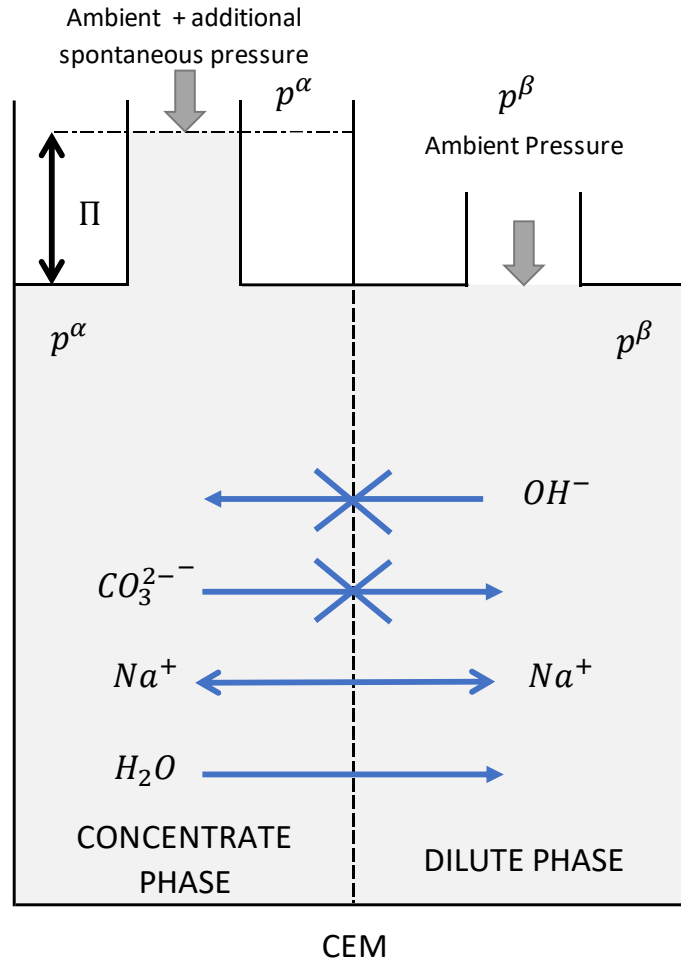


Figure 2.5: Schematic diagram of osmotic pressure (π) at thermodynamic equilibrium. (α -phase (Na_2CO_3) is separated from β -phase (NaOH) by a semipermeable CEM)

Referring to Figure 2.5, the build-up of osmotic pressure (π) in the concentrate phase is the same as the deficiency in chemical potential in the dilute phase. When the ions and water are all able to pass through a membrane, no osmotic pressure is exerted. When membranes have semipermeable characteristics, the osmotic pressure becomes important (Pyun, 2021). By applying the equality of chemical potential of water in the dilute phase, α , the concentrate phase, β , with the simultaneous molar inequality of Na_2CO_3 and NaOH in both phases, gives:

$$\mu_{\text{H}_2\text{O}}^{\alpha}(p^{\alpha}) = \mu_{\text{H}_2\text{O}}^{\beta}(p^{\beta}), \text{ with } \mu_{\text{Na}^+}^{\alpha}(p^{\alpha}) = \mu_{\text{Na}^+}^{\beta}(p^{\beta}) \quad (2.30)$$

Where $\mu_{\text{H}_2\text{O}}^{\alpha}(p^{\alpha})$ and $\mu_{\text{H}_2\text{O}}^{\beta}(p^{\beta})$ are the chemical potentials of water in the α and β phases respectively. The osmotic pressure of the system shown in Figure 2.5 is dependent on temperature and concentration (c_{eq}):

$$\Pi = (p^\alpha - p^\beta) = c_{eq}RT \quad (2.31)$$

Giving:

$$\mu_{H_2O}(p^\beta) = \mu_{H_2O}(p^\alpha) + RT \ln x_{H_2O} \quad (2.32)$$

Where x_{H_2O} is the mole fraction. Returning to the Donnan model in Figure 2.4, there is equality in hydrostatic chemical potential of water ($\eta_{H_2O}(p)$) in pure solvent in α - phase and in the solution β - phase, with simultaneous inequality of the chemical potential ($\mu_{RCL}(p)$) of a resin molecule RCL in both phases gives:

$$\eta_{H_2O}^\alpha(p) = \eta_{H_2O}^\beta(p) \text{ with } \mu_{RCL}^\alpha(p) \neq \mu_{RCL}^\beta(p) \quad (2.33)$$

The chemical potential and osmotic pressure in the α -phase are the respective reference levels, because $c_{H_2O}^\alpha > c_{H_2O}^\beta$.

$$RT \ln a_{H_2O}^\alpha + (\Pi = 0)v_{H_2O} = RT \ln a_{H_2O}^\beta + (\Pi \neq 0)v_{H_2O} \quad (2.34)$$

Where v_{H_2O} is the molar volume of solution. Giving,

$$RT \ln \frac{a_{H_2O}^\alpha}{a_{H_2O}^\beta} + \Pi v_{H_2O} = 0 \quad (2.35)$$

The combined hydrostatic chemical potential (p) and electrochemical potential of diffusible cations (z) for the equilibrium is valid (Luo et al., 2018):

$$\eta_{Na^+}^\alpha(p, z) = \eta_{Na^+}^\beta(p, z) \quad (2.36)$$

The chemical potential and osmotic pressure in the α -phase as the respective reference levels, as $C_{Na^+}^\alpha > C_{Na^+}^\beta$,

$$RT \ln a_{Na^+}^\alpha + \Pi^\alpha(\Pi = 0)v_{Na^+} + F\varphi^\alpha = RT \ln a_{Na^+}^\beta + \Pi^\beta(\Pi \neq 0)v_{Na^+} + F\varphi^\beta \quad (2.37)$$

Giving:

$$RT \ln \frac{a_{Na^+}^\alpha}{a_{Na^+}^\beta} + \Pi v_{Na^+} = F(\varphi^\beta - \varphi^\alpha) \quad (2.38)$$

Similarly, the equality of the combined hydrostatic chemical potential and electrochemical anion species for the equilibrium condition to be valid:

$$\eta_{CO_3^{2-}}^\alpha(p, z) = \eta_{OH^-}^\beta(p, z) \quad (2.39)$$

The chemical potential and osmotic pressure in the β -phase as the respective reference levels, as $C_{CO_3^{2-}}^\alpha > C_{OH^-}^\beta$,

$$RT \ln a_{CO_3^{2-}}^\alpha + \Pi^\alpha(\Pi \neq 0)v_{CO_3^{2-}} - F\varphi^\alpha = RT \ln a_{OH^-}^\beta + \Pi^\beta(\Pi = 0)v_{OH^-} - F\varphi^\beta \quad (2.40)$$

Giving,

$$RT \ln \frac{a_{CO_3^{2-}}^\alpha}{a_{OH^-}^\beta} + \Pi v_{CO_3^{2-}} = F(\varphi^\beta - \varphi^\alpha) \quad (2.41)$$

Equations (2.38) and (2.41) imply that the activity ratio of cation and anion is split into two contributions of osmotic and potential difference. It is shown below, there is less contribution from osmotic potential (Π), compared to electrochemical potential of diffusible ions (φ), so Π can be integrated into the activity ratio of water between the two compartments.

Subtracting the (2.41) from (2.38) gives:

$$\Pi = \frac{RT}{(v_{CO_3^{2-}} - v_{Na^+})} \ln \frac{a_{Na^+}^\alpha a_{OH^-}^\beta}{a_{Na^+}^\beta a_{CO_3^{2-}}^\alpha} \quad (2.42)$$

From (2.35) gives:

$$\Pi = \frac{RT}{v_{H_2O}} \ln \frac{a_{H_2O}^\alpha}{a_{H_2O}^\beta} \quad (2.43)$$

Combining (2.42) and (2.43) gives:

$$\left(\frac{a_{H_2O}^\alpha}{a_{H_2O}^\beta} \right)^s = \frac{a_{Na^+}^\alpha a_{OH^-}^\beta}{a_{Na^+}^\beta a_{CO_3^{2-}}^\alpha} \quad (2.44)$$

Where $s = \frac{(v_{Na^+} - v_{CO_3^{2-}})}{v_{H_2O}} = (p - q)$. As the right-hand side approximates to 1 due to Henrian activity (Pyun, 2021), $a_{H_2O} = 1$ at the standard state in a dilute solution. So (2.44) becomes:

$$(a_{Na^+}^\alpha)(a_{CO_3^{2-}}^\alpha) = (a_{\pm}^\alpha)^2 = (a_{Na^+}^\beta)(a_{OH^-}^\beta) = (a_{\pm}^\beta)^2 \quad (2.45)$$

As ($a = f \times c$), if the activity coefficients (f) for anion and cation are the same, activity product (a) can be replaced by concentration (c), to give:

$$(c_{Na^+}^\alpha)(c_{CO_3^{2-}}^\alpha) = (c_{Na^+}^\beta)(c_{OH^-}^\beta) \quad (2.46)$$

Substituting (2.43) into either (2.38) or (2.41) gives the membrane potential:

$$\varphi_{Don} = \varphi^{\beta} - \varphi^{\alpha} = -\frac{RT}{F} \ln \frac{a_{Na^+}^{\alpha}}{a_{Na^+}^{\beta}} \left(\frac{a_{H_2O}^{\alpha}}{a_{H_2O}^{\beta}} \right)^p = -\frac{RT}{F} \ln \frac{a_{CO_3^{2-}}^{\alpha}}{a_{OH^-}^{\beta}} \left(\frac{a_{H_2O}^{\alpha}}{a_{H_2O}^{\beta}} \right)^q \quad (2.47)$$

Where, $p = \frac{v_{Na^+}}{v_{H_2O}}$ and, $q = \frac{v_{CO_3^{2-}}}{v_{H_2O}}$ are molar volume ratios. The standard state Henrian activity for a dilute solution (lower concentration of non-diffusible resin cation R⁺ in the β – phase $\ll c_{Na_2CO_3}^{\alpha}$), $a_{H_2O}^{\alpha} = 1$, assuming the same activity coefficients of diffusible cations and anions, (17) reduces to:

$$\varphi_{Don} = \varphi^{\beta} - \varphi^{\alpha} = -\frac{RT}{F} \ln \frac{c_{Na^+}^{\alpha}}{c_{Na^+}^{\beta}} = -\frac{RT}{F} \ln \frac{c_{CO_3^{2-}}^{\alpha}}{c_{OH^-}^{\beta}} \quad (2.48)$$

Referring to the Figure 2.4 arrangement, the electrical neutrality and stoichiometric constraints give on each side (α -phase and β -phase) of the membrane:

$$c_{Na^+}^{\alpha} = c_{CO_3^{2-}}^{\alpha} = c_{Na_2CO_3}^{\alpha} \quad (2.49)$$

$$c_{Na^+}^{\beta} = c_{OH^-}^{\beta} + c_{R^-}^{\beta} \quad (2.50)$$

Adding the (2.49) and (2.50), we get charge neutrality and stoichiometric constraint on both sides of the membrane.

$$c_{Na^+}^{\alpha} + c_{Na^+}^{\beta} = c_{CO_3^{2-}}^{\alpha} + c_{OH^-}^{\beta} + c_{R^-}^{\beta} \quad (2.51)$$

Combining (2.46), (2.49) and (2.50), we get the quadratic equation:

$$c_{Na^+}^{\beta} (c_{Na^+}^{\beta} - c_{R^-}^{\beta}) - (c_{Na_2CO_3}^{\alpha})^2 = 0 \quad (2.52)$$

As $c_{R^-}^{\beta} \ll c_{Na_2CO_3}^{\alpha}$, (2.52) becomes:

$$c_{Na^+}^{\beta} = c_{Na_2CO_3}^{\alpha} + \frac{c_{R^-}^{\beta}}{2} \quad (2.53)$$

Equation (2.53) implies that permeating cations will dominate permeating anions due to the right side of the membrane containing the resin cation R⁺.

IEMs Permselectivity – Kraft Green Liquor Context

In an IEM system targeting the synthesis of NaOH from a Na₂CO₃ Green liquor feed, cation exchange membranes are required for Na⁺ passage. More challenging is the capture of Na₂S, or S²⁻ ions, and possible rejection of “deadload” CO₃²⁻, SO₃²⁻ and SO₄²⁻. Possible IEM mechanism for this is an anion exchange membrane strong transport efficiency for S²⁻ ions. Discussed in more detail below, S²⁻ ions may have better diffusion rates than CO₃²⁻, SO₃²⁻ and SO₄²⁻ ions, so even across a standard AEM, some preferential permselectivity for S²⁻ may occur. Table 2.12 below summarises possible membrane selection for a Kraft Green liquor IEM system.

Table 2.12: Green Liquor Ionic Species, desired separation, and ideal IEM

Green Liquor Ionic Species Separation Target	IEM	Comments
Na ⁺ from CO ₃ ²⁻ , SO ₃ ²⁻ and SO ₄ ²⁻	CEM	If monovalent selective, may be mechanism to remove trace Ca ²⁺ or Mg ²⁺ . CEM monovalent selective membrane is available and is widely used in table salt production.
CO ₃ ²⁻ , SO ₃ ²⁻ and SO ₄ ²⁻ from Na ⁺	AEM	Assisted with the application of an electrical potential across membrane cell.
S ²⁻ from CO ₃ ²⁻ , SO ₃ ²⁻ and SO ₄ ²⁻	AEM	S ²⁻ has better solubility/diffusion rates than CO ₃ ²⁻ , SO ₃ ²⁻ and SO ₄ ²⁻ which may affect separation across AEM.
Hydroxide generation/water spitting (H ₂ O → H ⁺ + OH ⁻)	AEM CEM BPM	Acid/Alkali cell can employ bipolar membranes (BPM) or combination of CEM and AEM membranes to control the flow of H ⁺ and OH ⁻ ions.

2.2.2 Permselectivity – IEM Microstructure and Effect of Process Conditions

The forced transport of ions through ion exchange membranes requires a concentration and/or an electrical potential gradient across the cell. Subsequently, the ion selectively between two counter-ions can be affected by their solubility (ion-exchange) and mobility in the membrane phase (Luo et al., 2018).

The membrane microstructure has been modelled in three different ways to assess the properties of ion exchange membranes and how ions transport through them.

- First, membranes have been modelled as homogeneous solutions, where ions transport as per the classical Donnan effect describe above.
- Second, membranes have been modelled taking into account the complex inconsistency on the sub-microscopic scale, taking into account the classical cluster network model of Nafion® (Luo et al., 2018).
- The third model is based on the microphase scale, representing the membrane as a gel and interstitial phases. The gel phase being made up of hydrophilic ion exchange groups that are fixed on polymer chains. The interstitial phase are voids in the membrane that are filled with electroneutral solution when the membranes are hydrated with salt solutions and is responsible for the transport of co-ions through ion exchange membranes. The size of the voids, which are affected by membrane hydration and swelling, impact on the depth of diffusion of electroneutral solution into the membrane (Sata, 2007c, Kreue, 2013).

In processes such as the chlor-alkali and table salt production, the hydration, swelling and void characteristics of an IEM change with process conditions (temperature, flow and electro-potential gradient) and solution conditions (ionic type, concentration, and gradient across membrane) (Ran et al., 2017). Referring to Table 2.6 above, the temperature, concentration and composition of Kraft Green liquor will differ from plant-to-plant, which will impact on membrane permselectivity properties and should be investigated. In Kraft recausticization process, the temperature of the Green Liquor is maintained above 85°C, to affect efficient CaCO₃ settling. This is a limitation of the recausticization process and does not imply an IEM process cannot receive the liquor at lower or higher temperature.

2.2.3 Permselectivity - IEM Transport Mechanisms

The four possible mechanisms for the transport of ions through in the membrane phase are diffusion, electro migration, convection and surface hopping (Luo et al., 2018). These mechanisms occur simultaneously and are complex.

There are three basic concepts that explain membrane ion transport phenomena: the Nernst-Planck flux equation, the theory of absolute reaction rate processes and the principle of irreversible thermodynamics (Sata, 2007b). Here the Nernst-Planck flux equation has been

chosen to describe the transport mechanism as it is proven generally applicable at defining ion transport through IEM, serves as the basis of quantitative treatment (Luo et al., 2018) and is simplest to describe.

The Nernst-Planck equation (Sata, 2007b) defines the ionic flux, J_i , as:

1. The sum of the convective transport of ions imposed by electro osmotic solvent (water) transfer (vC_i);
2. The Ion diffusion due to the concentration gradient $\left(D_i \frac{dC_i}{dx}\right)$.
3. The ion electro migration because of the electric potential gradient $\left(\frac{z_i F C_i D_i}{RT} \frac{d\varphi}{dx}\right)$.

Giving,

$$J_i = vC_i - D_i \frac{dC_i}{dx} - \frac{z_i F C_i D_i}{RT} \frac{d\varphi}{dx} \quad (2.54)$$

Where v is the convective velocity of the solvent (water), C_i , D_i and z_i are the concentration, diffusion coefficient, and valence of ion i , and x is the distance across the membrane.

Regarding the first two terms, the osmotic equilibrium is characterised by the equality of the hydrostatic chemical potential of diffusible water. The ion diffusion equilibrium is characterised by electro-potential equilibrium of diffusible ions (Pyun, 2021).

Of the three terms described by the Nernst-Planck equation, the electro potential gradient across the membrane is by far the most significant factor by a size of one to three magnitudes (Luo et al., 2018). It is most important in the context of the chlor-alkali process, production of table salt and in the context of Kraft Green Liquor regeneration if a CEM is employed for the selective recovery of sodium ions or AEM for sulphide ions.

Ions transported through IEMs as the result of electric gradient are carrying electrical current as per Faraday's law (Sata, 2007a).

$$i = \frac{I}{A} = F \sum_i^n |z_i| J_i \quad (2.55)$$

Where i is the current density, I is the current, and A is the effective membrane surface area for ion transport.

2.2.4 IEM Permselectivity and the Influence of Boundary Layers in IEM Systems

In the presence of water, the fixed ionic groups on the membrane are ionized and surrounded by a water molecule forming a hydration shell, as are mobile ions in solution. Interactions between counter-ions and fixed ionic groups on the membrane are influenced by both the coulombic force and the hydration effect of the ions (Luo et al., 2018). For traditional IEMs, the permselectivity of specific ions through an anion exchange membrane is governed by the balance of hydration energy of anions with hydrophilicity of the membranes, partially by the hydrated ionic size of the anions (Sato, 2000). Multivalent ions will in effect have high ion solubility, but lower mobility in common IEMs because of the larger hydration shell formed around the molecule creating more drag through solution.

In electrodialysis desalination, the boundary layer near the ion-exchange membrane is the limiting region for the overall rate of ionic separation due to concentration polarisation in that layer (Kim et al., 2012). The system operating conditions of current density and fluid dynamics influence the concentration polarisation in boundary layers (Nikonenko et al., 2010a). Under high current conditions, a sharp concentration gradient, creating substantial ionic diffusion, can drive targeted separation ratio for certain ions depending on their concentration and mobility in the solution (Kim et al., 2012).

In desalination electrolysis, an electrical potential across the membrane drives the current of ions across the cell, a low ion concentration boundary layer is developed on the side of the membrane that is being desalinated or depleted of ions (Nikonenko et al., 2010b). As the current density increases, the boundary layer concentration at the membrane decreases until the point at which the electrolyte concentration at the membrane-solution interface becomes zero, which is the limiting current density of the system. In most desalination systems, the limiting current density is not normally reached. When the current limit is approached in IEM desalination systems, complex phenomena including water splitting, membrane discharge and electro-convection occur (Nikonenko et al., 2010b), which complicate ion permselectivity and will be the case with an IEM process for Kraft Green liquor recovery at the limiting current density.

2.2.5 IEM Leakage and Current Efficiency in an IEM System

In a desalting cell, an ionic electrolyte solution is supplied to partitions comprised of AEMs and CEMs and an electrical current is passed through it, and ions and solutions pass through the membranes. In an electrolysis membrane cell, for example the chlor-alkali cell, an ionic anolyte (NaCl) is supplied to an anode partition and catholyte (Water + NaOH) is supplied to a cathode partition, with both partitions separated by a CEM.

In a large-scale IEM processes, not all parts of a unit are always consistent with values in the specifications (Tanaka, 2004). Pinholes can open in relatively low strength IEMs. Gaps may occur between the materials of the IEM process assembly. In the design of a lab IEM system, the design and scale will be such that the mechanical stresses on the IEM will be minimal and chances of pinholes or gaps in materials are small. Membrane integrity can be verified by method of standardised integrity test, using known ionic solutions with standard operation set points and verifying the consistency of performance of the membrane.

Another source of IEM leakage is when a pressure difference may occur between the desalting cell and concentrating cell in the case of electrodialysis or the anode and cathode in the case of an electrolysis membrane cell. This phenomenon will lower the performance of the IEM cell (Tanaka, 2004).

2.2.6 Summary of IEM Permselectivity Considerations in Context of Green Liquor

The permselectivity of IEMs are affected by the individual characteristics of the membrane and the conditions of the system in which they operate. These system conditions include the temperature, concentration, composition, and flowrates of solutions (Green Liquor) fed to the membrane cell. If applied, an electrical potential driving ion transport will change the boundary conditions either side of a membrane, also changing the permselectivity the IEM. Table 2.13 below summarises the IEM system conditions and the possible effect permselectivity. It is a research objective to evaluate the effect these system conditions have on the performance of an IEM Green Liquor recovery process.

Table 2.13: IEM System Conditions and Possible Impacts on Permselectivity

System Conditions	Influence to be Tested on Ion Permselectivity
Temperature Increasing	<p>As temperature increases</p> <ul style="list-style-type: none"> • Increased mobility/solubility of some ionic species • Increased overall ionic flux across membranes • Increased mobility/solubility of some ionic species decreases resistance to transport through solution • Decreasing resistance to transport decreases membrane transport energy requirement in case of ED or EMC • Decreased resistance to membrane transport may decrease membrane permselectivity (current leakage)
Green Liquor Feed Concentration Increasing	<p>Increasing Kraft Green liquor feed strength</p> <ul style="list-style-type: none"> • Increased Na⁺ concentration across CEM • Improved boundary conditions and permselectivity • Improved ionic flux across membranes and current efficiency (positive concentration gradient). Decreases electrical potential required to transport targeted flux • Decreased cell resistance due to increased ionic concentration of the cell.
Green Liquor Flowrate Increasing	<p>Increased Kraft Green Liquor feed flow</p> <ul style="list-style-type: none"> • Increased supply of Na⁺ across CEM • Improved turbulence in cell and ionic transport • Improved boundary conditions and permselectivity • Improved ionic flux across membranes and current efficiency (positive concentration gradient). Decreases electrical potential required to transport targeted flux • Decreased cell resistance due to increased ionic concentration of the cell.
Concentration of target ion Na ⁺ (NaOH) on opposite side of CEM	<p>Increased NaOH concentration on opposite side of CEM</p> <ul style="list-style-type: none"> • Decreased cell resistance due to increased ionic concentration of the cell • Negative Na⁺ concentration gradient across CEM increases cell voltage requirement to transport targeted flux • Deteriorated boundary conditions and permselectivity • Overall energy requirement to achieve targeted flux may increase or decrease depending on selectivity of CEM and potential for “current leakage”.

2.2.7 Other System Permselectivity Considerations – Ionic Radii and Cell Mobility

Ion transport through IEMs is governed by both the ion concentration and ion mobility in the membranes (Luo et al., 2018). Ion mobility is correlated to the valence and size of the ions. Ions with a higher valence, or larger ionic radius when the valence is the same, are preferentially exchanged into IEMs (Sata, 2007a). The ionic mobility in the membrane matrix depends on the radii (r) of the ions as well as their interaction with the fixed ionic groups, the Stokes ionic radii is the most widely adopted measure of reported hydrated ionic radii (Luo et al., 2018).

Stokes radius factors include not only size but solvent effects (Sata, 2007a) where a smaller ion with stronger hydration may have a greater radius than a larger ion with weaker hydration. This is because the smaller ion drags a greater number of water molecules with it as it moves through the solution. The mobility of a monovalent anion at infinite dilution, is inversely proportional to the ionic radius, in an aqueous solution (Luo et al., 2018). Divalent anions also have high mobility due to stronger coulombic force, even though they possess larger Stokes radii.

Table 2.14 and 2.15 below list the characteristics and properties for common cations and anions, those present in Kraft green liquor, such as the equilibrium of Na_2S with NaOH :



Table 2.14: Cation Mobility in Aqueous Solutions: Diffusion Coefficient, D , Stokes Radius, r (Haynes, 2014-2015), (Luo et al., 2018)

Present in Green Liquor	Cation	Radius, r (nm)	Width of hydration shell, Δr (nm)	Number of water molecules in this shell, n	Calculated Gibbs energy of hydration, ΔG	Experimental Gibbs energy of hydration, ΔG	Diffusion coefficient, D , of the ion in dilute aqueous solution ($10^{-5} \text{ cm}^2 \text{ s}^{-1}$)
Yes	H^+	0.28	(0.28)		-1050		9.31
Yes	Na^+	0.102	0.116	3.5	-385	-365	1.33
Yes/Trace	K^+	0.138	0.074	2.6	-305	-295	1.96
Trace	Mg^{2+}	0.072	0.227	10	-1940	-1830	0.705
Trace	Mn^{2+}	0.083	0.203	8.7	-1740	-1760	0.712
Trace	Ca^{2+}	0.1	0.171	7.2	-1515	-1505	0.793
Trace	Al^{3+}	0.053	0.324	20.4	-5450	-4525	0.559
Trace	Fe^{3+}	0.065	0.288	16.6	-4580	-4265	0.604

Table 2.15: Anion Mobility in Aqueous Solutions: Diffusion Coefficient, D, Stokes Radius, r (Haynes, 2014-2015), (Luo et al., 2018)

Present in Green Liquor	Anion	Radius, r (nm)	Width of hydration shell, Δr (nm)	Number of water molecules in this shell, n	Calculated Gibbs energy of hydration, ΔG	Experimental Gibbs energy of hydration, ΔG	Diffusion coefficient, D, of the ion in dilute aqueous solution ($10^{-5} \text{ cm}^2 \text{ s}^{-1}$)
Yes	OH ⁻	0.133	0.079	2.7	-380	-430	5.27
Yes	SH ⁻	0.207	0.031	1.7	-285	-295	1.731
Yes	CO ₃ ²⁻	0.178	0.076	4	-1195	-1315	0.96
Yes	S ²⁻	0.184	0.07	3.9	-1171	-1315	1.731
Yes	SO ₃ ²⁻	0.2	0.059	3.6	-1112	-1295	1.132
Yes	SO ₄ ²⁻	0.23	0.043	3.1	-1010	-1080	1.07

Table 2.14 above indicates that, in a Kraft Green liquor IEM system, Na⁺ and K⁺ will have higher diffusion coefficients and an advantage in ionic mobility in aqueous solution over trace elements Mg²⁺ and Ca²⁺. Table 2.15 indicates that desired OH⁻, SH⁻ and S²⁻ ions have a higher diffusion coefficient than CO₃²⁻, SO₃²⁻ and SO₄²⁻.

The differences in ionic mobility may be a mechanism for the selective separation of the desired ions from the “deadloads” using an IEM process such as electrodialysis or diffusion dialysis. If a concentrated stream of Na₂CO₃ may be isolated, it could then be effectively electrolysed in an IEM cell, to produce the desired NaOH and purge the CO₃²⁻ deadload as CO_{2(g)}.

2.2.8 Membrane Selection – Fouling, Scaling and Alkali Resistance

Kraft Green liquor with a high pH and temperature in the range of 80°C and 95° represents a potentially challenging fluid for some membranes. The clarified green liquor does not contain significant concentrations of organic matter because of the reboiler, however the high concentrations of dissolve solids introduce scaling potential that needs to be considered and managed in an IEM system design.

In conventional Green liquor recausticization systems, pirssonite, (Na₂CO₃·CaCO₃·2H₂O) is most commonly a cause of hard-scale build up in green liquor handling systems (Tran and Papangelakis, July 2013). This precipitation occurs when the concentration of sodium carbonate in the liquor exceeds the solubility of pirssonite. In the absence of CaCO₃, which will be the case with EDM, pirssonite scale may not be an issue, however high feed concentration may identify other scaling issues for membranes.

Membranes selected in a Green liquor alkali recovery system will need to have excellent thermal and mechanical properties, and good chemical resistance. Poly vinylidene difluoride (PVDF) is a membrane material with excellent thermal and mechanical properties and good chemical resistance, and is widely used for hollow fibre membranes, ion exchange membranes and ultrafiltration membranes (Liu et al., 2014). However, the hydrophobic nature of PVDF is a hindrance to alkali recovery, making it inefficient for spontaneous IEM alkali recovery processes like diffusion dialysis (Ye et al., 2015). To improve their hydrophilic properties, PVDF membranes have been blended with hydrophilic polymers, including poly sodium p-styrene sulfonate (PSSS), however more miscibility of blending components usually results in loss of hydrophilic components during diffusion dialysis (DD) process operation (Liu et al., 2014). An electro potential across the IEM cell can overcome this hydrophobic nature to effectively recover alkali, however this is still a resistance affecting system efficiency.

Membrane performance has been examined in the context of black liquor concentration, before multi-effect distillation, which possibly presents an even more challenging fluid than Green Liquor due to the presence of high concentration organics (Kevlich et al., 2017). Recently polyethersulfone (PES) membranes have been prominent in research into Black Liquor concentration because of their higher stability and rejection of organics and even inorganics (Kevlich et al., 2017). A general problem with many polymeric membranes for Black liquor treatment has been their short lifetime of generally less than 1.5 years, and a requirement for frequent cleaning, requiring significant capital and maintenance (Liua et al., 2004).

Green liquor will not impose the same organic load as Black liquor, which should translate to less frequent cleaning and greater membrane life. Also, whilst Green Liquor is kept above 80°C for the benefit of lime mud settling in the recausticization process, this is no longer necessary for the IEM process. Reducing Green liquor temperature may decrease stress on the IEM. This would, however, come at the expense of ionic mobility leading to increased system resistance.

2.3 IEM Systems – Evaluation in the Context of Kraft Green Liquor

IEMs are integrated into systems including diffusion dialysis (DD), electrodialysis (ED), electrodialysis reversal (EDR), substitutional electrodialysis-metathesis (EDM) and membrane electrolysis (ME). These systems have design and control parameters that can be manipulated to target the recovery and generation of targeted salts. The design and control parameters include membrane selection, arrangement, stream compositions, concentrations and temperatures, flowrate, and cell electric potential.

DD, ED, EDR, EDM and ME are evaluated in the context of their potential to regenerate Kraft Green liquor, which primarily requires conversion on Na_2CO_3 to NaOH . Retention of Na_2S and removal of deadload salts (Na_2CO_3 , Na_2SO_3 , Na_2SO_4 , $\text{Na}_2\text{S}_2\text{O}_3$) is highly desirable.

2.3.1 IEM Processes – Diffusion Dialysis

Diffusion dialysis (DD) is an IEM separation process driven by concentration gradient across the membrane and is used for the separation and recovery of primarily acid, but also alkali waste solutions and is a developed industrial process (Luo et al., 2011). As separation is driven primarily by concentration gradient, it is known as a spontaneous separation process, as it gives rise to an increase in entropy and decrease in Gibbs free energy, so it is thermodynamically favourable. DD IEM process is characterised by a low power requirement, low installation and operating cost (Xu, 2005).

DD has been successfully applied for recovery of acids and alkalis from the discharges of steel production, metal-refining, electroplating, cation exchange resin regeneration, non-ferrous metal smelting, aluminium etching, and tungsten ore smelting. The limitation of DD is its relatively low processing capability of waste acid and product concentration is limited by the equilibrium as ion transport as it is driven by concentration gradient only (Luo et al., 2011).

Application – Weak and Strong Acid Recovery

The application of acid recovery using DD centres around an AEM, where a feed solution of acid (for example HCl) contaminated with metal salts, is fed into a DD cell on one side of the membrane and pure water is fed on the other. The acid and its metal salts in the feed solution are attracted to the water side of the membrane due to concentration difference. The

presence of the AEM, the anion (e.g., Cl^- , SO_4^{2-} , CO_3^- , etc) are permitted passage, while the metal ions in the waste solution are much less likely to pass (Luo et al., 2011).

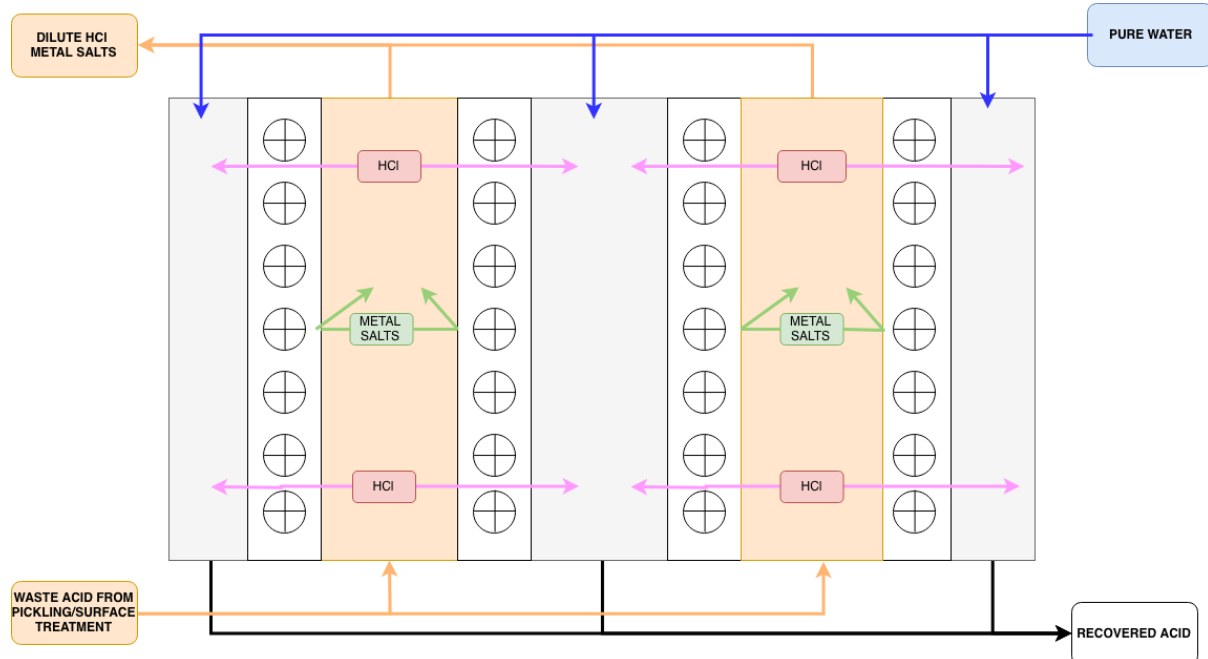


Figure 2.6: Principle of HCl recovery using Diffusion Dialysis

(Luo et al., 2013)

The H^+ ions in solution, although positively charged, are smaller in size compared to metal cations in solution and have low valence and high mobility that allows them to diffuse along with the Cl^- ions (Wang et al., 2013). This transport of H^+ ions is fundamental to acid recovery systems using DD. The properties of an ideal AEM include stability in acidic solution, high H^+ permeability, strong rejection of other metal ions, high water uptake but low water permeability (Wei et al., 2010).

Application – Alkali Recovery

The application of alkali recovery using DD centres around a CEM where a feed solution of alkali, for example NaOH contaminated with tungsten as Na_2WO_4 , is fed into the DD on one side of the membrane and pure water on the other (Luo et al., 2011). The NaOH and tungsten salts in the feed solution are attracted to the water side of the membrane due to concentration gradient. The presence of the CEM allows Na^+ passage through the membrane, while WO_4^{2-} is restricted. Like H^+ in the acid context, OH^- ions, whilst restricted, do have a

competitive transport advantage over WO_4^{2-} so diffuse with the Na^+ ions to meet the requirement of electrical neutrality.

The transport of OH^- ions is central to the alkali recovery by DD process. The relative slow transport of OH^- compared to H^+ ions in aqueous solutions, and hydrophobic nature of standard CEMs, generally makes alkali recovery DD comparatively less efficient to acid recovery DD. ED processes are more practical for alkali recovery (Yan et al., 2014). CEM membranes for alkali recovery systems need to have high OH^- permeability, strong rejection of other anions, relatively high-water uptake but low water permeability, whilst having strong alkali resistance (Wei et al., 2010).

Diffusion Dialysis Application Evaluation – Kraft Green Liquor Recovery

If DD were to be utilized, it could incorporate a CEM as per the tungsten contaminated NaOH example above. Green Liquor would be fed to the DD on one side of the CEM and pure water on the other. The Green Liquor salts would be attracted to the water side of the membrane due to concentration gradient. The presence of the CEM would promote the passage of Na^+ through the membrane. To meet the requirement of electrical neutrality, some anions will also pass through the membrane, those with a competitive transport advantage will diffuse in greater concentration. Referring to Table 2.15 above, OH^- has the highest diffusion coefficient followed by S^{2-} and SH^- , whilst CO_3^{2-} has the lowest. The product stream would then be expected to contain some of the NaOH and Na_2S from the green liquor but the Na_2CO_3 deadload would be expected to remain the green liquor (see Figure 2.7). There is no mechanism for conversion of Na_2CO_3 to NaOH so DD itself cannot regenerate Kraft Green Liquor.

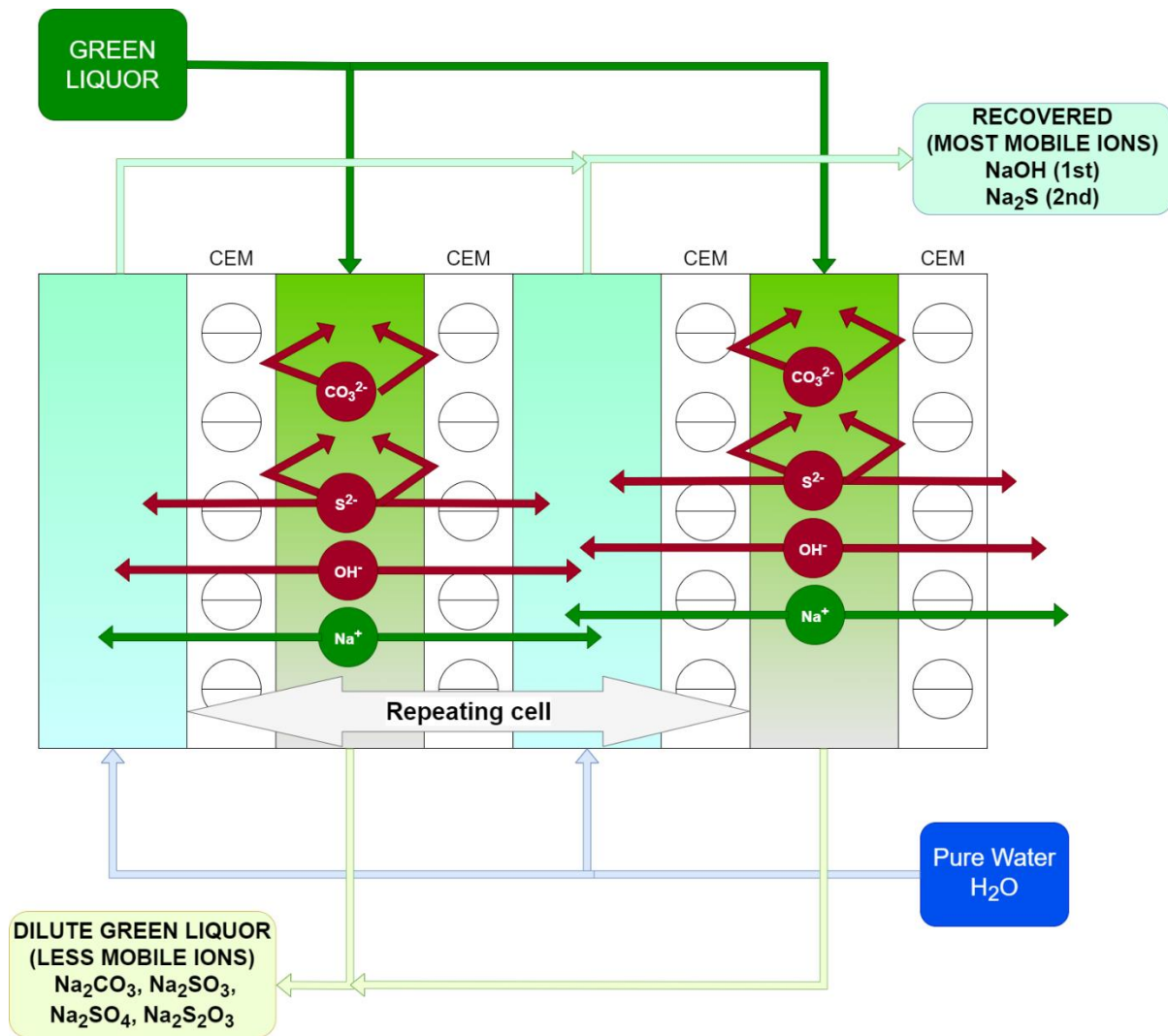


Figure 2.7: Hypothetical recovery of Green Liquor feed using counter current CEM DD system. OH⁻ and S²⁻ ions more mobile than competing CO₃²⁻.

2.3.2 IEM Process – Electrodialysis

Electrodialysis (ED) is an IEM separation process with the additional driving force of DC electrical potential difference existing between a positively charged anode and a negatively charged cathode (Phillip Murray, 1995). As per Figure 2.8 below, the electrodialysis IEM stack contains repeating cell pairs of a concentrate compartment and a diluate compartment, and two membranes - a cation selective membrane and an anion selective membrane. An electrodialysis cell stack can contain hundreds of repeating cell pairs between a cathode and anode (Ran et al., 2017).

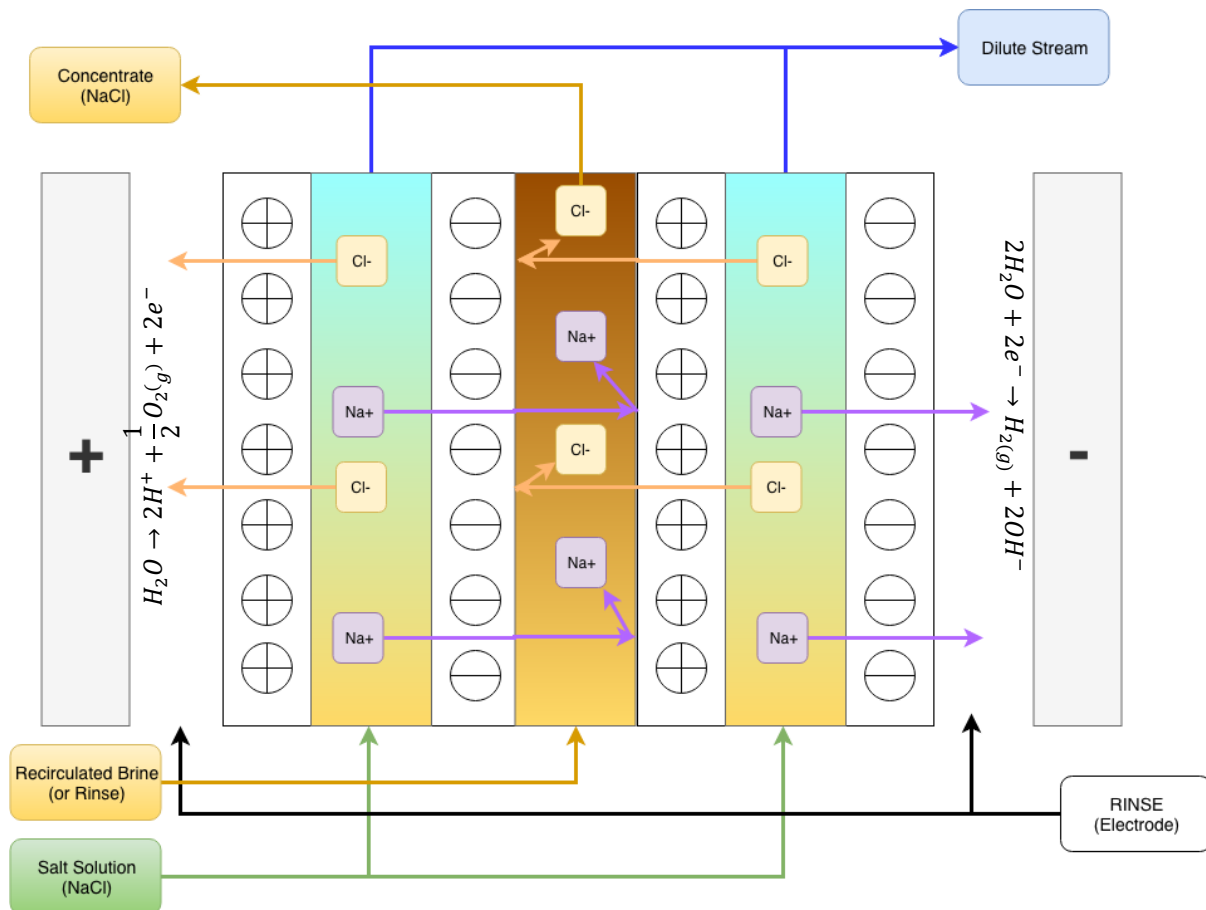
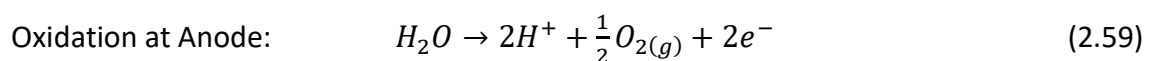
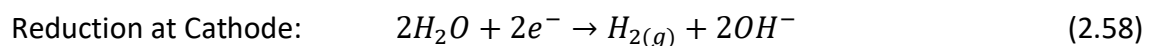


Figure 2.8: Example of Conventional Repeating IEM Stack for Desalination
(Ran et al., 2017)

A H_2O rinse is fed to anode and the cathode of the ED the following half reactions occur:



To preserve electrical neutrality, as the $NaCl$ saline feed is passed through the diluate compartment, cations are transported through negatively charged CEM attracted towards the cathode, where they are held by the repulsion of the next positively charged AEM. Anions are simultaneously transported in the opposite direction through an AEM towards the anode, where they are held by the repulsion of the next CEM. The feed is effectively demineralised, whilst the removed salts are removed in a sweeping concentrate stream (Ran et al., 2017).

Like reverse osmosis, the desalination capacity of an electro dialysis system is limited by the solubility of salts concentrated in the reject or concentrate stream, or scaling potential. In an ED system, as the electric potential increases the ion concentration at the boundary layer on

the depleted side of the membrane decreases until a limiting current density of the desalination system is approached.

Electrodialysis Application Evaluation – Kraft Green Liquor Recovery

Like conventional desalination systems, ED could be used to drive the separation of anions and cations from Green Liquor, if CO_3^{2-} ions are the slowest through solution (see Table 2.15) it may be a mechanism to separate the Na_2CO_3 deadload by removal of the more mobile other ions. This is depicted in Figure 2.9 below. The net effect of this arrangement would be removal of the Na_2CO_3 deadload, albeit with the production of a more dilute green liquor stream (Stream B) with all the other deadload salts. Stream A would be a Na_2CO_3 rich depleted green liquor. There is no mechanism for conversion of Na_2CO_3 to NaOH so ED itself cannot regenerate Kraft Green Liquor.

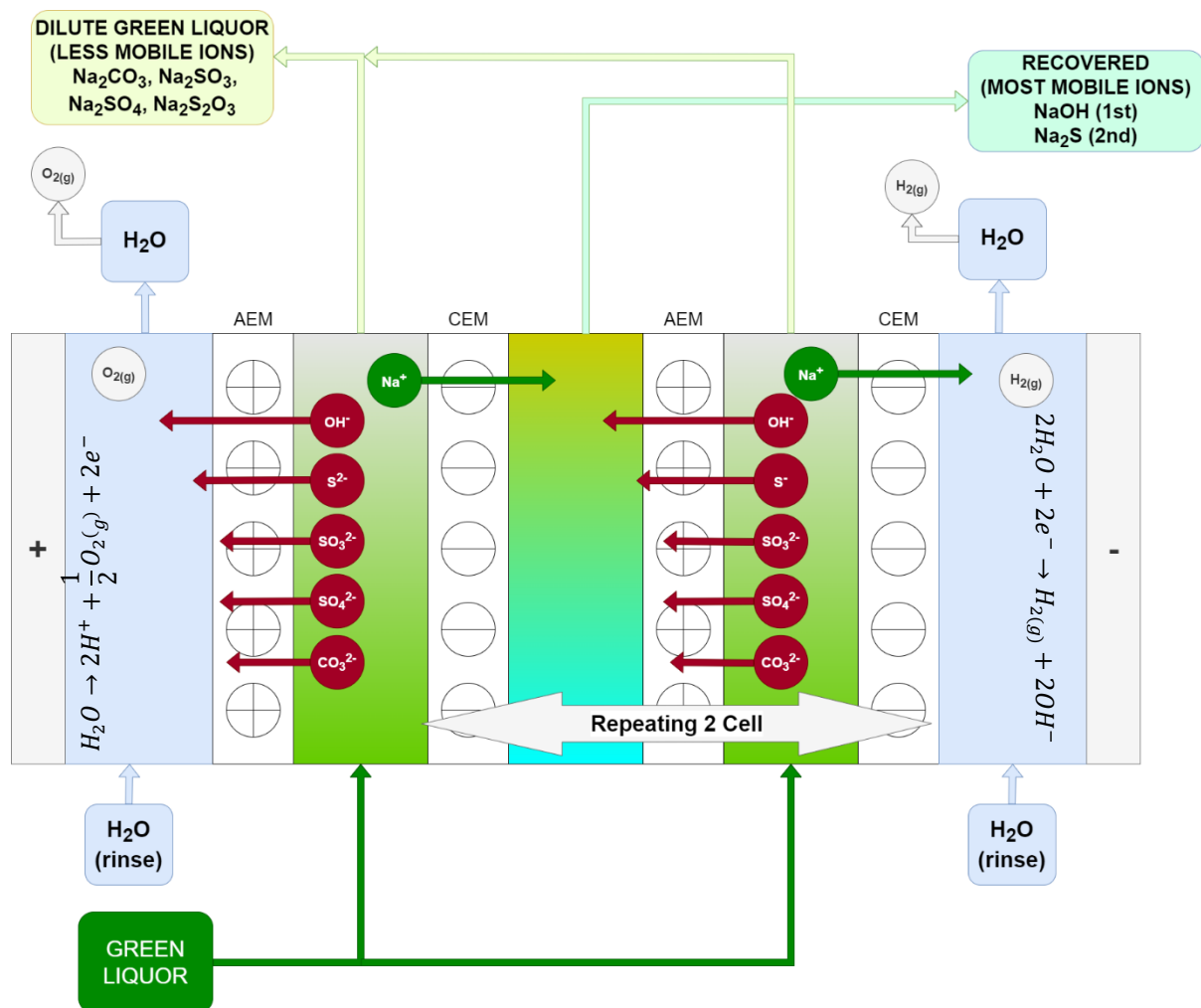


Figure 2.9: Electrodesalination of Green Liquor leaving least mobile ions Na_2CO_3

2.3.3 Electrodialysis Reversal (EDR)

EDR is an extension to ED, involving the reversal of the electrical charge to a membrane after designed periods of time (2 – 4 hours). The polarity reversal helps prevent the formation of scale on the membranes (Phillip Murray, 1995).

Figure 2.10 shows how in an EDR system the feed water is separated into three streams, desalinated product water, concentrated brine and electrode feedwater passing over the electrodes creating the electrical potential.

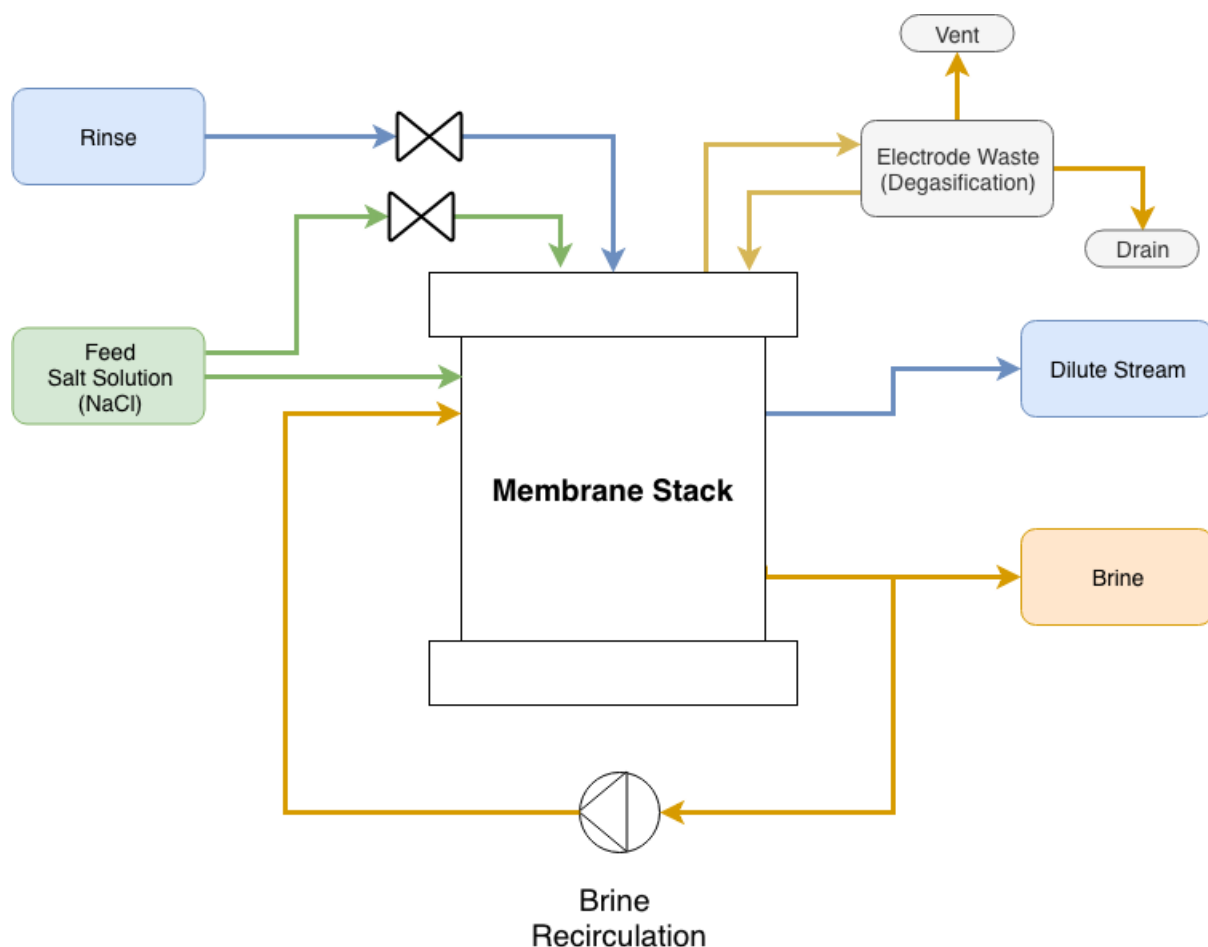


Figure 2.10: Conventional Repeating IEM Stack for Desalination
(Phillip Murray, 1995)

Figure 2.11 below shows how it is like ED, except for the presence of reversal valving.

The reverse of polarity reverses reactions occurring at the electrodes. At the cathode, hydrogen gas is produced with hydroxide ions, which raise the pH of the water, causing calcium carbonate precipitation for example in a desalination process (Ran et al., 2017). At

the anode electrode reactions produce acid, oxygen and some chlorine, and the acid tends to dissolve any calcium carbonate present and inhibit scaling. Valves in the electrode streams automatically switch flows in the two types of compartments, concentrate streams become demineralizing streams and demineralizing streams become concentrate (Phillip Murray, 1995). The EDR current reversal process detaches polarization films on membranes, breaks up freshly formed precipitate scale before they become damaging and reduces organic fouling on membranes. The EDR effectively acid cleans electrodes during anodic operation, decreasing the requirement for clean-in-place chemicals.

Electrodialysis Reversal (EDR) – Application to Kraft Green Liquor

Kraft Green liquor is characterised by its high TDS (up to 150 g/L) and low organic fouling potential by virtue of almost all liquor organics being burned off in the black liquor reboiler. For an ED application, however, the high TDS represents high potential for scaling on the system, so an EDR application has merit for scaling prevention.

For this investigation, scaling potential whilst important, is a secondary interest after whether an IEM ED process has the potential for recovery of Kraft Green liquor.

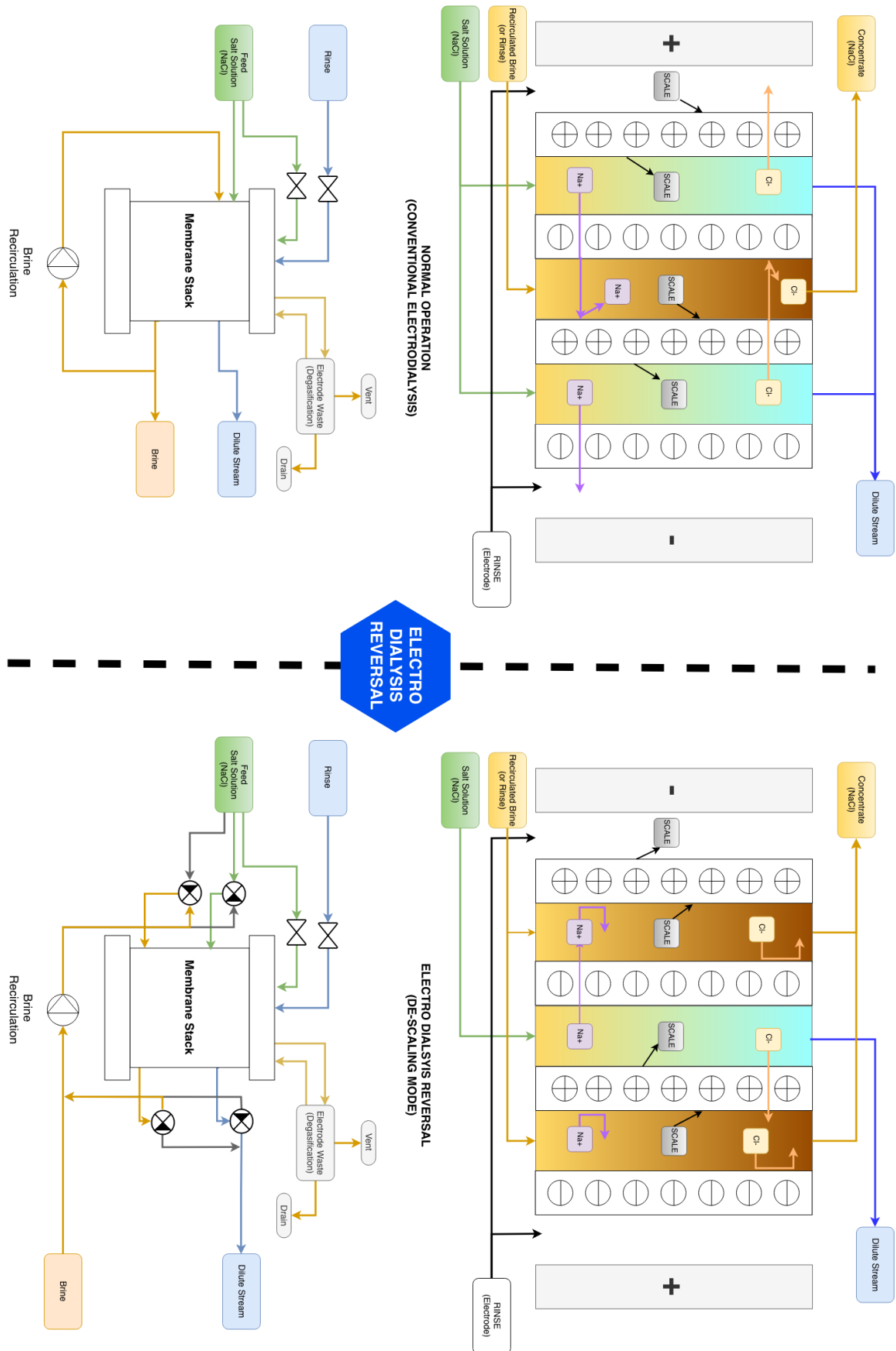


Figure 2.11: EDR Flow Diagram and Schematic (Phillip Murray, 1995)

2.3.4 Substitutional Electrodialysis – Metathesis

An extension to traditional ED is electro dialysis metathesis (EDM) or substitutional electro dialysis. EDM can involve a single substitution, where an acid or alkali can be derived from a corresponding salt form by replacing the counter ions with hydrogen or hydroxide ions (SELEMION(AGC), 2018). EDM can also involve multiple substitutions where a targeted salt, is derived by replacing counter ions with another cation or anion.

In an EDM system, there are four alternating ion-exchange membranes forming a quad of four compartments and the substitution solution is added to provide the exchangeable ions for the metathesis reaction (Camacho et al., 2017). In the reaction, the feed solution, AB, exchanges cations and anions with the substitutional solution CD, to form new product salts AD and CB, as per the reaction:



Metathesis Application – Desalination

Substitutional electro dialysis, EDM, has been used in novel desalination process where the sparingly soluble salts in brackish water are converted into highly soluble solutions (Tom Davis, 2012). In this EDM process, four alternating ion-exchange membranes form a repeating quad of four compartments and a substitutional solution, NaCl, is added to provide the exchangeable ions for the metathesis reaction, shown in Figure 2.12 below.

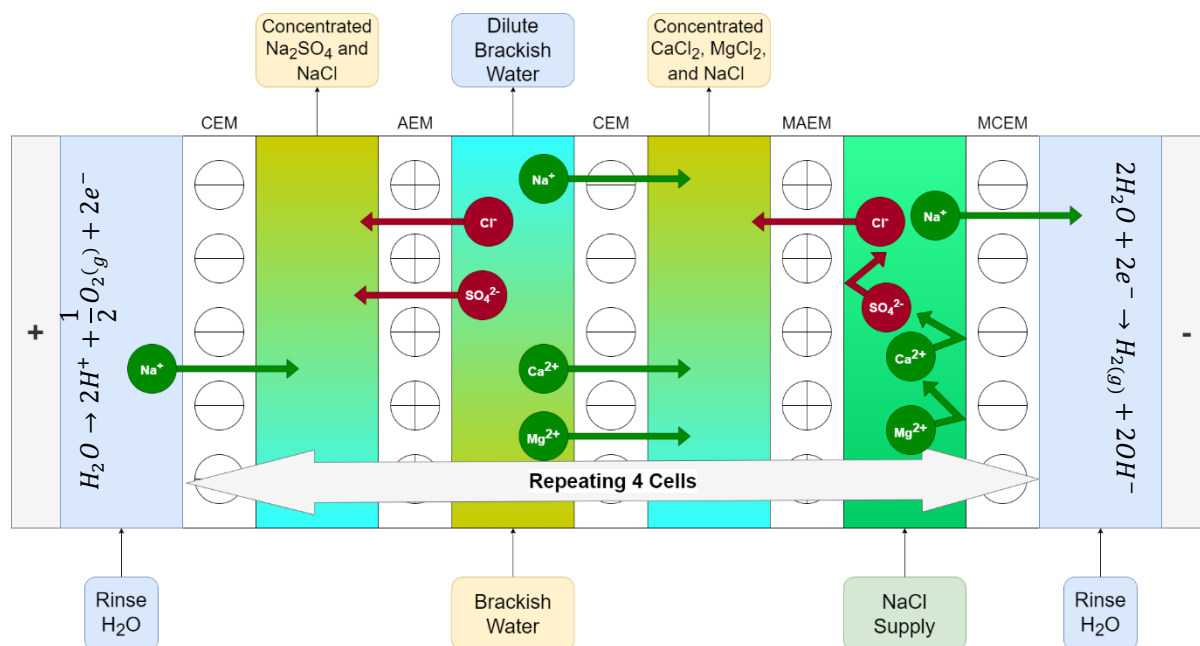


Figure 2.12: Example of Metathesis Desalination Process (Tom Davis, 2012)-
 (AEM – Anion Exchange Membrane, CEM – Cation Exchange Membrane, MAEM – Monovalent Anion Exchange Membrane, MCEM – Monovalent Cation Exchange membrane)

The brackish feed to the EDM, from the reject of reverse osmosis desalination system, is heavy in relatively low solubility calcium sulphate, which is a salt that commonly limits the recovery of reverse osmosis desalination systems. This arrangement causes the ions in the EDM feed to be separated into two highly soluble concentrate streams, one containing mostly chloride with cations and the other mostly sodium with anions (Tom Davis, 2012). Of the concentrate streams, the least soluble salt is sodium bicarbonate, which is over 40 times more soluble than calcium sulphate in the feed, allowing EDM to treat reverse osmosis concentrate streams to recover up to 95 percent of these streams as product water (Tom Davis, 2012).

Metathesis Application – Alkali and Acid Production with Bipolar Membranes

An application of EDM used bipolar membranes (EDBM) technology applied to brines to produce acids and bases with just two inputs: electric energy and brine (Wei et al., 2013). (Herrero-Gonzalez et al., 2020) demonstrated that using a saltwater reverse osmosis brine feed concentrations of HCl and NaOH of up to 3.3 M and 3.6M are obtained respectively. The specific energy consumption of the EDBM unit was in the range of 21.8 kWh/kg to 43.5 kWh/kg of HCl, being dependent on the applied current density of the cell. The substitutional reaction is as follows:

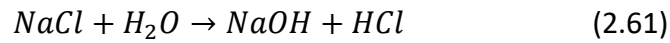


Figure 2.13 below shows an EDBM metathesis arrangement for alkali and acid production, using a NaCl brine feed to produce NaOH and HCl, with H₂O rinse at the anode and the cathode.

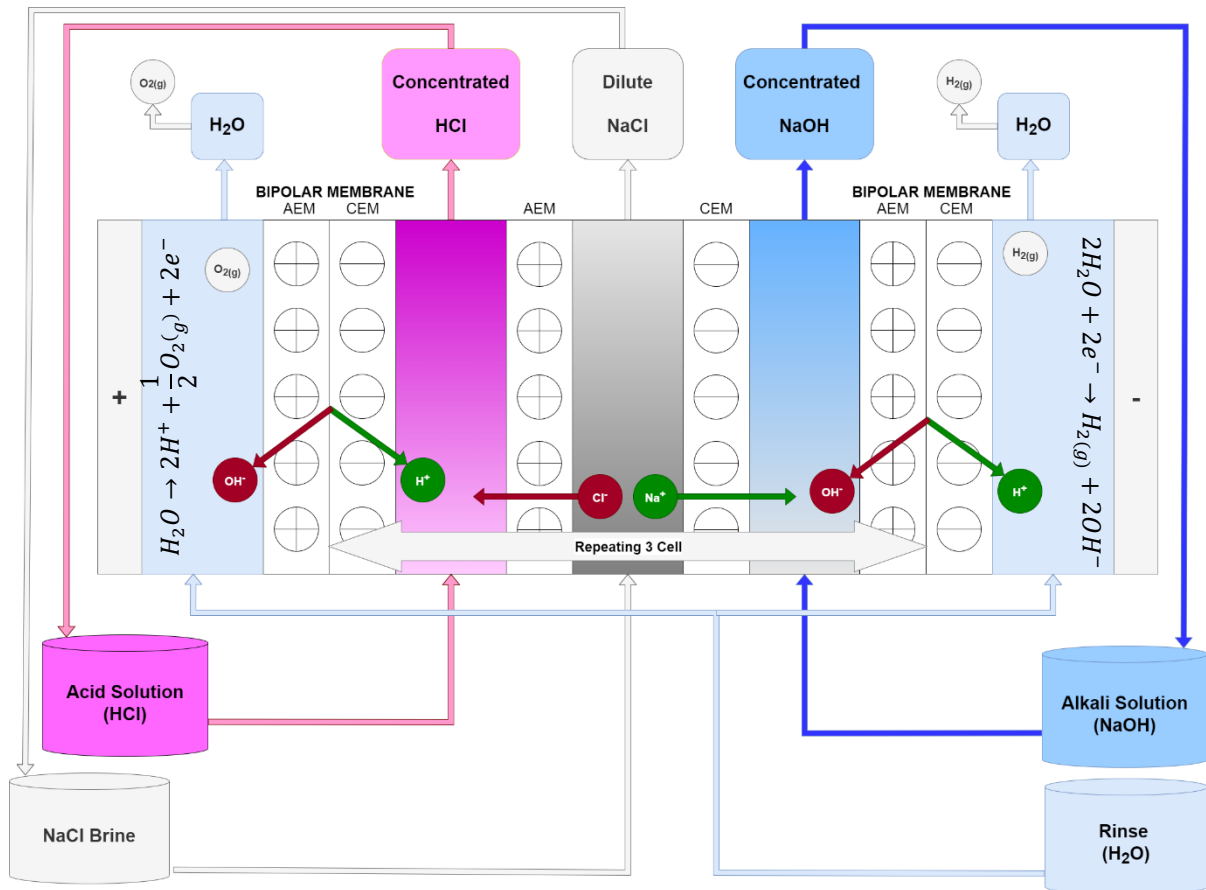
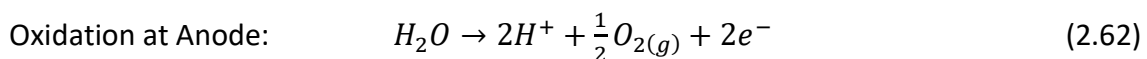
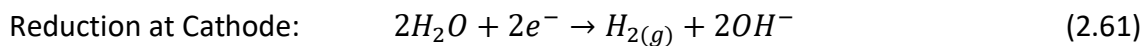
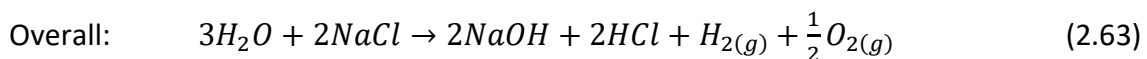


Figure 2.13: Example of NaOH and HCl production using EDM/EDBM (Herrero-Gonzalez et al., 2020).

In the EDBM metathesis single 3-cell arrangement shown in Figure 2.13 the following half reactions occur at the cathode and anode.



As NaCl is fed into the cell, Na⁺ and Cl⁻ move across the membranes to preserve electrical neutrality, producing NaOH and HCl.



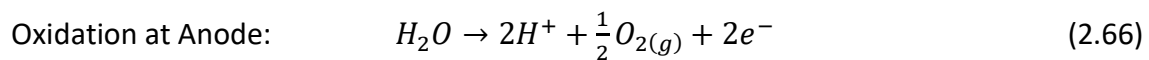
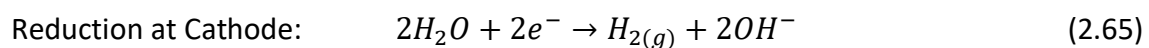
When the above 3 cell is repeated, the ratio of $O_{2(g)}$ and $H_{2(g)}$ production relative to NaOH and HCl reduces, as the reduction and oxidation reactions only occur at the anode and the cathode.

Metathesis Application – Alkali and Acid with Bipolar Membranes – Bauxite Mine

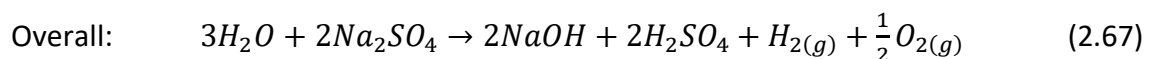
The CSIRO has researched an in-situ remediation process of bauxite residue centred around a three compartment bipolar-membrane electro dialysis system, generating NaOH and H_2SO_4 from an Na_2SO_4 feed from bauxite red mud storage (Kishida et al., 2017). The substitutional reaction is as follows:



The recovered NaOH can be reused in the Bayer process for further digestion of aluminium ore, while the H_2SO_4 is returned to the red mud storage to further neutralise the red mud with the aim of making it easier to manage. Figure 2.14 below illustrates this substitutional reaction:



As Na_2SO_4 is fed into the ED cell, Na^+ and Cl^- move across the membranes to preserve electrical neutrality.



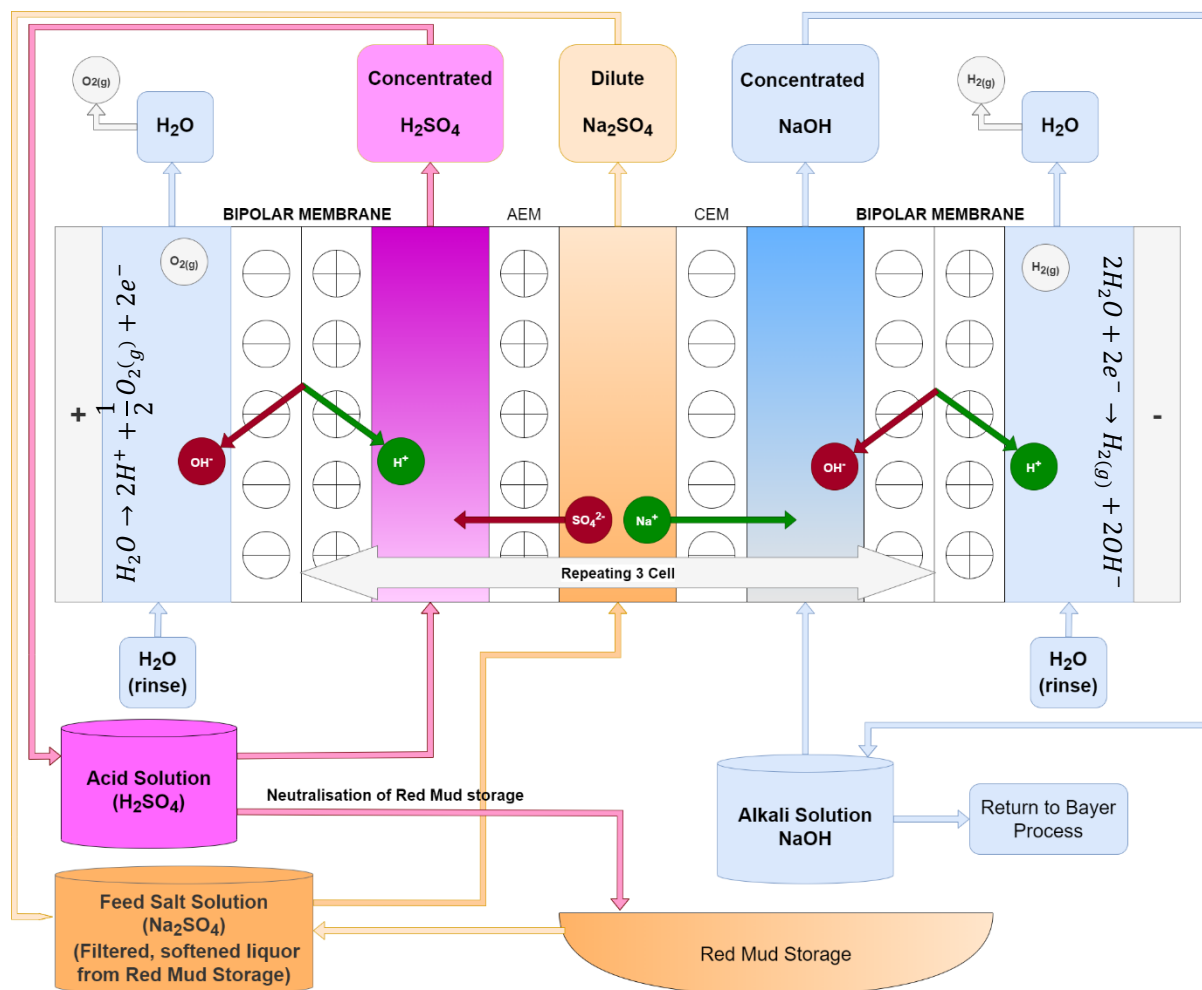


Figure 2.14: CSIRO In-situ remediation of Bauxite Red Mud.
Adapted from (Kishida et al., 2017)

Kraft Green Liquor Recovery with EDM – Possible Experimental Unit Arrangements:

The EDM bipolar membrane arrangements for acid and alkali production shown in figures 2.12 and 2.13 can be adapted for a Kraft Green Liquor feed. (Eswaraswamy et al., 2022), trialled a bipolar membrane EDM system to produce NaOH from a synthetic Green Liquor. Focussing on the production of NaOH only, the system was able to produce NaOH with a current efficiency of 88% and a specific energy of 4.7 kWh/kg (16.9 MJ/kg).

Whilst this arrangement can generate a NaOH product, there is an undesirable impact on Na₂S in the Green Liquor, which is required by the Kraft pulping process. This is illustrated in Figure 2.15 below.

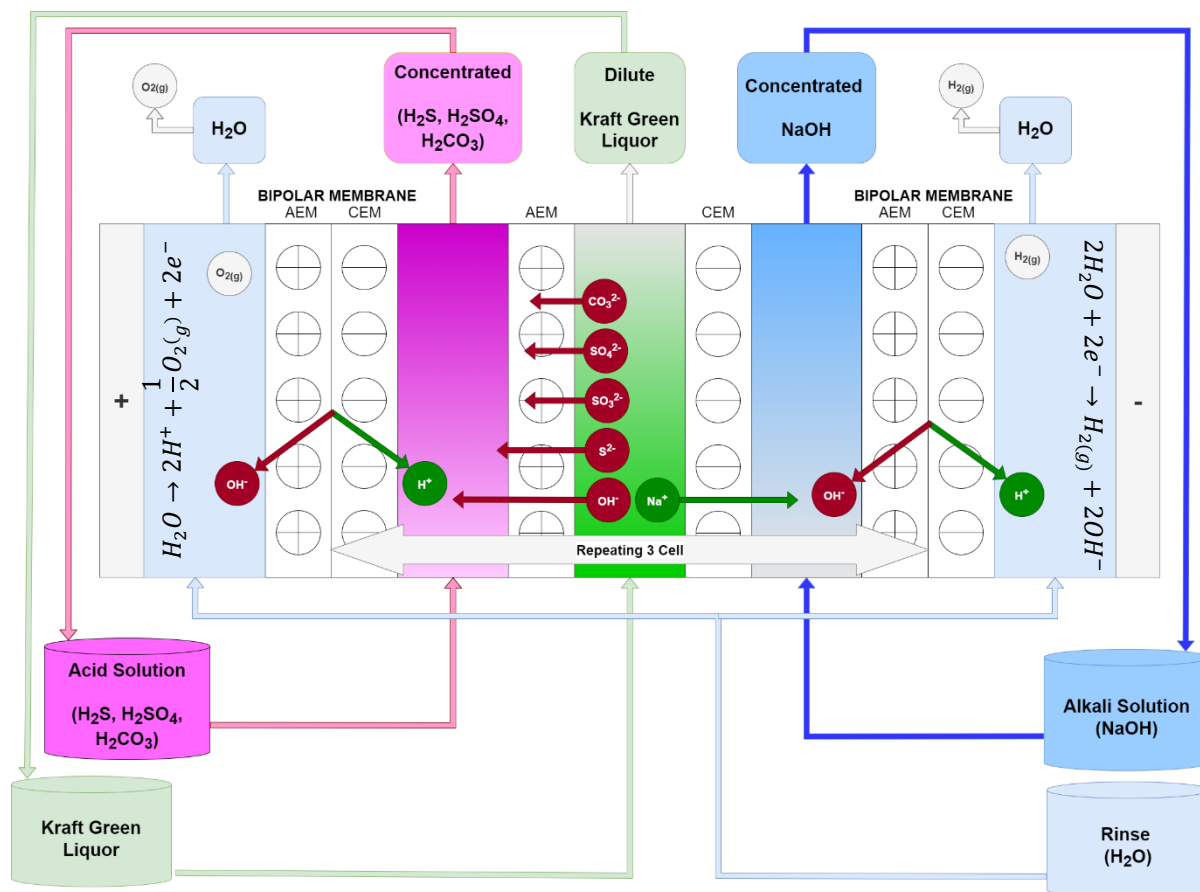
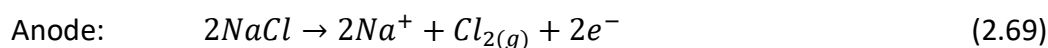
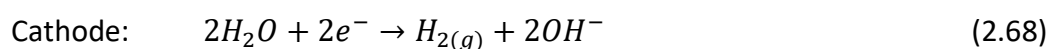


Figure 2.15: Kraft Green Liquor Regeneration with EDM – Acid and Alkali Generation

EDM using bipolar membranes is an established technique for the simultaneous production of alkali and acidic products from a brine feed, which can be used to generate NaOH from a Kraft Green liquor feed. The arrangement will, however, only result in the transfer of all other green liquor constituents, including valuable Na_2S , to an acidic stream that is of little practical use.

2.3.5 Membrane Electrolysis Cell (MEC)

Membrane electrolysis cells are extensively used in the chlor-alkali industry in the production of chlorine and sodium hydroxide. The chlor-alkali process involves the electrolysis of sodium chloride (brine) producing chlorine at the anode and sodium hydroxide at the cathode, via the reaction (O'Brien et al., 2005):



To prevent mixing between the anolyte and catholyte a separator is used through which sodium ions can be transported (O'Brien et al., 2005). The use of ion exchange membranes (IEMs) has revolutionised the Chlor-alkali industry, which has gradually transitioned from mercury-cell production to asbestos diaphragms to polymer IEMs. The motive for this change being concerns over mercury poisoning and pollution, notable occurrences being in Japan (Minamata) and Canada (Matsuyama et al., 2018).

The chloro-alkali membrane electrolysis cell consists of two compartments divided by an IEM as can be seen schematically in Figure 2.16.

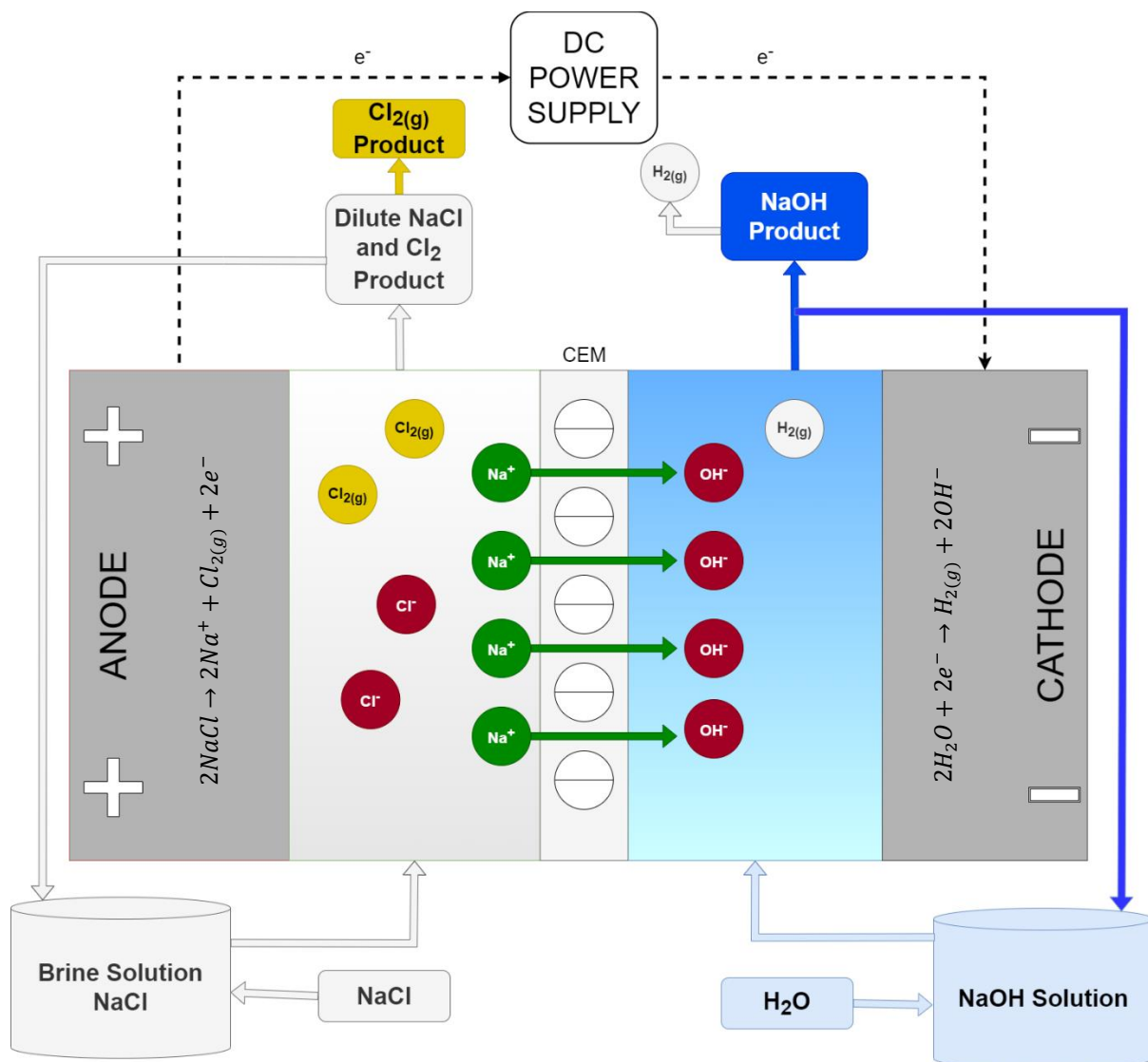


Figure 2.16: Chloro-Alkali Cell Schematic

A saturated NaCl solution is fed to the anode where chloride ions are oxidised to chlorine. The sodium ions migrate through the membrane to the cathode compartment and combine with the hydroxyl ions produced from the water reduction at the cathode (Simon et al., 2014a).

The electrolytic cell needs to be driven by an electric potential, given by the Gibbs free energy ($dG > 0$):

$$\Delta G = -nFE^0 \quad (2.71)$$

Where n is the number of moles transferred, F is the Faraday's constant and E^0 is the standard electrode potential. ΔG is the minimum electrical work that must be supplied to drive the electrochemical reaction. The standard electrode potential values are available in literature and the standard potential for an electrochemical cell can be calculated by combining the potentials of the two half reactions (oxidation and reduction).

The equilibrium electrode potentials ($E_{0,a}$ and $E_{0,c}$) corrected for the electrolytes concentration, temperature and pressure are given by (O'Brien et al., 2005):

$$E_{0,a} = E_a^0 + \left(\frac{dE_a^0}{dT}\right)_T (T - 25) + \frac{1}{2} \left(\frac{d^2E_a^0}{dT^2}\right)_T (T - 25)^2 + \frac{2.303RT}{F} \log \left[\frac{p_{Cl_2}^{1/2}}{[NaCl]} \right] \quad (2.72)$$

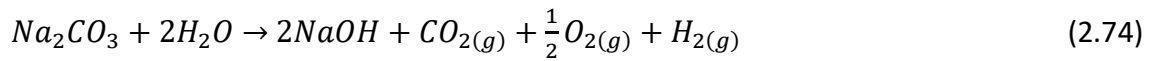
$$E_{0,c} = E_c^0 + \left(\frac{dE_c^0}{dT}\right)_T (T - 25) + \frac{1}{2} \left(\frac{d^2E_c^0}{dT^2}\right)_T (T - 25)^2 + \frac{2.303RT}{F} \log \left[\frac{a_{H_2O}^2}{p_{H_2} a_{OH}^{-2}} \right] \quad (2.73)$$

E_a^0 and E_c^0 are the anode and cathode standard electrode potentials and are a function of cell temperature (T), the partial pressures of chlorine and hydrogen (p_{Cl_2} and p_{H_2}) and the concentration of sodium chloride solution $[NaCl]$. $a_{H_2O}^2$ and a_{OH}^{-2} are the activity of water and hydroxyl ions and R is the ideal gas constant.

The modern-day industrial Thyssenkrupp Uhde "zero-gap" chlor-alkali electrolysis membrane cell produces NaOH at a rate of 2,035 kWh per 1 metric ton (7.3 MJ/kg NaOH) at membrane current density of 6 kA/m². Using a membrane electrolysis cell to investigate the viability of generating NaOH from a coal seam gas brine (Simon et al., 2014a), showed that at the same current density, NaOH is produced at the same rate from NaCl brine and Na₂CO₃ brine feed.

2.3.6 Kraft Green Liquor Recovery with MEC:

(Simon et al., 2014a) showed that an electrolysis membrane cell can produce a pure stream of NaOH from feed streams of Na₂CO₃ and H₂O, whilst producing H₂ and CO₂ gas products also, as per the overall reaction:



A schematic of the membrane electrolysis system used by (Simon et al., 2014a) is shown in Figure 2.17 below.

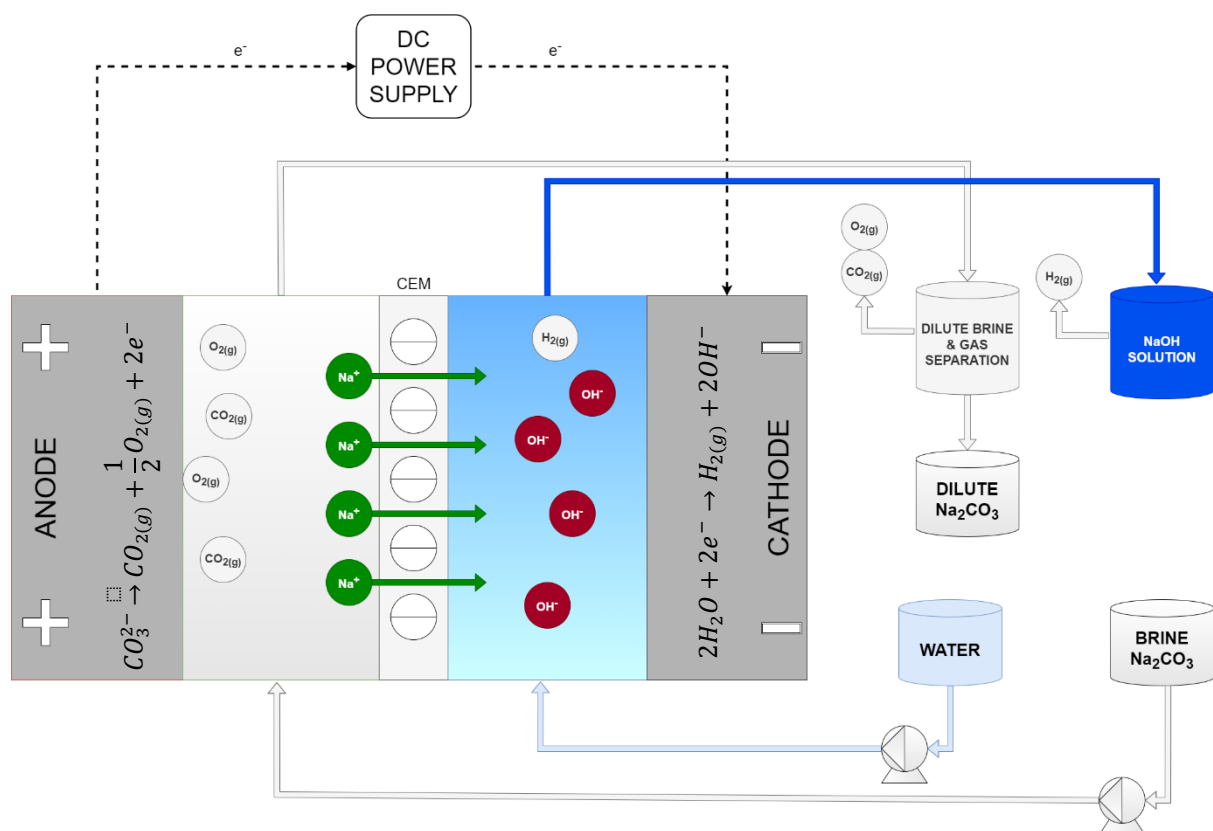


Figure 2.17: Schematic of electrolysis system used by (Simon et al., 2014a)

The MEC arrangement has the advantage that Na₂CO₃ is removed from the feed with the oxidation of carbonate (CO₃²⁻) at the anode with the half reaction:



The other IEM processes of DD, ED, EDR and EDM do not oxidise CO₃²⁻ due to the physical separation of Green Liquor from the electrodes.

A MEC process with a cationic exchange membrane (CEM) was used to convert Na_2CO_3 in Kraft Green Liquor to NaOH by (Goel et al., 2021) and (Mandal et al., 2021). In each study the specific energy of NaOH production (kJ/mol NaOH), CEM current density (A/m^2) and final NaOH concentration produced were defining metrics of the MEC operation. Trialling different CEMs (Goel et al., 2021) at a current density of $600 \text{ A}/\text{m}^2$ produced a NaOH solution of 46.8 g/L (1.17 M), at 372 kJ/mol NaOH. Using synthetic and industrial Kraft Green liquor feed solutions delivered to a MEC at a current density of $600 \text{ A}/\text{m}^2$ (Mandal et al., 2022) produced a NaOH solution of 94 g/L (2.35 M) at 454 kJ/mol NaOH.

A schematic for a membrane cell for the electrolysis of Kraft Green liquor is shown below in Figure 2.18. Once again, the sodium cations migrate through the cation selective membrane toward the negative cathode. The more complex group of anions produced by the electrolysis of the Green Liquor migrate toward the positive electrode.

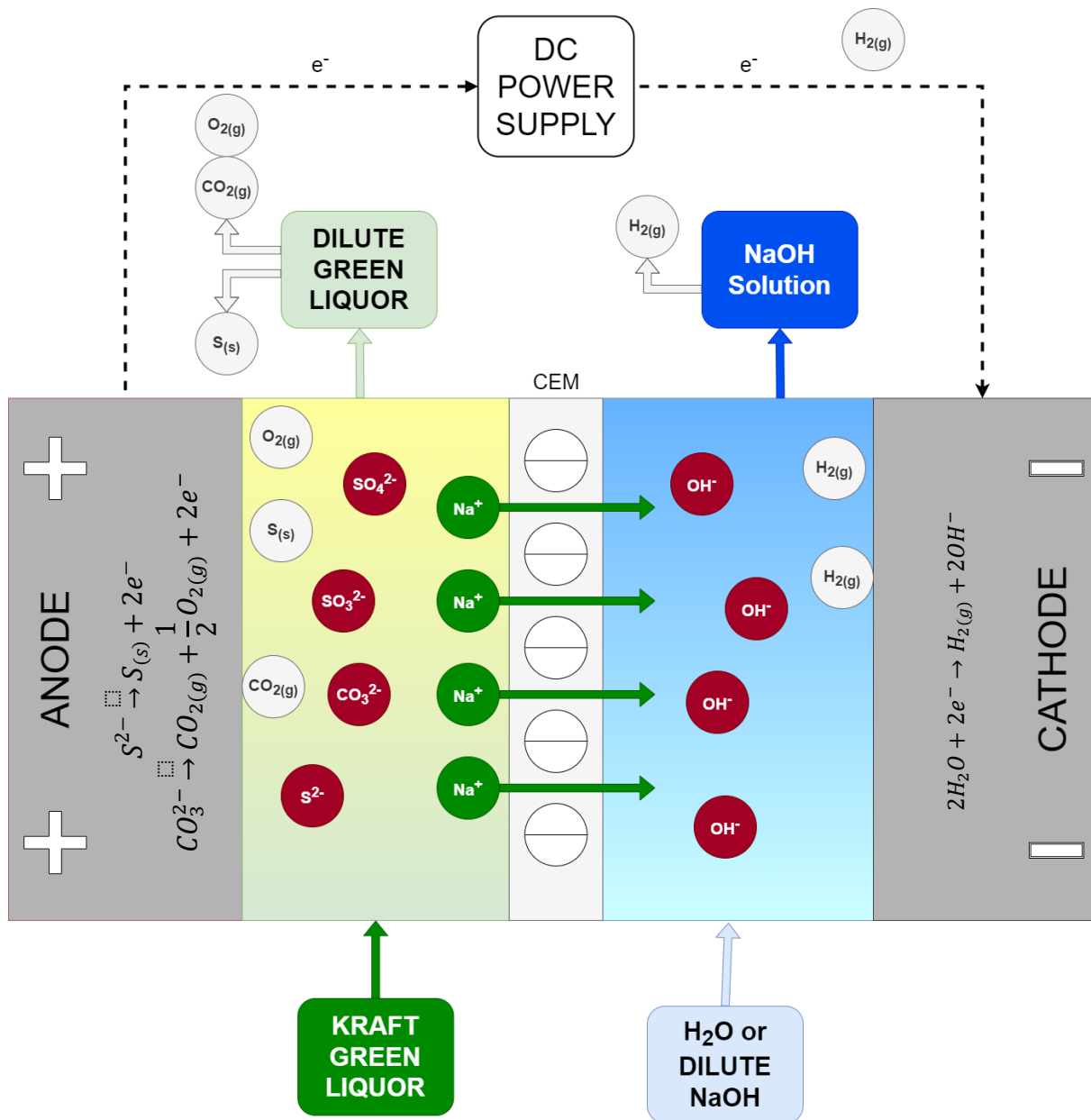
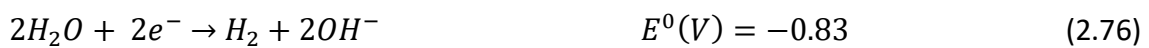


Figure 2.18: Schematic Kraft Green Liquor Electrolysis

Cathode:

Water molecules fed to the cathode side of the CEM can be reduced, as can sodium ions that have diffused from the anode through the CEM.



The reduction voltage for H₂O is much lower than for Na⁺, so the only product at the cathode is hydrogen gas and hydroxide.

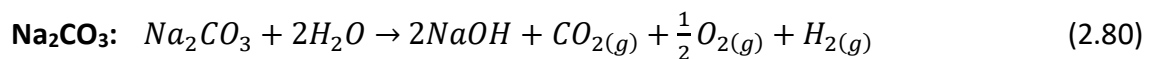
Anode:

Kraft Green liquor is approximately 60% Na₂CO₃, with 22% Na₂S, 8% NaOH and the balance Na₂SO₄, Na₂SO₃ and Na₂S₂O₃. Of the compounds, Na₂CO₃ and Na₂S have the lowest reduction voltage requirement, so are the easiest to reduce.

Main reactions at anode (most reducible ions):



Half reaction at the anode:



Half reaction at the anode:



The standard-state potential for the oxidation of Na₂S is slightly less than Na₂CO₃ but they are reasonably close, so it is expected that they will both be oxidised at the anode. Oxidation of Na₂S at the anode will present as a sulphide precipitate, whilst Na₂CO₃ will present as gas production (CO₂, O₂) at the anode. The elemental sulphur precipitate produced presents a potential for fouling or scaling on the anode and potentially membrane, which would need to be monitored.

As cell current density is increased, it is expected that cell resistance and voltage will also increase, where more Na₂CO₃ oxidation will occur. This will present in the form of greater gas production at the anode and higher concentration of NaOH at the cathode.

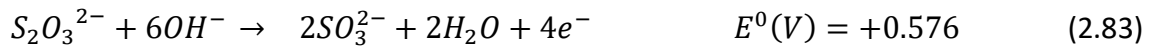
Other reactions - less oxidisable ions at the anode:

H₂O: Half reaction at the anode



The reduction potential for water to oxygen gas and hydrogen ions at the anode is expected to be negligible because the reduction potential is higher than that for Na₂S and Na₂CO₃

Na₂S₂O₃: Half reaction at the anode (in presence of 1M NaOH):



Na₂S₂O₃ will be reduced to Na₂SO₃ in the presence of 1 M NaOH. The typical green liquor of 100 g/L total dissolved solids will contain approximately 0.2 M NaOH, so this may be limited stoichiometrically. Any Na₂SO₃ production would not present in the form of precipitate, as the concentration would still significantly be below solubility limit.

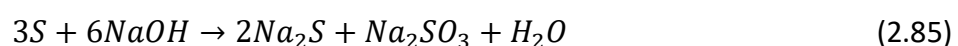
Na₂SO₃: Half reaction at the anode (in presence of 1M NaOH):



MEC has the potential to produce a pure solution of NaOH at concentrations much higher than that required by the conventional Kraft pulping process of 5 to 6% by weight. As a comparison, the AGC Selemion F-9010 chlor-alkali membrane is designed to produce NaOH at concentrations in excess of 35% weight at current efficiencies greater than 97% (Selemion, 2019a). If MEC can produce a NaOH product in greater concentrations than 6% by weight, it introduces the opportunity to decrease the volume of chemical that needs to be stored, heated, and transferred.

Na₂CO₃ is also the main deadload in the Kraft cycle. Whilst the conventional Kraft regeneration process using lime is limited by chemical equilibrium to around 80% conversion of Na₂CO₃ to NaOH, an MEC process can produce a pure aqueous solution greater than 35% NaOH by weight. The MEC will also produce hydrogen gas at the cathode, a potentially value product that can be used elsewhere in the Kraft process.

The query over the merits of MEC recovery Kraft Green liquor is whether Na₂S will be lost in the electrolysis process. Na₂S has a slightly lower reduction potential than Na₂CO₃. Referring to equation (2.79), the reduction of Na₂S will produce NaOH and an elemental sulphur precipitate. This sulphur precipitate could be separated from the anode discharge and combined with the concentrated NaOH cathode product to form Na₂S that can return to the cycle as per the reaction below:



The downside of this reaction is that the undesirable Na_2SO_3 is also formed, which is an undesired “deadload” chemical.

Whilst some S precipitate is expected to present in the anode discharge, given the raw Green Liquor is strongly alkaline, containing 10 -20g/L NaOH, much of the S precipitate formed will react and reform soluble Na_2S and Na_2SO_3 within the MEC before being discharged, as per (2.85). The Na_2S will continue to be converted to Na_2SO_3 until all the NaOH is exhausted, after which more S precipitate will begin to present in the discharge.

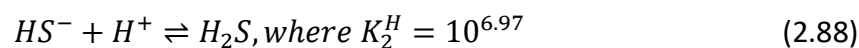
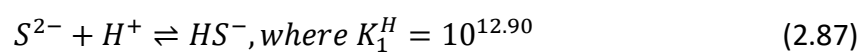
As the voltage across the cell increases with current density, the Na_2SO_3 will be converted to Na_2SO_4 as per (2.84), which will consume even more available NaOH.

The synthesised raw Green Liquor is strongly alkaline with pH greater than 13, which means that the S^{2-} ions present are mostly in the form of Na_2S . In this form, the Green Liquor is a clear light green colour, as the other Na_2CO_3 , NaOH, Na_2SO_3 , Na_2SO_4 and $\text{Na}_2\text{S}_2\text{O}_3$ are also colourless and well within their solubility limits.

In aqueous solution Na_2S disassociates depending on solution concentration of NaOH in solution, with the equilibrium reactions for S^{2-} , HS^- and H_2S in aqueous solutions with hydroxide (OH^-), are present in the following equilibrium:



The acid disassociation constant (pK_a) for H_2S can be sourced from literature (Dean, 1999) so the speciation of S species versus pH can be modelled.



So, the distribution of S species (ϕ) can be modelled using equations (2.88), (2.89) and (2.90).

The modelled output of these equations is shown in Figure 2.17 below.

$$\phi[\text{S}^{2-}] = \frac{1}{1 + K_1^H[\text{H}^+] + K_1^H K_2^H [\text{H}^+]^2} \quad (2.89)$$

$$\phi[\text{HS}^-] = \frac{K_1^H [\text{H}^+]}{1 + K_1^H [\text{H}^+] + K_1^H K_2^H [\text{H}^+]^2} \quad (2.90)$$

$$\phi[H_2S] = \frac{K_1^H K_2^H [H^+]^2}{1 + K_1^H [H^+] + K_1^H K_2^H [H^+]^2} \quad (2.91)$$

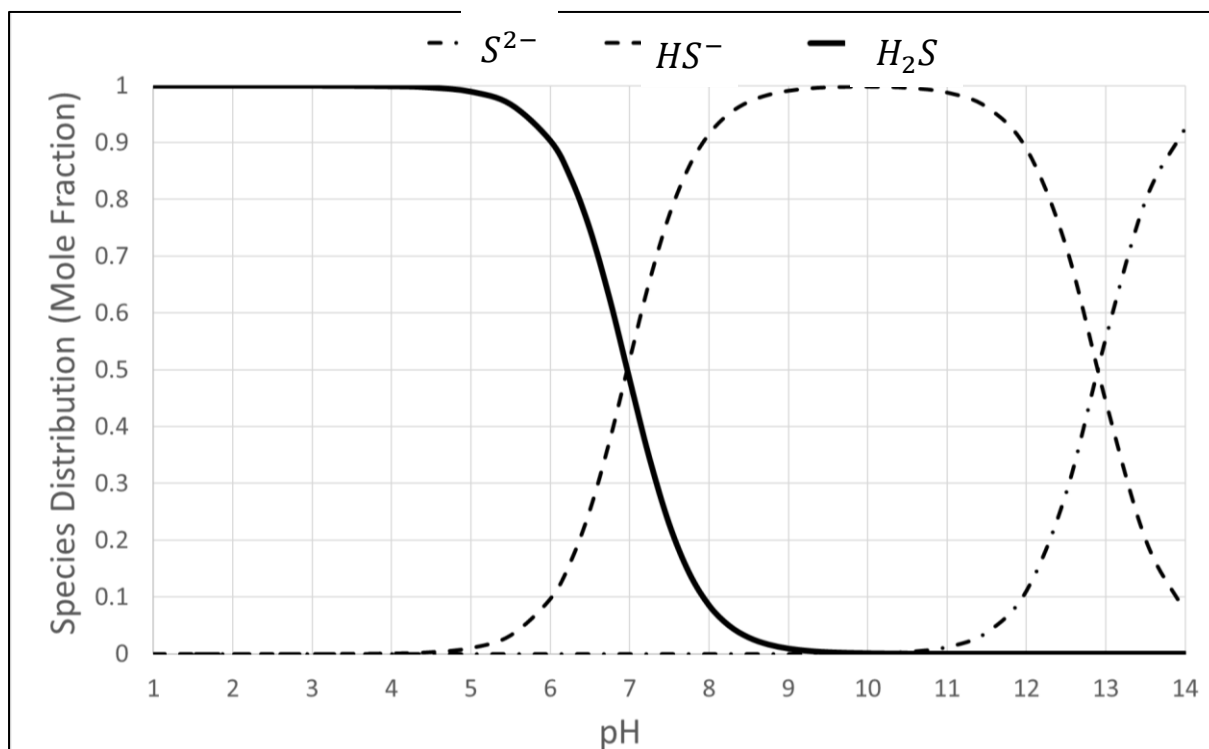


Figure 2.19: Modelled Speciation of S species in Aqueous Solution vs pH.
pKa values obtained from (Dean, 1999)

Raw Green Liquor is a strongly alkaline solution of pH normally greater than 13. Referring to Figure 2.19 at high pH the balance of S²⁻ species favours Na₂S which is pale green colour. As discussed above, as Na₂S is oxidised to S precipitate (2.79), the precipitate will combine with the available NaOH reducing the concentration of hydroxide, whilst at the same time Na₂CO₃ will be decreasing as it is reduced to CO₂ and O₂ gas. This will decrease the pH of the Green Liquor leaving the anode shifting the distribution of S²⁻ species toward Sodium Hydrogen Sulphide (NaHS) which is strong gold colour.

It is not expected that the MEC will drop the pH of the anode discharge below 9, so if any H₂S gas presents in the anode discharge, it will be H₂S that forms locally at the electrode surface and does not dissolve back into solution to form NaHS before discharge.

Eventually, as the MEC current density increases relative to Green Liquor flowrate and concentration, the S²⁻ is completely converted to weak alkali salt Na₂SO₃ and then to the neutral salt Na₂SO₄, the solution colour will fade from the yellow NaHS to clear or white Na₂SO₃ and Na₂SO₄ solution.

An MEC anode stream that is essentially Na_2SO_4 solution could be recirculated to the Kraft reboiler to be once again converted to Na_2S , however this is perhaps not ideal as it puts the Na_2S back into the Green Liquor before the MEC. This will result in an accumulation of Na_2S in a new recycle loop.

In summary, a key research objective is to characterise the condition of the Green Liquor leaving the electrolysis cell under a range of different operating conditions, including feed flow, concentration, temperature and current. To evaluate this, the following will be measured in the Green Liquor discharge in key experiments:

- Sodium (Na) and sulphur (S) concentration in the Anode Green Liquor liquid discharge to indicate mass of Na that has been transported across the membrane to the cathode.
- Remaining carbonate and hydroxide in the Green Liquor discharge as an indication of the balance of remaining, Na_2CO_3 and NaOH , but also to indicate the balance of Na_2S , Na_2SO_3 and Na_2SO_4 .
 - High concentration of carbonate and hydroxide indicates strong balance of Na_2S present.
 - Medium concentration of carbonate indicates decreasing presence of Na_2S , but possibly developing concentration of weaker alkaline Na_2SO_3 .
 - As the presence of carbonate and hydroxide decreases towards zero, it is an indication that any Na or S is present in the form of the neutral salt Na_2SO_4 .
- Characterisation of any precipitated solids in the anode liquid discharge to confirm the presence of sulphide precipitate as predicted by equation (2.79).

2.3.7 Key Operating Metrics of the Membrane Electrolysis Cell

Molar Production of NaOH (N_{Prod})

The electro potential across the MEC drives the electrolysis of Kraft Green Liquor, predominantly Na_2CO_3 and Na_2S , transporting Na^+ ions across the IEM towards the cathode. H_2O is fed to the cathode, where it is electrolysed to OH^- and H_2 gas. The OH^- combines with the Na^+ ions transported across the IEM to form NaOH.

The rate of NaOH production (N_{Prod}) is calculated using (2.92) below.

$$N_{Prod} \left(\frac{\text{mol}}{\text{hr}} \right) = (M[\text{NaOH}]_{out} - M[\text{NaOH}]_{feed}) \times Q_{Cathode} \quad (2.92)$$

Where:

$M[\text{NaOH}]_{out}$ = Molar concentration of NaOH in cathode discharge (mol/L)

$Q_{Cathode}$ = Volumetric flow rate of the cathode (L/hr)

$M[\text{NaOH}]_{feed}$ = Molar concentration of NaOH in cathode feed (mol/L).

Current Efficiency (ϵ)

The electro potential across the MEC drives a current of Na^+ across the IEM. If the MEC has 100% current efficiency, then the molar transport of Na^+ ions across the CEM and production rate of NaOH will follow Faraday's law. This theoretical 100% molar transport rate (N_{100}) is calculated using:

$$N_{100} \left(\frac{\text{mol}}{\text{hr}} \right) = \frac{I \text{ (C/sec)}}{96485 \text{ (C/mol)}} \times \left(\frac{3600 \text{ sec}}{1 \text{ hr}} \right) \quad (2.93)$$

However, the MEC will not deliver 100% current efficiency because of current leakage across the CEM. The previously defined Nernst-Planck equation is used to explain the sources current leakage, where the overall ionic flux, J_i , is:

$$J_i = vC_i - D_i \frac{dC_i}{dx} - \frac{z_i F C_i D_i}{RT} \frac{d\phi}{dx}$$

The electro potential gradient $\left(\frac{z_i F C_i D_i}{RT} \frac{d\phi}{dx} \right)$ is the most significant factor driving cation transport across the CEM from the anode to the cathode.

Current leakage can occur in the form of cations being convectively transported across the CEM by water (vC_i) due to a hydraulic or osmotic pressure differential between the anode and cathode compartments.

Current leakage can also occur in the form of ion diffusion from the cathode to the anode due to a concentration gradient ($D_i \frac{dC_i}{dx}$). The feed flow rates and concentration to the anode and cathode affect the average concentration of ions either side of the membrane and directly impact current leakage due to concentration gradient.

The MEC current efficiency (ε) is calculate using:

$$\varepsilon(\%) = \frac{N_{Prod}}{N_{100}} \times 100\% \quad (2.94)$$

Specific Energy of NaOH Production (kJ/mol NaOH)

The specific energy requirement of the MEC to produce a unit mass of NaOH is central to its evaluation against the conventional Kraft process. As per Joule's law the product of cell voltage (V) and current (I) give the instantaneous power (P) to the MEC.

$$P \left(\frac{kJ}{hour} \right) = V \left(\frac{J}{C} \right) \times I \left(\frac{C}{sec} \right) \times \left(\frac{3600 \text{ sec/hr}}{1000 \text{ J/kJ}} \right) \quad (2.95)$$

The energy requirement (E_{NaOH}) per mole of NaOH, E_{NaOH} , produced is given by:

$$E_{NaOH} \left(\frac{kJ}{mol \text{ NaOH}} \right) = P \left(\frac{kJ}{hour} \right) \div N_{Prod} \left(\frac{mol}{hr} \right) \quad (2.96)$$

Current Density (kA/m²)

Current density is a measure of the current applied across an electrolysis cell per membrane unit area. Industrial IEMs produced by AGC Selemion LTD and DuPont with their Nafion membrane for NaOH production in the chloralkali industry are typically designed to operate at a range of 4,000 to 6,000 A/m² (Selemion, 2019a).

For a MEC Green Liquor recovery process the chosen current density applied across CEM needs to be balanced against the membrane design, cell voltage, and the concentration of Na⁺ ions available for transport across the membrane.

For the diffusion of sodium ions (Na^+) across a CEM, the basic relationship between current (I), electrical motivation force (V) and net MEC resistance (R_{MEC}), can be used to evaluate the MEC system in the context of Ohm's law (Sadrzadeh and Mohammadi, 2009).

$$V = I \times R_{MEC} \quad (2.97)$$

MEC resistance, R_{MEC} , is a fundamental characteristic of the MEC system for a given set of MEC operation parameters, such as feed flows, concentration, and temperature.

Combining Joule's law (2.95) with Ohm's law (2.97) and the specific energy equation (2.96) gives:

$$E_{NaOH} \left(\frac{kJ}{mol NaOH} \right) = \left[(I^2 \times R_{MEC}) \times \left(\frac{3600 \text{ sec/hr}}{1000 \text{ J/kJ}} \right) \right] \div N_{Prod} \left(\frac{mol}{hr} \right) \quad (2.98)$$

Substituting in equation (2.94), N_{100} for N_{Prod} gives:

$$E_{NaOH} \left(\frac{kJ}{mol NaOH} \right) = \left[I^2 \times R_{MEC} \times \left(\frac{3600 \text{ sec/hr}}{1000 \text{ J/kJ}} \right) \right] \div (N_{100} \times \varepsilon) \times 100\% \quad (2.99)$$

Substituting in equation 2.93 for N_{100} gives

$$E_{NaOH} \left(\frac{kJ}{mol NaOH} \right) = \left[I^2 \times R_{MEC} \times \left(\frac{3600 \text{ sec/hr}}{1000 \text{ J/kJ}} \right) \right] \div \left(\frac{I}{F} \times \varepsilon \right) \times 100\% \quad (2.100)$$

This simplifies to:

$$E_{NaOH} \left(\frac{kJ}{mol NaOH} \right) = \frac{I \times R_{MEC} \times F}{\varepsilon} \times 100\% \quad (2.101)$$

Equation 2.101 shows that the specific energy of NaOH production using MEC will increase linearly with current density, with constant MEC current efficiency, ε .

A source current leakage in the MEC will be the form of ion diffusion from the cathode to the anode due to a negative concentration gradient $\left(D_i \frac{dc_i}{dx} \right)$. The concentration gradient of ions across the membrane is given by:

$$\Delta c_i = c_{iA,ave} - c_{iC,ave} \quad (2.102)$$

Where:

$c_{iA,ave}$ = Average concentration of ion i between the anode feed and discharge

$c_{iC,ave}$ = Average concentration of ion i between the cathode feed and discharge

Given by:

$$c_{iA,ave} = \frac{c_{iA,in} + c_{iA,out}}{2} \quad (2.103)$$

$$c_{iC,ave} = \frac{c_{iC,in} + c_{iC,out}}{2} \quad (2.104)$$

With cell temperature, feed flow and concentration to the anode and cathode constant, an increase in current density will increase $c_{iC,ave}$ and decrease $c_{iA,ave}$, moving the concentration gradient in a negative direction, increasing potential for current leakage, and decreased current efficiency, ε . Returning to equation 2.99, the decrease in current efficiency associated with increasing current density may further compound the increase in specific energy requirement.

Resistance

The MEC resistance is the sum of the resistance of the CEM (R_{CEM}), the resistance of the anolyte compartment (R_{anode}) and the resistance of the catholyte compartment ($R_{cathode}$):

$$R_{MEC} = R_{anode} + R_{CEM} + R_{cathode} \quad (2.105)$$

The electrical resistance of the anode (R_{anode}) or cathode ($R_{cathode}$) compartments is proportional to the electrical conductivity of the anolyte and catholyte and the dimensions of the MEC. Electrical resistance increases with channel depth or gap (d) and decreases with CEM cross-sectional (A) area (Sadrzadeh and Mohammadi, 2009).

For the anolyte and catholyte compartments, resistance is given by:

$$R_{anode} = \frac{d}{EC_{anode} \times A} \quad (2.106)$$

$$R_{cathode} = \frac{d}{EC_{cathode} \times A} \quad (2.107)$$

Where EC_{anode} and $EC_{cathode}$ are the electrical conductivity (EC) of the anolyte and catholyte respectively. The importance of channel depth to MEC resistance in the above equations explains the move towards “zero gap” electrolysis cell designs in the chloralkali industry. “Zero gap” refers to the installation of electrically conductive membrane supports that extend the anode and cathode up to the membrane surface. This reduced gap decreases the ohmic drop related to the ionic movement through the catholyte or anolyte gap, decreasing cell resistance (Hnát et al., 2019).

Based on the Nernst-Einstein equation the relationship between the molar limiting conductivity (Λ_{M_i}) and the diffusion coefficient for any ion in the Green Liquor is described (Sata, 2007d).

$$EC_{anode} = \sum_i \Lambda_{m,i} c_{iA,ave} = \left(\frac{F^2}{RT}\right) \sum_i z_i^2 D_i c_{iA,ave} \quad (2.108)$$

$$EC_{cathode} = \sum_i \Lambda_{m,i} c_{iC,ave} = \left(\frac{F^2}{RT}\right) \sum_i z_i^2 D_i c_{iC,ave} \quad (2.109)$$

Where:

- $\Lambda_{m,i}$ = Molar Conductivity of ion i (S.m²/mol)
- $c_{iA,ave}$ = Average concentration of ion i between the anode feed and discharge
- $c_{iC,ave}$ = Average concentration of ion i between the cathode feed and discharge
- z_i = Charge of ion i
- T = Temperature (K)
- R = Gas Constant (8.314 J/K.mol)
- F = Faraday's constant (96485 Coulomb/mol)
- D_i = Diffusion coefficient of ion i (m²/s)

The Nernst-Einstein equation predicts that as the average concentration of ions, $c_{i,ave}$, in solution increases, EC_{anode} also increases, decreasing relative compartment resistance, R_{anode} .

The temperature dependency of Λ_M can be represented by a typical Arrhenius-type equation of the form (Soriano et al., 2011):

$$\Lambda_{m,i}^0 = \Lambda_{m,i} \times e^{\left(\frac{-E_a}{RT}\right)} \quad (2.110)$$

$\Lambda_{m,i}$ is the pre-exponential molar conductivity factor and E_a is the activation energy of the ion, i . Generally, the molar conductivity ($\Lambda_{m,i}^0$) of aqueous solutions increase with temperature as the mobility of ions increases (D_i). This increased ionic mobility decreases the resistance of the anode compartment (R_{anode}), the CEM (R_{CEM}) and to the cathode compartment ($R_{cathode}$).

2.3.8 Summary of Evaluation of best IEM Technologies for Kraft Green Liquor Regeneration

To regenerate Green Liquor back into usable pulping liquor, which the conventional Kraft process refers to as White Liquor, there must be effective conversion of Na_2CO_3 to NaOH .

The IEM processes of diffusion dialysis (DD), electrodialysis (ED), electrodialysis metathesis (EDM) and membrane electrolysis (MEC) were evaluated in the context of Kraft Green Liquor recovery. DD and ED were not suitable as they are designed for purification and desalination functions and not alkali production, which is necessary for the conversion of Na_2CO_3 to NaOH . EDM in the form of an acid-alkali bipolar electrodialysis (BPED) arrangement can produce a NaOH product, however it would also produce unwanted side reactions involving the conversion of Na_2S to H_2S in an acidic discharge stream.

MEC was chosen over EDM as it is an established technique for NaOH production in the chloralkali industry and with a Green Liquor feed, it can oxidise the unwanted deadload carbonate (CO_3^{2-}) at the anode, removing it from the Green Liquor as $\text{CO}_{2(g)}$, whilst producing hydroxide at the cathode. There were identified possible side reactions associated with Na_2S at the MEC anode, however these indicated the conversion to more neutral salts of S, Na_2SO_3 and Na_2SO_4 , which may be recovered, rather than highly undesirable H_2S produced in the case of EDM.

MEC has also been shown to be able to produce NaOH from a Na_2CO_3 feed source (Simon et al., 2014a) and from green liquor (Mandal et al (2022), Eswaraswamy et al (2022) and Goel et al (2021). A strong high purity NaOH stream can be produced, but the potential for side reactions that can result in undesirable effects such as Na_2S loss, Na_2S gas generation at the anode, and precipitation of elemental sulphur have not been fully explored in the literature. This research investigates the effect of process conditions on the production of NaOH and the impact on the Green Liquor leaving the MEC anode.

2.4 Research Objectives Identified from Literature Review

Selecting MEC as the preferred IEM technology defines the research objectives are identified.

1. Design, build and commission a bench scale MEC apparatus for the recovery of Kraft Green Liquor (Chapter 3).
2. Design a standard test to confirm the integrity of the electrolysis cell membrane at the beginning of each trial (Chapter 4)
3. Evaluate the ability of MEC to recover Kraft Green Liquor by examining the effect of key process parameters on the performance of the electrolysis cell (Chapter 5):
 - a. Temperature
 - b. Anode (Green Liquor) feed flow rate
 - c. Anode (Green Liquor) feed concentration
 - d. Cathode feed concentration (0 g NaOH/L – 100g NaOH/L)
 - e. Electrolysis Cell Current density
4. Evaluate the impact on the Green Liquor leaving the electrolysis membrane cell anode, with focus on required Na₂S and remaining Na₂CO₃ deadload (Chapter 5):
 - Measurement of remaining carbonate and hydroxide in the Green Liquor discharge as indication of reduction of deadload Na₂CO₃ in the Green Liquor.
 - Characterisation of remaining Na and S of the Anode liquid discharge.
 - Characterisation of any precipitated solids in the Anode liquid discharge to confirm Na₂S reduction to elemental sulphur precipitate.
5. Measure the rate of hydrogen production at the cathode as a potential beneficial product of the MEC recovery of Kraft Green Liquor (Chapter 5)
6. Identification and justification of optimal operational parameters for Kraft Green Liquor Recovery (Chapter 5)
7. Evaluate the performance of high and low resistance ion exchange membranes in an electrolysis membrane cell in the recovery of Kraft Green liquor (Chapter 6).
8. Identify key deficiencies of the MEC in the recovery of Kraft Green liquor with a key focus on Na₂S recovery and other deadload
9. Identify possibilities for future research for the development of ion exchange membrane process for the recovery of Kraft Green liquor

Chapter 3 Experimental Methods

3.1 Introduction

The objective of the Kraft Green liquor recausticization process using lime (CaO) is the conversion of Na_2CO_3 to NaOH, while retaining Na_2S . The limitation of the conventional process is the extent of chemical reaction being restricted to approximately 80%, so a significant deadload of Na_2CO_3 remains in the Kraft pulping cycle and is a major source of process inefficiency.

In the Chapter 2 literature review the mechanics of ion exchange membranes were discussed and current ion exchange membrane process were detailed. The ion exchange processes were evaluated based on their potential for Na_2CO_3 to NaOH conversion and Na_2S conservation.

The outcome of the literature review was that the membrane electrolysis cell (MEC) was identified as a promising ion exchange membrane technology for the recovery of Kraft Green liquor due to its greater capacity for the conversion of Na_2CO_3 to NaOH over the other arrangements.

The challenge in the use of MEC for this application is the unknown effect it may have on the required Na_2S in the Green Liquor leaving the MEC anode. Na_2S has a slightly lower reduction potential (-0.41V) compared to Na_2CO_3 (-0.69V), so it is expected to be oxidised to a sulphur (S) precipitate. The S precipitate will also react with available NaOH in solution to form Na_2S and Na_2SO_3 , which will continue to be oxidised in the MEC, ultimately towards Na_2SO_4 . The composition of the Green Liquor in the MEC anode will be transformed depending on the cell current density, relative to the Green Liquor feed concentration and flow rate. It is a key objective of this research to determine the impact of MEC treatment on the Kraft Green liquor. The ability to retain Na_2S is central to the evaluation of the merits of MEC as an alternative to the conventional recausticization process.

The Kraft Green Liquor feed used in this research was synthesized by mixing chemicals in proportions taken from literature (Biermann, 1996a). A synthesized Green Liquor was utilised due to its reproducibility and the poor reliability of accessing an industrial Green Liquor supply due to COVID-19 lock downs in Victoria, Australia during 2020-21.

The experimental methods detailed in Chapter 3 were designed to achieve the objectives of research:

1. Development and fine tuning of MEC arrangement for the recovery of Kraft Green liquor (Chapter 4)
2. Design of a standard test to confirm the integrity of the electrolysis cell membrane at the beginning of each trial (Chapter 4)
3. Evaluation of the effect of key process parameters on the performance of the MEC (Chapter 5):
 - Temperature (Solution feed to the electrolysis cell)
 - Anode (Green Liquor) feed flow rate
 - Anode (Green Liquor) feed concentration
 - Cathode feed concentration (0 – 100 g NaOH/L)
 - Electrolysis cell current density (A/m²)

The key performance indicators are the efficiency with which the applied current to the MEC generates NaOH at the cathode and the voltage required to drive the cell current. The combination of the cell current efficiency (ε) and voltage (V) are used to determine the units of NaOH generated per unit of applied energy supplied (E_{NaOH}). The Nernst Planck equation is used as a tool to explain the impact the each of the parameters on cell current efficiency and resistance or voltage.

The MEC NaOH production performance is evaluated against the benchmarks of the conventional Kraft recovery process using lime, where NaOH production efficiency is approximately 8 MJ/kg NaOH produced and approximately 0.98 kg CO₂ is emitted per kg NaOH produced (based on a diesel fuel source).

As above, Na₂S, which is critical to the Kraft pulping process will also be oxidised in the electrolysis membrane cell with Na₂CO₃. The expectation is that the oxidation of Na₂S will present as a solid sulphur precipitate in the electrolysis cell discharge and potentially also as scale on the electrode and possibly also the membrane. Not all the Na₂S will leave as S precipitate since some will be converted to Na₂SO₃ and Na₂SO₄ also.

Meanwhile, as Na₂CO₃ is oxidised and freed Na⁺ ions diffuse through the cation exchange membrane to form NaOH at the cathode and Na₂S is oxidised, the concentration of S and Na

in the Green Liquor will also decrease. The concentration of carbonate in the Green Liquor discharge will also decrease as confirmation of the reduction of the deadload Na_2CO_3 .

The anode discharge was analysed to achieve the following research objective:

4. Evaluate the impact on the Green Liquor leaving the electrolysis membrane cell anode:
 - Characterisation of any precipitated solids in the anode Green Liquor discharge to confirm Na_2S oxidation to sulphur precipitate.
 - Measurement of remaining Na^+ and S^{2-} of the anode Green Liquor discharge
 - Measurement of remaining carbonate and hydroxide in the anode Green Liquor discharge as indication of reduction of deadload Na_2CO_3 in the Green Liquor.

The above measurements were used to give strong indication of the composition of Na_2CO_3 , NaOH , Na_2S , Na_2SO_3 , Na_2SO_4 and $\text{Na}_2\text{S}_2\text{O}_3$ remaining in solution and confirm the impact on the Green Liquor leaving the MEC anode.

5. Measure the rate of hydrogen production at the cathode as a potential beneficial product of the MEC recovery of Kraft Green Liquor (Chapter 5)
6. Identification of optimal operational parameters for Kraft Green Liquor Recovery (Chapter 5)
7. Trial identified optimal operation parameters using a series of high and low resistance cation exchange membranes to identify most suitable or recovery of Kraft Green liquor (Chapter 6):
 - AGC-Selemion SX-1831 (Low resistance cation exchange membrane)
 - AGC-Selemion SX-1811 (Balanced grade cation exchange membrane)
 - AGC-Selemion SX-2301WN (High selectivity cation exchange membrane)
 - AGC-Selemion SX-2301WNY (High selectivity cation exchange membrane)
 - AGC-Selemion F-9010 (NaOH production membrane)
 - Dupont Nafion N-324 (NaOH production membrane)

The evaluation of the above experimental results will allow for final discussion and conclusions on remaining research objectives:

8. Identify key deficiencies of the MEC in the recovery of Kraft Green liquor with a key focus on Na₂S recovery and other deadload (Chapter 7).
9. Identify possibilities for future research for the development of ion exchange membrane process for the recovery of Kraft Green liquor (Chapter 7).

3.2 Conceptual Framework - Integration of EMC into the Kraft Cycle

Figure 3.1 below shows how an electrolysis membrane cell (EMC) can integrate into the Kraft pulping cycle.

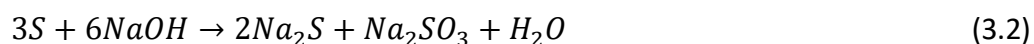
The feed to the anode side of the membrane electrolysis cell is Green Liquor, which is comprised of the smelted salts leaving the Kraft Reboiler dissolved in water and clarified. As per Table 2.6 in Chapter 2, a conventional Kraft Green liquor will be between 100 g/L and 150 g/L total dissolved solids (TDS). The TDS feed concentration to the electrolysis cell is not limited to 150 g/L, as the feed brine to the chlor-alkali process can well exceed 225 g/L (Rabbani et al., 2014). The maximum Green Liquor concentration is more a limitation of solution solubility, which can be more than 200 g/L. Table 3.3 details the solubility limits of each of the Green Liquor constituents. In this experimentation, the brine concentration was varied between 100 to 200 g/L to evaluate its impact on cell performance over this range.

Industrially, the temperature range of the Kraft Green liquor is between 75 and 90 °C, as per Table 2.6 above. The Green liquor is kept at an elevated temperature to accelerate CaCO₃ settling when Na₂CO₃ is contacted with CaO (Tran, 2008). For the MEC, increased Green Liquor temperature will decrease cell voltage and reduce membrane resistance (Luo et al., 2018) impacting selectivity, however is not critical to the process like it is to CaCO₃ settling, so for that reason the feed to the electrolysis membrane cell was evaluated between 40°C and 80°C.

The discharge from the anode is returned to the Green Liquor feed tank via a cyclone separator to isolate any precipitated elemental sulphide formed in the oxidation of Na₂S, as per the reaction:



The sulphide precipitate is added to the concentrated NaOH stream to be converted to Na₂S.



As Na_2CO_3 is oxidised, CO_2 and O_2 gas will be produced at the anode, as per the half reaction.



These gases can be separated from the anode discharge and sent to the Kraft reboiler.

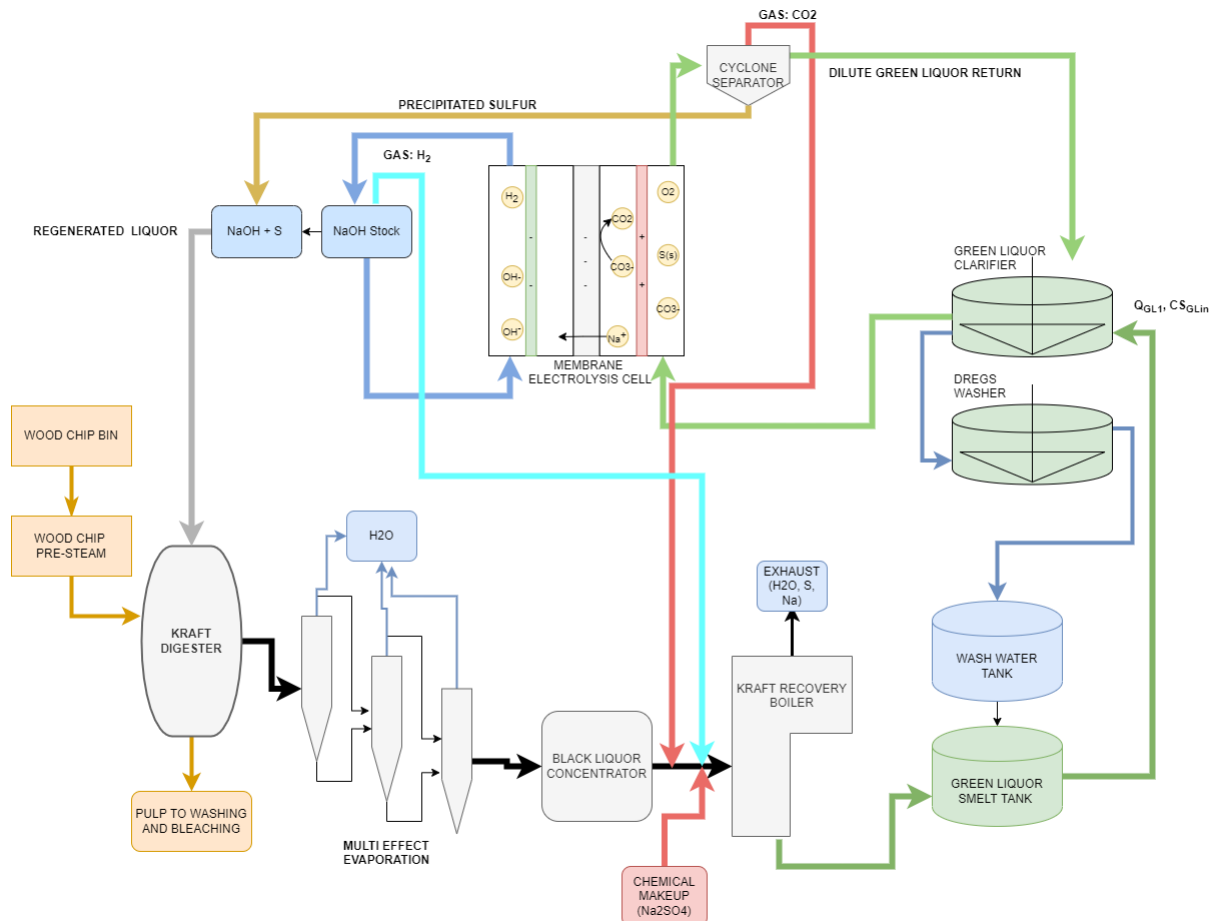


Figure 3.1: Possible Integration of MEC into the Kraft Cycle

Concentration of NaOH in the feed to the cathode is dependent on whether the cathode product is recycled through the electrolysis membrane cell. In the Chlor-Alkali process, the NaOH product is recycled to the extent that NaOH concentration can be more than 32% by weight and achieve current efficiencies greater than 95% (Selemion, 2019a).

Referring to Table 2.6, Chapter 2, regenerated “White” Kraft pulping liquor requires a concentration of NaOH of approximately 50 to 60 g/L, or approximately 5% by weight. Producing a NaOH solution of any higher concentration will allow the storage of a greater mass of NaOH in smaller volume. The range tested in this research was from 0 to 100 g

NaOH/L to evaluate the impact of different concentration gradients of sodium ions across the cation exchange membrane on selectivity and overall cell efficiency.

Finally, as they will have different performance, the replacement of the conventional lime driven recausticization process with a membrane electrolysis cell (MEC) will impact the composition of the recirculated brine in the Kraft cycle. The change to the Green Liquor feed returned to the MEC is considered in Table 3.1 below.

Table 3.1: Change in Green Liquor Composition with Integration of MEC into Kraft Cycle

	Conventional Process Composition of 100g/L Green Liquor	MEC Process Integration - Removal of Lime from the Kraft Cycle - 100% conversion of Na₂CO₃ to NaOH
Na ₂ CO ₃	60 g/L	<p>The conventional lime “recausticization” process is limited to approximately 80% conversion of Na₂CO₃ to NaOH by chemical equilibrium. The 20% remaining Na₂CO₃ returns to the cycle as “deadload”. MEC cathode product will be essentially 100% NaOH solution, so the concentration of Na₂CO₃ in the White Liquor will be zero. This Na₂CO₃ reduction will carry over to the Black Liquor and then back to the Green Liquor.</p> <p>A 20% reduction in Na₂CO₃ would represent a decrease in Green Liquor concentration from 60g/L to 48 g/L.</p> <p>Referring to Figure 3.1, the Green Liquor leaving the MEC anode is returned to the feed reservoir. The concentration of Na₂CO₃ in the anode discharge stream will decrease as it is oxidised and converted to NaOH. In selected experiments the concentration of remaining carbonate and hydroxide in the anode discharge was measured by titration to confirm the rate of Na₂CO₃ oxidation.</p>
Na ₂ S	22 g/L	<p>Na₂S has a redox potential slightly lower than Na₂CO₃ so is expected to oxidise significantly to solid S. Solid S should appear in the anode discharge. This can be separated and returned to the product NaOH to form Na₂S under controlled conditions.</p> <p>The concentration of Na₂S in the Kraft cycle is maintained by topping up lost chemical by adding Na₂SO₄ to the process before the reboiler, where it is reduced to Na₂S. For this reason, the concentration of Na₂S in Green Liquor is not expected to change.</p>
Calcium	Trace only. Calcium is normally lost from cycle via scale and dregs, so does not accumulate.	Introduction of MEC will largely eliminate calcium from process loop, other than that introduced with wood chips and water supply. Regenerated liquor would no longer be visually “White Liquor”.
Potassium	Trace introduced with woodchips but can accumulate due to solubility.	MEC will not selectively reject Potassium and it does participate in pulping and will accumulate at similar rate to ?.
NaOH	8 g/L	No significant change is expected in these lower concentration constituents. The NaOH concentration is a function of the concentration in the White Liquor and woodchip digestion, which should reach the same equilibrium. Na ₂ SO ₄ is introduced to the reboiler where it is reduced with no process change. Na ₂ SO ₃ and Na ₂ S ₂ O ₃ are in same equilibrium with Na ₂ S, NaOH and Na ₂ SO ₄ , so no significant change considered.
Na ₂ SO ₃	3 g/L	
Na ₂ SO ₄	6 g/L	
Na ₂ S ₂ O ₃	3 g/L	

3.3 Synthesis of Kraft Green Liquor:

Industrial Green Liquor is typically in the range of 100 to 150 g/L concentration. To evaluate the impact of Green Liquor feed concentration on the performance of the electrolysis membrane cell a slightly larger range was chosen, 100 to 200 g/L, this allowed for clearer detection of the impact of feed concentration and simplified the chemical batching process. For all experimental trials, a single large batch of 200 g/L Green Liquor was first synthesised. A portion of the produced 200 g/L solution was then separated and diluted to 100 g/L to ensure consistent distribution of constituents in the Green Liquor across all experiments.

The Green Liquor solution was prepared by dissolving in DI water, at room temperature, with constant mixing, the constituents in the proportions given in Table 3.2 below, which reflect proportions found in industry literature (Chandra, 2004, Kevlich et al., 2017).

Table 3.2: Compositions of Synthesised Kraft Green Liquor

Constituents	Green Liquor Composition (g/L)	Green Liquor Composition (g/L)
TDS	100	200
NaOH	8	16
Na ₂ S	22	44
Na ₂ CO ₃	60	120
Na ₂ SO ₃	2.5	6
Na ₂ SO ₄	5	12
Na ₂ S ₂ O ₃	2.5	6

The brine solutions were prepared by dissolving analytical grade NaOH, Na₂S, Na₂CO₃, Na₂SO₃, Na₂SO₄, Na₂S₂O₃ in Milli-Q water. The solubility limits of each of the components is given in Table 3.3 below, which shows that at a Green Liquor feed concentration of 200 g/L, all components were readily soluble at room temperature. In preparation of the solution, the Na₂CO₃ and NaOH components are added to the water first to form a strong alkali solution, followed by the addition of the remaining sulphur containing compounds. The strong alkali solution ensures the formation of stable Na₂S solution when added, rather than undesired NHS or H₂S, as per reactions (2.2) and (2.3).

Table 3.3: Solubilities of Salts Present in Kraft Green Liquor

	Molecular Weight (g/mol)	Solubility at 25°C (g/L)	Solubility at high temp
NaOH	40.0	1000	3370 g/L at 100°C
Na ₂ S	78.0	186	390 g/L at 50°C
Na ₂ CO ₃	106.0	340	430 g/L at 100°C
Na ₂ SO ₃	126.0	27	
Na ₂ SO ₄	142.0	139	42.7 g/L at 100°C
Na ₂ S ₂ O ₃	158.1	700	2310 g/L at 100°C

3.4 Membrane Electrolysis Cell:

The membrane electrolysis system used was designed so that it could be disassembled and reassembled with custom membranes, spacers, and electrodes (See Figure 3.2 below) when required. This system was designed, and purpose built for this research.

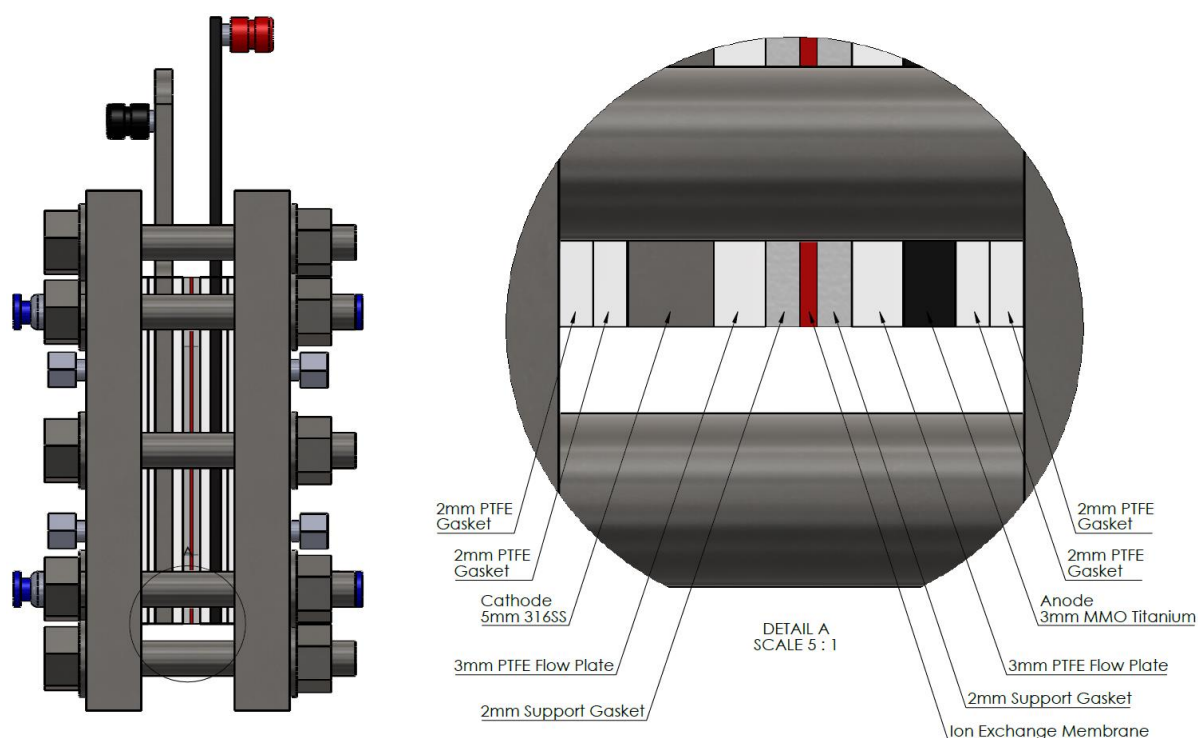


Figure 3.2: Electrolysis Membrane Cell Assembled

The anode material was grade 2 titanium commonly used in chlorate manufacturing with a coating of ruthenium iridium. The ruthenium iridium coating is a type of mixed metal oxide (MMO), which are catalytic coatings that also increase durability. The anode was supplied by

Boiji Quanjin Industry and Trade Company, China. The cathode was fabricated from 5mm 316 stainless steel plate.

Flow to an available membrane area of 60 mm x 60 mm was distributed by a 3 mm thick polytetrafluoroethylene (PTFE) flow plate (See Figures 3.3, 3.4 and 3.6) with 2mm deep milled distribution channels. A 2 mm PTFE membrane support gasket is placed on top of the flow plate, resulting in a channel depth of 5 mm. PTFE was chosen because it is resistant to high alkaline solutions and suitable for temperatures up to 200°C.

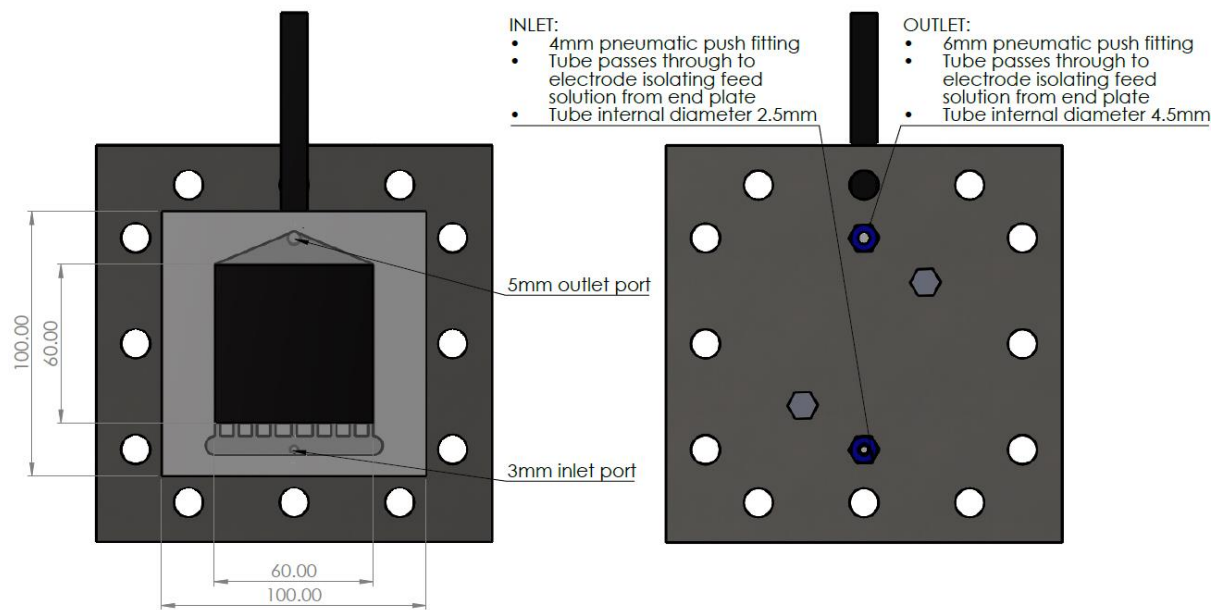


Figure 3.3: Anode Assembly with Flow Plate

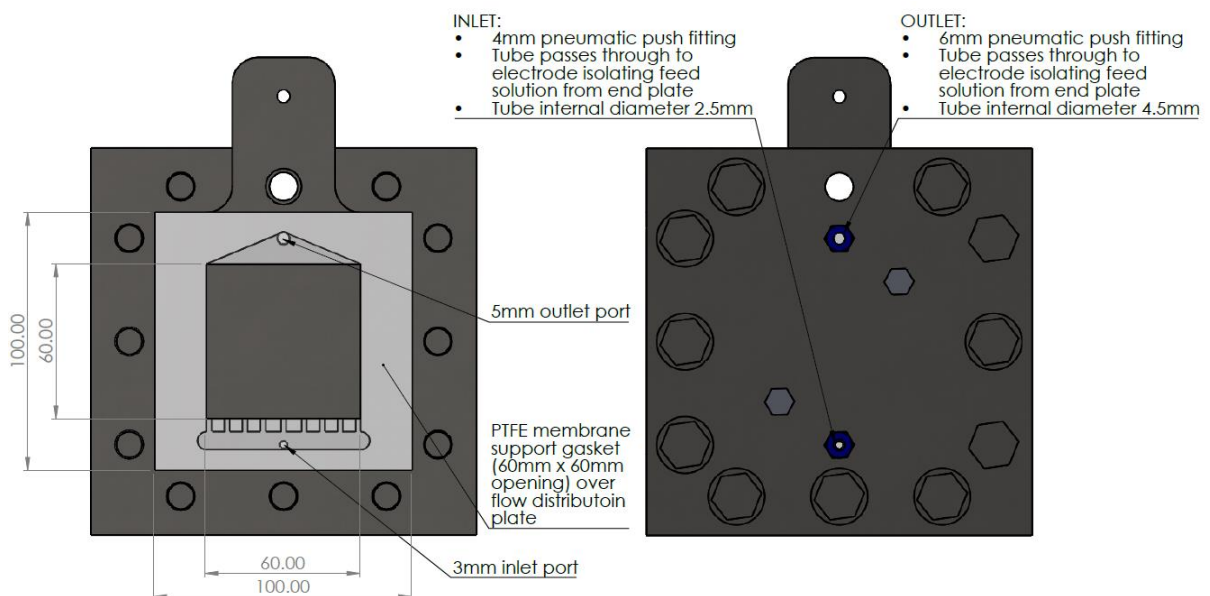
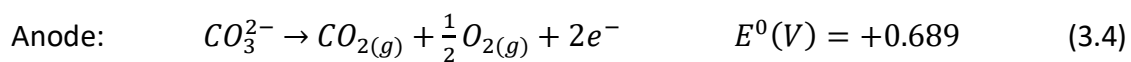


Figure 3.4: Cathode Assembly with Flow Plate

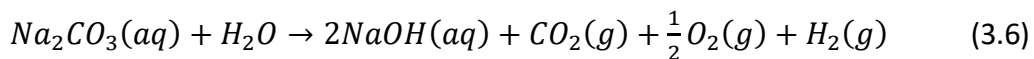
As the electrolysis process can generate gases at the cathode and the anode, the flow through the cell was designed in the vertical direction, with the inlets to both sides of the electrolysis cell located at the bottom and outlets at the top to prevent gas lock. The inlet at the bottom was 3 mm diameter, with larger 5mm outlets at the top to ease the discharge of any gases generated during electrolysis.

In the initial development of the electrolysis cell design the outlet diameter was 3mm, however during commissioning of the experimental arrangement (Chapter 4), the outlet was found to restrict the discharge of gas from the cell. Detailed in Chapter 4, pre trials were performed on the electrolysis cell with a 100 g Na₂CO₃/L feed to the anode and demineralised water feed to the cathode. The electrolysis of Na₂CO₃ is as follows:

Half Reactions:



Overall:



As per the reactions above, CO₂ and O₂ gas is produced at the anode and H₂ gas is produced at the cathode. As per Faraday's law, as cell current is increased by increasing the voltage potential, gas generation increases proportionally. During commissioning, detailed in Chapter 4, when the cell current was set to 3 amps (833 amps/m²) cell voltage equalised at approximately 3.5 volts. However, when it was increased to 5 amps (1,389 amps/m²) cell voltage increased exponentially above 12 volts. The design current density of the membrane being used (AGC SX-1831WN) was greater than 5000 amps/m² suggested that something other than the membrane was causing the increased resistance.

When the electrolysis cell discharge diameter was increased to 5mm, the cell voltage decreased to less than 5 volts at a current set point of 5 amps, confirming that the discharge restriction was the major contributor to the increased resistance. This indicated that with the smaller 3mm diameter outlets, gas was possibly accumulating in the cell and decreasing the available membrane area.

Unrestricted gas discharge from the cell was found to be a very important feature of the cell design for several reasons. Free gas discharge is very important to ensure the membrane area remains flooded, so ion transfer is unimpeded. Gas build-up on either side of the membrane can also contribute to hydraulic pressure differential across the membrane, which could drive the transport of water across the membrane, affecting the efficiency of the overall system. Finally, a cycle of gas build-up, followed by discharge, followed by build-up can create a pressure pulsation wave through the cell, potentially stressing the membrane.

3.4.1 Membrane Supports:

The membrane area of 60mm x 60mm and channel depth of 5mm (3mm flow plate + 2mm support gasket) resulted in an effective channel volume of 18 millilitres. In the 5mm channel or “gap” between the electrode and the membrane a support mesh was installed on both sides of the membrane.

The first function of the mesh was to give structural support to the membrane during operation, where an increased production of gas can create pulsating flow as gas repeatedly builds up and is pushed out of the cell with incoming feed. The second function of the mesh was to promote even distribution of feed across the membrane surface. The third function of the electrically conductive mesh was to extend the anode and cathode up to the membrane surface. This reduced gap decreases the ohmic drop related to the ionic movement through the catholyte or anolyte gap, potentially decreasing cell resistance (Hnát et al., 2019).

On the MMO-Titanium anode side, the mesh was an MMO coated titanium supplied by Shaanxi Yunzhong Metal Technology, China. On the 316SS Cathode side, the mesh was a fine nickel woven mesh supplied by Anping Count Bolin Metal Co, China. These are both shown in Figures 3.5 and 3.6 below.

In Chapter 4, the electrolysis cell is trialled with and without the membrane supports to examine their effect on the performance of the electrolysis cell.

Figures 3.5 and 3.6 show photographs of the disassembled electrolysis cell and Figure 3.7 is a photograph of the assembled cell. The plates align together with PTFE pins.

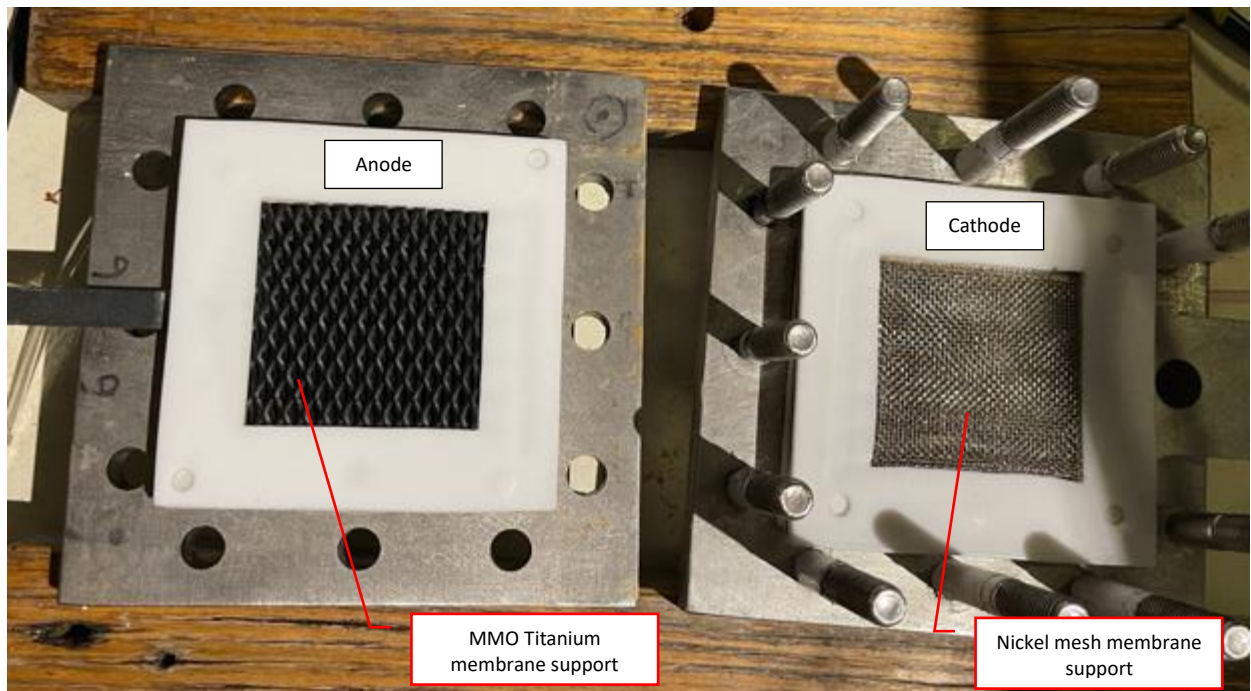


Figure 3.5: Dismantled Membrane Electrolysis Cell (Anode left, Cathode Right)

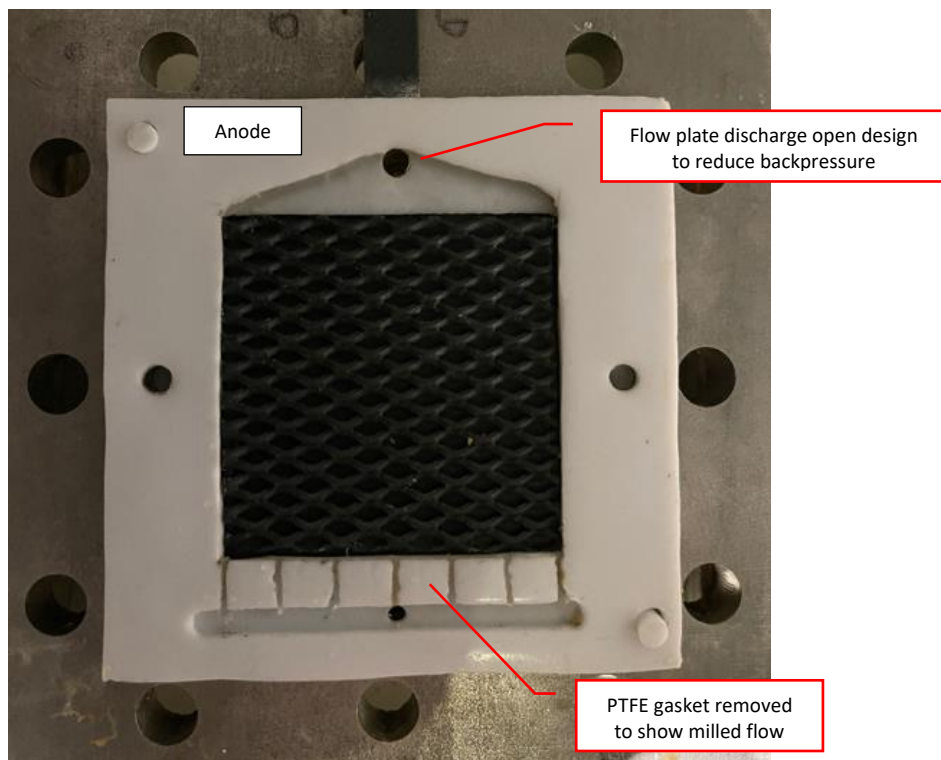


Figure 3.6: MMO Titanium Anode (PTFE Gasket removed to show flow plate)

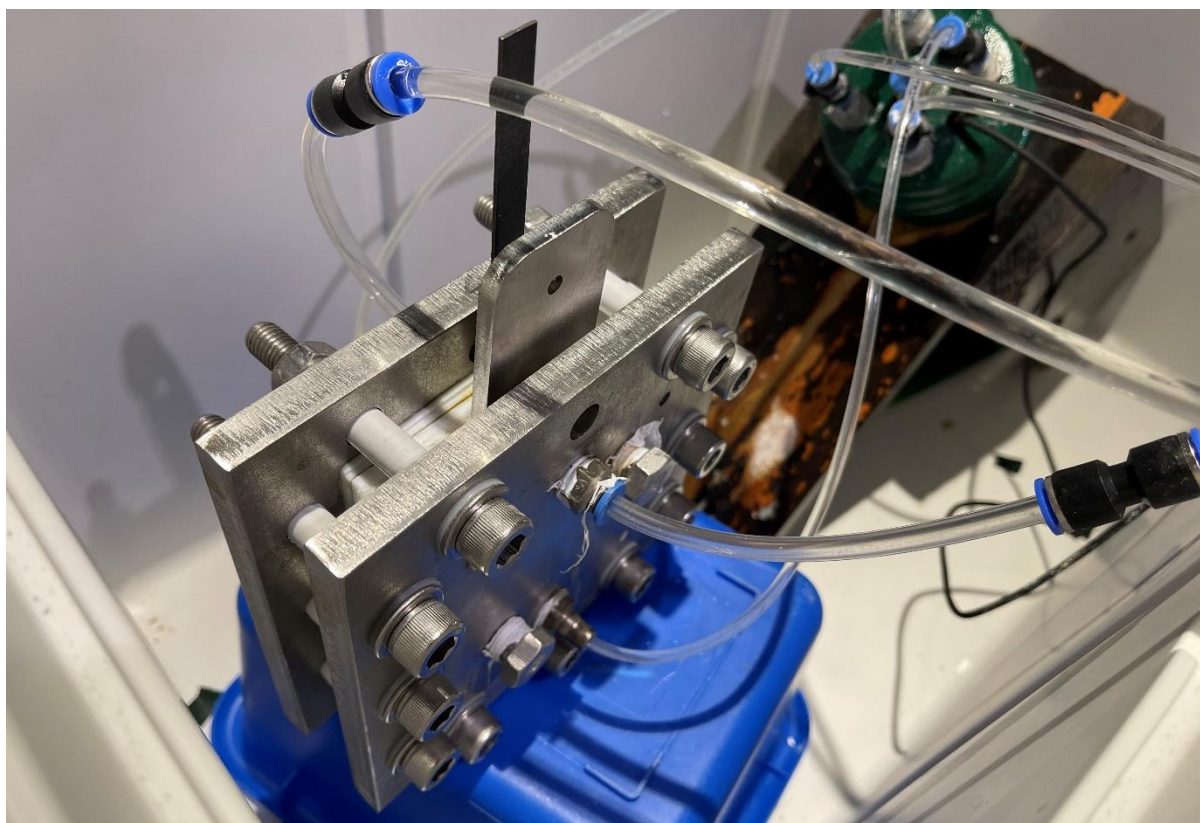


Figure 3.7: Assembled Membrane Electrolysis Cell in Insulated Container

3.5 MEC Feed Flow, Concentration and Current Range

3.5.1 Design Objective

As per the research aim, in Chapter 5 the effect of key process parameters on the performance of the electrolysis cell were evaluated:

- Cathode feed flow rate (mL/hr)
- Cathode feed concentration (g/L)
- Anode feed concentration (g NaOH/L)
- Current Density (amps/m²)
- Temperature

In the production of NaOH from a Green liquor feed, the key performance parameter will be energy per unit NaOH produced (kJ/mol NaOH) as it is affected by each of the above process parameters.

The other key research aim is to evaluate the impact on the Green Liquor leaving the electrolysis cell anode with a focus on the required Na₂S and the remaining Na₂CO₃ deadload. The objective of the experimental design was to choose an operating range from low to high that will impose a measurable effect on the Green Liquor production and quality leaving the MEC anode.

3.5.2 Calculation of Experimental MEC Maximum Current range

To identify the impact of Green Liquor feed flow, concentration, and cell current on the performance of the MEC (MJ/kg NaOH) and the impact on the Green Liquor quality leaving the MEC anode, ranges must be chosen that will impose a measurable effect.

With increasing MEC current density with all other parameters constant, Na₂CO₃ will be increasingly converted to CO₂ and O₂ at the anode and Na⁺ ions will be increasingly transported across the IEM to the cathode to form NaOH. As Na⁺ ion transport across the IEM increases relative to Na⁺ feed in the supply, the concentration of Na⁺ on the depleted (anode) side of the IEM will decrease. Simultaneously, the concentration of Na⁺ at the cathode will increase, gradually moving towards a negative concentration gradient across the membrane. A negative concentration gradient across the membrane will promote the leakage of Na⁺ back towards the anode, decreasing the efficiency of the MEC. It is an objective of this research to measure any decreasing current efficiency that may occur with increasing current density, so it is important to select current ranges that will potentially identify this.

Current Limit 1 – Na⁺ ion availability for transport across IEM

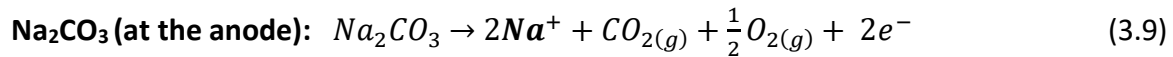
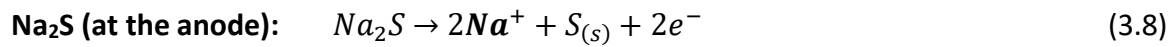
The transport of Na⁺ ions through the cation exchange membrane will follow Faraday's law and increase proportionally to the applied current (Simon et al., 2014b):

$$N \left(\frac{\text{mol}}{\text{s}} \right) = \frac{I}{F} \quad (3.7)$$

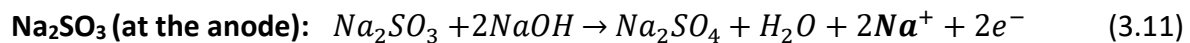
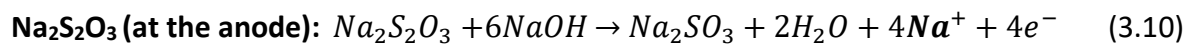
Where N is the molar transport of cations through the membrane, I is the applied current (A) and F is the Faraday constant (96485 C/M).

The proposed absolute limit of the MEC cell current applied is proportional to the quantity of oxidisable components in the Green Liquor feed that will provide free Na⁺ ions that can be transported across the cation exchange membrane.

Na₂S and Na₂CO₃ when oxidised provide sources of Na⁺ that can transport across the membrane to form NaOH, as per the reactions below.



Na₂S₂O₃ and Na₂SO₃ can be oxidised to Na₂SO₃ and Na₂SO₄ respectively in the presence of 1M NaOH, providing free Na⁺ ions to transport. However, given this is dependent on the availability of free NaOH, which is also being consumed by other reactions, notably (2.83, 2.84, 2.85), it is discounted.



The composition of the synthesised Green Liquor is given in Table 3.3 above. In this research two Green Liquor flow rates were trialled, 175 and 350 mL/hr, and two Green Liquor concentrations were also be trialled, 100 and 200 g/L. This flow range was chosen knowing that the maximum design current density of the IEM is approximately 5.0 kA/m², at the lower flowrate of 175 mL/hour with lower Green Liquor feed concentration of 100 g/L this allowed the MEC to affect significant change on the feed Green Liquor, which is an objective of this research to observe. At the highest feed concentration and flowrate, 200 g/L and 350 mL/H, the impact on the Green Liquor would be far less noticeable. Table 3.4 below gives the maximum current that can be applied to the electrolysis cell before the available Na⁺ that can be transported across the membrane becomes exhausted.

The maximum current that can be applied across the membrane cell is limited by the availability of sodium ions fed into the cell, Na_{feed} (mol/s). Na_{feed} is a function of the Green Liquor feed flow (Q_{GL}) and the molar concentration (mol/L) of Na⁺ in the feed solution C_{GLi} , which is only comprised of Na₂CO₃ and Na₂S only. The Na⁺ in Na₂S₂O₃ and Na₂SO₃ is not included because it relies on the presence of NaOH to reduce to Na₂SO₄, so may not be available if the NaOH in solution is not available.

$$Na_{feed} \left(\frac{mol}{s} \right) = Q_{GL} \times C_{GLi} \quad (3.12)$$

The maximum current that can be applied across the electrolysis membrane cell is:

$$I_{limit}(amps) = Q_{GL} \times C_{GLi} \times F \quad (3.13)$$

Table 3.4: MEC Experimental Cell – Na⁺ Current Limitation (Na₂CO₃ and Na₂S)

Green Liquor Feed		Na ⁺ Current Limitation	
Concentration (g/L)	Flowrate (mL/hr)	Maximum current $I_{limit}(amps)$	Maximum MEC Current Density (kA/m ²)
100	175	8.0	2.2
100	350	15.9	4.4
200	175	15.9	4.4
200	350	31.8	8.8

Current Limit 2 – IEM maximum current density and MEC hydraulic limit

The AGC Selemion and Nafion membranes used in this research when installed in commercial electrolyzers typically operate at current densities of approximately 5 kA/m², and in the range of 4 to 6 kA/m² (Selemion, 2019a).

As detailed above, this research is utilising a scaled down bench scale MEC, so the current density will possibly be limited by the hydraulics of the MEC. The current (amps) limitation of the experimental MEC were identified in Chapter 4 electrolysis equipment pre-commissioning, where the MEC was trialed using a 100 g Na₂CO₃/L feed to produce NaOH. During these pre-trials the MEC showed stable operation at a current of 5 amps (1.4 kA/m²) for a period of several days. Over shorter periods the MEC was operated at 10 amps (2.8 kA/m²), imposing a higher cell resistance, which may over longer periods of time cause the MEC to increase in temperature.

For comparison, in a similar experiment performed by (Simon et al., 2014b) where NaOH was produced from analytical grade NaCl, NaHCO₃ and Na₂CO₃ using an AGC Engineering Ltd, Japan electrolysis cell with Selemion cation exchange membrane, the maximum current density utilised was 900 A/m².

Based on the above, a maximum current setpoint of 5 amps (1.4 kA/m²) was considered a reasonable maximum setting for Chapter 5, where the MEC was evaluated under all other parameters.

Current Limit 3 – Evaluation of impact on Green Liquor leaving MEC Anode

It is a research objective to identify the impact on the Green Liquor leaving the electrolysis cell. As current density increases relative to the Green Liquor feed and concentration the impact on the anode discharge will increase. In order of increasing reduction potential, the following will happen to the Green Liquor (Chapter 2 reference equations in brackets):

1. Na_2S :
 - a. Oxidised to S-precipitate, Na^+ ions migrate across the IEM to cathode (2.78)
 - b. S-precipitate will combine with available NaOH to form Na_2SO_3 (2.85)
 - c. With decreasing pH as OH^- is consumed, Na_2S (colourless) will convert to NaHS (yellow) (2.2, 2.3)
 - d. As all the $\text{Na}_2\text{S}/\text{NaHS}$ is oxidised to Na_2SO_3 , discharge will go turn white/clear
 - e. Some S-precipitate will present in the anode discharge
2. Na_2CO_3 :
 - a. Oxidised to CO_2 and O_2 , Na^+ ions will migrate across the IEM to cathode (2.80)
3. $\text{Na}_2\text{S}_2\text{O}_3$ and Na_2SO_3 :
 - a. Will be oxidised to Na_2SO_3 and Na_2SO_4 respectively, if NaOH is available (2.83, 2.84).

To drive the reduction of the Green Liquor all the way from step 1 to step 3, the current range is approximately identified in Table 3.4 above. The maximum current density that can be reasonably applied to the electrolysis cell is approximately 10 amps, this will allow for the complete reduction of Green Liquor when the feed flow is 175 mL/hr and 100 g/L, which requires only 8 amps.

3.6 Feed Pre-heater

The temperature of the feed streams to the electrolysis membrane cell will impact on membrane permselectivity and cell resistance (Ran et al., 2017), so its impact will be examined as part of this experimentation.

In the Kraft process, Green Liquor is generally controlled at above 85°C, to affect efficient CaCO₃ settling in the recausticization process.

The temperature range chosen for this experimentation was 40°C to 80°C. 40°C was chosen as the minimum set point as it is above the ambient environment temperature where the experimentation is being performed and can be heated to this point. 80°C was chosen as the maximum set point, as it is in the approximate temperature of typical green liquor commercially. The 40°C difference between the two set points should be sufficient to illustrate the impact of temperature on the electrolysis membrane cell performance.

Preheater design:

The electrolysis cell feed preheater was sized for the maximum heat transfer requirements required, which occurs during highest experimental flow rates with the highest temperature set point.

Maximum conditions chosen were:

- Temperature of feed streams:
 - Anode feed (Green liquor), $T_{Ain} = 10^{\circ}\text{C}$
 - Cathode feed (Demineralised water), $T_{Cin} = 10^{\circ}\text{C}$
 - Electrolysis Cell feed temperature (post preheater), $TEMC = 80^{\circ}\text{C}$
- Flow rates (2 x required maximum):
 - Anode feed (Green liquor), $Q_{Ain} = 500\text{mL/H}$
 - Cathode feed (Demineralised water), $Q_{Cin} = 500\text{mL/H}$

The specific heat capacities of feed solutions are:

- Water = $4.184 \text{ J}\cdot\text{kg}^{-1}\cdot\text{K}^{-1}$
- Sodium Hydroxide (100g/L) = $4.00 \text{ J}\cdot\text{kg}^{-1}\cdot\text{K}^{-1}$ (Solvay Chemicals Liquid Caustic Soda)
- Kraft Green Liquor (100g/L) = $3.0 \text{ J}\cdot\text{kg}^{-1}\cdot\text{K}^{-1}$

The specific heat capacity of Kraft Green liquor decreases with increasing dissolved solids from 100g/L to 150g/L.

For preheater sizing, a heat capacity of $4.2 \text{ J}\cdot\text{kg}^{-1}\cdot\text{K}^{-1}$ was chosen for all streams to ensure the preheater heating element was not undersized. The minimum required heating element size is hence:

$$P = [(Q_{anode} \times SG_{brine}) + (Q_{cathode} \times SG_{water})] \times c_p (T_{HXout} - T_{HXin}) \times \frac{1 \text{ hour}}{3600 \text{ sec}} \quad (3.14)$$

Where:

$P (W)$ = Heating element (minimum) power capacity (W)

Q_{anode} = Feed flowrate to anode (green liquor) (mL/hour)

SG_{brine} = Specific Gravity of Green liquor solution (kg/L)

$Q_{cathode}$ = Feed flowrate to cathode (water/NaOH solution) (mL/H)

SG_{water} = Specific Gravity of water (kg/L)

c_p = Specific heat capacity ($4.2 \text{ J}\cdot\text{kg}^{-1}\cdot\text{K}^{-1}$)

T_{HXout} = Temperature of preheater outlet (353.15K)

T_{HXin} = Temperature of preheater feed (283.15)

Based on the above conditions, at 100% heat transfer efficiency, the maximum heating power requirement is 82 watts.

The preheater was comprised of a 2,000mL steel heating vessel containing propylene glycol heating fluid with 500-watt cartridge heating element. The temperature of the preheater was controlled to within $\pm 2^\circ\text{C}$ of a temperature set point using a thermostat. Items are displayed in Figure 3.8 below.



Figure 3.8: Electrolysis membrane cell feed preheater – Clockwise from top left:

- 2000mL preheater vessel (filled with propylene glycol heat transfer solution)
- Preheater heat exchange tubing (316SS) – 6mm (4.5mm internal diameter)
- Inkbird Preheater temperature controller
- 500-watt preheater cartridge element

To allow the feed solutions to increase in temperature to the feed setpoint, it was required that the internal heat exchange tubing (see Figure 3.8) had sufficient surface area to allow required heat transfer.

As per above, the highest rate of heat transfer was required when the feed solution temperature was lowest and temperature setpoint highest. The temperature of the preheater was set above the temperature set point (85°C).

T_{HXin} = Temperature of feed brine into preheater = 10°C

T_{HXout} = Temperature of feed brine leaving preheater = 80°C

T_{HX} = Temperature of preheater heat transfer fluid (propylene glycol) = 85°C

This gives the following log mean temperature difference across the heater exchanger tubing:

$$dT_{mean} = \frac{(T_{HX} - T_{HXout}) - (T_{HX} - T_{HXin})}{\ln\left(\frac{(T_{HX} - T_{HXout})}{(T_{HX} - T_{HXin})}\right)} \quad (3.15)$$

$$dT_{mean} = 25.8^{\circ}\text{C}$$

The heat exchange tubing chosen is 6mm 316 stainless steel tube (4.5mm internal diameter).

The overall heat transfer coefficient for the preheater is calculated using equation below:

$$\frac{1}{U \times A_m} = \frac{1}{h_1 \times A_1} + \frac{dx_{wall}}{A_m \times k_{316SS}} + \frac{1}{h_2 \times A_2} \quad (3.16)$$

Where:

U = Overall heat Transfer Coefficient for preheater (W/m²K)

A_m = Overall mean surface area of preheater tubing

h_1 = Heat transfer coefficient of brine at $T_{HXin} + dT_{mean}$.

= 2000W/m²K (Source Perry. Low turbulence, so free convection only)

h_2 = Heat transfer coefficient of propylene glycol at 85°C

= 800W/m²K (Source Perry. Low turbulence, so free convection only)

A_1 = Tube internal surface area per unit length (m²/m) – 4.5mm internal diameter.

A_2 = Tube external surface area per unit length (m²/m) – 6mm outside diameter.

dx_{wall} = Tube wall thickness (m)

k_{316SS} = Thermal conductivity of 316SS

= 14.3 W/m.K

Solving for the universal heat transfer coefficient, U, for the preheater at highest flowrate (500mL/H) and highest temperature (80°C) the result is:

$$U = 499.8 \text{ W/m}^2.\text{K}$$

For the maximum heating requirement of 82watts, a minimum tube length of 362mm was required.

The preheater as shown in Figure 3.8 above has 500mm of 6mm 316 stainless steel heat exchange tube for each feed line, exceeding the minimum requirement for temperature control.

3.7 Experimental Flowsheet

Figure 3.9 below shows the experimental flowsheet used for all Green Liquor trials (Chapter 5 and 6).

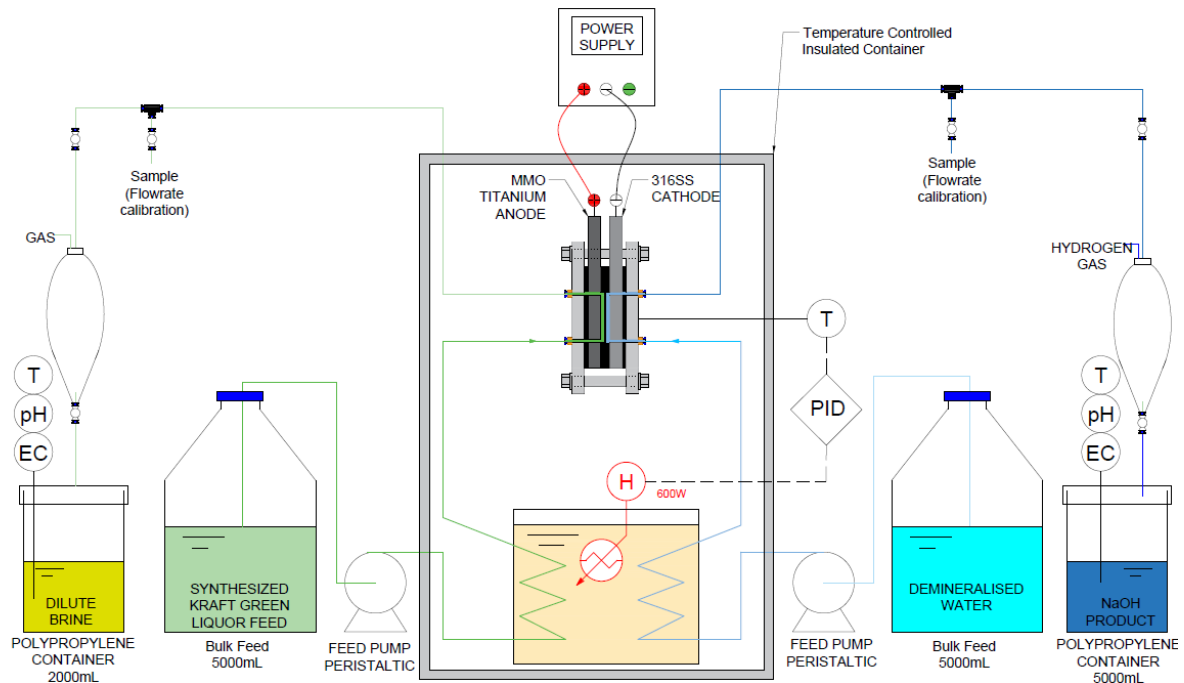


Figure 3.9: Experimental flowsheet

Referring to Figure 3.9, the electrolysis membrane cell and feed preheater were stored within an insulated container to control the equipment to the temperature setpoint of the feed preheater.

The equipment arrangement on either side of the electrolysis membrane cell was mirrored with a BT100M variable speed peristaltic pump (see Figure 3.10 below) with chemical resistant Norprene peristaltic hose. On either side of the electrolysis membrane cell, the pumps drew Green Liquor and water from feed storage tanks and transferred it to the preheater via 4mm (2.5mm internal) polyurethane tubing. From the preheater to the electrolysis membrane cell outlet, again 4mm polyurethane tubing was used.

On the discharge of the electrolysis cell, larger 6mm polyurethane tubing was used. The larger tubing diameter was required on the discharge due to the production of gas within the electrolysis cell, which needed to be released as efficiently as possible to avoid accumulation within the cell and increasing cell resistance.

The 6mm tubing discharged into 250mL polypropylene separation flasks before feeding into the product tanks. The purpose of the separation flask was to allow for gas liquid separation and simple sample collection.

Two programmable power supplies were used during the experimentation. For lower currents (0.5 to 3.0A), a Tenma 72-2685 linear adjustable power supply was used. For higher currents (3.0 to 40.0A), a Powertech MP-2091 laboratory power supply was used. These are shown below in Figure 3.10.



Figure 3.10: Experimental Equipment

(Clockwise from top left): BT100M Variable Speed Peristaltic Pump, Tenma 72-2685 benchtop power supply (0 to 3.0A) and Powertech MP-3091 benchtop power supply (3.0A to 40A)

3.8 Experimental Measurements

Each experimental trial was video recorded, and the following online measurements were logged continually:

- MEC voltage
- MEC current
- MEC cell temperature

The following measurements were recorded with regular sampling and verification:

- NaOH concentration (mol/L) – MEC cathode discharge
- Gas production rate (L/H) – MEC cathode (hydrogen)
- MEC anode and cathode feed flowrates (mL/hr)

The above measurements were required to calculate the MEC NaOH production efficiency (MJ/kg NaOH) for comparison to the conventional Kraft process.

Key experiments were chosen where the impact on the Kraft Green Liquor was most significant. In these experiments regular samples of the anode product were taken to verify:

- Change in Green Liquor discharge (MEC – anode):
 - Remaining Na and S concentration in liquid phase
 - Remaining carbonate and hydroxide in liquid phase
 - Composition of any precipitate

3.8.1 Electrolysis Cell Voltage and Current

The MEC power supply was programmed to modulate the cell voltage to achieve the experimental current set point.

The programmable power display detailing instantaneous cell current, and voltage was continually captured by the video camera recording each experiment. The programmable power supply gave readings to a current resolution of 0.01 amps and voltage to 0.01 volts.

A Fluke 17B+ digital multimeter was used verify the cell power supply reading whenever the current setpoint was adjusted during each trial, with no error being detected.

3.8.2 Electrolysis Cell Temperature

During each experiment, the MEC cell and preheater were placed inside a polystyrene container to insulate the experimental equipment to help maintain the equipment at consistent temperature.

The MEC preheater was controlled to a temperature set point by the Inkbird Temperature controller. A temperature setpoint is input into the temperature controller, for example 42°C, and the heating element is triggered to start when the temperature of the cell drops below 40°C.

An Inkbird temperature logger was placed inside the insulated container to monitor the ambient temperature inside. Being in the same container as the preheater in a relatively small space, the ambient temperature inside the insulated container closely followed the temperature of the preheater.

The outside temperature of the MEC cell components was periodically checked using a Stanley Infrared Thermometer (Stht0-77365), accurate to within 2°C. This was used to measure the temperature of the MEC outer plates, anode, and cathode. These readings were only taken periodically as they required opening the insulated container, and unlike the preheater, which was in direct contact with the MEC feed, was considered a less accurate indication. The infrared temperature measurement was primarily used during the initial start-up of each experiment, to verify that the MEC unit had reached the experimental temperature set point.

3.8.3 NaOH Concentration (MEC Cathode discharge) – Standard Titration

For each experimental trial current set point two 14mL samples were taken of the MEC cathode discharge, once the cell voltage had stabilised. Stabilisation took approximately 60 minutes after the current setpoint was adjusted and two samples 15 minutes apart were taken to confirm stable concentration of NaOH (mol/L).

The concentration of NaOH in each sample was confirmed twice by standard titration procedure using 0.1M HCl titrant and phenolphthalein indicator.

3.8.4 NaOH Concentration (MEC Cathode discharge) – Electrical Conductivity

In experimental pre-trials, Chapter 4, the MEC anode NaOH was recirculated to the anode feed reservoir with large enough volume to immerse an online conductivity meter (YSI Professional Plus – Multiparameter).

As the MEC anode product was almost a pure NaOH aqueous solution, conductivity can be used as an online measurement for NaOH by referencing concentration vs electrical conductivity data tables and graphs (Rosemount_Analytical, 2010).

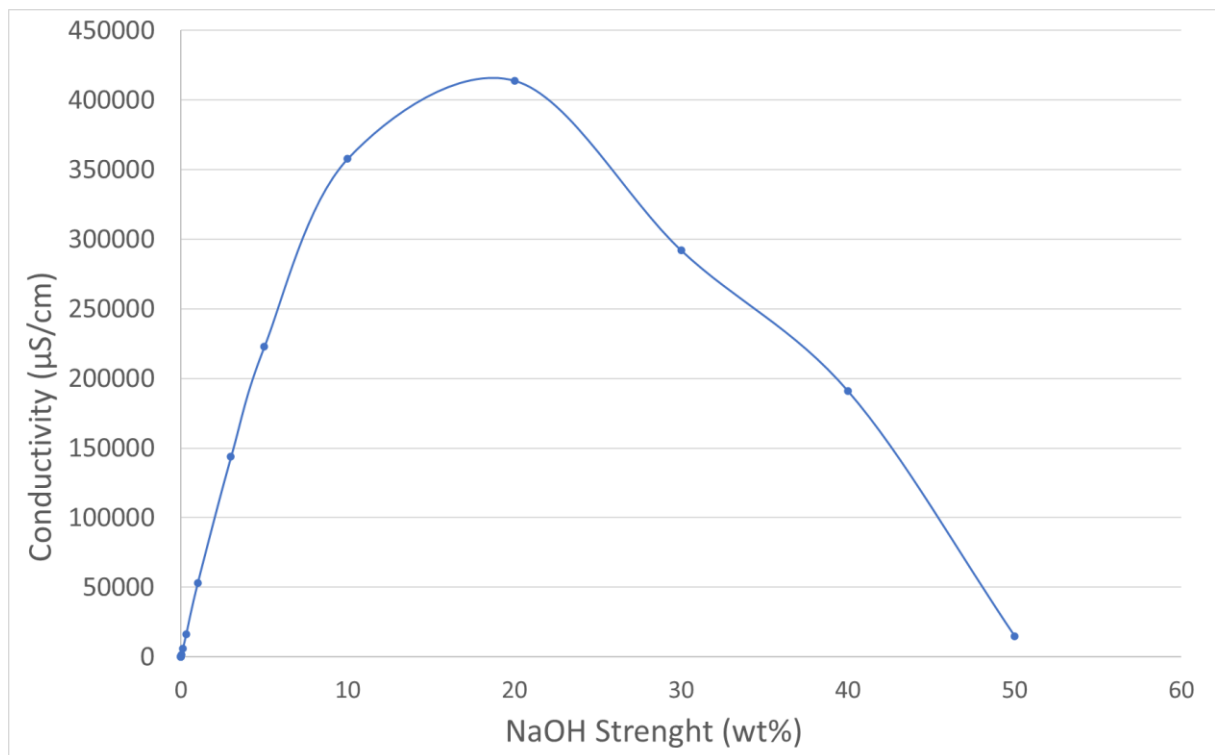
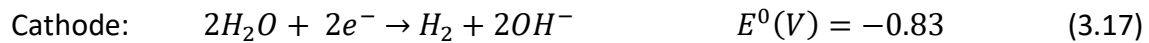


Figure 3.11: Electrical Conductivity (µS/cm) vs NaOH (wt%)
(Rosemount_Analytical, 2010)

3.8.5 Gas-Hydrogen Production Measurement

In all electrolysis experiments, either a demineralised water stream or a 100g/L NaOH solution were supplied to the cathode. As the reduction potential for H₂O is lower than NaOH, the reaction at the cathode was:



Hydrogen gas was produced at the cathode and measuring the rate that it was being produced was used as a direct comparison to the current imposed to confirm cell performance.

The production rate of hydrogen gas at the cathode was measured by collecting the gas in a 100mL volumetric flask over a timed period (t).

To collect the hydrogen in the 100mL flask (V), the flask was first filled with demineralised water by submerging it in a larger vessel to evacuate all air. The flask was then turned upside down with its neck still submerged under water, to not allow any water or gas to escape.

The discharge line from the electrolysis cell cathode was then diverted to the inlet of the flask underwater, discharging all H₂ gas into the flask and displacing the water in the flask. The time (t) taken to displace 100mL of water was measured to allow the calculation of a volumetric flow rate, Q (L/hr).

The temperature (T) of the demineralised water vessel was recorded as it would be close the final temperature of the hydrogen gas after it has bubbled through it. Local atmospheric pressure (P) conditions were recorded also. This allowed for the calculation of molar production rate (\dot{n}) of H₂ gas as per the ideal gas formula:

$$\dot{n} = P \times V \div (R \times T) \times \left(\frac{3600sec/hr}{t} \right) \quad (3.18)$$

Where:

\dot{n} = molar production of H₂ gas (moles/hr)

P = atmospheric pressure (Pa),

V = Volume of the flask (0.0001 m³)

R = Gas constant (8.3145 J.K⁻¹.mol⁻¹)

T = Temperature of gas (K)

t = Time taken for H₂ to fill 100mL flask (sec)

3.8.6 MEC feed flow rates (Q_{anode} , $Q_{cathode}$)

The feeds to the cathode and anode were supplied by BT100M variable speed peristaltic pump. The peristaltic pump chemical tubing was selected based on chemical resistance to strong NaOH and N₂S solution and the design flow range for the experimental trials. For all trials MasterFlex® 06442-12 Chem-Durance® Bio Norprene tubing was used in the peristaltic pump.

During experimental commissioning (Chapter 4), the peristaltic pump speeds were fine tuned to achieve the targeted flowrates 175 and 350 mL/hr, which were linearly related to the peristaltic pump speed at 10% and 20% respectively.

At the beginning of each trial (Chapter 5 and 6), the condition of the peristaltic pump tubing was inspected for any deformation and replaced if necessary. Following this, the anode and cathode peristaltic pump suction lines were connected to the respective feed tanks and discharges to the inlets of the MEC feed preheater, as per Figure 3.9 above. With the power supply turned off, the peristaltic pumps were then started at the trial speed (10% for 175 mL/hr) and circulated through the MEC equipment. The MEC, preheater and tubing were confirmed as being charged with solution once it began to be discharged into the conical separation flasks above the product tanks.

The peristaltic pump flowrates were then confirmed by closing the valve on the conical separation flask discharge and capturing a volume (V) over a time (t) of 10 minutes or greater. The volume was measured in a 25mL or 50mL measuring cylinder, depending on the volume captured. The flowrate (Q) was confirmed by:

$$Q_{pump} = \frac{V}{t} \quad (3.19)$$

The flow measurement was repeated twice per pump for each experimental trial. The peristaltic pumps performed well, as measured flowrates were consistent with pump speed for all experimental trials. The peristaltic hose was changed every 4 trials, so no hose deformation was ever detected, which assisted pumping consistency also.

3.8.7 MEC Molar Production of NaOH (N_{Prod})

The voltage potential across the MEC drives the electrolysis of Kraft Green Liquor, predominantly Na_2CO_3 and Na_2S , transporting Na^+ ions across the IEM towards the cathode. H_2O is fed to the cathode, where it is electrolysed to OH^- and H_2 gas. The OH^- combines with the Na^+ ions transported across the IEM to form NaOH.

The rate of NaOH production (N_{Prod}) is calculated using (3.20) below.

$$N_{Prod} \left(\frac{\text{mol}}{\text{hr}} \right) = M[\text{NaOH}]_{out} \times Q_{Cathode} \quad (3.20)$$

Where:

$M[\text{NaOH}]_{out}$ = Molar concentration of NaOH in cathode discharge (mol/L)

$Q_{Cathode}$ = Volumetric flow rate of the cathode (L/hr), as measured by method (3.8.6)

In experiments where a NaOH solution (100g NaOH/L) is fed to the cathode, the calculation becomes:

$$N_{Prod} \left(\frac{\text{mol}}{\text{hr}} \right) = (M[\text{NaOH}]_{out} - M[\text{NaOH}]_{feed}) \times Q_{Cathode} \quad (3.21)$$

Where:

$M[\text{NaOH}]_{feed}$ = Molar concentration of NaOH in cathode feed (mol/L).

3.8.8 Current Efficiency (ϵ)

The voltage potential across the MEC drives a current of Na^+ across the IEM. If the MEC has 100% current efficiency, then the molar transport of Na^+ ions across the membranes and production rate of NaOH will follow Faraday's law. This theoretical 100% molar transport rate (N_{100}) is calculated using (3.22).

$$N_{100} \left(\frac{\text{mol}}{\text{hr}} \right) = \frac{I \text{ (C/sec)}}{96485 \text{ (C/mol)}} \times \left(\frac{3600 \text{ sec}}{1 \text{ hr}} \right) \quad (3.22)$$

However, the MEC does not deliver 100% current efficiency because of current leakage across the CEM. The previously described Nernst-Planck equation can be used to explain current leakage. Whilst the electro potential gradient across the membrane is by far the most significant factor driving cation transport in the MEC, cations can be convectively transported

across the CEM by water due to a pressure differential, or ion diffusion can occur due to a negative concentration gradient across the CEM.

The MEC current efficiency (ε) was calculate using (3.23).

$$\varepsilon(\%) = \frac{N_{Prod}}{N_{100}} \times 100\% \quad (3.23)$$

3.8.9 Specific Energy for NaOH Production (kJ/mol NaOH)

The energy requirement of the MEC to produce a unit mass of NaOH is central to its evaluation against the conventional Kraft process. For each experimental data point, the cell voltage (V) and current (I) are recorded to give the instantaneous power (P) to the MEC.

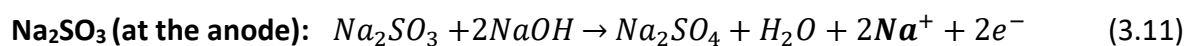
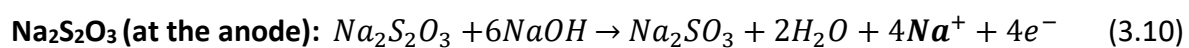
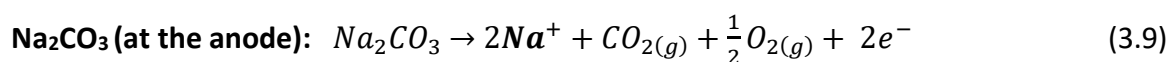
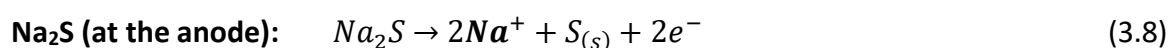
$$P \left(\frac{kJ}{hour} \right) = V \left(\frac{J}{C} \right) \times I \left(\frac{C}{sec} \right) \times \left(\frac{3600 \text{ sec/hr}}{1000 \text{ J/kJ}} \right) \quad (3.24)$$

The energy requirement (E_{NaOH}) per mole of NaOH, E_{NaOH} , produced is given by:

$$E_{NaOH} \left(\frac{kJ}{mol \text{ NaOH}} \right) = P \left(\frac{kJ}{hr} \right) \div N_{Prod} \left(\frac{mol}{hr} \right) \quad (3.25)$$

3.8.10 Impact on Green Liquor – MEC Anode Discharge

The extent of impact on the Green Liquor leaving the MEC anode proportional to current applied relative to the anode feed concentration and flow rate. As per above, the following key reactions were occurring:



As per reactions above, with increasing current applied to the MEC, the following will occur to the MEC discharge:

- Decreasing concentration of Na^+ as it migrates across the IEM towards the cathode.
- Some sulphur, S, precipitate presenting in the discharge as S^{2-} is oxidised to $S_{(s)}$, as per equation (3.8)

- Decreasing concentration of carbonate, CO_3^{2-} , as it is converted to CO_2 and O_2 at the anode, as per equation (3.9).
- Decreasing concentration of hydroxide, OH^- , as:
 - It combines with $\text{S}_{(s)}$ to reform Na_2S , as per equation (3.2)
 - It combines with $\text{Na}_2\text{S}_2\text{O}_3$ and is oxidised to Na_2SO_3 , as per (3.10)
 - It combines with Na_2SO_3 and is oxidised to Na_2SO_4 , as per (3.11)
- As carbonate and hydroxide are consumed, the Green Liquor feed pH, 14, will decrease. If all the Na_2S , $\text{Na}_2\text{S}_2\text{O}_3$ and Na_2SO_3 are oxidised, it will be predominantly the neutral salt Na_2SO_4 .

To measure and evaluate the impact MEC has on the Green Liquor leaving the anode, key experiments were chosen where the impact on the Green Liquor would be greatest, which was when MEC current density was highest relative to Green Liquor feed flow rate and concentration. Samples were taken at each current set point and the Green Liquor liquid, and any precipitate was analysed.

Inductively Coupled Plasma Optical Emission Spectrometry (ICP-OES)

ICP-OES is an analytical technique used for the detection of chemical elements. It is a type of emission spectroscopy that used the inductively coupled plasma to produce excited atoms and ions that emit electromagnetic radiation at wavelengths characteristic of a particular element (EPA, 2018). ICP-OES was used to measure the remaining sodium and sulphur in the MEC anode discharge.

Due to their high concentration of total dissolved solids, over 100 g/L, the Green Liquor samples were diluted, and samples were digested with strong acid on heating block. The parameters analysed in the ICP-OES analysis are detailed in Table 3.5 below.

Table 3.5: ICP-OES Analysed Elements

Element	Symbol	Reason for selection in ICP-OES Analysis	Anticipated range of result (mg/L)
Sodium	Na	Main element present	Very high presence
Sulphur	S	Main element present	Very high presence
Potassium	K	Can be a trace contaminant of NaOH and Na ₂ CO ₃	Trace presence
Calcium	Ca	Trace contaminant of make-up water	Trace presence
Iron	Fe	Trace contaminant in Na ₂ S	Trace presence
Iridium	Ir	Oxide coating on titanium cathode	Trace presence

HCl Acid Titration – Green Liquor Na₂CO₃ and NaOH Measurement

As per reactions (3.8), (3.9), (3.10) and (3.11) above, as the current applied to the MEC increases the hydroxide and carbonate present is being consumed, decreasing the pH of the Green Liquor leaving in the anode discharge.

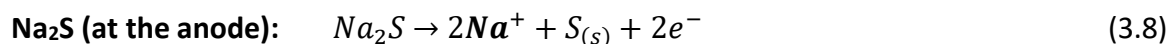
A 902 Titrande (Figure 3.12 below) high-end potentiometric titrator was used to measure the remaining Na₂CO₃ and NaOH concentration in the MEC anode discharge via method of endpoint titration.



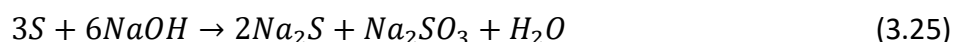
Figure 3.12: Metrohm 902 Titrande Potentiometric Titrator for endpoint titration

Scanning Electron Microscopy (SEM) – Green Liquor Discharge Precipitate Composition

As per reaction (3.8) the reduction of Na_2S at the cathode will produce a sulphide precipitate.



Some of this precipitate reacts with available NaOH in the Green Liquor feed to form Na_2S and Na_2SO_3 as per (3.25).



A precipitate presented in the MEC anode discharge in most trials, generally presenting in greater quantity with higher current set points relative to Green Liquor feed flow and concentration. The precipitates were separated from the bulk liquid by first siphoning off the bulk liquid to the point that only a slightly wet solid precipitate remained, visually greater than 50% precipitate. Figure 3.13 below shows an example of solid precipitate settled at bottom of 14mL sample vile before liquid is siphoned off.



Figure 3.13: Example of precipitate formed at bottom of an MEC anode sample
(Prior to liquid being syphoned off)

The fine granular precipitate was removed from the sample with a small spatula, leaving most of the remaining liquid, but was still slightly wet. The quantity of solid precipitate removed is shown in Figure 3.14 below.



Figure 3.14: Trial 14 (Chapter 5) – Example MEC precipitate extracted.

Image shows precipitate on Scanning Electron Microscope sample mount (10mm diameter).

The very small amount of precipitate extracted was placed on sample mounts for analysis using Scanning Electron Microscopy (SEM), as shown in Figure 3.14. The sample mounts were 10mm in diameter and had pure carbon adhesive tape to attach the precipitate. The samples were fully dried before analysis, as were platinum coated in a vacuum chamber before analysis in the SEM.

The relatively small sample amount made physical measurement of mass before and after drying impractical. The presence of liquid introduced analysis error of the actual precipitate, as soluble elements (Na_2CO_3 , Na_2SO_3 , Na_2SO_4) in the liquid would add to the final precipitate being analysed once dried.

The Scanning Electron Microscope used was the ThermoFischer Phenom Pharos G2 Desktop FEG-SEM, as shown in Figure 3.15 below. The FEG-SEM performs elemental analysis (EDS) using x-ray spectrometry by method of silicon drift X-ray radiation detection. It incorporates a silicon nitride (SiN_x) window for detection of elements from Boron (B) to Californium (Cf) (ThermoFischer_Scientific). The detector can scan and analyse a precipitate surface area of 25mm^2 and give a reading in the form of an atomic concentration and weight concentration.

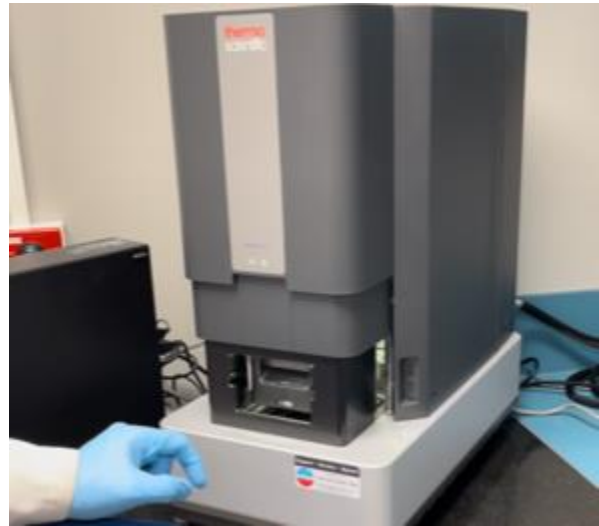


Figure 3.15: Thermoscientific Phenom Pharos G2 Desktop FEG-SEM

Clockwise from top left: Vacuum precoating of samples; Thermoscientific Phenom Pharos G2 Desktop FEG-SEM Scanning Electron Microscope; SEM image display; Microscope display of samples in SEM unit

3.9 Start Up and Pre-Trial Performance Verification Procedure:

Prior to starting each experimental trial, a standard start-up procedure was performed, followed by an equipment integrity test. A standard 100g Na₂CO₃/L solution was used as anode feed as per Figure 3.16 below.

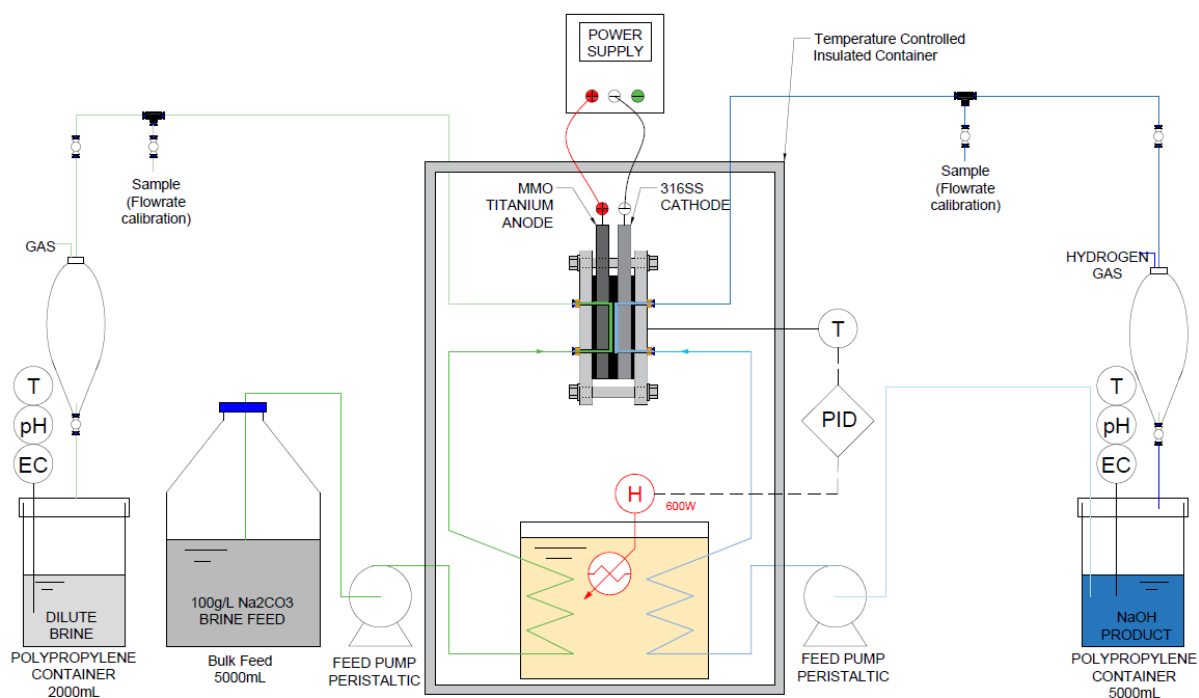


Figure 3.16: Experiment Schematic – Preparation and standardised test.
(Constant 100g/L Na₂CO₃ feed)

The purpose of this standard procedure was to ensure the repeatability of results and to ensure proper operation of the experimental equipment before beginning experiments using Kraft Green liquor.

The key performance indicator for each pre-start trial was the MEC voltage at which the system was stabilised. After verifying MEC feed flowrates, preheater temperature, current set point, if voltage stabilised at a level higher or lower than normal, it would be an indicator of a problem with the experimental set up.

Errors in experimental set up that may cause a higher MEC resistance or voltage could be:

- A leak or blockage on one of the feed lines to the MEC causing reduced feed flow.
- A restriction on the MEC discharge causing a build-up of gas within the cell
- A poor or disconnected electrical connection to the electrodes

Errors in experimental set up that may cause a reduced MEC resistance or voltage could be:

- A tear or hole in the membrane resulting in leakage between the anode and cathode.
- A short circuit in the power supply to the MEC

All the above issues were always unlikely to occur, with the only issue that ever presented on occasion being small leaks on the MEC feed line due to bad push fitting connections made during assembly. This was always identified during the pre-trial integrity test and fixed before starting the main experiments.

3.9.1 MEC charging and Preheater Start-up

In this standard start up procedure the MEC was charged with demineralised water at the cathode and a standard solution of sodium carbonate (100g/L Na_2CO_3) at the anode for sufficient time to allow a minimum of three full passes of the system. The preheater was set to 40°C, a temperature it would reach within 2 or 3 minutes from start-up.

The volume of electrolysis cell that must be charged, on each side of the membrane, was:

- Electrolysis Membrane Cell: 14cm³
- Feed Preheater tubing: 5cm³
- Polyurethane tubing: 3 cm³
- Total volume: 22cm³

The feed peristaltic pumps were set at 175 mL/h. The minimum charging time was 15 minutes, which allowed for three full fluid passes of the MEC.

3.9.2 Standard MEC Integrity Test

Without changing any other parameter, the electrolysis cell current (power supply) was set to 3 amps. The cell was allowed to run for 45 minutes to confirm stabilisation of voltage (resistance) across the membrane.

This result was compared to previous experimental runs to confirm integrity of the experimental arrangement. A sample of the NaOH product was taken for later titration to confirm molar concentration and the hydrogen production rate was also measured.

Once confirmed, the 100g/L Na₂CO₃ solution feed was changed for Kraft Green liquor and depending on the experiment, the demineralised water was changed to NaOH solution or remained as demineralised water feed.

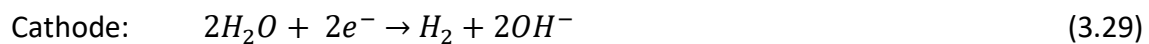
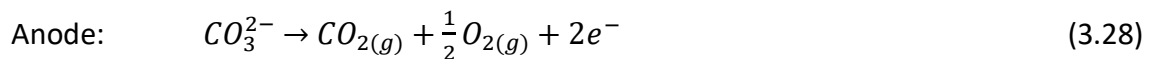
The standard MEC integrity test was performed before every experimental trial and the results are presented in Figure A.2.

3.10 Performance of MEC with Na₂CO₃ Feed (Chapter 4)

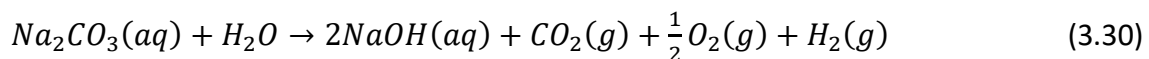
This series of three experiments used a 100 g Na₂CO₃/L single solute as substitute for Green Liquor. The objective of these experiments was the development of the experimental arrangement and methods to be used with a Green Liquor feed solution in Chapter 5 and 6.

The electrolysis of Na₂CO₃ is as follows:

Half Reactions:



Overall:



With a voltage imposed across the MEC, CO₃²⁻ ions at the anode are oxidised to CO_{2(g)} and O_{2(g)}. Sodium ions migrate through the CEM to the cathode compartment and combine with the hydroxide ions from the reduction of water at the cathode to produce NaOH.

A series of experiments were identified that would substantiate progression to a mixed solute synthetic Green Liquor solution:

1. Effect of “Zero Gap” versus “Open Channel” MEC Configurations
2. Voltage stabilisation time after current change
3. Production of NaOH solution greater than 3.0 M (120 g NaOH/L)

3.10.1 Effect of “Zero Gap” versus “Open Channel” MEC Configuration

This set of experiments evaluated the merit of the anode and cathode membrane supports to confirm if they should be used in subsequent experiments using Green Liquor.

Two experiments were performed, one with membrane supports in a “zero gap” configuration and one without supports in an “open channel” configuration. In the “zero gap” configuration the anode membrane support was iridium oxide coated expanded titanium mesh and the cathode membrane support was a woven pillow of nickel mesh. In the “open channel” arrangement there was a 5mm gap between the electrodes and the membrane. All other process parameter settings for the “zero gap” and “open channel” experiments were identical and are given in Table 3.6.

Table 3.6: “Zero Gap” versus “Open Channel” Experiment Settings

Parameter		Setting
Preheater Temperature Set Point		60°C
Cell prestart recirculation (no power)		15 minutes
Current Set Point (Target)		1 amp
Membrane		AGC Selemion SX-1811 (Balanced grade IEM for selectivity and low voltage)
Membrane area		6cm x 6cm
ANODE	Cell Arrangement:	Closed loop
	Feed Reservoir Volume	1000 mL
	Feed Na ₂ CO ₃ concentration (g/L) at start of trial	100 g/L
	Feed (recirculation) flow rate	200 mL/hour
CATHODE	Cell Arrangement:	Product returned to Feed
	Feed Reservoir Volume	1000 mL
	Feed NaOH concentration (g/L) at start of trial	0 g/L (Demineralised water)
	Feed (recirculation) flow rate	200 mL/hour

The arrangement for both experiments in Figure 3.17 shows the product streams from the anode and cathode were returned to their respective feed reservoirs in a closed loop arrangement. Change in concentration of NaOH at the cathode and Na₂CO₃ at the anode was monitored using online conductivity sensors as per Figure 3.11 and with final concentration of NaOH confirmed using HCl titration.

Before commencing each experiment, the standard MEC charging procedure was performed (section 3.9.1), then the standard integrity test (section 3.9.2). Following this the MEC process

parameters were set to those in Table 3.6, where the MEC current set point on the programmable power supply was set to 1 A (278 A/m²).

During each experiment the cell voltage was recorded as a measure of cell resistance as the MEC stabilised after the change in current set point. The merit of “zero gap” vs “open channel” arrangement was evaluated based on time taken for the MEC to stabilise after initialising a current set point change, and the final voltage that the systems stabilised at.

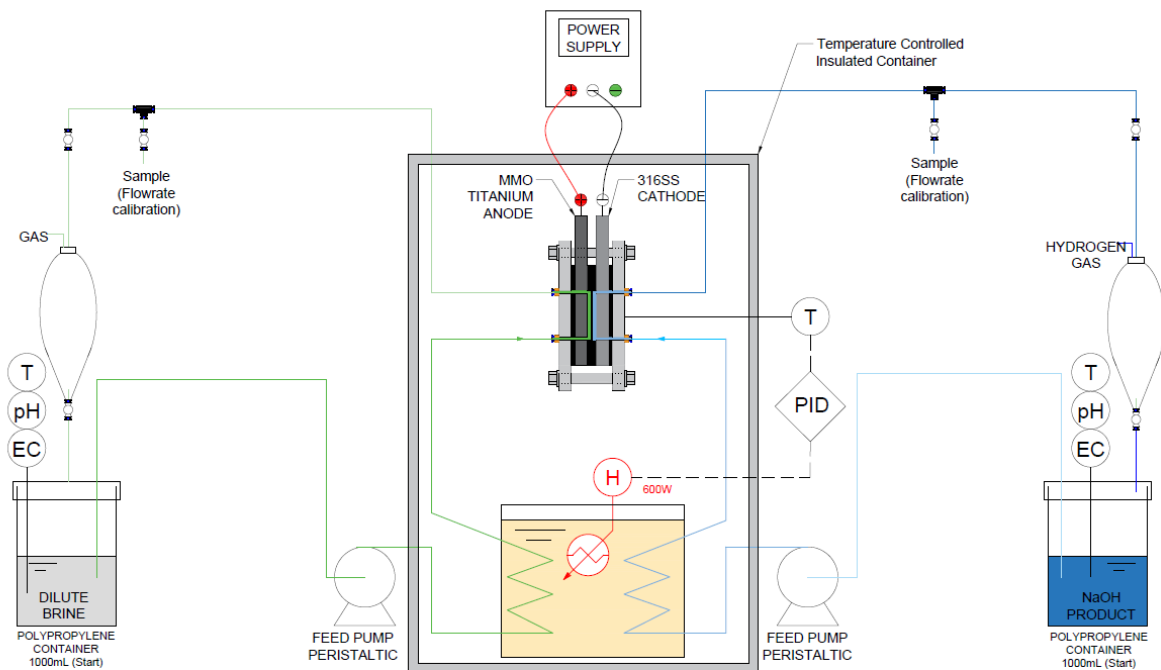


Figure 3.17: Experimental Schematic - “Zero Gap” versus “Open Channel”

3.10.2 Voltage Stabilisation Time After Current Adjustment

The objective of this experiment was to monitor how long the MEC voltage takes to stabilise after a current set point change. Observations made during this experiment was used to design experiment procedures used in subsequent experiments using Green Liquor.

In this experiment the discharge from the anode and cathode was not returned to the feed solution, so the feed concentration to the anode and cathode remained constant throughout.

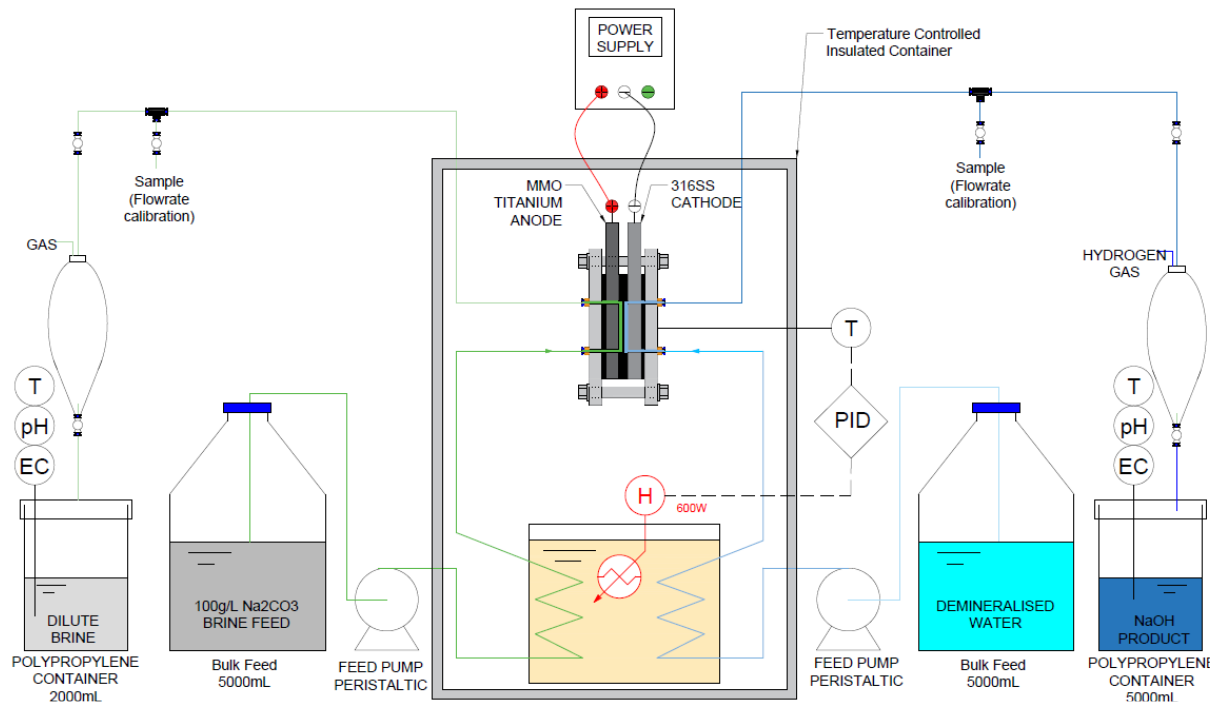


Figure 3.18 – Experimental Schematic - “Voltage Stabilisation Time”

The experimental details of Pre-Trial 2 are given in Table 3.7.

Table 3.7: Trial 2 Operation Setpoints

Parameter		Set Point
Preheater Temperature Set Point		60°C
Cell prestart recirculation (no power)		15 minutes
Current Set Point (Target)		0.5, 1.0, 1.5, 0.5, 1.0
Membrane		AGC Selemion SX-1811 (Balanced grade IEM for selectivity and low voltage)
ANODE	Cell Arrangement:	Product to separate vessel
	Membrane Support	Iridium oxide coated pressed titanium mesh “Zero-Gap”
	Feed Reservoir Volume	1000 mL
	Feed Na ₂ CO ₃ concentration (g/L) at start of trial	100 g/L
	Feed flow rate	350 mL/hour
CATHODE	Cell Arrangement:	Product to separate vessel
	Membrane Support	Woven Nickel mesh “Zero-Gap”
	Feed Reservoir Volume	1000 mL
	Feed NaOH concentration (g/L) at start of trial	0 g/L (Demineralised water)
	Feed (recirculation) flow rate	350 mL/hour

3.10.3 Production of Strong NaOH Solution by Recirculation of Anode Product

In pre-trial 3 the MEC was arranged in a flow through arrangement as per Figure 3.19. This trial was run for an extended period (12 days) where fresh Na_2CO_3 solution (100 g/L) was fed to the anode at a constant rate, and the feed to the cathode was recirculated. As the MEC anode product was returned to the anode feed, the concentration of NaOH gradually increased in concentration.

The purpose of pre-trial 3 was to observe the performance of the MEC over an extended period, and the impact of recirculating the MEC anode product back to the feed. An online conductivity sensor was installed in the anode feed reservoir as an online indicator of NaOH concentration, as per Figure 3.11.

Apart from the observed increase in concentration of NaOH in the anode feed, any change in volume in aqueous solution in the anode feed reservoir was an indication of water being transported across the IEM.

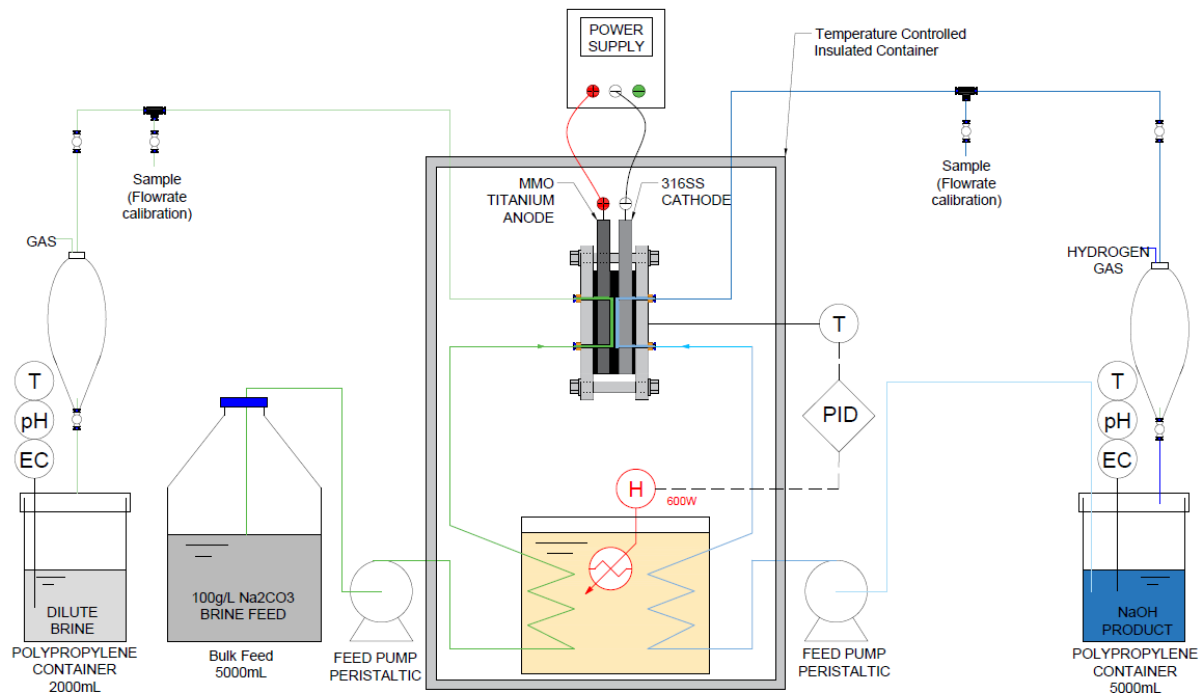


Figure 3.19 – Experimental Schematic - “Production of Strong NaOH Solution”

The experimental details of Pre-Trial 3 are given in Table 3.8.

Table 3.8: Pre-Trial 3 Settings

Details		Trial 3
Preheater Temperature Set Point		60°C
Cell prestart recirculation (no power)		15 minutes
Current Set Point (Target)		1.5 to 3.0 amps
Membrane		AGC Selemion SX-1811 (Balanced grade IEM for selectivity and low voltage)
ANODE	Cell Arrangement:	Product to separate vessel
	Membrane Support	Iridium oxide coated pressed titanium mesh "Zero-Gap"
	Feed Na ₂ CO ₃ concentration (g/L)	100 g/L
	Feed flow rate	350 mL/hour
CATHODE	Cell Arrangement:	Product Recirculated to Feed
	Membrane Support	Woven Nickel mesh "Zero-Gap"
	Feed Reservoir Volume	Starting Volume = 1000 mL
	Feed NaOH concentration (g/L) at start of trial	0 g/L (Demineralised water)
	Feed (recirculation) flow rate	350 mL/hour

3.11 Establishing Operating Parameters Using Synthesized Green Liquor

In the experimental pre-trials (Chapter 4) an experimental arrangement was developed and fine-tuned by trialling a 100g/L Na_2CO_3 solution feed to the anode and demineralised water to the cathode. Practical current density and flow ranges for the more complex Green Liquor solution were identified and for the electrolysis cell.

The objective of Stage 1 experiments (Chapter 5) was to evaluate the potential for this experimental arrangement to regenerate Kraft Green liquor. The successful regeneration of Kraft Green liquor was assessed based on the efficiency of conversion of Na_2CO_3 to NaOH , the preservation of the required Na_2S and the minimisation of unwanted deadloads. The experimental arrangement for these trials is shown in Figure 3.20 below.

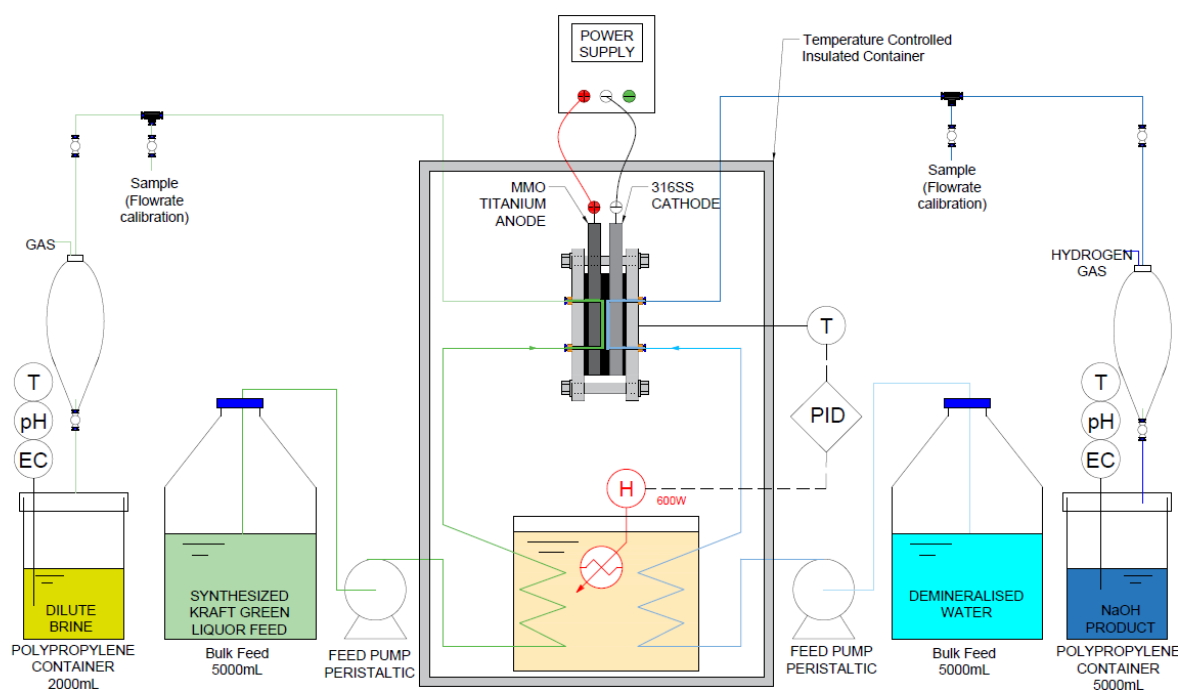


Figure 3.20: Experimental Schematic for trials with Kraft Green Liquor

Each of parameters detailed in Table 3.9 were systematically varied to measure and evaluate their impact on the electrolysis cell performance and identify optimal settings for Kraft Green Liquor recovery. As detailed in Table 3.9, anode (Green Liquor) feed flow, anode (Green Liquor) feed concentration, cathode (NaOH) feed concentration and MEC feed temperature were all evaluated across two data points, requiring a total of 16 experimental trials. In each trial, 5 current settings were also tested. Table 3.10 below lists the 16 trials performed, where trials 14 and 16 were also repeated to confirm results.

Table 3.9: Stage 1 Experimental Parameters

Parameter	Number of Data Points	Low Point	High Point
Anode (Green Liquor) Feed Flow, (mL/hr)	2	175	350
Anode (Green Liquor) Feed Strength (g/L)	2	100	150
Cathode (Demin/NaOH) Feed Flow (mL/hr)	1	175	175
Cathode (NaOH) Feed Strength (g/L)	2	0	100
Preheater temperature (°C)	2	40	80
Total Number of Trials =	(2 x 2 x 2 x 2) = 16		
Current settings (amps)	5	1	5
Minimum number of data points:	16 x 5 = 80		
Membrane	AGC-9010		

Varying four experimental parameters across two data points, as detailed in Table 3.9, required 16 experimental trials. Table 3.10 below details the 16 trials and their respective operation settings for each trial. Each trial also includes five current setpoints, giving a total of 80 experimental data points.

Table 3.10: Stage 1 Experimental Trials Operation Settings (5 Current set points per trial)

Trial Number	Feed Temperature (°C)	Anode (Green Liquor) Feed Flow (mL/hr)	Anode (Green Liquor) Feed Concentration (g/L)	Cathode (NaOH) Feed Concentration (mL/hr)	Cathode (NaOH) Feed Concentration (g NaOH/L)
1	40	175	200	175	0
2	80	175	200	175	0
3	40	350	200	175	0
4	80	350	200	175	0
5	40	175	200	175	100
6	80	175	200	175	100
7	40	350	200	175	100
8	80	350	200	175	100
9	40	175	100	175	0
10	80	175	100	175	0
11	40	350	100	175	0
12	80	350	100	175	0
13	40	175	100	175	100
14*	80	175	100	175	100
15	40	350	100	175	100
16*	80	350	100	175	100

*Trials 14 and 16 were repeated to confirm results. The anode discharge from these trials was evaluated to confirm impact on Kraft Green Liquor leaving MEC anode discharge.

In each experimental trial in Stage 1, the AGC-9010 membrane was selected. This AGC-9010 membrane was selected because it is the AGC-Selemon latest generation fluorinated ion exchange membrane used to produce NaOH in electrolysis membrane plants. It is PTFE fabric reinforced for high mechanical strength and temperature tolerance, which makes it suitable for contact with Kraft Green Liquor and the temperature ranges used in this experimental trial.

At the beginning of each trial, the standard start-up procedure was performed, where the MEC equipment was first primed as detailed in section 3.9.1 and followed by the standard integrity check as per section 3.9.2.

Following this, the MEC was changed to Kraft Green Liquor feed and the experimental trial started. Each trial included 5 current set points, starting from 1 amp, and increasing to 5 amps in increments of 1 amp. As informed by pre-trial tests (Chapter 4), the MEC was allowed to stabilise for 60 minutes for each current setpoint. The standard schedule for each experimental trial is detailed in Table 3.11 below, which also details the MEC cathode (NaOH) and anode (Green Liquor) discharge sampling schedule, and the schedule for H₂ gas production measurements at the cathode discharge as per section 3.8.5 above.

Table 3.11: Standard Schedule for each Experimental Trial

Time Interval Start	Time Interval End	Stage	Anode Feed	Sampling Schedule		
				Cathode		Anode Sampling (Green Liquor)
				NaOH (15mL)	H ₂ gas flow measurement	
0:00:00	0:15:00	Priming Period	100 g/L			
0:15:00	0:30:00		Na ₂ CO ₃			
0:30:00	0:45:00	Membrane Integrity Test	100 g/L Na ₂ CO ₃			
0:45:00	1:00:00					
1:00:00	1:15:00					
1:15:00	1:30:00			Sample 0		
1:30:00	1:45:00	Start-up Stabilisation	Synthesized Green Liquor			
1:45:00	2:00:00					
2:00:00	2:15:00	1 Amp	Synthesized Green Liquor			
2:15:00	2:30:00					
2:30:00	2:45:00			Sample 1		
2:45:00	3:00:00			Sample 2		Sample 1
3:00:00	3:15:00	2 Amp	Synthesized Green Liquor			
3:15:00	3:30:00					
3:30:00	3:45:00			Sample 3		
3:45:00	4:00:00			Sample 4	Measurement	Sample 2
4:00:00	4:15:00	3 Amp	Synthesized Green Liquor			
4:15:00	4:30:00					
4:30:00	4:45:00			Sample 5		
4:45:00	5:00:00			Sample 6	Measurement	Sample 3
5:00:00	5:15:00	4 Amp	Synthesized Green Liquor			
5:15:00	5:30:00					
5:30:00	5:45:00			Sample 7		
5:45:00	6:00:00			Sample 8	Measurement	Sample 4
6:00:00	6:15:00	5 Amp	Synthesized Green Liquor			
6:15:00	6:30:00					
6:30:00	6:45:00			Sample 9		
6:45:00	7:00:00			Sample 10	Measurement	Sample 5

3.11.1 MEC NaOH Production Performance Evaluation

Section 3.8 above detailed the experimental measurements taken during each trial.

The measurements taken allowed the calculation of MEC current efficiency (ϵ) which is a key parameter for the comparison of each experimental arrangement.

Combining MEC current efficiency to the logged MEC voltage (V) allowed the calculation of units NaOH generated per unit energy supplied (E_{NaOH}). This is the key parameter that was used in the comparison of MEC Kraft Green liquor NaOH production to the conventional Kraft recausticization process.

3.11.2 MEC Impact on Kraft Green Liquor (Na₂S)

Section 3.8 above detailed the experimental measurements taken to evaluate the impact on Kraft Green Liquor in the MEC discharge. Two key trials were chosen to achieve the research objectives:

- Characterisation of any precipitated solids in the anode liquid discharge to confirm Na₂S reduction to sulphide precipitate.
- Measurement of remaining Na and S of the anode liquid discharge
- Measurement of remaining carbonate and hydroxide in the Green Liquor discharge as an indication of reduction of deadload Na₂CO₃ in the Green Liquor.

Referring to Table 3.10 above, trials 14 and 16 were chosen because they have the lowest Green Liquor feed concentration (100 g/L) relative to cell current, so the impact on the Green Liquor is most significant. Trials 14 and 16 were chosen over trials 10 and 12, because a 100 g NaOH/L solution feed to the cathode was more reflective of what an actual Kraft Green Liquor MEC recovery process requires.

Trials 14 and 16 were run to higher current ranges, up to 10 amps and 16 amps respectively to display the effect on the Kraft Green liquor towards its limit of available Na₂CO₃ and Na₂S.

3.12 Comparison of Membrane Performances

The optimal MEC cell settings identified during experimental Stage 1 (Chapter 5) were trials 7 and 8 and the conditions are detailed in Table 3.12 below.

Table 3.12: Trial Settings

Trial Number	Anode Feed Strength-GC (g TDS/L)	Anode Feed Flowrate-GF (mL/hr)	Cathode Feed Strength-CC (g TDS/L)	Feed Preheater Temperature-T (°C)
7	200	350	100	40
8	200	350	100	80

In stage 2 experimentation (Chapter 6) these settings identified were applied to a series of different IEMs with differing design characteristics. The same experimental arrangement and schedule as Stage 1 was adopted, as detailed in Figure 3.20 and Table 3.11 above.

3.12.1 Ion Exchange Membranes (IEMs) Selection

A key difference between the trialled IEMs was their designed resistance and selectivity for the transport of Na⁺ ions.

AGC-Selemon SX-1831 (SELEMION(AGC), 2018)

- Low resistance/voltage membrane for high capacity – low selectivity
- Fluorinated cation exchange membrane for electrolysis and electro-dialysis. All materials that make up the membrane (including the reinforcement fabric) are fluorinated resins for robust chemical resistance.
- PTFE fabric reinforced for high strength for operation and handling

AGC-Selemon SX-1811 (SELEMION(AGC), 2018)

- Balanced grade ion exchange membrane for ion selectivity and low voltage.
- Fluorinated cation exchange membrane for electrolysis and electro-dialysis. All materials that make up the membrane (including the reinforcement fabric) are fluorinated resins for robust chemical resistance.
- PTFE fabric reinforced for high strength for operation and handling

AGC-Selemon SX-2301WN (SELEMION(AGC), 2018)

- Higher membrane resistance for high cation selectivity
- Fluorinated cation exchange membrane for electrolysis and electro-dialysis. All materials that make up the membrane (including the reinforcement fabric) are fluorinated resins for robust chemical resistance.
- PTFE fabric reinforced for high strength for operation and handling

AGC-Selemon SX-2301WNY (SELEMION(AGC), 2018)

- Based on the SX-2301WN membrane but has gas-releasable zirconia coating on both surfaces leading to lower electrical resistance.

AGC-Selemon F-9010 (Selemon, 2019a)

- Latest generation fluorinated ion exchange membrane used to produce NaOH in electrolysis membrane plants.
- Irreversible, having carboxylic layer preventing OH⁻ from passing through the layer
- Zirconia coating on both surfaces of the membrane
- Chemically resistant to chlorine and NaOH
- PTFE fabric reinforced for high mechanical strength and temperature tolerance
- Low resistance with high current efficiency

Dupont Nafion N-324

- Perfluoro sulfonic acid (PFSA) cation exchange membrane

- Irreversible membrane
- Chemically resistant to chlorine and NaOH
- PTFE fabric reinforced for high mechanical strength and temperature tolerance

Table 3.13 below summarises the membrane structural characteristics.

Table 3.13: Membrane Structural Characteristics (SELEMION(AGC), 2018)

Parameter	SX-1831	SX-1811	SX-2301WN/ SX-2301WNY	F-9010	N-324
Counter ion	Na ⁺	Na ⁺	Na ⁺	Na ⁺	Na ⁺
Thickness (μm)	360	330	330	150	150
Ion exchange capacity (meq/g)	1.25	1.1	1.0	1.0	>0.92

3.12.2 IEM Performance Evaluation

In this series of trials, the IEM selection in the electrolysis cell was the only parameter that was varied allowing for the direct comparison of performance. The key evaluation criteria again would be:

- MEC voltage (V)
- MEC current efficiency (ϵ)
- Resultant energy requirement to produce NaOH, E_{NaOH} (MJ/kg)

Low resistance membranes with higher designed exchange capacity would display lower MEC voltage, however lower cell current efficiency. The objectives of the IEM trials and performance comparisons was to identify the preferred IEM type, high or low resistance, for Kraft Green Liquor recovery.

Chapter 4 Performance of MEC with Na₂CO₃ Feed

The primary focus of this chapter is to assess the performance of the MEC using a standard single solute solution of Na₂CO₃, allowing direct comparison with similar experiments performed by other researchers such as (Simon et al., 2014b) and allowing confirmation of the settings necessary for further experimentation.

The results from three experiments using a 100 g Na₂CO₃/L feed solution as a substitute for Green Liquor are presented. The outcome of these experiments was the development of the experimental arrangement and methods to be used with a Green Liquor feed solution in Chapter 5 and 6.

A series of experiments were identified that would substantiate progression to a mixed solute synthetic Green Liquor solution:

1. Effect of “Zero Gap” versus “Open Channel” MEC Configurations
2. Voltage stabilisation time after current change
3. Production of NaOH solution greater than 3.0 M (120 g NaOH/L)

4.1 Effect of ‘Zero Gap’ and ‘Open Channel’ feed Configurations.

The objective of this experiment was to evaluate the merit of the anode and cathode membrane supports to confirm if they should be used in subsequent experiments using Green Liquor.

The functions of the electrically conductive membrane supports are:

- Provide structural support to the membrane during operation,
- Promote the even distribution of feed across the membrane surface, and
- Extend the anode and cathode up to the membrane surface, reducing the distance of ionic movement through the catholyte and anolyte, potentially decreasing the cell resistance. This is referred to as “zero gap”.

Two experiments were performed, one with membrane supports in a “zero gap” configuration and one without supports in an “open channel” configuration. In the “zero gap” configuration the anode membrane support was iridium oxide coated expanded titanium

mesh and the cathode membrane support was a woven pillow of nickel mesh. In the “open channel” arrangement there is a 5mm gap between the electrodes and the membrane.

The common parameters used in both “zero gap” and “open channel” experiments were.

- Preheater temperature set point: 60°C
- Current set point: 1 amp (278 amps/m²)
- Membrane: Selemion SX-1811 (Balanced grade IEM for selectivity and low voltage)
- Anode feed: 100 g Na₂CO₃/L at 200 mL/hr
- Cathode feed: Demineralised water at 200 mL/hr

The arrangement for both experiments is shown in Figure 4.1 showing the product streams from the anode and cathode were returned to their respective feed reservoirs in a closed loop arrangement. Change in concentration of NaOH at the cathode and Na₂CO₃ at the anode were monitored using online conductivity sensors as per Figure 3.11, with the final NaOH concentration confirmed by HCl titration.

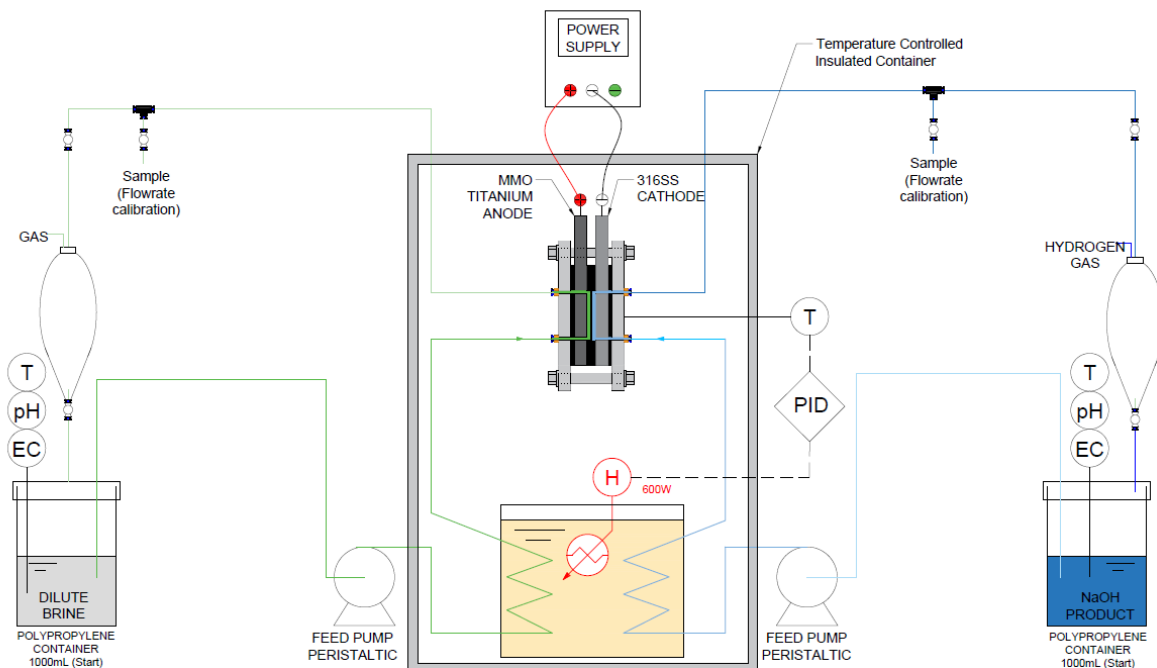


Figure 4.1: Flowsheet – Open Channel versus Zero Gap

During each experiment the cell voltage was recorded as a measure of cell resistance and the electrical conductivity of the product NaOH was logged using an online analyser, as described in section 3.8.4. The concentration of the final NaOH product was confirmed by standard titration method using 0.1M HCl titrate.

Before commencing each experiment, the standard MEC charging procedure was performed, then the standard integrity test. Following this the MEC process parameters were set to the experiment process parameters listed above.

4.1.1 Resistance: Analysis of Effect of Zero Gap versus Open Channel

With the same current (I) applied across the MEC in both experiments, voltage (V) is a direct indicator of MEC resistance (R_{MEC}), as per Ohms Law.

$$R_{MEC} = \frac{V}{I} \quad (4.1)$$

The MEC resistance is the sum of the resistance of the CEM (R_{CEM}), the resistance of the anolyte compartment (R_{anode}) and the resistance of the catholyte compartment ($R_{cathode}$):

$$R_{MEC} = R_{anode} + R_{CEM} + R_{cathode} \quad (4.2)$$

With the same CEM adopted in both experiments any change in overall resistance is attributable to $R_{cathode}$ and R_{anode} . The resistance of either compartment increases with distance (d) between the electrode and the membrane and decreases with increasing compartment electrical conductivity (EC_{anode}) and cross-sectional area (A).

$$R_{anode} = \frac{d}{EC_{anode} \times A} \quad (4.3)$$

With the same feed temperatures, flowrates and concentrations to the anode and cathode, the installation of conductive membrane supports, extending the electrode to the membrane decreases d and should affect a decrease in MEC voltage.

After 2 hours of operation, the MEC voltages had stabilised in both experiments and MEC and the effect on MEC resistance of “zero gap” versus “no gap” could be established. The data is given in Table 4.1 below.

Table 4.1: Experiment 1 – NaOH production

	“Open Channel” Configuration	“Zero Gap Channel” Configuration	Change (%)
Current (A)	1	1	-
Voltage (V)	2.8	2.6	-7.1%
Calculated Resistance, R_{MEC} (Ω)	2.8	2.6	-7.1%

This simple analysis confirms that the conductive membrane supports achieved a 7.1% reduction in overall MEC resistance. This only one data point, however it does confirm the merit of the “zero gap” arrangement and is enough justification to move forward with the use of this arrangement in subsequent experimentation with Green Liquor.

In this experiment, feed concentration to the anode was 100 g Na₂CO₃/L and the feed to the cathode was demineralised water. This implies an anolyte with high electrical conductivity, and a catholyte feed with very low conductivity. Whilst “zero gap” offered a 7.1% decrease in R_{MEC} under these conditions, it would be interesting to evaluate under both lower and higher feed concentration conditions, to evaluate the importance of “zero gap”. Equation 4.2 suggests that as EC_{anode} decreases, R_{anode} increases, so the relative importance of R_{anode} to the overall R_{MEC} increases, so the importance of “zero gap” or d would be greater.

4.1.2 MEC Stabilisation: Analysis of Effect of “Zero Gap” versus “Open Channel”

Figure 4.2 showed the cell voltage and cathode product NaOH trends for the “zero gap” and “open channel” experiments from the moment that a current is first applied across the MEC.

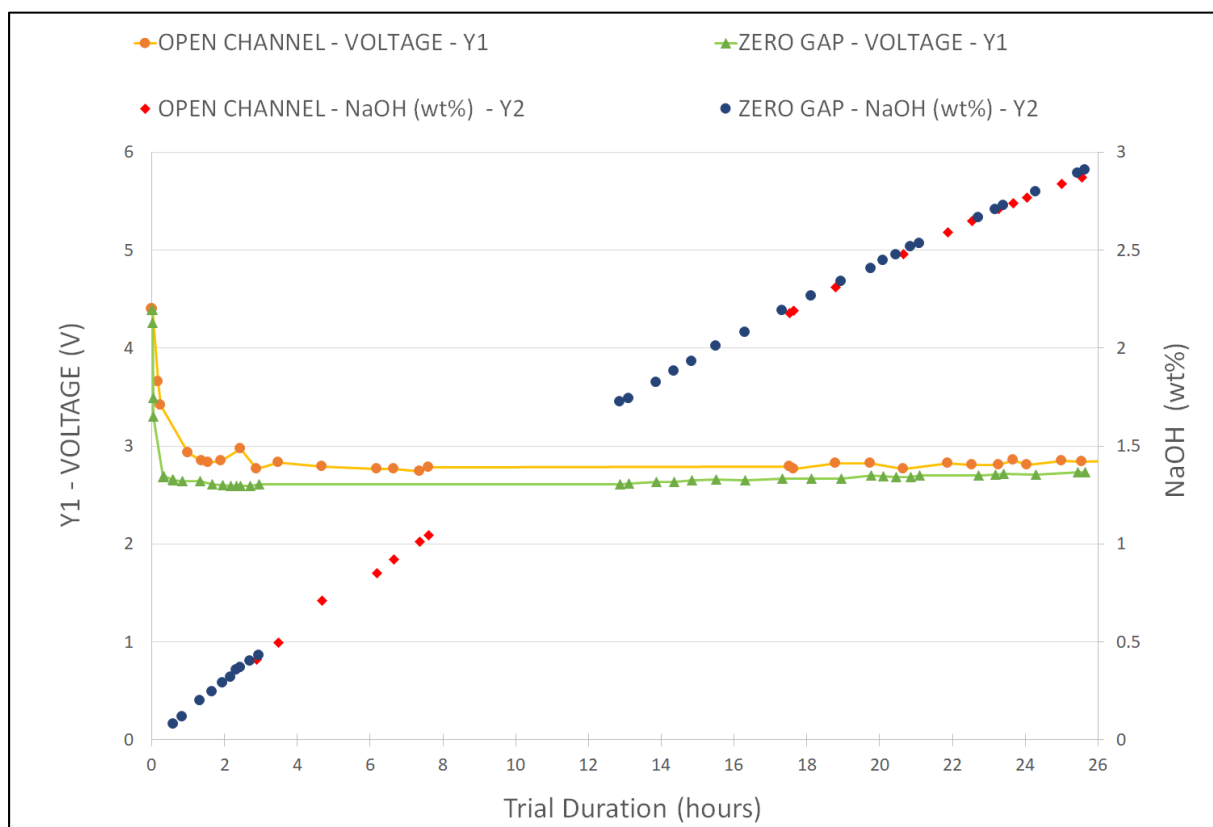


Figure 4.2: Zero Gap versus Open Channel configuration – Voltage and NaOH Production

In both the “open channel” and “zero gap” experiments the starting voltages were both approximately 4.4 V, indicating that at initial start up the resistance of the MEC arrangements were very similar.

However, soon after the current set point is set to 1 A the “zero gap” arrangement settles faster and at a lower voltage than the “open channel” arrangement. In the “zero gap” experiment, voltage reduces from 4.4 V to a stable voltage of 2.6 V within 60 minutes, after which the MEC voltage remains stable, with any variation not exceeding 0.02 V. In comparison, the unrestricted flow path offered by the “open channel” configuration, voltage takes 240 minutes to reduce from 4.4 V to a stable voltage of 2.8 V, and after which there was still some minor instability in MEC voltage of around 0.05 V. The membrane supports promoting the even distribution of feed across the membrane surface can explain the improved stability of the “zero gap” arrangement.

The faster transition to stable voltage exhibited by the “zero gap” arrangement can be attributed to the oxidation and reduction reaction occurring closer to the membrane surface decreasing the distance of ionic movement through solution to the CEM allowing it to stabilise faster. Titanium “zero gap” membrane supports are now commonly retrofitted to existing chloralkali plants, offering the benefit of even distribution of current across the membrane, increase voltage stability (TiAnode, 2022)

4.1.3 Specific Energy (kJ/mol NaOH): Analysis of Effect of “Zero Gap” versus “Open Channel”

With MEC anode product returned to the feed reservoir, the instantaneous concentration of NaOH at the cathode was measured using an electrical conductivity sensor in the cathode feed reservoir. Figure 4.2 shows negligible difference between the measured NaOH in the “zero gap” and “open channel” experiments over time. This result confirms that the conductive membrane supports had negligible impact on MEC current efficiency.

After 24 hours of operation samples were taken from the cathode product and the concentration of NaOH was confirmed using standard titration method. The results of titrations performed on the final NaOH are shown in Table 4.2, which also shows the calculated specific energy of NaOH production for both experiments.

Table 4.2: “Open Channel” versus “Zero Gap” – Specific Energy of NaOH Production

Feed channel configuration	Concentration NaOH after 1440 minutes (mol/L) (Titration)	Volume of NaOH product after 1440 minutes (mL)	Average Cell Voltage (v) over 24 h	Power consumption over 1440 minutes (kJ)	NaOH production rate (kJ/mol)
“Open Channel”	0.693	1100	2.8	242	318
‘Zero Gap’	0.690	1120	2.6	225	291
Change	-0.4%	+1.8%	-7.7%	-7.7%	-9.3%

Table 4.2 shows that the final NaOH concentration for the “zero gap” and “open channel” experiments had negligible effect on produced NaOH concentration, with the final concentrations measured to be within 0.4%. This result coincides with the online conductivity measurements used as an indication of NaOH concentration. This confirms that the conductive membrane supports had negligible impact on MEC current efficiency.

The overall specific energy of NaOH production in a “zero gap” arrangement was 9.3% lower than the “open channel” arrangement at 291 kJ/mol NaOH.

4.1.4 Comparison to Similar Research with 100 g NaCO₃/L Feed

For comparison of results, Simon et al., 2014, produced NaOH from a Na₂CO₃ feed using a similar electrolysis membrane cell arrangement over a current density range of 100 to 900 A/m², a summary of their results is presented in Table 4.3 below.

Table 4.3: NaOH from Na₂CO₃ Comparison experiment performed by Simon et al., 2014

	Simon et al., 2014	‘Zero Gap’ Configuration
Current Density (A/m ²)	300	278
Preheater Temperature (°C)	No Preheater (Ambient temperature)	60
Na ₂ CO ₃ feed concentration (g/L)	100	100
IEM type, (Thickness and resistance type)	AGC Selemion (440 μm, low)	AGC Selemion SX-1811 360 μm, balanced)
MEC Membrane area (cm ²)	200	36
MEC channel depth height (gap) (cm)	0.2	0
Cell Flow (L/H)	0.40	0.20
Specific Energy Requirement (kJ/mol)	833	291

The difference in specific energy requirement between the two experiments can be attributable to many possible factors, including the electrolysis cell membrane area, flow distribution and IEM resistance.

In both experiments with and without mesh the feed was preheated to 60°C decreasing cell resistance, while the feed was not preheated in Simon et al., 2014. The IEM used by Simon et al., 2014 was also stated as being very low resistance, whilst the AGC SX 1811 membrane used in experiment 1 is described by the manufacturer AGC Selemion as a balanced grade ion exchanger membrane for ion selectivity and low voltage. A higher selectivity IEM with favourable IEM concentration gradient will deliver much higher MEC current efficiency than the 55% by Simon et al., 2014.

4.1.5 “Zero Gap” versus “Open Channel”

It has been established that the ‘Zero Gap’ feed channel configuration using a 100g/L Na₂CO₃ solution as a surrogate for Green Liquor generates NaOH at a lower specific energy than “open channel”. The conductive membrane supports had no measurable affect MEC current efficiency, however by decreasing the overall MEC resistance a reduction in overall specific energy was achieved.

Further, the experiments illustrate that voltage stability is established nearly four times faster compared to the open channel configuration. Implementing ‘Zero Gap’ feed channel configuration shows that MEC resistance is reduced, and the time required for the cell to reach equilibrium is significantly reduced. Consequently, all future experiments will adopt the ‘zero Gap’ configuration.

4.2 Voltage Stabilisation Time after Current Adjustment

The purpose of this experiment was to observe the time that the MEC voltage takes to stabilise after a current set point change. The observations during this experiment were used in the design of experimental procedures and the times given for each current set point when using Green Liquor that will be reported in chapters 5 and 6.

In this experiment, the anode feed concentration was kept constant at 100g/L Na₂CO₃. The cathode feed was demineralised water.

This experiment ran for 600 minutes, during which time the current was increased in increments of 0.5 A from 0.5 to 1.5 A, and then back down again. The intention of this current variation pattern was to observe the time required to achieve stable cell voltage and whether the cell would stabilise at the same cell voltage after decreasing back down from higher current set points. The experimental flowsheet is shown in Figure 4.3.

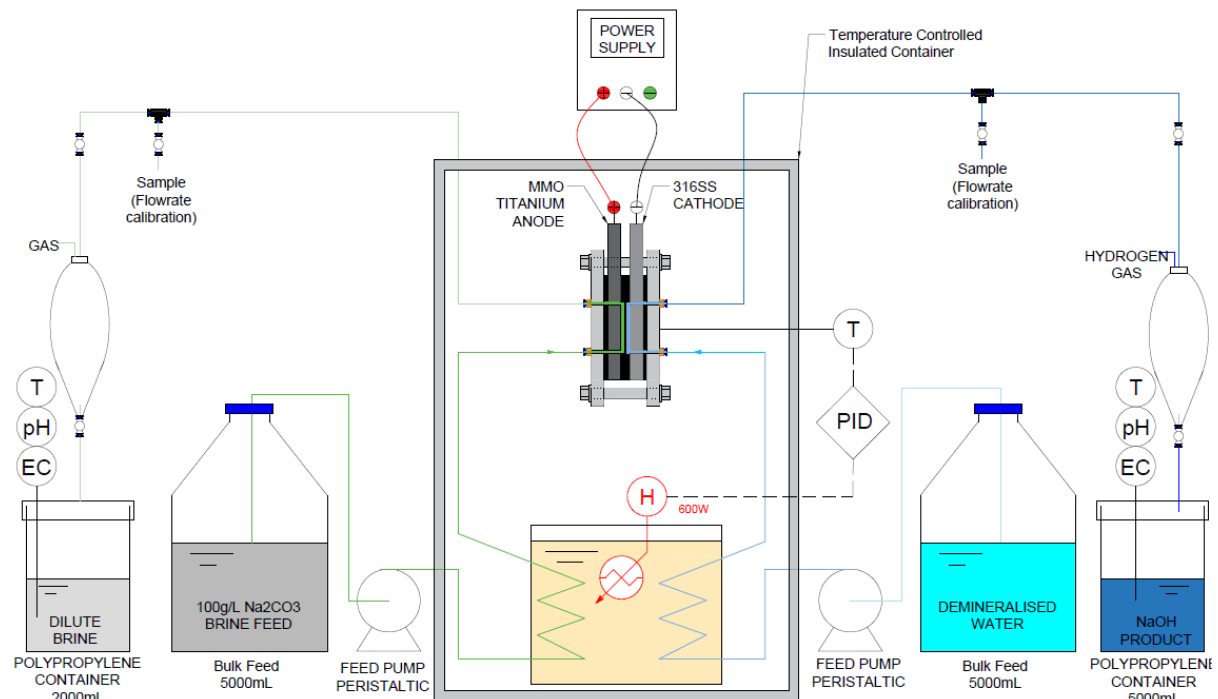


Figure 4.3: Flowsheet – Voltage Stabilisation Time

The parameters used in Experiment 2 are detailed in Table 3.7 in Chapter 3 Experimental Methods. The consistent parameters during Experiment 2 were:

- Preheater temperature set point: 60°C
- Membrane: Selemion SX-1811 (Balanced grade IEM for selectivity and low voltage)
- Anode feed: 100 g Na₂CO₃/L at 350 mL/hour
- Cathode feed: Demineralised water at 350 mL/hour

After starting feed streams to the anode and the cathode for 15 minutes without applying voltage across the MEC, the power supply current set point was adjusted to 0.5 amp and the programmable power supply began controlling the MEC voltage to achieve the set point.

Figure 4.4 below shows the MEC voltage and current trends during this experiment where the MEC current set point was first set to 0.5 amps, voltage allowed to stabilise, increased to 1.0

and then 1.5 amps and allowed to stabilise and then again reduced 0.5 amps and 1.0 amps to confirm the MEC voltage returned to previous voltage.

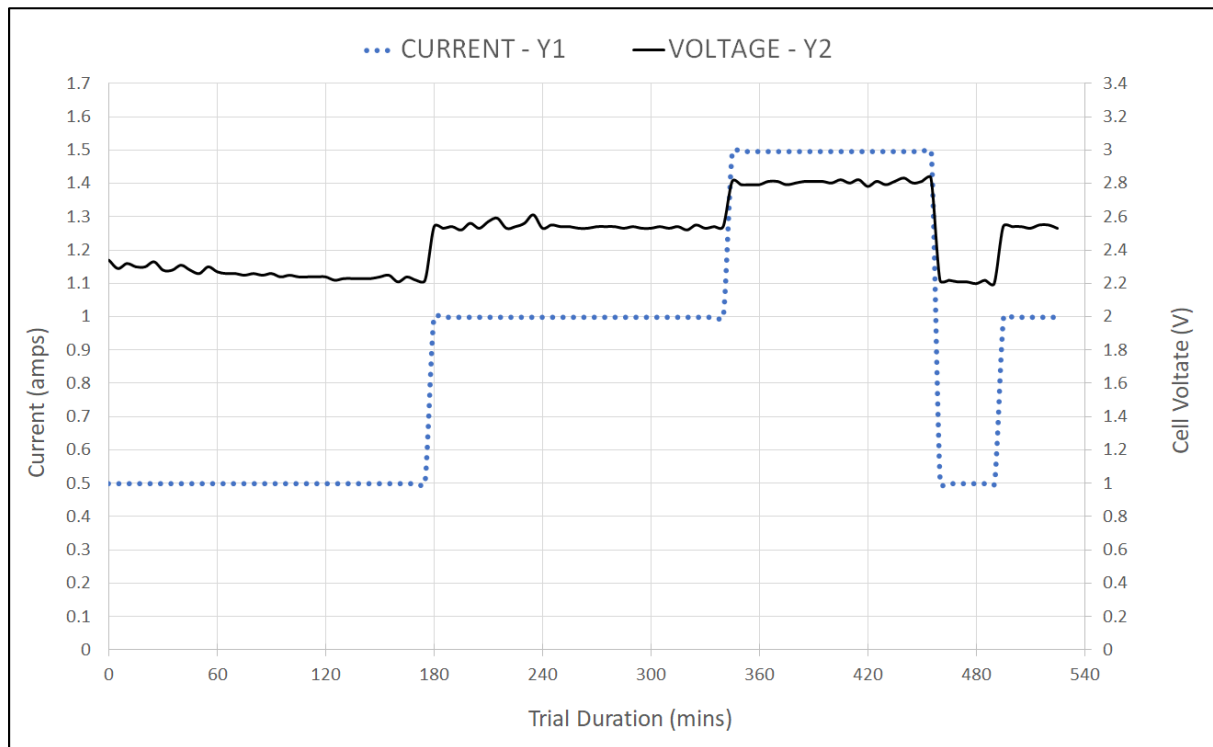


Figure 4.4 – Voltage Stabilisation Time after Current Adjustment

100g/L Na₂CO₃ Feed, Temperature: 60°C, Flow: 350mL/H, Membrane: AGC Selemion

Figure 4.4 shows that after the MEC current set point was set to 0.5 amps, upon start up, the MEC voltage was approximately 2.4 volts, and then took approximately 120 minutes to stabilise at 2.2 volts. After confirming the stable voltage at 180 minutes, the MEC current set point was increased to 1.0 amps and the MEC voltage stabilised at 2.55 volts in a comparatively faster within 60 minutes. To ensure stable voltage, the MEC ran at 1.0 amps for almost another 180 minutes before increasing MEC current to 1.5 amps. Again, the MEC voltage stabilised quickly within 60 minutes, at 2.8 volts.

Following this, when the MEC current set point was returned to 0.5 and then 1.0 amps, the MEC voltage again stabilised at 2.2 volts and 2.55 volts, however on this occasion far more quickly.

4.2.1 MEC Time to Reach Equilibrium

Each time the MEC current set point is adjusted the thermodynamic equilibrium of the system is shifted. At the instant that the MEC current set point is increased, the programmable power

supply automatically increases cell voltage, which increases the rate of oxidation and reduction reactions occurring at the anode and cathode respectively to match the current setpoint as per Faraday's law.

The concentration of free sodium ions (Na^+) at the anode increases, which diffuse through the CEM toward the cathode to preserve electrical neutrality. After the MEC current was first increased from 0 to 0.5 amps, the gradual decrease in MEC voltage from 2.34 to 2.25 volts over 60 minutes shows that the resistance of the system is decreasing over that time. This infers that after the current set point is changed, it took 60 minutes for the MEC to reach thermodynamic equilibrium.

As stated previously the MEC resistance is the sum of resistances across the anode and cathode compartments and the CEM.

$$R_{MEC} = R_{anode} + R_{CEM} + R_{cathode} \quad (4.2)$$

The resistance in the anode and cathode compartments change the electrical conductivity of the compartments. For the anode:

$$R_{anode} = \frac{d}{EC_{anode} \times A} \quad (4.3)$$

The electrical conductivity of the compartment changes with concentration of ions in solution. Given that the feed concentrations and flowrates are kept constant during this experiment, the resistance of the anolyte and catholyte compartments don't change. This means the CEM resistance must be changing in the membrane phase, R_{CEM} .

When current is changed from 0 to 0.5 A, the MEC voltage was initially 2.34 V, before stabilising at 2.25 V after 60 minutes. The decrease in R_{CEM} over that period can be explained by the fact that at the instant before the current was set to 0.5 A, the net flux of Na^+ ions through the membrane close to zero, so the concentration of Na^+ ions in the membrane was less, resulting in a higher R_{CEM} . The moment after the current was set to 0.5 A, a current of Na^+ ions began to diffuse through the CEM, changing the concentration gradient across the membrane and increasing the average concentration of Na^+ ions in the membrane phase, decreasing R_{CEM} .

When the MEC current was increased from 0.5 to 1.0 amps, and then 1.0 to 1.5 amps the time taken for the voltage to stabilise was only 30 minutes. This indicates there was a bigger shift

in thermodynamic equilibrium when the MEC current is increased from 0 to 0.5 amps, than from 0.5 to 1.0 amps or 1.0 to 1.5 amps.

4.2.2 Voltage Stabilisation Time:

The outcomes determined from the experiments using a single solute solution of 100 g/L as Na_2CO_3 provide a system configuration for mixed solute green liquor solution. In summary, the following criteria will be used in experiments in conjunction with Green Liquor.

In Chapter 5 and 6 the MEC experiments will be performed with Kraft Green Liquor under different conditions where current will be adjusted. It is critical that the MEC is allowed to reach equilibrium before any samples or measurements are taken.

Experiment 2 has the following outcomes for the design of MEC experiments with Kraft Green Liquor:

- At the start of all experiments using Green Liquor and reported in Chapter 5 and 6 the MEC Charging, and Preheater Start-up procedure is first followed, detailed in section 3.9.1, running for 30 minutes.
- Following this is the standard MEC Standard Integrity Test, detailed in section 3.9.2 in Chapter 3, running for an additional 60 minutes.
- Following this, the MEC anode feed is switched to Kraft Green liquor for a period of 30 minutes with no voltage applied across the MEC
- Following this, the current set point to the MEC is first switched to 1 amp and allowed to run for 60 minutes before MEC voltage is confirmed stable and cathode product samples (NaOH) are taken.
- The above start up steps add up to a total duration of 180 minutes. The standard schedule for each experimental experiment is detailed in Table 3.11 in Chapter 3.

4.3 Production of Strong NaOH Solution by Recirculation of Anode Product

The objective of this experiment was to confirm that the MEC arrangement can produce a NaOH concentration greater than 2.5 M (100 g/L) by recirculating the cathode product back to the feed reservoir until the concentration target is achieved. The feed to the anode was a single solute 100 g Na_2CO_3 /L solution surrogate for Kraft Green liquor. The anode discharge

was not returned to the anode feed reservoir, so feed concentration to the anode remained constant at 100 g Na₂CO₃/L. The experimental arrangement is given in Figure 4.5.

In future experiments with Green Liquor, a 100 g NaOH/L solution will be used to evaluate the effect of cathode feed concentration on MEC performance. Proving that the MEC can produce a product of 100 g NaOH/L here validates the application of a 100 g NaOH/L feed to the MEC cathode in future Green Liquor experiments.

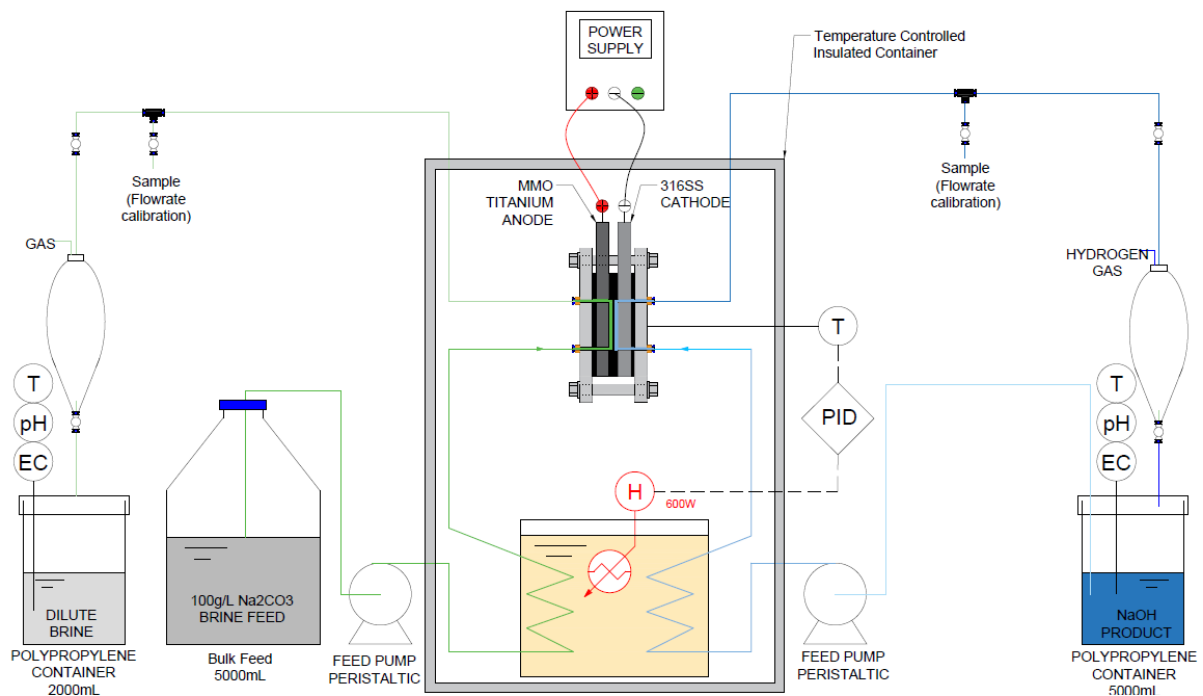


Figure 4.5: Flowsheet Production of Strong NaOH Solution – Anode Recirculation

The process parameters during were:

- Preheater temperature set point: 60°C
- “Zero gap” configuration
- Membrane: Selemion SX-1811 (Balanced grade IEM for selectivity and low voltage)
- Anode feed: 100 g Na₂CO₃/L at 350 mL/hour
- Cathode feed: Demineralised water at commencement at 350 mL/hour recirculated

4.3.1 Production of NaOH Solution

The MEC operated reliably over the 10-day experiment period, eventually producing a NaOH product of 3.5 M (140 g NaOH/L), more than that required by the Kraft Pulping process.

The MEC voltage, current and NaOH molar concentration over time is shown in Figure 4.6 below. The electrical conductivity of the recirculated cathode product was continually monitored over time as indicator of NaOH concentration.

At the commencement of the experiment, the MEC current set point was 1.5 A and the cell voltage remained stable at 2.83 V. After 5 days, the concentration of NaOH at the cathode increased to above 80 g NaOH/L (2.0 M), achieving the required concentration for conventional Kraft pulping.

An important observation over the first 5 days was that the volume of the recirculated NaOH solution had slowly increased from the initial volume of 1000 mL to 1500 mL, indicating the slow transport of water across the membrane from the anode to the cathode was occurring.

Osmotic pressure driving the transport of water from the anode to the cathode is one explanation, however at the beginning of the experiment the cathode feed was demineralised water while the anode feed was 0.94 M Na_2CO_3 , implying a negative osmotic pressure. By day 5, when the molar concentration of NaOH at the cathode had increased to approximately 2.0 M, so gradually the osmotic pressure would begin to favour transport of water toward the cathode, however this does not explain the slow but steady transport of water from the beginning of the experiment.

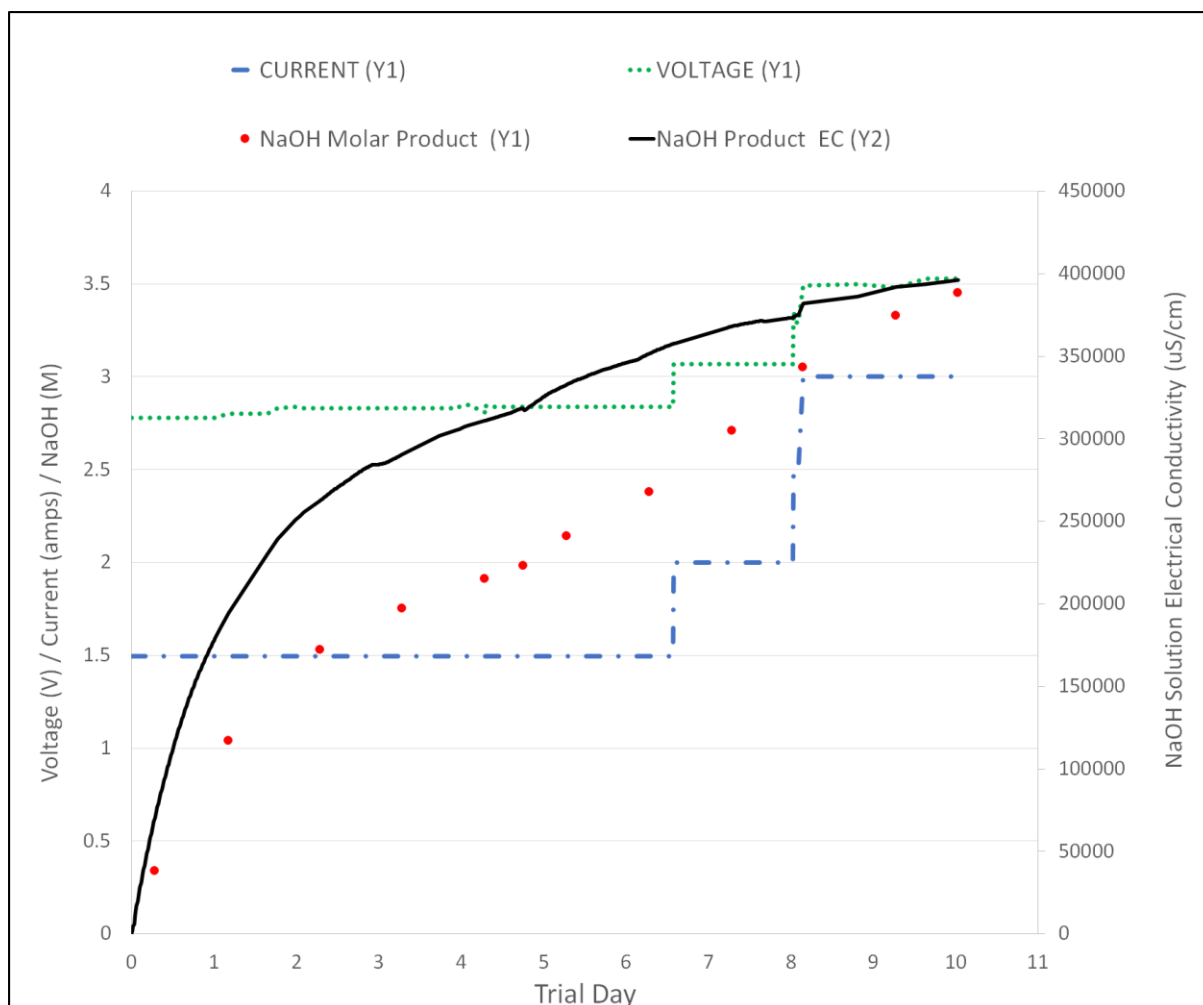
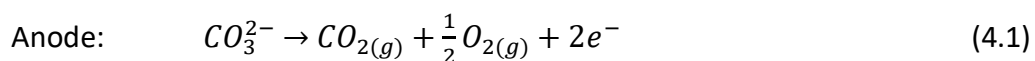


Figure 4.6: Cell Voltage and NaOH Production over Time

The transport of water from the anode to the cathode could also be explained by electro osmosis or a hydraulic pressure differential across the membrane. Electro-osmosis is the motion of a liquid induced by an applied potential across the membrane (Sata, 2007d).

The transport of water from the anode to the cathode could be better explained by a hydraulic pressure differential across the IEM caused by the unequal generation of gas on either side of the IEM.

Recalling the electrolysis reactions occurring at the anode and the cathode are:



At the anode, 1.5 moles of gas are produced ($CO_{2(g)} + \frac{1}{2}O_{2(g)}$), while at the cathode only 1.0 moles of gas are produced (H_2). The inlets (2.5mm ID) and outlets (4.5mm ID) of the electrolysis cell are identical, however given that more gas is produced at the anode, it can be assumed there will be a slight pressure differential across the membrane. Whilst small, any pressure differential will drive the passage of water and transport solute through the membrane.

On day 5, 500 mL was purged from the NaOH product, to return the volume to 1000mL, whilst maintaining the current at 1.5 A. A very slight increase in gradient can be seen in the rate of NaOH concentration increase (EC curve), as the same flux is feeding into a smaller volume. NaOH had increased to 2.5 M by the end of day 7, which exceeds requirement for Kraft pulping of 1.5 M.

On day 7, the cell current was increased to 2.0 A and then again to 3.0 A on day 9. On both occasions. Slight inflections in the EC curve can be seen on both these occasions.

4.3.2 Discussion – Increase in Catholyte Volume and Implications for Green Liquor Experiments:

The observed increase in the recirculated catholyte (NaOH) solution volume over time indicated the transport of water across the IEM due to either an osmotic or hydraulic pressure differential or both. A volume increase became evident after one day of operation and after a period of five days, the cathode feed reservoir was measured to have increased from 1000 to 1500 mL. This indicates an approximate average diffusion rate of 4 mL/hour.

In the Green Liquor experiments the MEC feed flow rate ranges, for both anode and cathode, were from 175 to 350 mL/hour.

With a feed rate of 350 mL/hour to the cathode, an average water diffusion rate of 4 mL/hour through the CEM from the anode represents approximately a one percent dilution of the NaOH product. If the cathode product is diluted by one percent, this would be reflected by a one percent reduction in the calculated MEC current efficiency, which will be considered when discussing results using Kraft Green Liquor.

4.4 Summary of Outcomes

The outcomes determined from the experiments in Chapter 4 using a single solute solution of 100 g/L as Na_2CO_3 provided a system configuration for experiments using mixed solute green liquor solution. In summary,

- The “zero gap” arrangement using conductive membrane supports were shown to decrease MEC resistance, increase system stability and decrease the time required for the MEC to stabilise after start-up so will be used in all future experiments with Green Liquor.
- The observed time taken for the MEC to reach a state of equilibrium after current set point adjustments was used to develop the standard experiment schedule detailed in Table 3.11.
- The MEC was shown to be able to produce a NaOH product concentration of 140 g/L. To evaluate the impact of NaOH feed concentration to the MEC cathode, 0 g NaOH/L (demineralised water) and 100 g NaOH/L feed solutions will be tested with a Green Liquor feed to the anode in Chapter 5 and Chapter 6 investigations.

Chapter 5 ESTABLISHING OPERATING PARAMETERS USING SYNTHESIZED GREEN LIQUOR

The outcomes determined from the experiments in Chapter 4 using a single solute solution of 100 g/L as Na_2CO_3 provided a system configuration for experiments using mixed solute green liquor solution. In this chapter, this system configuration is used to investigate the effect of key process variables on NaOH production using mixed solute green liquor solution.

5.1 Objectives of MEC Green Liquor Trials:

5.1.1 Development of Optimum Operating Parameters for NaOH Production

The objective of this research is the evaluation of the capability of the Membrane Electrolysis Cell (MEC) to convert Na_2CO_3 in Kraft Green Liquor into NaOH. The experiments presented in this chapter evaluate the effect of the key process parameters on the performance of the MEC, which are:

- Current density (A/m^2)
- Anode Green Liquor feed concentration (g/L)
- Anode Green Liquor feed flow (mL/hour)
- Cathode feed NaOH concentration (g NaOH/L)
- Feed Temperature ($^{\circ}\text{C}$)

The systematic evaluation of the effect of these parameters determined the ideal MEC process set points for the conversion of Na_2CO_3 in Kraft Green liquor to NaOH. Each experimental trial was video recorded, and the following online measurements were logged continually:

- Voltage (V)
- Current (A)
- Temperature ($^{\circ}\text{C}$)

The following measurements were recorded with regular sampling and verification as reported in Chapter 3.

- NaOH concentration (mol/L) – MEC cathode discharge
- MEC anode and cathode feed flowrates (mL/hr)

Performance indicators were developed using the data collected to understand the impact of each adjustment to the operating environment. Optimum performance outcomes were established as a benchmark for comparative trials using different membrane materials that are reported in the next chapter.

- Molar production rate of NaOH (mol/hour), N_{prod}
- Current efficiency (%), ε
- Specific energy for NaOH production (kJ/mol NaOH), E_{NaOH}

5.1.2 Evaluation of MEC Anode Discharge

Na₂S, is also critical to the Kraft pulping process and is also be oxidised in the electrolysis membrane cell with Na₂CO₃. The expectation is that the oxidation of Na₂S will present as a solid sulphur precipitate in the electrolysis cell discharge and potentially also as scale on the electrode and possibly also the membrane. Not all the Na₂S will leave as S precipitate since some will be converted to Na₂SO₃ and Na₂SO₄ also.

Meanwhile, as Na₂CO₃ is oxidised and Na⁺ ions diffuse through the cation exchange membrane to form NaOH at the cathode and Na₂S is oxidised, the concentration of Na in the Green Liquor will also decrease. The concentration of carbonate in the Green Liquor discharge will also decrease as confirmation of the reduction of the deadload Na₂CO₃.

The impact on the Green Liquor leaving the MEC anode was evaluated by:

- Measurement of remaining carbonate and hydroxide in the MEC anode Green Liquor discharge using HCl Acid Titration.
- Measurement of remaining Na⁺ and S²⁻ of the anode Green Liquor discharge
- Characterisation of any precipitated solids in the anode Green Liquor discharge.

5.1.3 Evaluation of MEC Hydrogen Production Potential with Kraft Green Liquor

The reduction voltage for H_2O is much lower than for Na^+ , so the only product at the cathode is hydrogen gas and hydroxide. Hydrogen is a potentially beneficial biproduct of the MEC recovery of Kraft Green Liquor. Potential reactions at the cathode are:



The rate of hydrogen production (mol/hour) should generally follow Faraday's Law, as there is no mechanism within the MEC that would promote H_2 gas forming at the cathode diffusing through the CEM toward the anode. The rate of hydrogen production was measured (mol/hour) in all experiments for current set points above 2A and compared to the applied current to give a hydrogen production efficiency.

5.2 Experimental Summary

The electrolyser configuration established previously and defined in chapter 3 was used in all experiments performed to establish the optimum operating conditions. The MEC anode and cathode products are discharged to separate containers, so there is no recirculation and the feed to the MEC anode and cathode is consistent for each individual experiment.

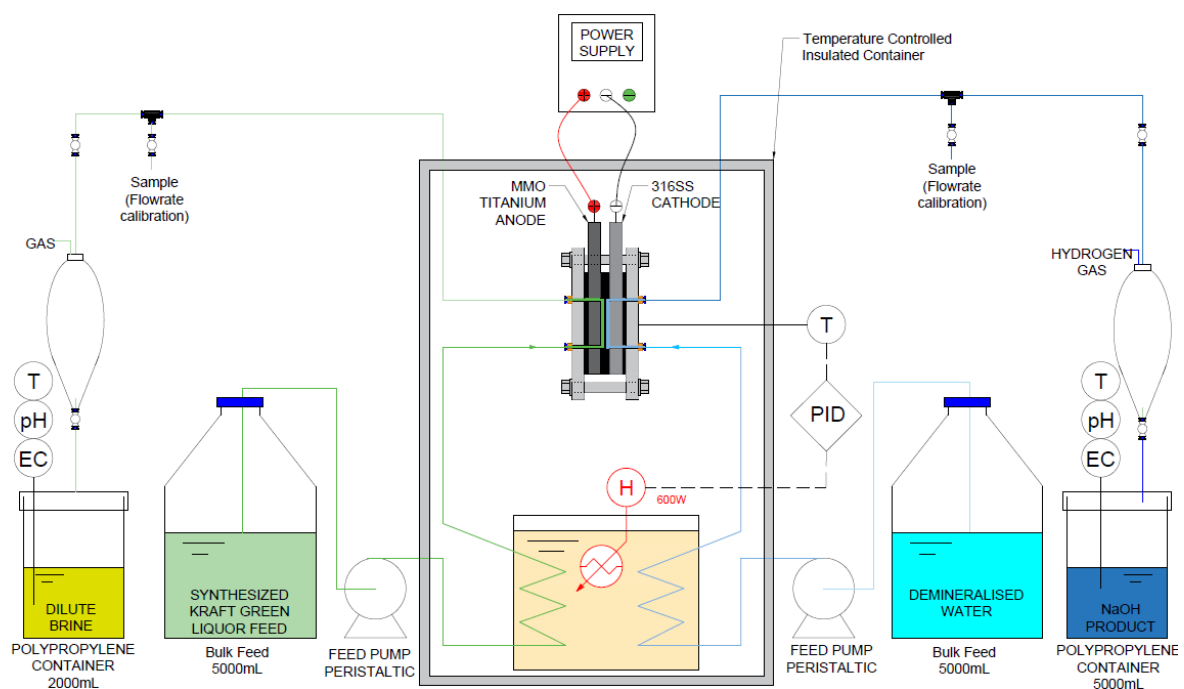


Figure 5.1: MEC Experimental Arrangement for trials with Kraft Green Liquor

The AGC-F-9010 membrane was selected for these experiments because it is the AGC-Selemon latest generation fluorinated ion exchange membrane used to produce NaOH in electrolysis membrane plants. It is PTFE fabric reinforced for high mechanical strength and temperature tolerance, which makes it suitable for contact with Kraft Green Liquor and the temperature ranges used in this experimental trial. A new AGC-9010 membrane was used in each experimental trial.

5.3 Experiment Trials

Varying four experimental parameters across two data points, required 16 experimental trials. Table 5.1 below details the 16 trials and their respective operation settings for each trial. Each trial also includes five current setpoints, giving a total of 80 experimental data points. Trials 14 and 16 were repeated to confirm results and the anode discharge from these trials was evaluated to confirm the impact on Kraft Green Liquor leaving the MEC anode discharge.

Table 5.1: Green Liquor Experimental List and Operation Settings

Experimental Trial Number	Feed Temperature (T) (°C)	Anode Feed Flow (AF) (mL/hr)	Anode Feed Concentration (AC) (g/L)	Cathode Feed Flow (mL/hr)	Cathode Feed Concentration (CC) (g NaOH/L)
1	40	175	200	175	0
2	80	175	200	175	0
3	40	350	200	175	0
4	80	350	200	175	0
5	40	175	200	175	100
6	80	175	200	175	100
7	40	350	200	175	100
8	80	350	200	175	100
9	40	175	100	175	0
10	80	175	100	175	0
11	40	350	100	175	0
12	80	350	100	175	0
13	40	175	100	175	100
14*	80	175	100	175	100
15	40	350	100	175	100
16*	80	350	100	175	100

*Trials 14 and 16 were repeated to confirm results. The anode discharge from these trials was evaluated to confirm impact on Kraft Green Liquor leaving MEC anode discharge.

At the beginning of each trial, the standard start-up procedure was performed, where the MEC equipment was first primed and was followed by the standard integrity check. The MEC was changed to Kraft Green Liquor feed and the experiment commenced and operating data was recorded. Each trial included 5 current set points, starting from 1 amp, and increasing to 5 amps in increments of 1 amp. As informed by previous experiments the MEC was allowed to stabilise for 60 minutes for each current setpoint. The standard schedule for each experiment is given in Table 3.11 of the Chapter 3.

The experimental results for all 16 trials are presented in Appendix A. Figure 5.2 below shows the results of Trial 1 to illustrate the presentation of results.

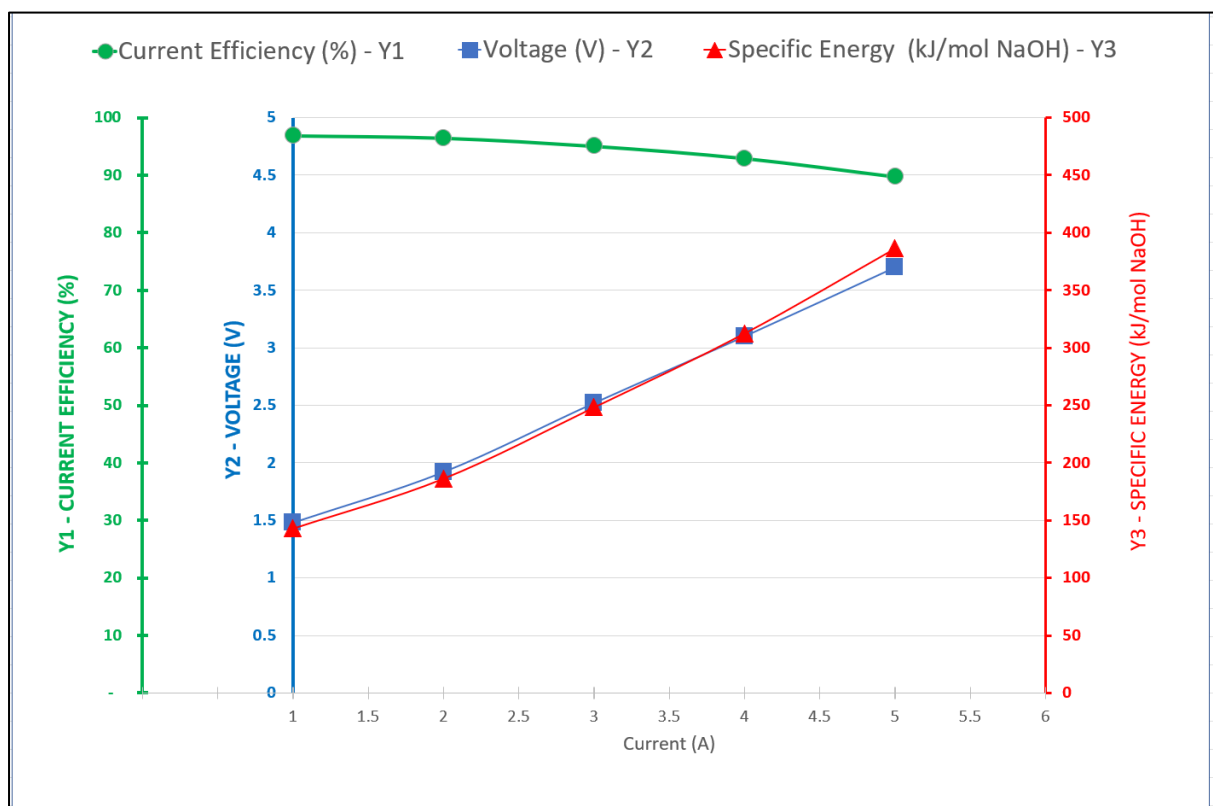


Figure 5.2: Trial 1: Current Efficiency, Voltage and Specific Energy

Temperature = 40°C, Green Liquor Flow = 175 mL/H, Green Liquor Concentration = 200 g/L, Cathode Feed Concentration = 0 g NaOH/L. (See Appendix A for Trials 2 to 16)

5.4 Effect of Applied Current Density

The applied power to the MEC provides the energy required to oxidise the constituents of Green Liquor at the anode and reduce water at the cathode. At the same time the electro-potential across the MEC drives a current of Na^+ ions across the CEM from the anode to the cathode to form NaOH.

The relationship between the specific energy requirement (E_{NaOH}) and current (I) is given by the formula developed in chapter 2, showing E_{NaOH} increases linearly with I with all other parameters constant.

$$E_{\text{NaOH}} \left(\frac{\text{kJ}}{\text{mol NaOH}} \right) = \frac{I \times R_{\text{MEC}} \times F}{\varepsilon} \times 100 \quad (5.1)$$

The other parameters being:

- F = Faraday's constant (96485 Coulomb/mol)
- R_{MEC} = Resistance of the MEC system
= $R_{\text{anode}} + R_{\text{CEM}} + R_{\text{cathode}}$
- ε = Current efficiency

With increasing current, the transport of Na^+ ions across the CEM will increase resistance of the anolyte compartment (R_{anode}) but decrease the resistance of the catholyte compartment (R_{cathode}), so the overall system resistance (R_{MEC}) remains relatively constant.

Generally, the specific energy increased with increase in applied current in all trials. However, observations that require analysis include:

- A. In trials 1, 2, 3 and 4, where a demineralised water was fed to the cathode, the rate of specific energy increase was linear with increasing current.
- B. In trials 5, 6, 7 and 8, where NaOH was fed to the cathode, specific energy increased at a higher rate and exhibited a positive deviation at 3 A in trials 5 and 6.
- C. In trials 9, 10, 13 and 14, gas presented at the anode between 3 and 4A, but not until higher in other trials.
- D. In trials 9, 10, 11 and 12 there were evident deviations in the specific energy curves with increasing current set point

Observations A and B are explained by decreasing current efficiency with increasing current density in the discussion below. Observation C and D are discussed in the context of oxidation reactions occurring at the anode following

5.4.1 Current versus Specific Energy and Current Efficiency

As the current applied across the CEM increases, the average concentration of ions at the cathode is increasing and the average concentration of ions at the anode is decreasing, shifting the concentration gradient across the membrane in favour of diffusion leakage from the cathode back to the anode. This explains why a decrease in current efficiency was observed in all trials with increasing current density.

As per equation 5.1, the specific energy increases with decreasing current efficiency.

In Trial 1, 2, 3 and 4 it was observed that specific energy increased with MEC current and voltage. In each of these trials the feed to the cathode was demineralised water, so the concentration gradient in Trials 1, 2, 3 and 4 strongly favoured the transport of ions from the cathode to the anode facilitating a relatively high system current efficiency.

In Trial 2, at 1 A the MEC current efficiency was almost 100%, which only diminished to 90% at 5 A (see Figure 5.3). This meant that the current efficiency in this trial was relatively constant with only a 10% change, compared to voltage which increased from 1.26 to 3.2 V, an increase of 154%. This result confirms that in arrangements where the concentration gradient strongly favours the diffusion of ions from the cathode to the anode, increases in specific energy are almost entirely attributable to the voltage required to drive the oxidation and reduction reactions, and the transport of ions across the MEC.

Figure 5.3 shows how in Trial 2 the rate of specific energy increase follows the rate of voltage increase closely, indicating current leakage had a small overall impact on MEC performance in Trial 2. As current increased from 1 to 5A, specific energy increased from 118 to 336 kJ/mol NaOH, a 185% increase.

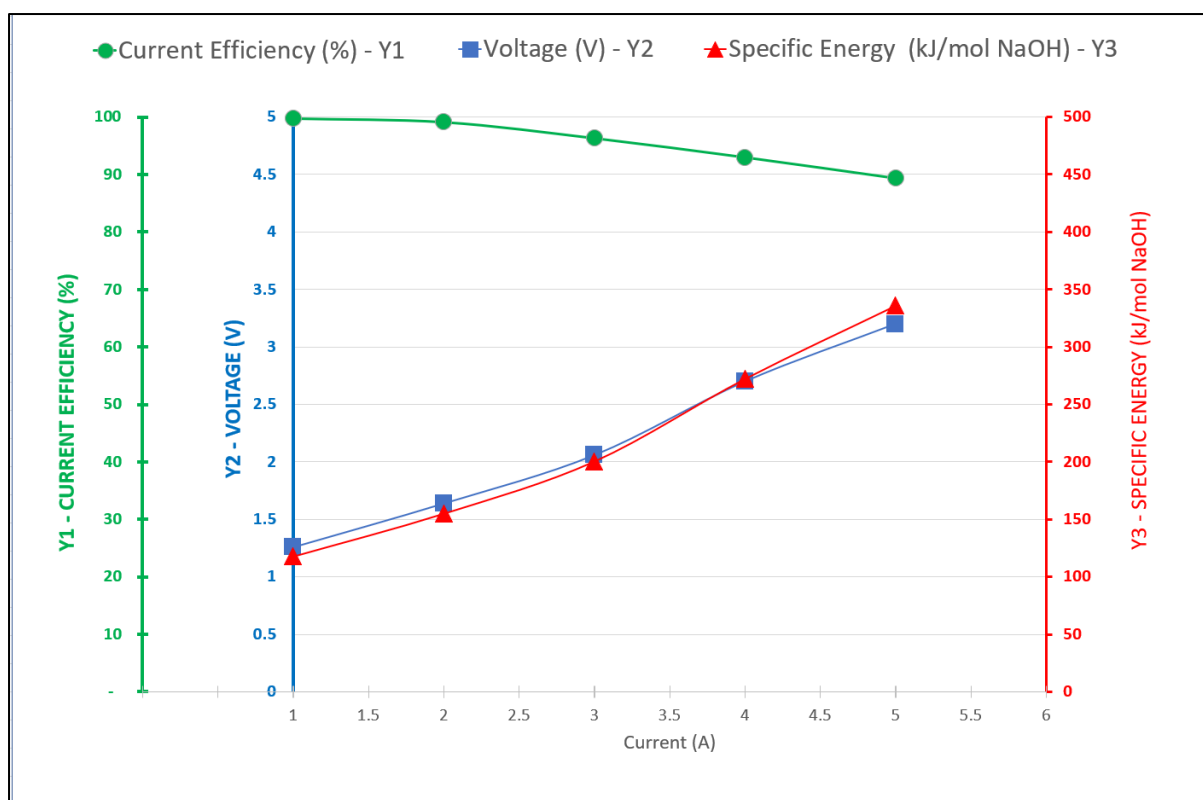


Figure 5.3: Trial 2: Current Efficiency, Voltage and Specific Energy

Temperature = 80°C, Green Liquor Flow = 175 mL/H, Green Liquor Concentration = 200 g/L, Cathode Feed Concentration = 0 g NaOH/L.

In contrast, in trials 5, 6, 7 and 8, 100 g NaOH/L solution was fed to the cathode, resulting in an unfavourable ion concentration gradient across the anode. Focussing on Trial 6 for direct comparison to Trial 2, the feed concentration to the cathode was 100 g NaOH/L, whilst the Green Liquor feed was 200 g/L at 175 mL/hr and 80°C (see Figure 5.4). The unfavourable concentration gradient in Trial 6 caused significant current leakage across the membrane, where at 1 A the current efficiency was 79% and decreased to 63% at 5 A, representing a 20% decrease.

Figure 5.4 shows that in Trial 6, the voltage and specific energy trends moving further away from each other, which is attributed to the decreasing current efficiency. Similar behaviours are seen in Trials 5, 7 and 8.

The overall impact on MEC performance in Trial 6 is that as current increased from 1 to 5 A the specific energy increases from 136 to 461 kJ/mol, a 238% increase, compared to 185% in Trial 2.

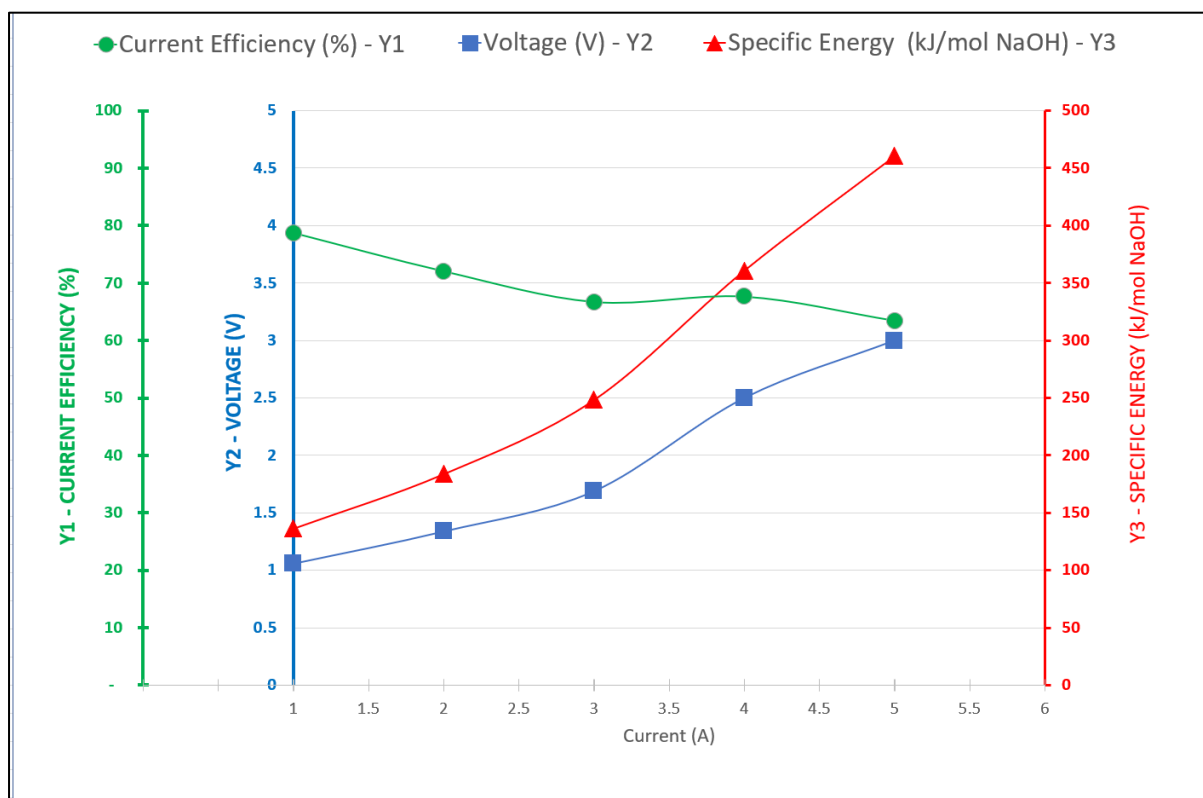


Figure 5.4: Trial 6: Current Efficiency, Voltage and Specific Energy

Temperature = 80°C, Green Liquor Flow = 175 mL/H, Green Liquor Concentration = 200 g/L, Cathode Feed Concentration = 100 g NaOH/L.

The parameters in Trial 8 were the same as Trial 6, except flow to the anode increased to 350 mL/hr. This meant that the residence time of the anolyte in the anode compartment was less than half the time, decreasing the rate of concentration reduction at the cathode by half. Figure 5.5 shows that in Trial 8, the current efficiency increased to 98% and 70% at 1 A and 5 A respectively, and the specific energy of production only increased from 104 to 306 kJ/mol NaOH, or 194%, compared to 238% in Trial 6. This confirms that in an MEC application with increasing current density, reductions in current efficiency can be managed with increased flow to the anode.

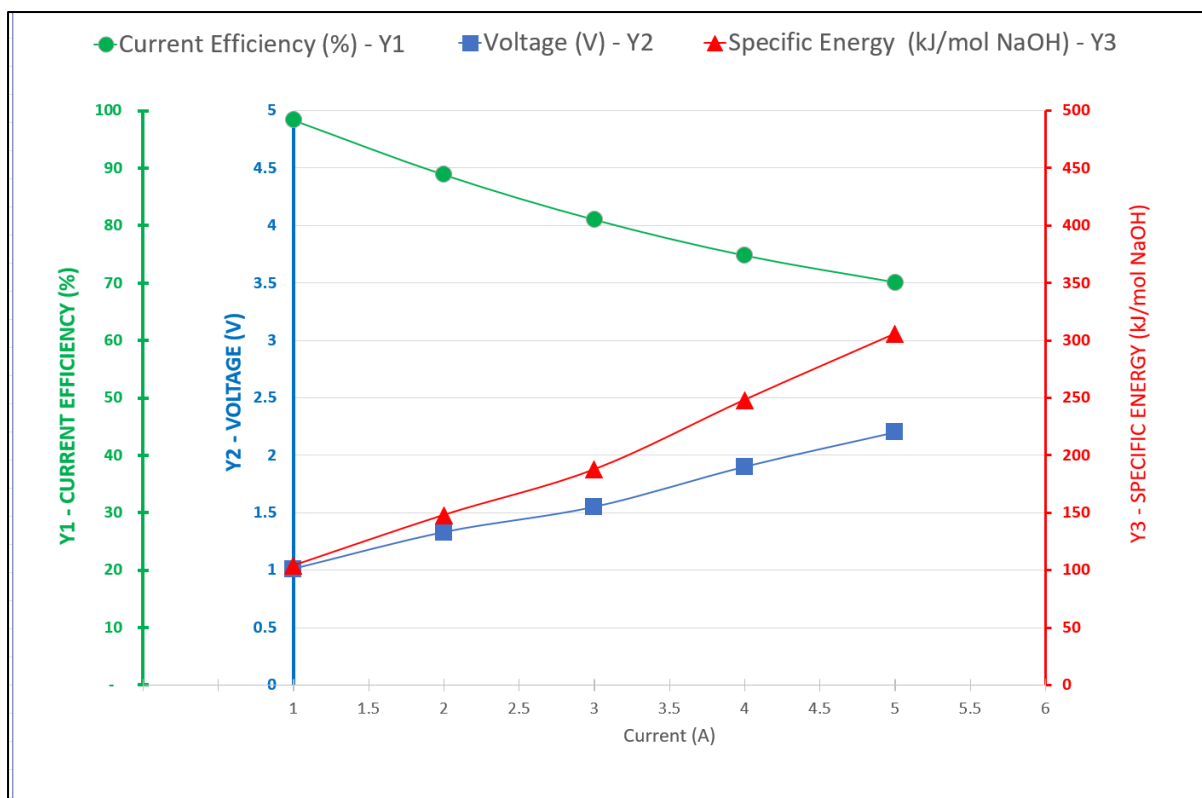


Figure 5.5: Trial 8: Current Efficiency, Voltage and Specific Energy

Temperature = 80°C, Green Liquor Flow = 350 mL/H, Green Liquor Concentration = 200 g/L, Cathode Feed Concentration = 100 g NaOH/L.

The results of all sixteen trials showed that increasing current density across the MEC decreases current efficiency, due to concentration gradient across the membrane shifting in favour of diffusion from the cathode back to the anode. The improved current efficiencies in Trial 8, compared to Trial 6, show the importance of balancing the feed to the anode with increasing current MEC current density.

5.4.2 Current Density and Oxidation Reactions at the Anode – Effect on Specific Energy

With Green liquor feed to the MEC the main reduction (anode) and oxidation (cathode) reactions occurring are given below to illustrate the potential gas production on either side of the CEM.

Cathode (half reaction):



Anode (half reaction for Na₂S and Na₂CO₃):



As per (5.2) there is H₂ gas produced at the cathode. In all experiments the rate of hydrogen production at the cathode was measured at each current set point above 2 amps. The results of these measurements are presented in section 5.12. The molar production rate of hydrogen gas followed the imposed current set point for all trials very closely, reflecting the relatively low complexity of the reduction reactions occurring at the cathode.

The reactions at the anode are more complex. At the anode the Green Liquor is comprised of largely Na₂S and Na₂CO₃. The NaOH, Na₂SO₃, Na₂SO₄ and Na₂S₂O₃ oxidation reactions are less important, especially at low currents, because they have higher oxidation potentials and are present in much smaller concentrations.

Whilst gas (H₂) production rate was measured at the cathode, production at the anode was only observed as occurring or not occurring because of the relatively lower rate of gas production at the anode and corrosive nature of Green Liquor making measurement not possible.

The point at where gas production began to present at the anode was affected by Green Liquor feed concentration and flow rate but was not affected by preheater temperature or cathode feed concentration (g NaOH/L). Table 5.2 below records the point in each experiment trial where gas began to present at the anode.

Table 5.2 – Gas Presentation at the Anode

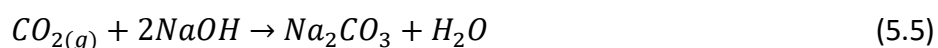
Trial	Green Liquor Feed Concentration (g/L)	Green Liquor Feed Flow (mL/h)	MEC Current when gas presented (A)
T9, T10, T13, T14	100	175	3 to 4
T11, T12, T15, T16	100	350	5 to 6
T1, T2, T5, T6	200	175	5 to 6
T3, T4, T7, T8	200	350	8 to 10*

Note: *T1, T2, T7 and T8 were run to a current of 10 amps to identify gas production point.

Table 5.4 shows that as the Green Liquor feed flow rate and concentration increased, gas did not begin to present at the anode until higher current set point.

Reasons for delay in gas ($CO_{2(g)} + \frac{1}{2}O_{2(g)}$) presentation in the anode discharge are:

- a) Preferential oxidation of Na_2S due to the slightly lower oxidation potential of S^{2-} .
- b) Any $CO_{2(g)}$ produced at the anode reacts with available $NaOH$ to form Na_2CO_3 and H_2O :



- c) Any $O_{2(g)}$ produced is readily soluble in low concentrations that it is produced

HCl titration performed on the MEC anode discharge are presented in section 5.11. These titrations show a consistent decrease in Na_2CO_3 and $NaOH$ concentration in the MEC anode discharge validating (b) and (c). The titration results for Trial 14 are shown in Figure 5.5 below.

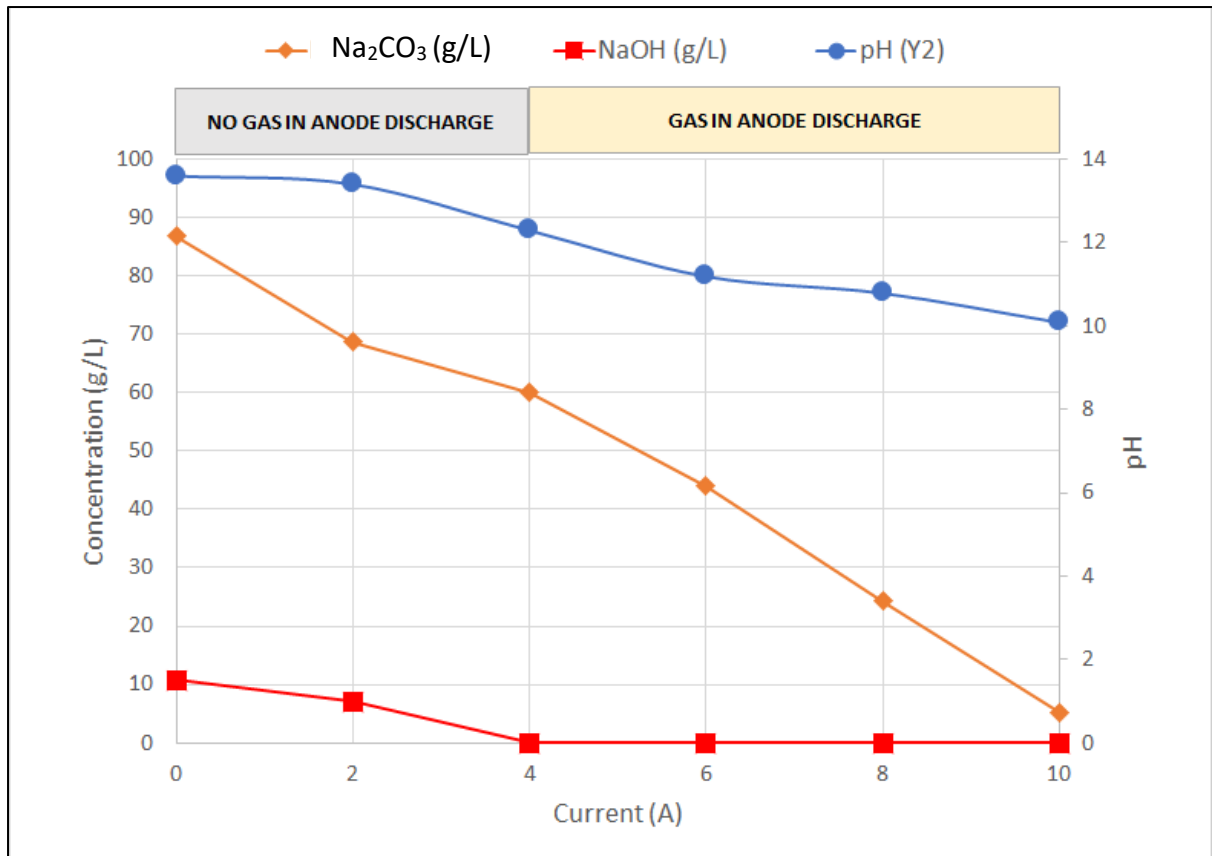


Figure 5.6: Trial 14 (Repeat) MEC Green Liquor Discharge Residual NaOH and Na₂CO₃

Referring to Figure 5.6, between the 2 and 4 A current set points, the residual NaOH concentration is exhausted. Interestingly this corresponds with the presentation of gas in the MEC anode discharge between 3 and 4 amps, which indicates CO₂ gas is no longer reacting with any available NaOH.

The complex reactions occurring at the anode offer explanation for deviations that present in the specific energy trends for each trial. Figure 5.7 below shows the results of Trial 14, corresponding to the titration results shown in Figure 5.6.

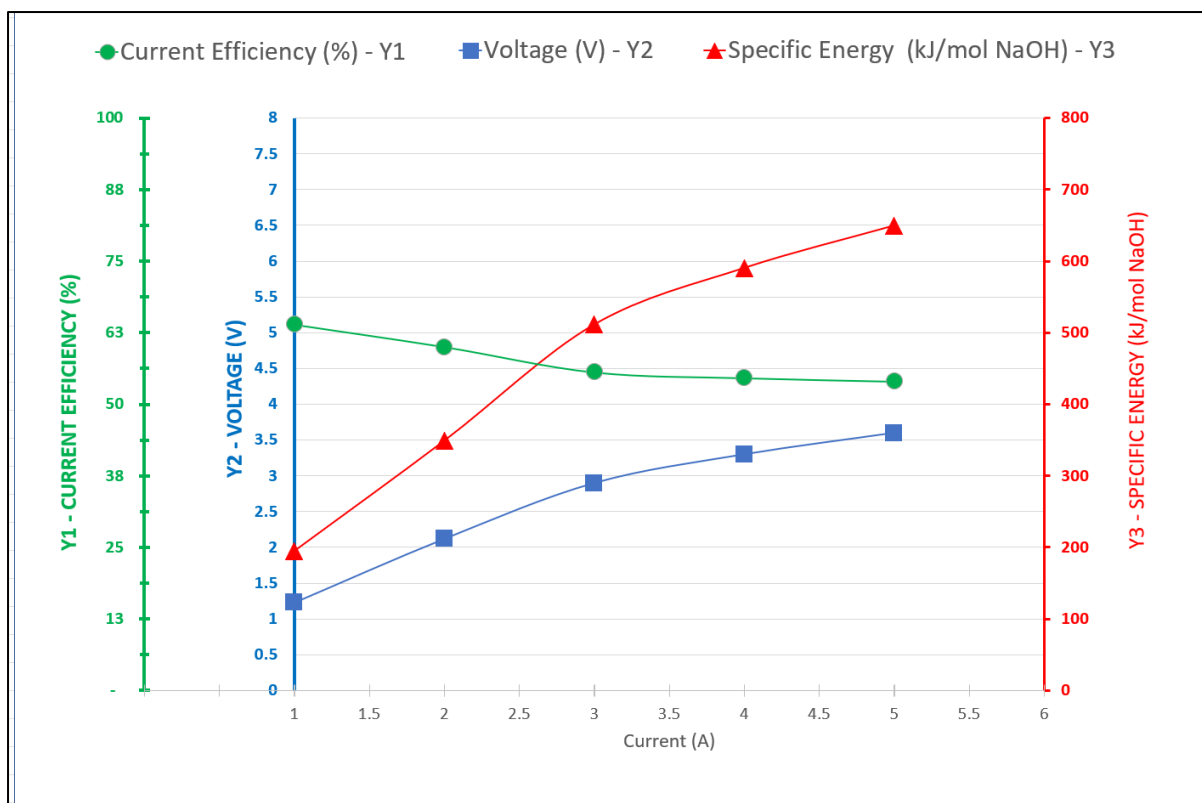


Figure 5.7: Trial 14: Current Efficiency, Voltage and Specific Energy

Temperature = 80°C, Green Liquor Flow = 175 mL/H, Green Liquor Concentration = 100 g/L, Cathode Feed Concentration = 100 g NaOH/L.

After current is increased above 3 A there is a deviation in the specific energy of NaOH production. This could be linked to the onset of gas production at current set points at or around 3 to 4 amps. Similar deviations can be seen in Trials 11 and 12 ('S' Shape), while the curve in Trial 13 resembles Trial 14 (see Appendix).

5.4.3 Optimal Current Set Point for Green Liquor Recovery

The specific energy (E_{NaOH}) required for NaOH production increases with the current applied across the MEC, incentivising reduced current densities in MEC design. However, the power requirement must be balanced against practical application of membrane area.

In industrial chlor-alkali applications the AGC F-9010 CEM is designed for current densities typically between 4 and 6 kA/m² (Selemion, 2019a). In the context of the lab-scale 6cm x 6cm MEC employed here, this represents a current range of 14 to 21 A. Given the Green Liquor was a more complex solution than NaCl with components of lower solubility and ionic mobility, the experimental current range was decreased to 1 to 5 A (0.28 to 1.39 kA/m²).

For comparison, similar research by (Mandal et al., 2022), using MEC with CEM composed of graphene oxide (GO) and SPEEK (sulfonated poly ether ether ketone) to generate NaOH from a Kraft Green liquor feed, trialled current densities between 0.15 and 0.75 kA/m². In earlier research by (Mandal et al., 2021), a comparatively very low current density range of only 15.2 to 37.9 A/m² was trialled using a sulfonated styrene-divinylbenzene cross-linked copolymer), CEM from M/s Permionics Membranes, India. Meanwhile (Goel et al., 2021) using SPK CEM incorporating sulphonated graphene oxide (SGO) generated NaOH from a Green Liquor feed at a current density of 0.60 kA/m².

(Simon et al., 2014a) using MEC generated NaOH from a 100g Na₂CO₃/L feed solution, using a CEM (Selemion CMF, AGC Engineering Ltd. Tokyo Japan) trialled current densities from 0.10 to 0.90 kA/m². The current efficiency and specific energy results of these trials are summarised in Table 5.3 below for comparison.

Table 5.3: Comparison of Current (kA/m²) and MEC Performance – Similar Trials

Author	Anode Feed	Cathode Feed	Membrane	Range*	Current Density Reported (kA/m ²)	Current Efficiency Range (%)	Resultant Specific Energy Reported (kJ/mol)
(Simon et al., 2014a)	100 g Na ₂ CO ₃ /L	0 g NaOH/L	AGC PTFE	L	0.10	50	600
				H	0.90	60	1800
(Mandal et al., 2022)	Green Liquor (140 g TDS /L)	0 g NaOH/L	GO SPK	L	0.15	63	500
				H	0.75	67	576
(Mandal et al., 2021)	10 g Na ₂ CO ₃ /L	0 g NaOH/L	Permionics India	L	0.015	50	612
				H	0.038	52	630
(Goel et al., 2021)	Green Liquor	0 g NaOH/L	GO SPK	L	0.60	61.4	372
				H	0.60	61.4	372
This trial	Green Liquor (100 – 200 g/L)	0 g NaOH/L	AGC Selemion	L	0.28	98	100
				H	1.39	65	452
		100 g NaOH/L	PTFE F-9010	L	0.28	70	150
				H	1.39	52	650

*The range L and H represent the low and high current ranges tested in the respective research papers.

The conventional lime kiln in the Kraft pulping cycle requires approximately 10 MJ/kg CaO produced (Tran, 2008). This energy is delivered to the lime kiln by burning a fossil fuel source most commonly natural gas, fuel oil or waste oil (Francey et al., 2011). After reacting with Na₂CO₃ to produce NaOH, this equates to an estimated fuel energy requirement of 320 kJ/mol NaOH produced.

Referring to Table 5.3, the previous research producing NaOH from Green Liquor using MEC produced it at a specific energy higher than 320 kJ/mol. Of the sixteen trials performed here, Trial 4 (224 kJ/mol) and Trial 8 (306 kJ/mol) produced NaOH at a specific energy below 320 kJ/mol at 5 A (1.39 kA/m²). Trial 4 and 8 were both performed at 80°C, with Green Liquor feed flow and concentration of 375 mL/hr and 200 g/L respectively, illustrating the importance temperature and increased concentration of ions at the anode has on performance.

In the following sections the impact of Green Liquor feed flow, Green Liquor feed concentration, Cathode feed concentration and preheater temperature are further evaluated at the current set point of 5 A (1.39 kA/m²).

5.5 Effect of Green Liquor Feed Concentration on MEC NaOH Production

Increasing the Green Liquor feed concentration (100 to 200 g/L) increases the average concentration of ions in the anode chamber. This will shift the CEM concentration gradient in favour of ion diffusion from the anode to the cathode. The average concentration of Na⁺ ions (*i*) in the anode ($c_{iA,ave}$) is given by:

$$c_{iA,ave} = \frac{c_{iA,in} + c_{iA,out}}{2} \quad (5.6)$$

As Na⁺ ions migrate across the CEM the concentration of Na⁺ ions the anode discharge ($c_{iA,out}$) can be calculated using mass balance.

$$\text{Change in moles Na}^+ \text{ anode} = - \text{Change in moles Na}^+ \text{ cathode} \quad (5.7)$$

Expressed as:

$$Q_{Anode} \times (c_{iA,out} - c_{iA,in}) = -Q_{Cathode} \times (c_{iC,out} - c_{iC,in}) \quad (5.8)$$

Substituting 5.6 into 5.8 and solving for $c_{iA,out}$:

$$c_{iA,out} = c_{iA,in} - \frac{Q_{Cathode} \times (c_{iC,out} - c_{iC,in})}{Q_{Anode}} \quad (5.9)$$

Table 5.4 below gives the average concentration gradient measured for each trial at 5 A as per the outcome of the evaluation of current densities previous.

Table 5.4: Average CEM Concentration Gradient for all Trials

Trial Number	Anode Feed Flow (mL/hr)	Anode Feed Green Liquor Concentration (g/L)	Cathode Feed NaOH Concentration (g/L)	Cathode Na ⁺ Concentration (M)		Anode Na ⁺ Concentration (M)		Average Na ⁺ Concentration Gradient (M) ($c_{iA,ave} - c_{iC,ave}$)
				$c_{iC,in}$ (measured)	$c_{iC,out}$ (measured)	$c_{iA,in}$ (measured)	$c_{iA,out}$ (calculated)	
1	175	200	0	0.00	0.99	4.08	3.10	3.10
2	175	200	0	0.00	0.98	4.08	3.10	3.10
3	350	200	0	0.00	0.99	4.08	3.59	3.34
4	350	200	0	0.00	0.99	4.08	3.59	3.34
5	175	200	100	2.50	3.24	4.08	3.35	0.85
6	175	200	100	2.50	3.17	4.08	3.41	0.91
7	350	200	100	2.50	3.26	4.08	3.70	1.01
8	350	200	100	2.50	3.24	4.08	3.71	1.03
9	175	100	0	0.00	0.96	2.04	1.09	1.09
10	175	100	0	0.00	0.93	2.04	1.12	1.12
11	350	100	0	0.00	0.96	2.04	1.56	1.32
12	350	100	0	0.00	0.89	2.04	1.59	1.37
13	175	100	100	2.50	3.19	2.04	1.35	-1.15
14	175	100	100	2.50	3.07	2.04	1.47	-1.03
15	350	100	100	2.50	3.14	2.04	1.72	-0.94
16	350	100	100	2.50	3.05	2.04	1.77	-0.87

A pairwise comparison of trials with common process parameters but different feed concentrations is shown in Table 5.5 and Figure 5.8.

An increase in Green Liquor feed concentration decreased the MEC voltage in all trial pair comparisons (see Table 5.5). This is easily explained by Ohm's law as the increased concentration of ions in the anode compartment, increases the electrical conductivity of the anode compartment (EC_{anode}),

$$EC_{anode} = \sum_i \Lambda_{m,i} c_{iA,ave} \quad (5.10)$$

Which decreases the anolyte compartment resistance (R_{anode}).

$$R_{anode} = \frac{d}{EC_{anode} \times A} \quad (5.11)$$

Referring to Figure 5.7, in all trial comparisons the magnitude of the voltage drops increases with temperature, suggesting increased Green Liquor feed concentration is even more important at higher temperatures.

Table 5.5: Anode Feed Concentration from 100 to 200 g/L all Trials at 1.39 kA/m² (5 A)

Trials Compared	Common Trial Parameters			Change in Concentration Gradient (M)		Change in Voltage, V (%)	Change in Current Efficiency, ϵ (%)	Change in Specific Energy, E_{NaOH} (%)
	Anode Feed Flow (mL/hr)	Cathode Feed Conc. (g NaOH/L)	Preheater Temperature Set Point (°C)	$(c_{iA,ave} - c_{iC,ave})$				
				From	To			
T1 vs T9	175	0	40	1.09	3.10	-11.9%	3.1%	-14.6%
T2 vs T10	175	0	80	1.12	3.10	-16.9%	5.9%	-21.5%
T3 vs T11	350	0	40	1.32	3.34	-17.9%	3.4%	-20.6%
T4 vs T12	350	0	80	1.37	3.34	-38.6%	10.6%	-44.5%
T5 vs T13	175	100	40	-1.15	0.85	-15.4%	6.5%	-20.6%
T6 vs T14	175	100	40	-1.03	0.91	-24.2%	23.9%	-38.9%
T7 vs T15	350	100	80	-0.94	1.01	-24.3%	18.7%	-36.3%
T8 vs T16	350	100	80	-0.87	1.03	-31.3%	34.5%	-48.9%

The increased average concentration of Na⁺ ions ($c_{iA,ave}$) at the anode improves the concentration gradient in favour of ion diffusion from the anode to the cathode. Table 5.7 displays the change in concentration gradient ($c_{iA,ave} - c_{iC,ave}$) in each trial, showing that it moves in favour of passage of ions from the anode to the cathode in all cases, predictably resulting in an increase in current efficiency (ϵ) in all trials.

In trials where 100 g NaOH/L solution is being supplied to the anode, the improvement in concentration gradient is most significant, going from negative to positive, greatly improving

the current efficiency. In Figure 5.8, the results right of middle display the impact on current efficiency where 100 g NaOH/L solution is being fed to the cathode and current efficiency increases by 34.5% when comparing Trials 8 and 16.



Figure 5.8: Effect of Increasing Anode Feed Concentration (100 to 200 g/L) on MEC Performance at 1.39 kA/m² (5 A), arrows indicate effect of increasing temperature.

In the case of Trials 8 and 16, at a MEC temperature of 80°C, cathode feed of 100 g NaOH/L, and anode feed rate of 350 mL/h, the requirement for the higher concentration Green Liquor feed is clear with a 48.9% reduction in specific energy requirement for NaOH production and is shown in Table 5.6 below.

Table 5.6: Comparison of Trial 8 and 16 results at 1.39 kA/m²

	Trial 16	Trial 8	Change (%)
Temperature (°C)	80	80	-
Cathode Feed (g NaOH/L)	100	100	-
Anode Feed Flow (mL/hr)	350	350	-
Anode Feed Concentration (g/L)	100	200	100
Voltage (V)	3.2	2.2	-31.3
Current Efficiency, ε (%)	52	70	+34.5
Specific Energy (kJ/mol NaOH)	598	306	-48.9

A Green Liquor feed concentration of 200 g/L was adopted for further experiments that will be reported in Chapter 6. The basis for selecting a concentration of 200 g/L was that MEC voltage decreases, current efficiency increases, and the overall specific energy required to produce NaOH decreases.

5.6 Effect of Anode Green Liquor Feed Flow on MEC NaOH Production

Increasing the Green Liquor feed flow rate from 175 to 350 L/hr decreases the residence time of solution in the anode chamber, so affects an increase in the discharge ion concentration ($c_{iA,out}$) and increases the average concentration of ions in the compartment, $c_{iA,ave}$. The effect of increasing a $c_{iA,ave}$ on concentration gradient, voltage and current efficiency was presented when discussing increasing Green Liquor feed concentration.

Table 5.7, and Figure 5.9 pair the trials with common process parameters apart from an increase Green Liquor feed flow from 175 to 350 L/hr. The experiment results here show the effect of increasing Green Liquor feed flowrate follows the same trend as increasing feed concentration, but the decrease in voltage and increase in current efficiency is not as large because the change in concentration gradient is not as large.

Table 5.7: Anode Feed Flow from 175 to 350 mL/hr all Trials at 1.39 kA/m² (5 A)

Trials Compared	Common Trial Parameters			Change in Concentration Gradient (M)		Change in Voltage, V (%)	Change in Current Efficiency, ε (%)	Change in Specific Energy, E_{NaOH} (%)
	Anode Feed Conc. (g/L)	Cathode Feed Conc. (g NaOH/L)	Preheater Temperature Set Point (°C)	$(c_{iA,ave} - c_{iC,ave})$				
				From	To			
T9 vs T11	100	0	40	1.09	1.32	-7.1%	0.0%	-7.1%
T10 vs T12	100	0	80	1.12	1.37	-9.1%	-3.5%	-5.8%
T1 vs T3	200	0	40	3.10	3.34	-13.5%	0.3%	-13.7%
T2 vs T4	200	0	80	3.10	3.34	-32.8%	0.8%	-33.3%
T13 vs T15	100	100	40	-1.15	-0.94	-5.1%	-7.2%	-34.8%
T14 vs T16	100	100	80	-1.03	-0.87	-15.2%	-4.6%	-11.1%
T5 vs T7	200	100	40	0.85	1.01	-15.2%	3.4%	-17.9%
T6 vs T8	200	100	80	0.91	1.03	-26.7%	10.4%	-33.6%

Doubling anode feed flow from 175 to 350 mL/hr does not increase $c_{iA,ave}$ as much as doubling anode feed concentration from 100 to 200 g/L. For example, Trial 1 (175 mL/hr and 200 g/L) and Trial 11 (350 mL/hr and 100 g/L) have the same mass feed flow rates of Na^+ ions to the anode. However, the concentration of $c_{iA,out}$ in Trial 1 and Trial 11 is 3.10 and 1.56 mol/L respectively. It should be noted that the experimental MEC is lab-scale, so the membrane area is small relative to pilot of industrial scale. With larger membrane areas concentration polarisation between the anode compartment inlet and outlet can become more significant, so the importance of high feed flow rates would be more significant.

Referring to Figure 5.8, in all trial comparisons the magnitude of the voltage drops increases with temperature, suggesting increased Green Liquor feed flow rate is even more important at higher temperatures.

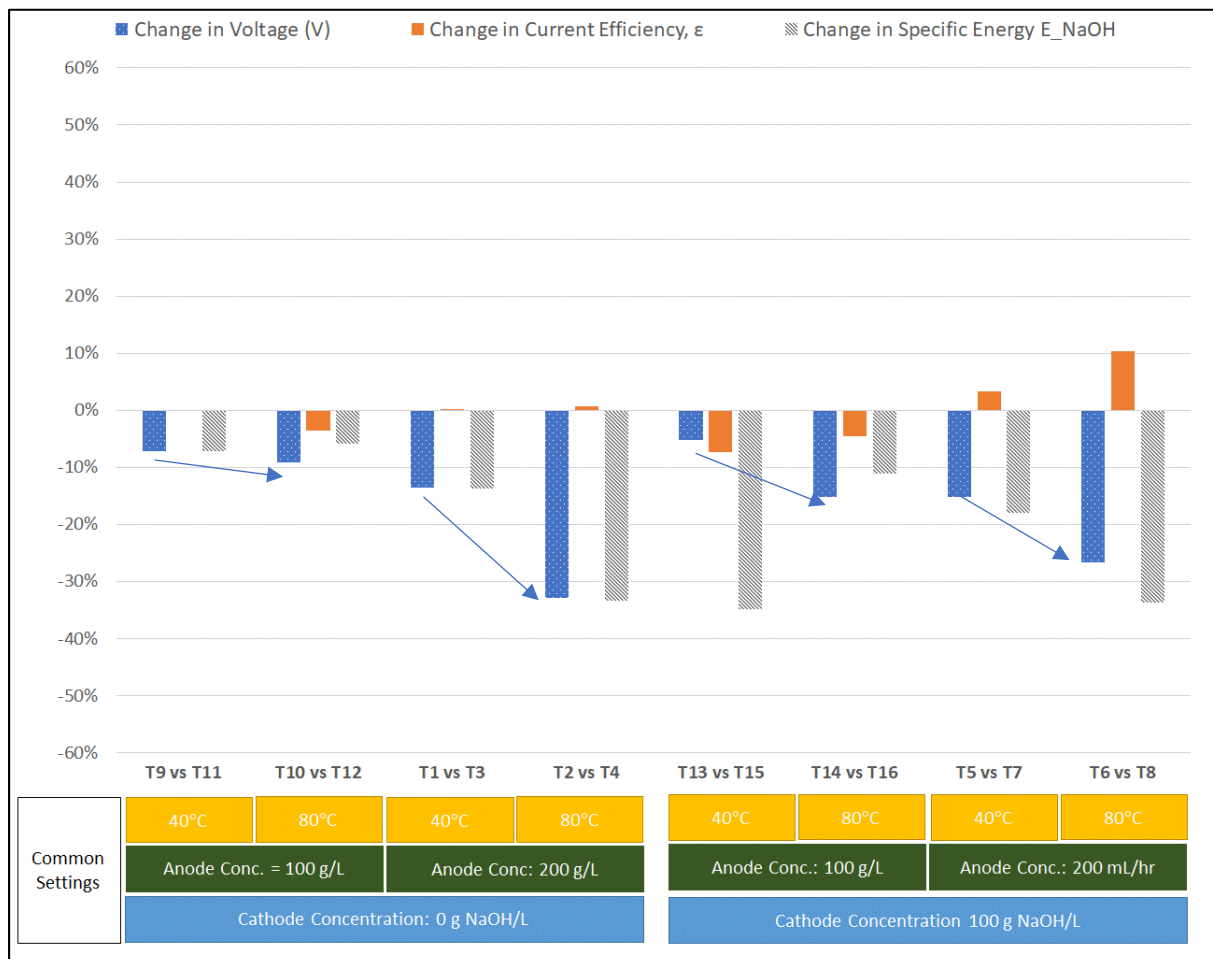


Figure 5.9: Effect of Increasing Anode Feed Flowrate (175 to 350 mL/hr) on MEC Performance at 1.39 kA/m² (5 A) arrows indicate effect of increasing temperature.

In the case of Trials 6 and 8, at a MEC temperature of 80°C, cathode feed of 100 g NaOH/L, and anode feed concentration of 200 g/L, the benefit of the higher Green Liquor feed flow is clear with a 33.6% reduction in specific energy requirement for NaOH production and is shown in Table 5.8 below.

Table 5.8: Comparison of Trial 6 and 8 results at 1.39 kA/m²

	Trial 6	Trial 8	Change (%)
Temperature (°C)	80	80	-
Cathode Feed (g NaOH/L)	100	100	-
Anode Feed Flow (mL/hr)	175	350	100
Anode Feed Concentration (g/L)	200	200	-
Voltage (V)	3	2.2	-26.7
Current Efficiency, ϵ (%)	63	70	+10.4
Specific Energy (kJ/mol NaOH)	461	306	-33.6

In experimentation presented in Chapter 6, where different membranes were trialled, a high Green Liquor feed flow rate of 350 mL/L was adopted on the basis that a high flow rate results in a lower MEC voltage, higher current efficiency, and a lower overall specific energy required to produce NaOH.

5.7 Effect of Cathode Feed Concentration on MEC NaOH Production

Increasing the Cathode feed concentration from 0 to 100 g NaOH/L increases the average concentration of ions in the cathode chamber, decreasing the MEC CEM concentration gradient from the anode to the cathode, and in some cases, making it negative. Table 5.9, and Figure 5.10 pair the trials with common process parameters apart from an increase cathode feed concentration from 0 to 100 g NaOH/L.

The average concentration of Na⁺ ions (*i*) in the cathode ($c_{iC,ave}$) is given by:

$$c_{iC,ave} = \frac{c_{iA,in} + c_{iA,out}}{2} \quad (5.12)$$

Table 5.9: Cathode Feed Conc. from 0 to 100 g NaOH/L all Trials at 1.39 kA/m² (5 A)

Trials Compared	Common Trial Parameters			Change in Concentration Gradient (M)		Change in Voltage, V (%)	Change in Current Efficiency, ϵ (%)	Change in Specific Energy, E_{NaOH} (%)
	Anode Feed Flow. (mL/hr)	Anode Feed Conc. (g/L)	Preheater Temperature Set Point (°C)	$(c_{iA,ave} - c_{iC,ave})$				
				From	To			
T9 vs T13	175	100	40	1.09	-1.15	-7.1%	-24.9%	28.5%
T10 vs T14	175	100	80	1.12	-1.03	-6.5%	-36.0%	51.7%
T11 vs T15	350	100	40	1.32	-0.94	-5.1%	-30.4%	41.6%
T12 vs T16	350	100	80	1.37	-0.87	-6.7%	-40.1%	62.2%
T1 vs T5	175	200	40	3.10	0.85	-10.8%	-22.5%	19.5%
T2 vs T6	175	200	80	3.10	0.91	-6.3%	-29.0%	37.1%
T3 vs T7	350	200	40	3.34	1.01	-12.5%	-20.0%	13.7%
T4 vs T8	350	200	80	3.34	1.03	2.3%	-22.1%	36.5%

As per the increase in $c_{iA,ave}$ at the anode, an increase in $c_{iC,ave}$ at the cathode affects a decrease in resistance at the cathode. The experimental results showed a decrease in overall MEC voltage in all cases where the 100 g NaOH/L solution was fed to cathode, although the decrease was only in the range of 5 to 10%, compared to 10 to 40% when the Green Liquor feed concentration was increased from 100 to 200 g/L. Notably in the comparisons of trial 4 and 8, when the anode feed flow and concentration were 350 mL/hr and 200 g/L respectively and the MEC temperature 80°C, the increase in cathode feed from 0 to 100 g NaOH/L affected a slight increase in voltage of 2.3%.

The increased average concentration of Na⁺ ions ($c_{iC,ave}$) at the cathode shifts the concentration gradient in favour of ion diffusion from the cathode to the anode. Table 5.9 displays the change in concentration gradient ($c_{iA,ave} - c_{iC,ave}$) in each trial, showing that it

moves in favour of the leakage of ions from the cathode to the anode in all cases, predictably resulting in a decrease in current efficiency (ϵ) in all trials.

Referring to Figure 5.10, in trials where 200 g/L Green Liquor solution is being supplied to the anode, the reduction in concentration gradient is less significant, so the reduction in current efficiency is less.

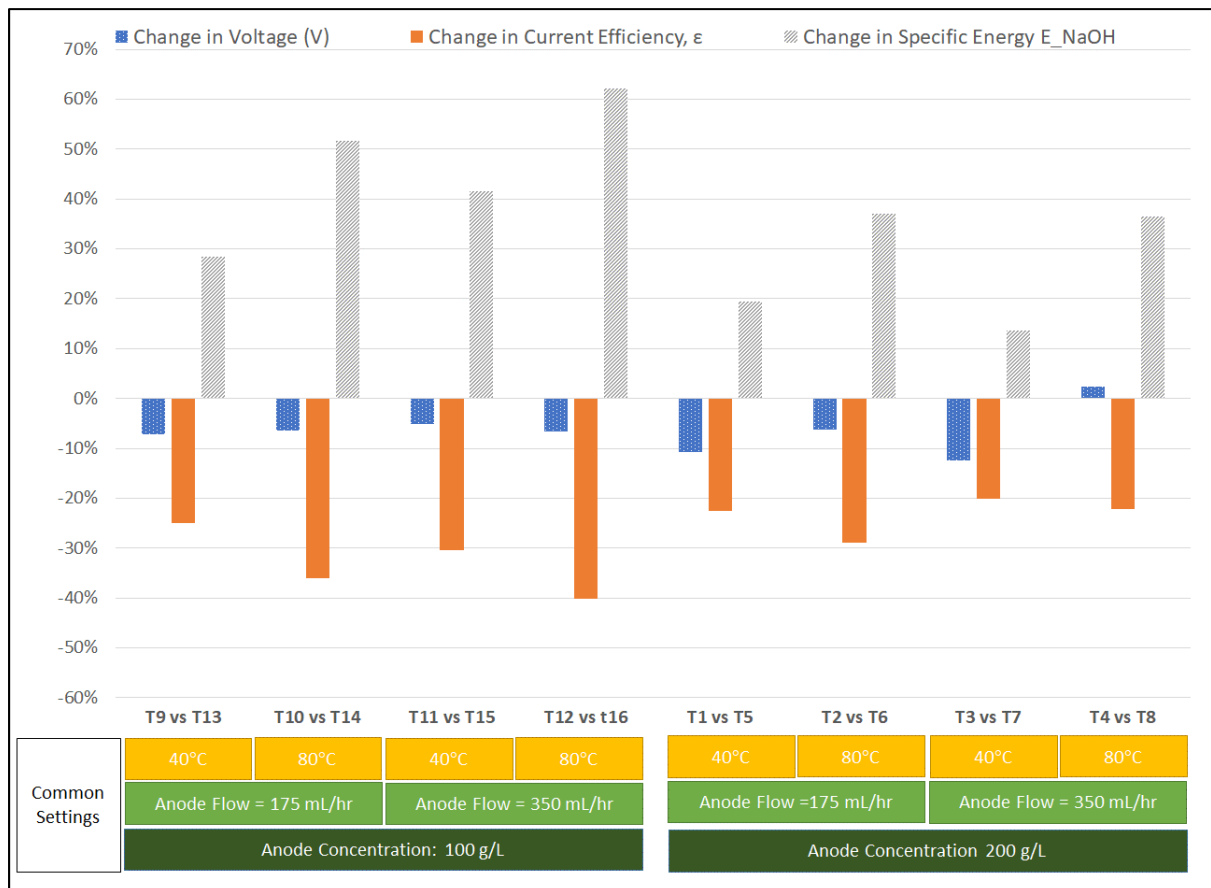


Figure 5.10: Effect of Increasing Cathode (NaOH) Feed Concentration (0 to 100 g NaOH/L) on MEC Performance at 1.39 kA/m² (5 A)

The experimental data confirmed that as NaOH concentration increases at the cathode, the MEC voltage does decrease, however the relative decrease in current efficiency results in an overall increase in the specific energy required to produce NaOH.

This mechanism is very important to understand, however the Kraft pulping process requires a minimum NaOH concentration of 60 g/L. In experimentation presented in Chapter 6 a cathode feed concentration of 100 g NaOH/L was adopted on this basis because producing a concentration of lower concentration would be of little relevance to the Kraft pulping cycle.

5.8 Effect of Preheater Temperature on MEC NaOH Production

Increasing the temperature of the anode and cathode feed to the MEC increases the molar conductivity ($\Lambda_{m,i}^0$) of Na^+ ions in solution which increases with temperature. The effect on the diffusion coefficient (D_i) is described by Nernst-Einstein equation the (Sata, 2007a):

$$D_i = \frac{RT}{z_i^2 F^2} \Lambda_{m,i}^0 \quad (5.13)$$

Table 5.10, and Figure 5.11 pair the trials with common process parameters apart from an increase MEC preheater temperature set point. The experimental results show confirm that an increase in temperature from 40°C to 80°C decreases MEC voltage in all cases, illustrating an increase in ionic mobility with the increase in temperature.

According to the Nernst-Planck equation the rate of membrane diffusion due to concentration gradient increases with ion mobility, here defined as the diffusion coefficient (D_i). The trials in Table 5.10 and in Figure 5.10 are presented in order of concentration gradient.

Table 5.10: MEC Preheater Temperature from 40 to 80°C all Trials at 1.39 kA/m² (5 A)

Trials Compared	Common Trial Parameters			Change in Concentration Gradient (M)		Change in Voltage, V (%)	Change in Current Efficiency, ϵ (%)	Change in Specific Energy, E_{NaOH} (%)
	Anode Feed Flow (mL/hr)	Anode Feed Conc. (g/L)	Cathode Feed Conc. (g NaOH/L)	$(c_{iA,ave} - c_{iC,ave})$				
				From	To			
T3 vs T4	350	200	0	3.34	3.34	-23.2%	25.1%	-40.9%
T1 vs T2	175	200	0	3.10	3.10	-13.5%	-0.5%	-13.1%
T11 vs T12	350	100	0	1.32	1.37	-10.3%	-6.5%	-4.0%
T9 vs T10	175	100	0	1.09	1.12	-8.3%	-3.1%	-5.4%
T7 vs T8	350	200	100	1.01	1.03	-21.4%	-2.6%	-19.3%
T5 vs T6	175	200	100	0.85	0.91	-9.1%	-8.8%	-0.3%
T15 vs T16	350	100	100	-0.94	-0.87	-17.6%	-17.2%	-0.6%
T13 vs T14	175	100	100	-1.15	-1.03	-7.7%	-17.4%	11.7%

Looking at the orange current efficiency bars on Figure 5.11, moving from left to right, the most positive concentration gradient to the most negative, the current efficiency is improving on the left and getting worse on the right. In case of Trials 13 and 14 which have the most negative concentration gradient, the decrease in current efficiency is more significant than voltage decrease, resulting in an overall increase in specific energy.

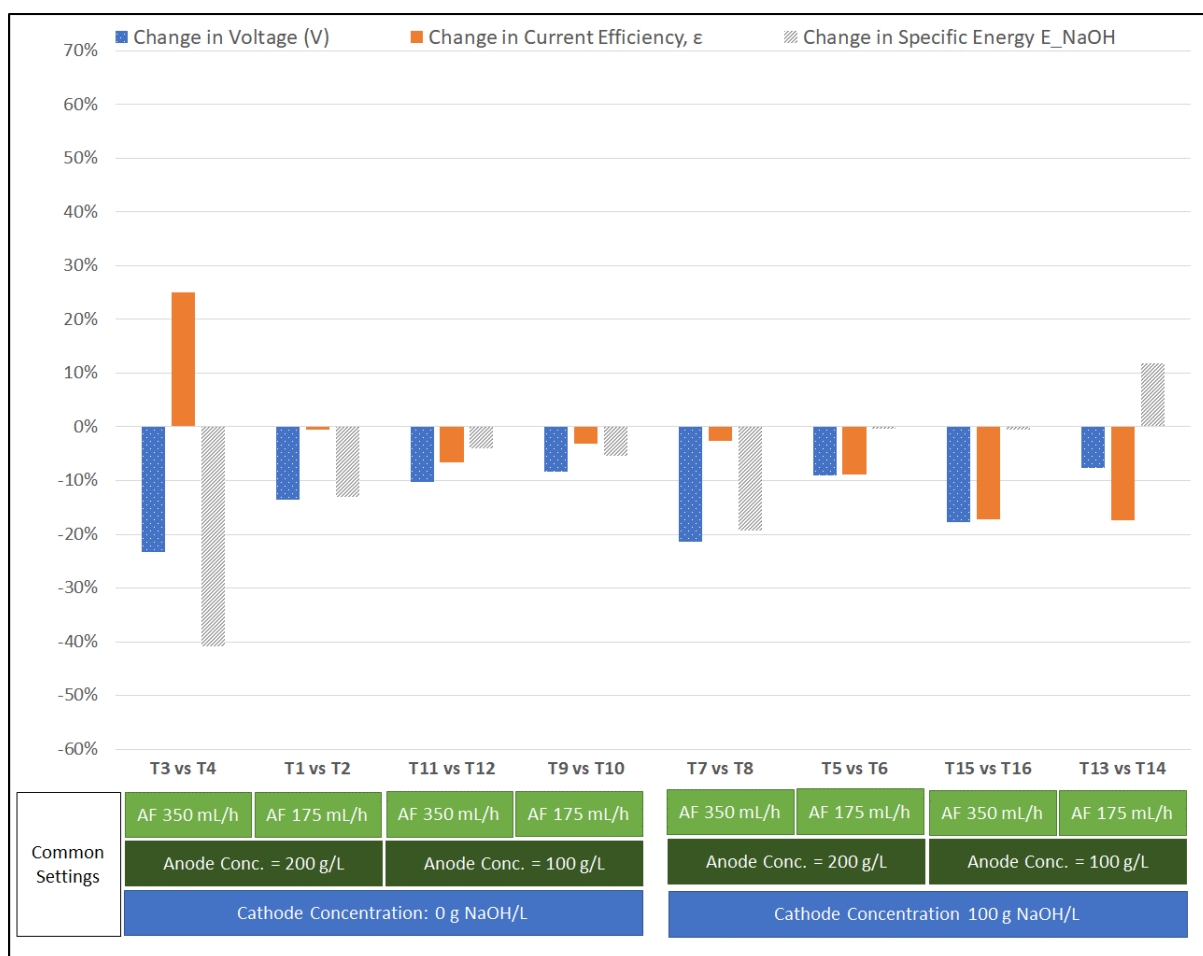


Figure 5.11: Effect of Increasing Preheater Temperature (40 to 80°C) on MEC Performance at 1.39 kA/m² (5 A)

Green Liquor feed concentration and flowrates to be used in future experiments will be 200 g/L and 350 mL/hr respectively, while the feed to the cathode will be 100 g NaOH/L. These set points were trialled at 40°C in Trial 7 and 80°C in Trial 8. Table 5.11 below compares the MEC performance in Trials 7 and 8 at 1.39 kA/m².

Table 5.11: Comparison of Trial 7 and 8 results at 1.39 kA/m²

	Trial 7	Trial 8	Change
Temperature (°C)	40	80	+40
Cathode Feed (g NaOH/L)	100	100	-
Anode Feed Flow (mL/hr)	175	350	-
Anode Feed Concentration (g/L)	200	200	-
Voltage (V)	2.8	2.2	-21.4%
Current Efficiency, ε (%)	72	70	-2.7%
Specific Energy (kJ/mol NaOH)	379	306	-19.3%

The results in Table 5.11 shows that an increase in temperature from 40°C to 80°C resulted in a decrease in voltage of 21% and a decrease in current efficiency of 2.7%, so there is an overall significant decrease in the specific energy required to produce NaOH (-19.3%).

The experimentation performed in this chapter showed that the MEC operates more efficiently at higher temperature with the AGC F 9010 high selectivity membrane. In experimentation presented in Chapter 6, the CEM's being evaluated will be of both high and low resistance or selectivity. Given that temperature affects membrane resistance, comparing the effect on both high and low selectivity membranes is of interest, so both 40°C and 80°C temperature set points were trialled and presented in Chapter 6

5.9 Evaluation of MEC Anode Discharge

The impact of MEC treatment on the Green Liquor composition was most significant in the experiment trials where current density was high and Green Liquor feed flow and concentration was low.

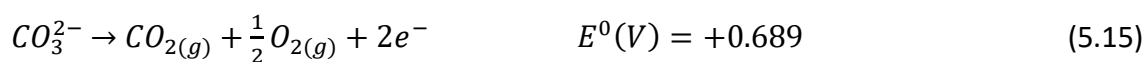
To examine the effect of MEC treatment on the Green Liquor discharge, Trials 14 and Trial 16 were repeated as they are trials where any changes in Green Liquor composition would be most evident as they are trials with low Green Liquor concentration. The current range tested was increased to amplify the effect on the Green Liquor discharge for measurement. Table 5.12 below shows the settings for Trial 14 and 16 and the tested current ranges.

Table 5.12: Trial 14 and Trial 16 Process Parameters – Trials Repeated

	Trial 14	Trial 16
Temperature (°C)	80	80
Cathode Feed (g NaOH/L)	100	100
Anode Feed Flow (mL/hr)	175	350
Anode Feed Concentration (g/L)	100	200
Current minimum (A)	2 (0.56 kA/m ²)	2 (0.56 kA/m ²)
Current maximum (A)	10 (2.78 kA/m ²)	10 (2.78 kA/m ²)

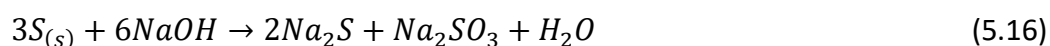
Na₂CO₃ (60 wt%) and Na₂S (22 wt%) were the two main constituents of the synthesised Green Liquor, while NaOH is also present (8 wt%). Na₂SO₃, Na₂SO₄ and Na₂S₂O₃ are also present in smaller concentrations and their oxidation potentials are higher, so they are less significant in the MEC anode.

The two main half reactions occurring at the anode are:



The products of the above half reactions both react with the NaOH present in the Green Liquor and any NaOH that may leak from the cathode back to the anode. It has been shown above that at a current density of 1.39 kA/m² (5 A) the current efficiency of Trial 14 and 16 was 54% and 52% respectively, indicating significant leakage of NaOH from the cathode to the anode.

The half reaction product reactions with NaOH are as follows:



The reactions above indicate the following should be observed in the MEC discharge:

1. NaOH concentration decrease with increasing current until exhausted.
2. Na₂CO₃ concentration will decrease, but CO₂ gas will not present until NaOH is exhausted
3. Na₂S oxidation will produce an elemental sulphur (S) precipitate and will start to present when any NaOH is no longer present in solution.
4. Na₂SO₃ has relatively low solubility, so as Na₂S is converted to Na₂SO₃, this may exceed the saturation limit and start to form precipitate also.

Figure 5.12 shows the titration results for anode discharge in the repeated Trial 14. These results, previously presented as Figure 5.6 in Section 5.4.2, are here paired with a photograph of the anode samples to show the visual changes in Green Liquor that took place during the trial at the different current settings. The results for Trial 16 are presented in Appendix B. Referring to Figure 5.12, at 4 A there is no NaOH remaining in the anode discharge, which corresponds to the visual observation of gas beginning to present in the anode discharge and some solid precipitate in the anode sample photo.

With increasing current, the quantity of solid precipitate in the sample is increases indicating greater more conversion of Na₂S to an elemental sulphur precipitate or Na₂SO₃ has exceeded its solubility. At 10 A the quantity of precipitate has decreased, possibly suggesting Na₂SO₃ is being converted to the more soluble Na₂SO₄.

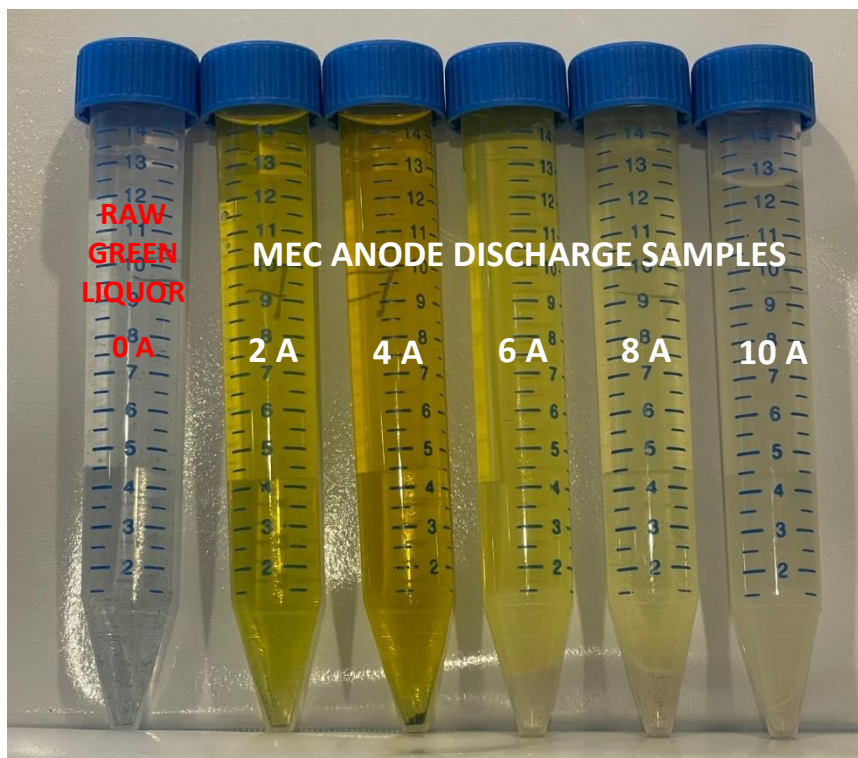
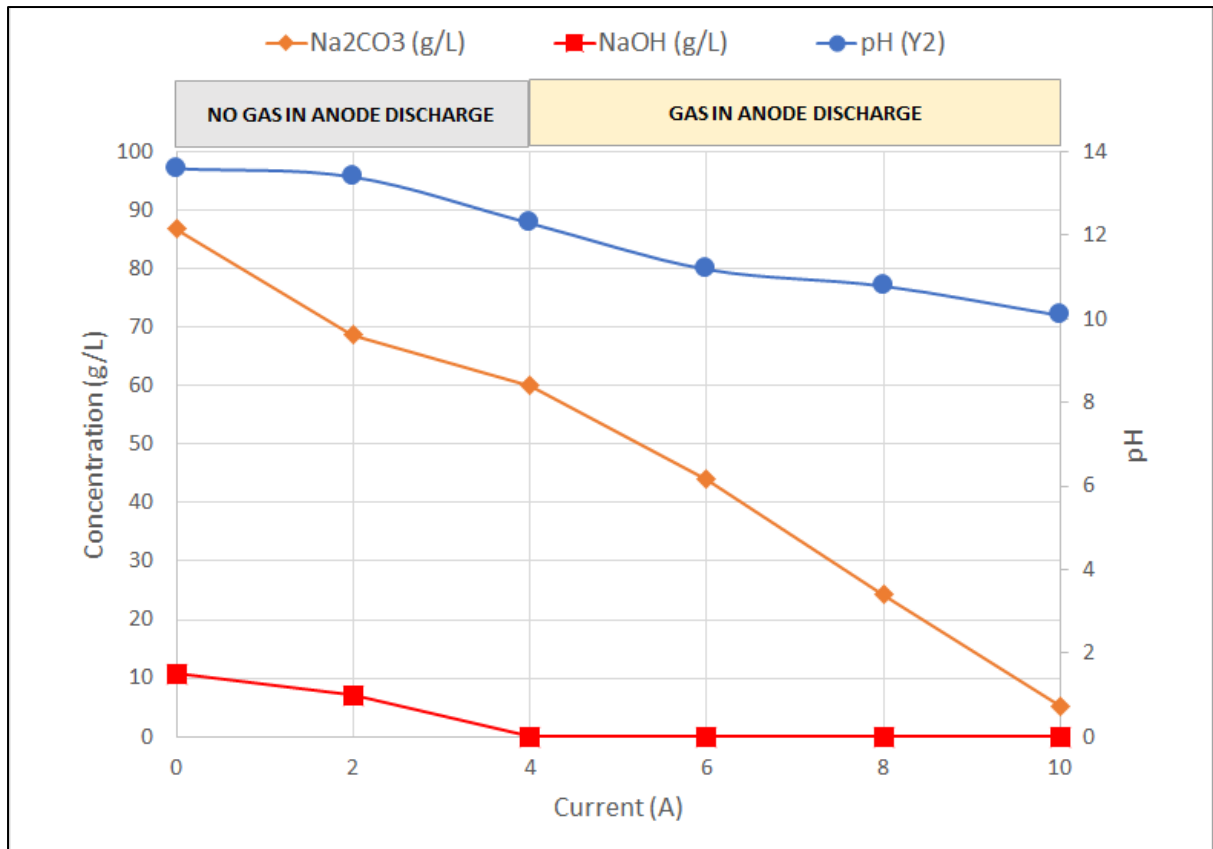


Figure 5.12: Trial 14 (Repeated): Titrations (Graph) and Green Liquor Samples (Photo)
 Top: MEC Anode Discharge Residual NaOH and Na₂CO₃.
 Bottom: Photo of Samples taken: Raw Green Liquor, 2 A, 4 A, 6 A, 8 A and 10 A)

With the low Green Liquor feed flow rate and concentration, the decreasing in NaOH, Na₂CO₃ and pH of the MEC discharge was most significant in Trial 14. Photographs of samples taken from trial 14 in Figure 5.12 illustrate the colour of the anode discharge at 2 and 4A is deep yellow. This corresponds to the modelled speciation of S species shown in Figure 5.13 below. As pH decreases the balance of S species shifts from S²⁻ to HS⁻, which presents as the deep yellow colour. As current increases from 4 to 10 A the yellow colour of the samples begins to fade to clear. This colour change can be explained by reactions (5.14) and (5.16) above, as Na₂S is converted to S_(s), some of which combines with NaOH to form the more neutral colourless salt Na₂SO₃.

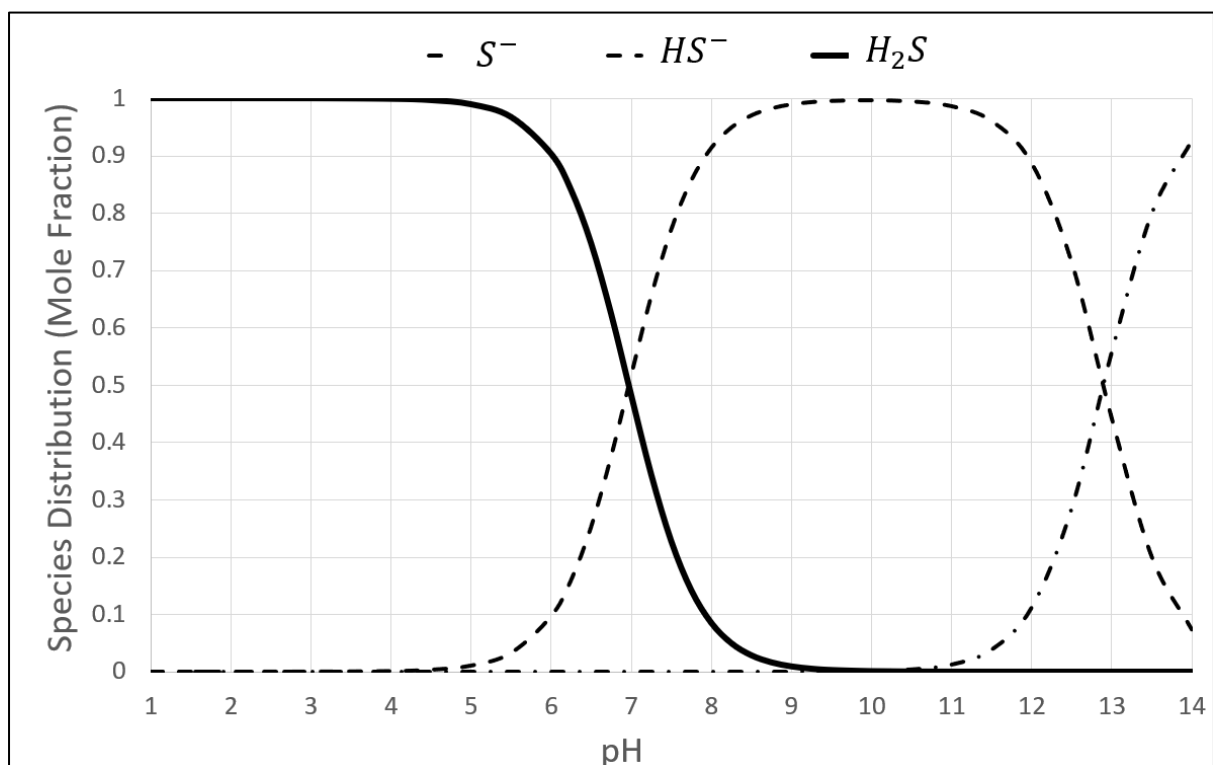


Figure 5.13: Modelled Speciation of S species in Aqueous Solution vs pH. pKa values obtained from (Dean, 1999)

Residual concentrations of Na⁺ and S²⁻ ions present in the MEC anode discharge in the repeated Trials 14 and 16 were measured with results for Trial 14 shown in Figure 5.14 below and Trial 16 in Appendix B. Any precipitate formed in the MEC discharge was not included in the ICP-OES sample, so the results presented are representative of the liquid phase only.

The ICP-OES results for Na in the MEC anode discharge show the reduction in Na concentration is linear with MEC increasing current.

The ICP-OES results for S in the MEC anode discharge show that the concentration of S remains relatively constant at all current set points. This indicates that only a small portion of the S in the Green Liquor feed leaves as elemental S precipitate in the anode discharge. This indicates that any S precipitate formed as per reaction 5.14 is almost completely converted to Na_2SO_3 and Na_2S as per reaction 5.16. The relatively small amount of precipitate presenting in the anode discharge suggest that the Na_2SO_3 is oxidising further to Na_2SO_4 .

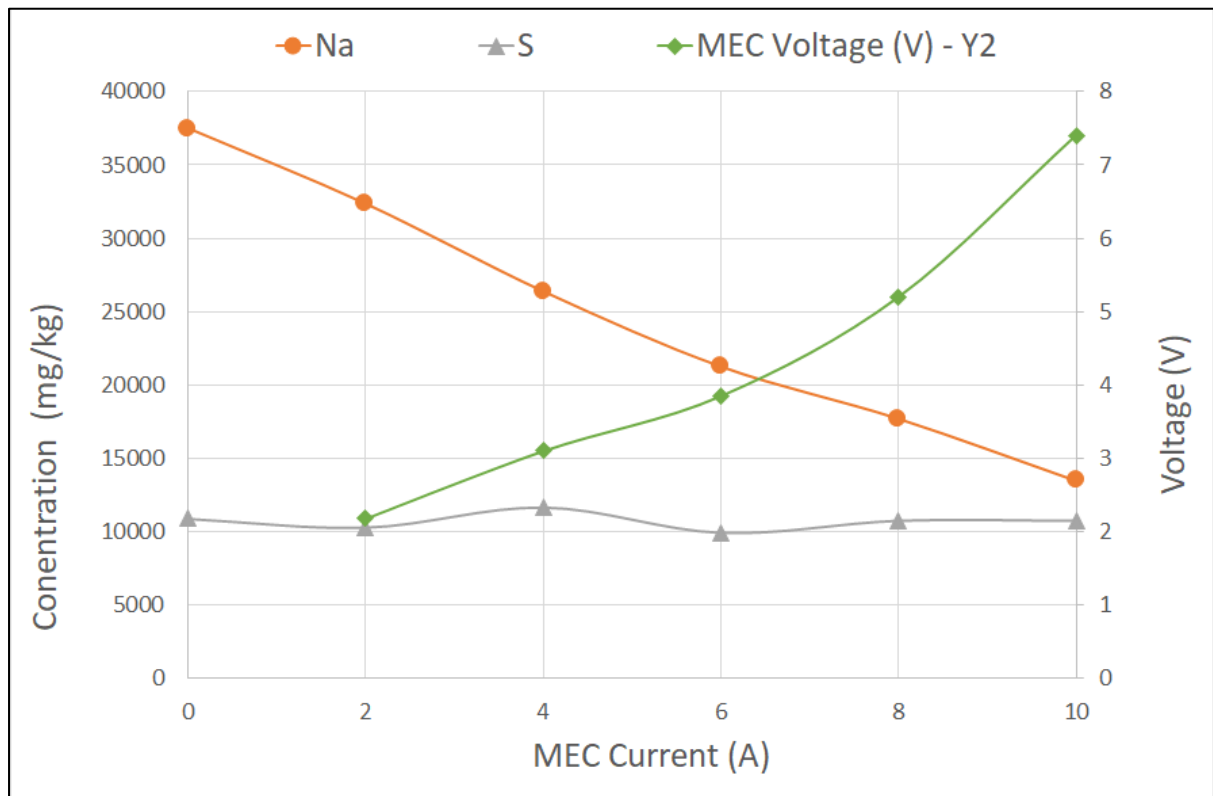


Figure 5.14: MEC Anode Discharge Trial 14 – Liquid Phase Analysis by ICP-OES

ICP-OES analyse also performed on selected samples of the cathode discharge in Trial 14 to detect any S leakage across the membrane from the anode to the cathode. Figure 5.15 below shows the results of the ICP-OES analysis performed on the cathode discharge and confirms that there is a negligible leakage of S^{2-} ions across the CEM. This confirms that essentially all the S entering the MEC anode compartment leaves in the anode discharge stream.

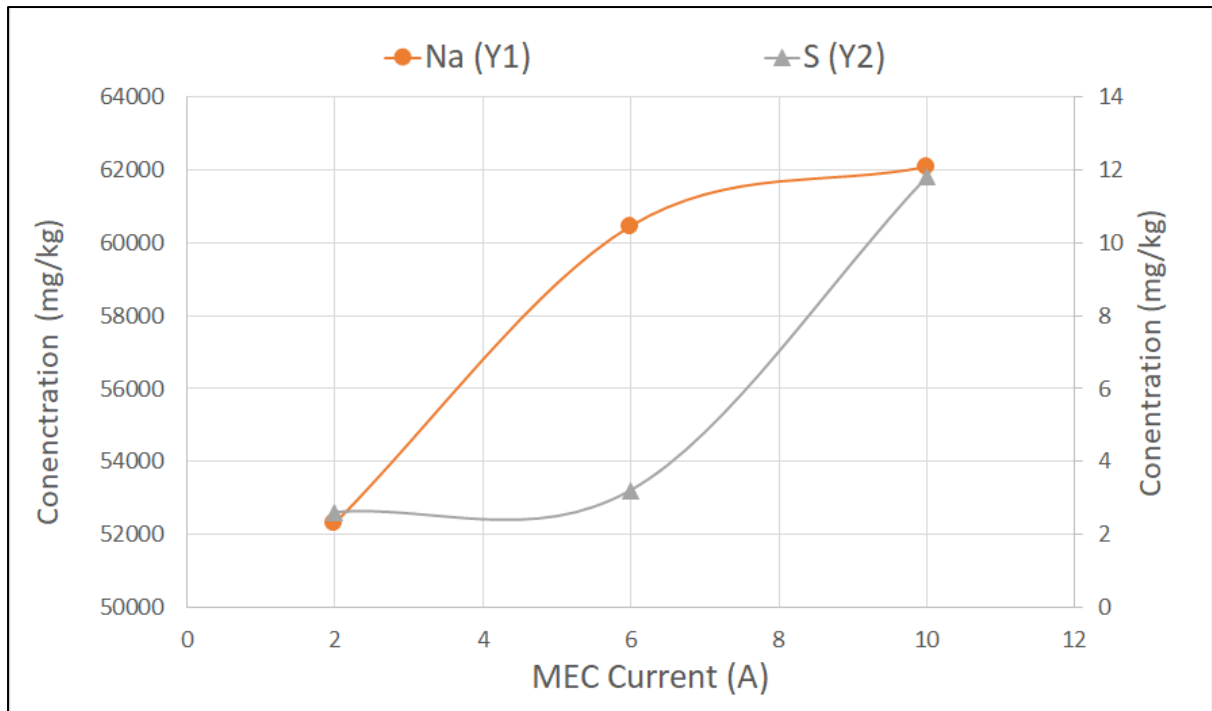


Figure 5.15: MEC Cathode Discharge Trial 14 – Liquid Phase Analysis by ICP-OES

In Trial 14, at current set point above 4 A precipitate began to present in the anode discharge. This is shown in Figure 5.16 where the colour change is clearly visible in the photograph. Samples of the precipitate were taken from the anode discharge at 6, 8 and 10 A, where there was enough to perform analysis using Scanning Electron Microscopy (SEM).

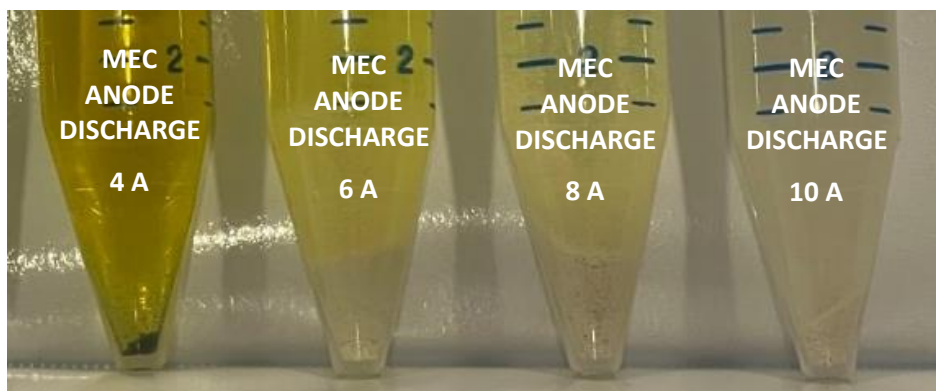


Figure 5.16: Trial 14 – Close-up of precipitate formed in MEC Anode Discharge

Figure 5.17 below shows an example of a SEM image of the precipitate from the anode discharge from Trial 14 at 6A. This is an example of a spot test at a focal width of 26µm at 10 kV.

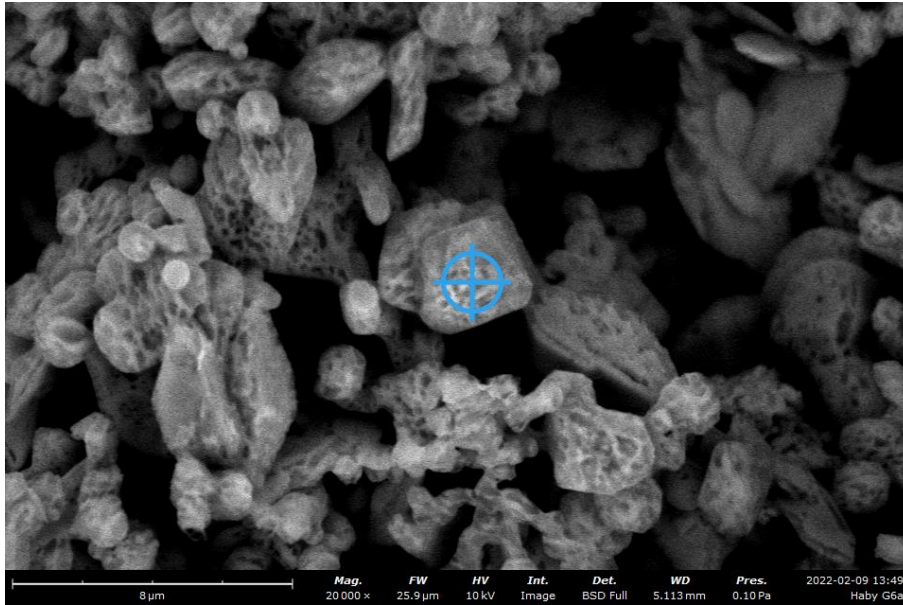


Figure 5.17: SEM Photograph Spot Test Example (Trial 14 – Current Set Point 6A)
 Settings: FW: 26μm, SEM mode: 10 kV

Figure 5.18 below shows an example of a SEM map scan of a precipitate sample from Trial 14 at 8A. The SEM maps show the measured presence of most prevalent elements, which is then graphed below.

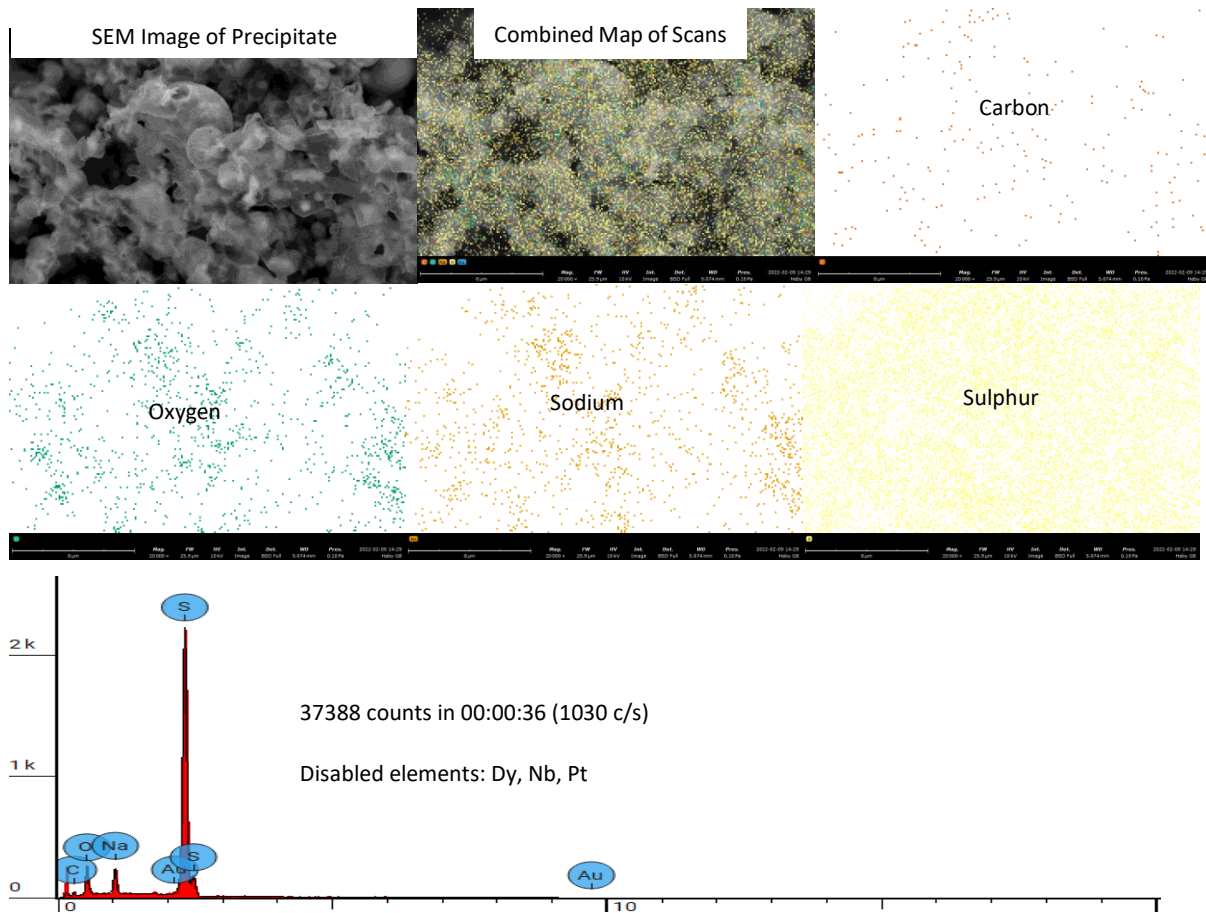


Figure 5.18: Map Test Example Results (Trial 14: 8 amps) – FW: 26μm, SEM mode: 10 kV

The summary results of all the SEM scans for MEC anode precipitate discharges at 6, 8 and 10 A are detailed in tables 5.13, 5.14 and 5.15.

Table 5.13: Composition of MEC Anode Discharge Precipitate by SEM – Trial 14 6A

Sample Tests	Carbon	Oxygen	Sodium	Sulphur
	Average (weight concentration %)			
10	20	3	2	74
10	40	4	2	54

Table 5.14: Composition of MEC Anode Discharge Precipitate by SEM – Trial 14 8A

	Sample Tests	Carbon	Oxygen	Sodium	Sulphur
Average (weight concentration %)	5	5	9	4	80
Average (atomic concentration %)	5	12	15	5	68

Table 5.15: Composition of MEC Anode Discharge Precipitate by SEM – Trial 14 10A

	Sample Tests	Carbon	Oxygen	Sodium	Sulphur
Average (weight concentration %)	5	10	10	4	76
Average (atomic concentration %)	5	20	15	4	60

The results at 6A, 8A and 10A show a high concentration of S relative to other elements in the anode precipitate, indicating the formation of an elemental sulphur precipitate, S_(s).

In all cases, there is a measured presence of Na, O and C precipitate sample. This can be explained by the preparation of precipitate samples for SEM analysis. The precipitate samples were taken from the bottles shown in Figure 5.16 using a small spatula. The precipitate sample could not be completely separated from the liquid and was slightly wet with solution before drying and analysis with SEM. As a result, a small amount of liquid phase solution could dry on the precipitate sample. Any Na₂CO₃, Na₂SO₃ or Na₂SO₄ in the liquid phase would add to the precipitate sample, and could explain the presence of Na, O and C in the SEM results.

The SEM uses carbon adhesive to attach the precipitate sample to the SEM mount. The presence of this adhesive would also contribute to an inflated C measurement.

5.9.1 Outcomes of MEC Anode Discharge Analysis

The outcomes of the MEC Anode discharge analysis are significant for the application of MEC for the recovery of Kraft Green liquor.

MEC can successfully convert Na_2CO_3 in Kraft Green Liquor to a NaOH stream of concentrations greater than 100 g NaOH/L, more than that required by the Kraft Pulping process. Analysis of the Green Liquor discharge showed the deadload Na_2CO_3 concentration diminishing linearly with MEC current density.

However, the impact on the Na_2S is important and analysis here shows that it is being converted to the neutral salt Na_2SO_3 , and likely Na_2SO_4 . In the conventional Kraft Cycle, Na_2SO_4 is reduced to Na_2S in the Kraft Recovery boiler. A similar reduction process will be needed after the MEC to convert the Na_2SO_3 and Na_2SO_4 in the MEC anode discharge to Na_2S , so it can be reintroduced to the Kraft cycle.

5.10 MEC Hydrogen Production Results

Water molecules fed to the cathode side of the CEM can be reduced, as can sodium ions that either enter with the cathode feed or have diffused through the CEM from the anode. The two possible half reactions at the cathode are:



The reduction potential for H_2O is much lower than Na^+ , so it was anticipated that essentially only reaction 5.18 would occur at the cathode. This is confirmed in the results shown in Figure 5.19 below as the measured hydrogen production for all trials is linear with the applied current, following Faraday's law with close to 100% efficiency.

The key observation is that the changing parameters in each trial, anode feed concentration, anode feed flow, cathode feed concentration and temperature did not significantly impact the molar production rate of hydrogen gas at the cathode beyond the accuracy of the measurement technique.

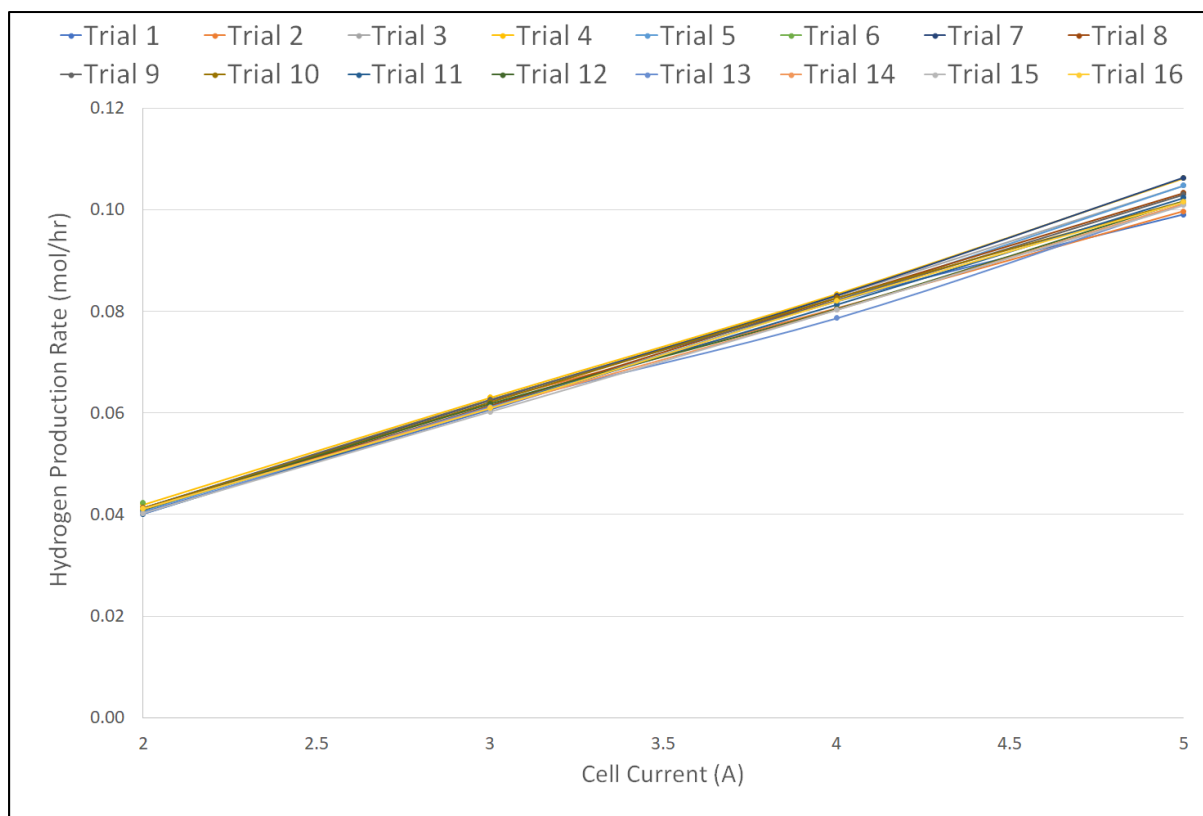


Figure 5.19: Hydrogen Gas Production (mol/hr) versus MEC Current – ALL TRIALS

The Hydrogen gas production was measured at currents above 2 A, as the production rate at 1 A was not fast enough to complete the measurement between current set points. The gas production was measured by capturing the H₂ gas in a submerged flask of known volume (100 mL).

The time to capture the sample at 2 A took 2.5 times as long as the sample taken at 5 A. This increased measurement time gives more accuracy of measurement, as any error in time measurement is less significant to the overall time. At 5 A, the time to capture 100 mL was less, so any error in time recording caused a greater error in flow measurement. This explains why the results at 2 A are much closer together than at 5 A.

5.11 The Way Forward

The experiments reported in this chapter were developed with the express intention to inform subsequent experiments using a variety of IEM materials from two membrane manufacturers: Selemion and Nafion. Analysis of the data reported established optimum settings for further experiments to determine specific membrane performance.

The level of process parameters established through the testing regime reported in this chapter have identified the operating conditions for further work. The operating parameters will remain consistent across the five membranes selected to enable performance comparisons to be made and develop metrics that reflect the operational metrics to meet the research objectives established in Chapter 1.

- Green Liquor Flow Rate: 350 mL/hr
- Green Liquor Feed Concentration: 200 g/L
- Anode feed Flow Rate: 175 mL/hr
- Anode feed concentration: 100 g NaOH/L
- Green Liquor feed Temperature Set Point: 40 and 80°C

The variety of membranes provided by the two manufacturers provided an opportunity to understand the importance of Green Liquor feed temperature with respect to ion selectivity and permeability, particularly in the case of the membranes supplied by Selemion. Selemion supplied five membrane materials, some that exhibited higher selectivity than others and feed temperature was considered a significant factor in assessing performance across the diversity of membrane materials available. Consequently, two Green Liquor feed temperature settings will be evaluated to assess the NaOH recovery performance based on the differing membrane characteristics of the five membrane materials. Two Green Liquor feed temperature settings will be used to better understand the permeability and selectivity of the various membrane materials in addition to NaOH recovery performance.

The higher temperature setting reflects current practices employed in the paper industry while the lower temperature may provide other benefits that include lowering energy demand by heating the smelt and potentially reducing GHG emissions. Temperature has a major impact on IEM resistance and selectivity and will have varying levels of impact on high and low resistance CEMs. Whilst in the case of the AG C F-9010 CEM a temperature of 80°C produced NaOH at lower specific energy levels that might not be the case with the other CEMs to be tested.

Chapter 6 Membrane Performance

Previously reported experiments in chapter 4 established the foundation for the configuration of MEC test equipment by including 'Zero Gap' mesh and defining core operational modes. Further experiments reported in chapter 5 established optimum operating conditions to determine the performance of the membrane-based system used to recover NaOH. The capability of the MEC to convert Na_2CO_3 in Kraft Green Liquor to NaOH was investigated by systematically varying the key process parameters of the system and evaluating their effect on MEC current efficiency and the specific energy requirement to produce NaOH.

The parameters identified are:

- Green Liquor Flow Rate: 350 mL/hr
- Green Liquor Feed Concentration: 200 g/L
- Anode feed Flow Rate: 175 mL/hr
- Anode feed concentration: 100 g NaOH/L
- Green Liquor feed Temperature Set Point: 40 and 80°C

The variety of membranes provided by the two manufacturers provided an opportunity to understand the importance of Green Liquor feed temperature with respect to ion selectivity and permeability, particularly in the case of the membranes supplied by Selemion. Two MEC feed temperature settings will be used to better understand the permeability and selectivity of the various membrane materials in addition to NaOH recovery performance.

Industrial IEMs produced by AGC Selemion LTD and DuPont with their Nafion membrane for NaOH production in the chloralkali industry are typically designed to operate at a range of 4 to 6 kA/m^2 (Selemion, 2019a). At the temperature set point of 40°C, the tested current range will be 1 A to 5 A (1.39 kA/m^2). At the temperature set point of 80°C, the current range will be increased to 10 A (2.78 kA/m^2) to better reflect industrial application for comparison.

6.1 Objectives of Membrane Trials:

Previously reported experiments were performed on a single membrane, the AGC Selemion F-9010 CEM. The objective of experiments and the resulting data analysed and reported in this chapter is to evaluate the MEC capability to convert Na_2CO_3 in Kraft Green Liquor to NaOH using the established settings identified in chapter 5, but varying the type of CEM used.

The CEMs assessed are identified in Table 6.1 below are of varying design for resistance, cation selectivity and ion exchange capacity. Temperature generally increases molar conductivity and the ion diffusion coefficient (Sadrzadeh and Mohammadi, 2009). Temperature changes may impact the selectivity and resistance of one type of CEM compared to another consequently, two temperature operating conditions were evaluated to consider the inherent differences between the membrane materials used and described in Table 6.1.

Table 6.1: Cation Exchange Membranes (CEM) Selected for Comparison.

	Membrane	Manufacturers Description	Thickness (µm)	Ion Exchange capacity (IEC) (meq/g)	Design Type
A	AGC-Selemion SX-1831WN	<p>Low resistance/High capacity/Low selectivity</p> <ul style="list-style-type: none"> - Fluorinated CEM for electrolysis and electro dialysis - Fabricated from fluorinated resins for chemical resistance - PTFE fabric reinforced for strength - (Selemion, 2020c) 	360	1.25	Low Selectivity
B	AGC-Selemion SX-1811WN	<p>Medium resistance/Medium capacity/Medium selectivity</p> <ul style="list-style-type: none"> - Fluorinated CEM for electrolysis and electro dialysis - Fabricated from fluorinated resins for chemical resistance - PTFE fabric reinforced for strength - (Selemion, 2020b) 	330	1.1	Medium Selectivity
C	AGC-Selemion SX-2301WN	<p>High resistance for high cation selectivity</p> <ul style="list-style-type: none"> - Fluorinated CEM for electrolysis and electro dialysis - Fabricated from fluorinated resins for chemical resistance - PTFE fabric reinforced for strength - (Selemion, 2020a) 	330	1.0	High Selectivity
D	AGC-Selemion SX-2301WNY	<p>High resistance for high cation selectivity</p> <ul style="list-style-type: none"> - Fluorinated CEM for electrolysis and electro dialysis - Fabricated from fluorinated resins for chemical resistance - Gas releasable zirconia coating on surfaces to lower resistance - PTFE fabric reinforced for strength - (Selemion, 2020a) 	330	1.0	High Selectivity
E	AGC-Selemion F-9010	<p>Low resistance with high current efficiency/ High selectivity:</p> <ul style="list-style-type: none"> - Latest generation membrane used to produce NaOH - Irreversible due to carboxylic layer preventing OH⁻ passage - Zirconia coating to lower resistance - Resistant to NaOH (and chlorine) - PTFE fabric reinforced - (Selemion, 2019b) 	150	1.0	High Selectivity
F	Dupont Nafion N-324	<p>Low resistance with high current efficiency/ High selectivity:</p> <ul style="list-style-type: none"> - Perfluoro sulfonic acid (PFSA) CEM - Irreversible membrane due to layer preventing OH⁻ passage - Resistant to NaOH (and chlorine) - PTFE fabric reinforced - (Nafion, 2017) 	150	>0.92	High Selectivity

The ion-exchange capacity (IEC) is a measure of active sites or functional groups responsible for ion exchange in polymer electrolyte membrane and can be determined using acid-base titration method (Luo et al., 2018). The IEC value (meq/g) is determined by the following equation:

$$IEC = V_{NaOH} \times S_{NaOH} / W_{dry} \quad (6.1)$$

Where W_{dry} is the dry weight of the membrane in grams, V_{NaOH} and S_{NaOH} are the volume and strength of the NaOH used in the titration (Kumar et al., 2018). The number of active sites on the membrane correlates to the membrane's conductivity, or inversely to its resistance to counter ions or selectivity rejection of counter ions.

In Table 6.2 above, the membranes are listed in order of their manufacturer's design ion exchange capacity from highest to lowest, or least selective to most selective.

In each experiment, the following measurements are made:

- Voltage (V)
- Current (A)
- Cell temperature (°C)
- NaOH concentration (mol/L) – MEC cathode discharge
- MEC anode and cathode feed flowrates (mL/hr)
- MEC Molar production rate of NaOH (mol/hour), N_{prod}

The performance of each CEM was evaluated based on:

- MEC current efficiency (%), ε
- MEC specific energy for NaOH production (kJ/mol NaOH), E_{NaOH}

The CEM with superior NaOH production performance was compared against the benchmarks of the conventional Kraft recovery process using lime, where the specific energy of NaOH production is 320 kJ/mol NaOH produced and approximately 0.49 kg CO₂ is emitted per kg NaOH produced (based on a diesel fuel source).

6.2 Membrane Performance at 40°C

Temperature generally increases molar conductivity and the ion diffusion coefficient (Sadrzadeh and Mohammadi, 2009). Temperature changes may impact the selectivity and resistance of one type of CEM compared to another, so it is important to compare performance at two temperature operating conditions.

The performance of the different membranes is first analysed at a temperature set point of 40 °C at a current range of 1 to 5 A.

6.2.1 Current Density vs Voltage at 40°C

Figure 6.1 shows the results for MEC current versus voltage at 40°C for each CEM. At 40°C, voltage is shown to increase linearly with increasing current in the tested current range from 1 to 5 A. Across the current range the AGC SX-1831WN CEM consistently presents the lowest voltage which corresponds to it having the highest IEC of 1.25 meq/g, meaning it has the most available sites per unit membrane mass available for ion exchange, decreasing its resistance.

The AGC-1811 WN membrane has the next highest IEC, at 1.1 meq/g, and across the current range it has the second lowest voltage consistently, however this was matched by the AGC SX-2301WNY membrane. The AGC SX-2301WNY membrane has an IEC of 1.0 meq/g, however the membrane has a gas-releasable zirconia coating designed to lower its resistance, which may explain why it had equivalent voltage performance to the AGC SX2301WNY, even though its IEC is lower. Thin zirconia surface coatings can significantly contribute to the permeability of targeted ions by improving the surface exchange kinetics (Park et al., 2020), decreasing the voltage required to drive Na⁺ ions through the membrane. In comparison, the equivalent membrane without surface coating, AGC SX-2301WN shows a consistently higher voltage across the current range.

The Nafion N-324 has a slightly higher voltage than the AGC F-9010 membrane across the current range reflecting its marginally lower quoted capacity, 0.95 compared to 1.0 meq/g. The similar performances of these membranes reflect their similar structural design for the chloralkali industry.

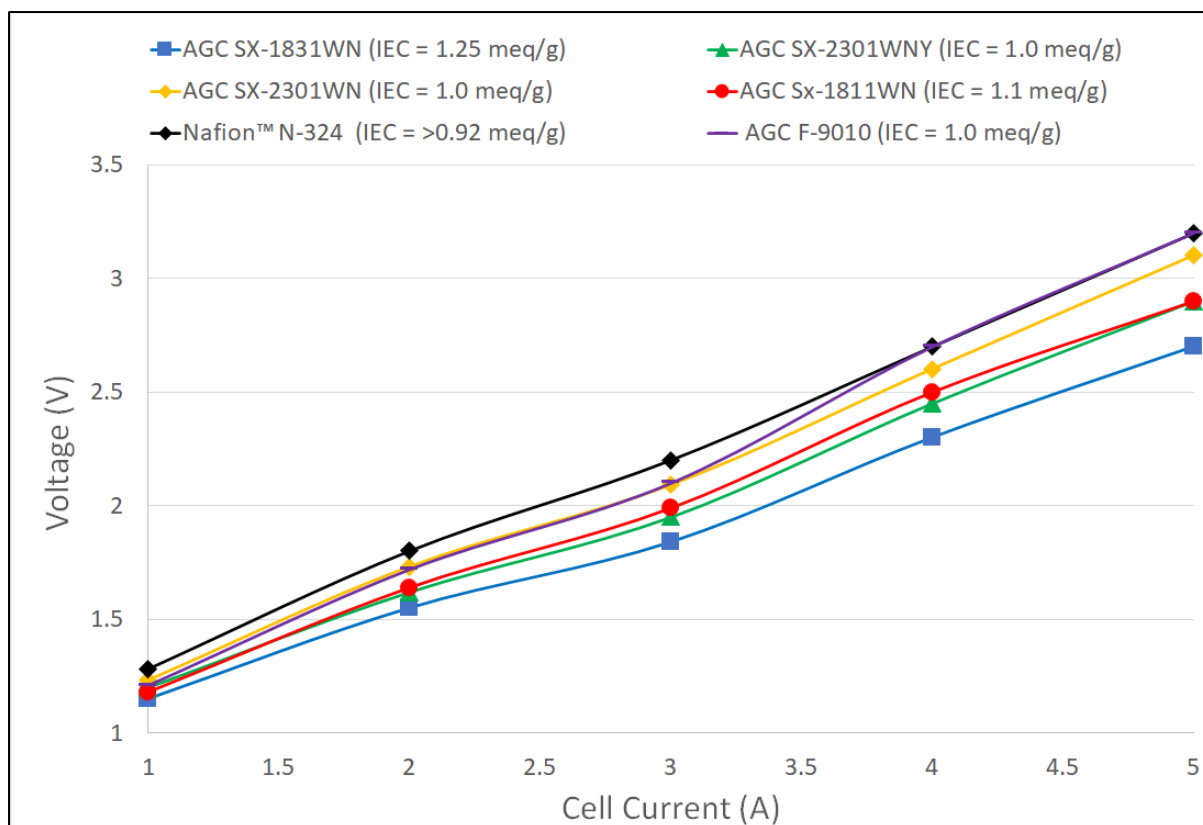


Figure 6.1 –Current (A) vs Voltage (V) – All Membranes at 40°C

6.2.2 Current Density vs Current Efficiency at 40°C

Figure 6.2 shows the results for MEC current versus current efficiency at 40°C for each CEM. At 40°C all membranes show some decrease in current efficiency from 1 to 5 A, consistent with the concentration gradient moving in favour of the diffusion of ions from the cathode to the anode.

At 40°C, the decrease in current efficiency across the current range is more significant for the high selectivity membranes, than the higher capacity membranes. The high selectivity AGC SX-2301WN membrane decreased from 88% to 67% over the 1 to 5 A current range, compared to the high capacity AGC SX-1831WN membrane only decreased 3%, from 44% to 41%, across the current range.

Overall, the AGC SX-2301WN and AGC SX-2301WNY delivered the highest current efficiency over the current range. These membranes showed very similar current efficiency performance, reflecting the fact that they have the same design capacity (1.0 meq/g) and

membrane structure. The zirconia coating whilst decreasing the CEM voltage, did not show any effect on the current efficiency performance.

As current increased to 5 A, the high selectivity membranes all presented very similar current efficiency performance of between 65 and 67%.

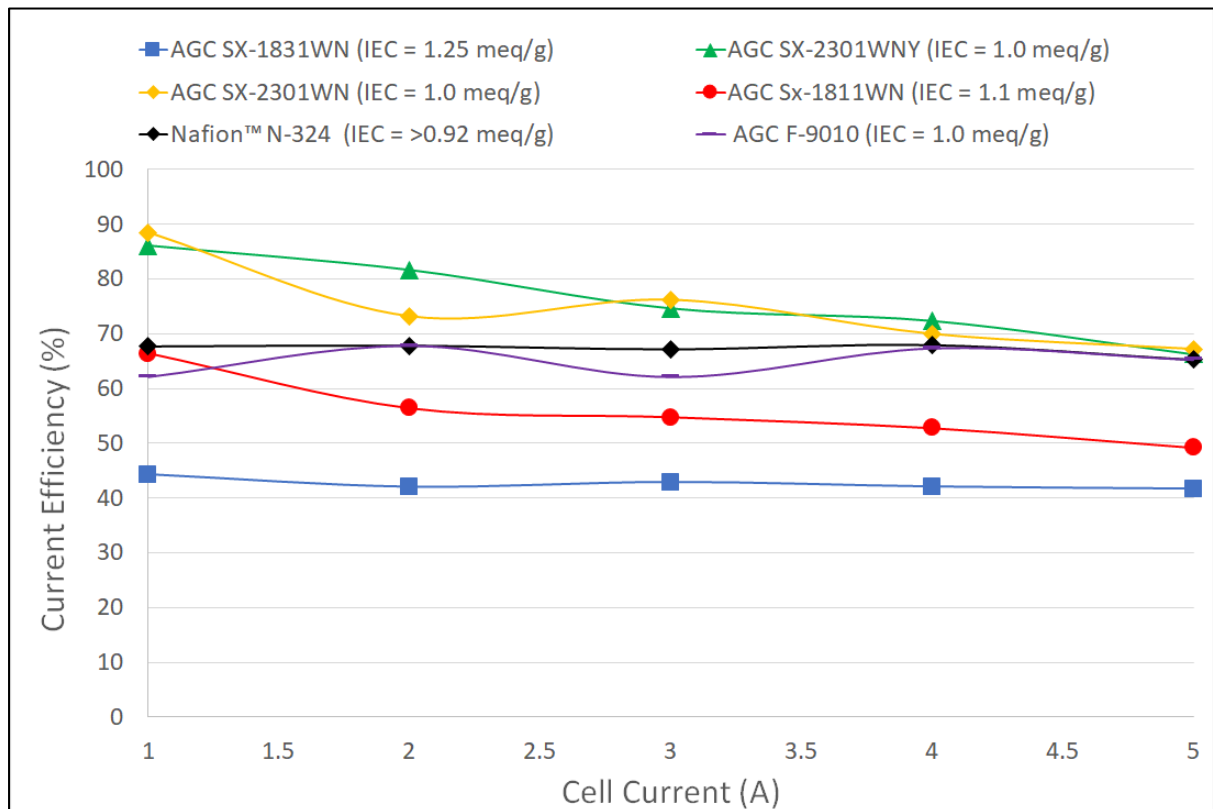


Figure 6.2: Current (A) vs Current Efficiency (%) – All Membranes at 40°C

6.2.3 Current Density vs Specific Energy of NaOH Production at 40°C

Figure 6.3 shows the results for MEC current versus specific energy of NaOH production at 40°C for each CEM across the current range of 1 to 5 A.

Across the current range and at the specific set of process parameters, the membrane of high capacity AGC-SX1831WN (1.25 meq/g) showed consistently the highest specific energy. The benefit of higher capacity and lower resistance is consistently outweighed by the negative effect of current leakage. This is not surprising as with a feed concentration of 100 g NaOH/L, the concentration gradient favours the passage of ions back to the anode, increasing the importance of membrane selectivity.

The high selectivity (1.0 meq/g) membranes showed similar overall specific energy performance. The AGC SX-2301 WNY is identified as having best overall specific energy performance across the current range, attributable to its lower voltage that can be linked to the membrane’s zirconia coating improving the membrane surface exchange kinetics.

The medium capacity AGC-1811WN membrane displayed specific energy performance between the low and high selectivity membranes.

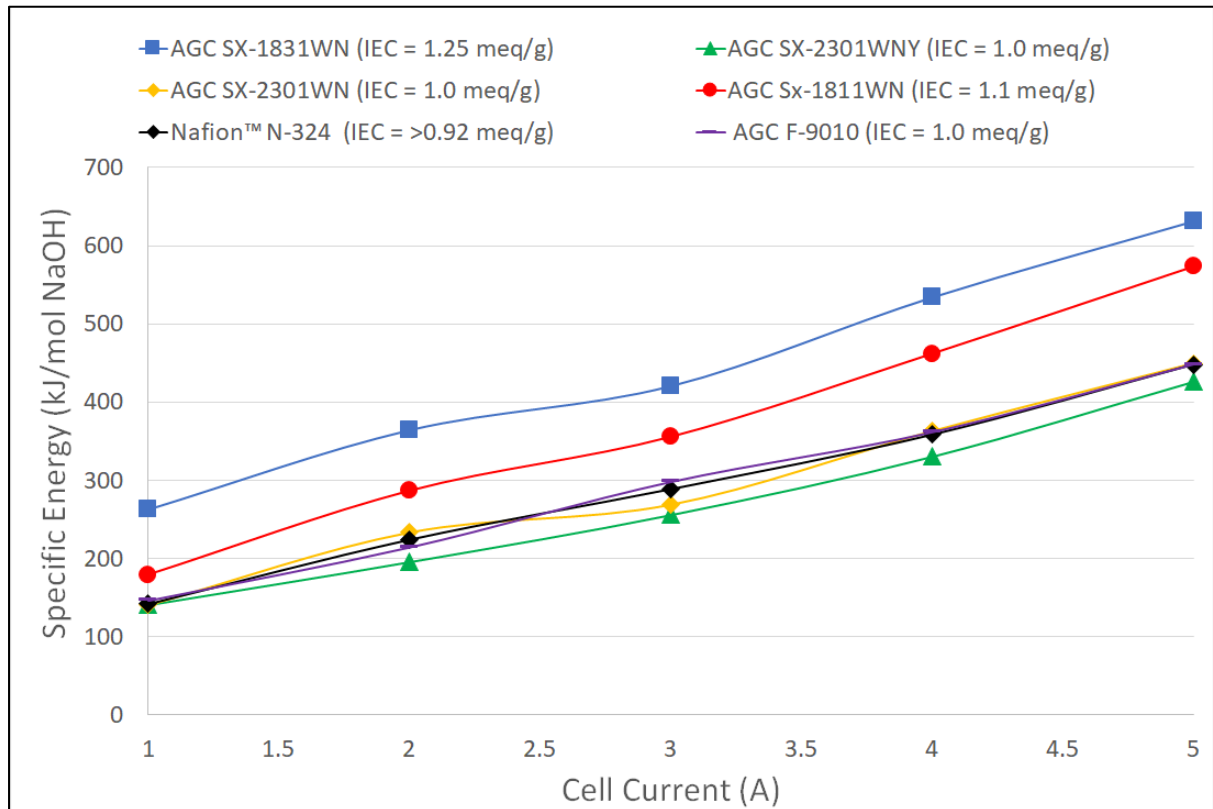


Figure 6.3: Current (A) vs Specific Energy (kJ/mol NaOH) – All Membranes at 40°C

6.2.4 Comparison Membrane Performance at 40°C and 5 A (1.39 kA/m²)

Table 6.2 and Figure 6.4 below compare the performance of each membrane at 40°C focussing on the current set point of 5 A, corresponding to a current density of 1.39 kA/m². The best performed membrane at this set of parameters was the AGC SX-2301WNY membrane, which produced NaOH at a specific energy 5% lower than the other high selectivity membranes of 1.0 meq/g ion exchange capacity (IEC). Each of high selectivity membranes showed similar current efficiency performance, but the lower voltage of the AGC SX-2301WNY membrane increased its overall performance.

The AGC Selemion membrane specification for AGC SX-2301WNY states that the membrane is based on the SX-2301WN CEM, however it has a gas-releasable zirconia coating on both surfaces of the CEM leading to lower electrical resistance (Selemion, 2020c). Based on the process parameters used in this experiment, the gas-releasable zirconia coating provided a 5% decrease in the specific energy required to produce NaOH.

Table 6.2: Comparison Membrane Performance at 40°C and 1.39 kA/m² (5 A)

Membrane	Design IEC (meq/g)	Voltage (V)	NaOH Conc. (M)	Current Efficiency (%)	Specific Energy	
					(kJ/mol NaOH)	Comparison to best
AGC SX-1831WN (Low Selectivity)	1.25	2.7	2.95	42	631	48%
AGC Sx-1811WN (Medium Selectivity)	1.10	2.9	3.03	49	574	35%
AGC SX-2301WNY (High Selectivity)	1.0	2.9	3.21	66	426	0%
AGC SX-2301WN (High Selectivity)	1.0	3.1	3.22	67	449	5%
Nafion™ N-324 (High Selectivity)	> 0.95	3.2	3.18	65	448	5%
AGC F-9010 (High Selectivity)	1.0	3.2	3.17	65	448	5%

The higher capacity (lower selectivity) SX-1831WN CEM and SX-1811WN have low relative resistance compared to the other high selectivity membranes. The reaction at the cathode releases H₂ gas and negatively charged hydroxide ions (OH⁻), creating a negative charge at the cathode. The cathode compartment produces a negative charge and has high concentration of hydroxide ions close to the membrane as 100 g NaOH/L solution is fed to the cathode. The balance of charge between the membrane φ^m and solution φ^s is expressed as the Donnan potential, φ_{Don} .

$$\varphi_{Don} = \varphi^m - \varphi^s \quad (6.2)$$

As the build-up of OH⁻ ions in the cathode compartment increases, the potential for leakage back across the membrane increases. In the case of membranes SX-1831WN and SX-1811WN they may perform better relative to the higher selectivity membranes in applications where the required concentration of NaOH in the cathode product is lower, so current leakage is less

significant, and can be outweighed by the benefit in voltage reduction. This could be proven with further experimentation trialling a demineralised water feed to the cathode.

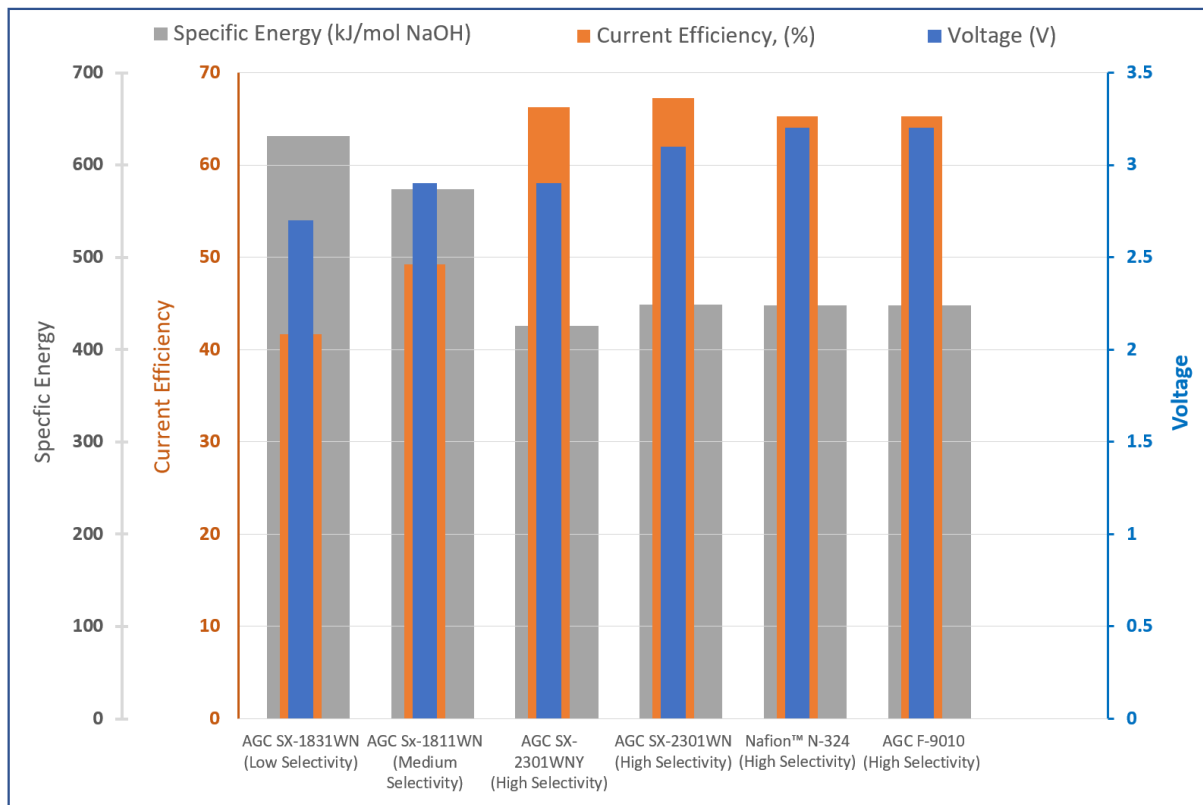


Figure 6.4 – Comparison of Membrane Performance at 40°C at 1.39 kA/m² (5 A)

The AGC SX-2301 WNY is identified as having best overall specific energy performance at a current density of 1.39 kA/m² at 40°C and the other specified operating parameters. At these operating parameters, performance benefit attributable the zirconia coating on AGC SX-2301 WNY is estimated to be a 5% reduction in specific energy requirement, given the membrane performance can be directly compared to the SX-2301 WN which does not have the coating.

6.3 Membrane Performance at 80°C

Temperature generally increases molar conductivity and the ion diffusion coefficient (Sadzadeh and Mohammadi, 2009). Temperature changes may impact the selectivity and resistance of one type of CEM compared to another, so it is important to compare performance at two temperature operating conditions.

The performance of the different membranes is now analysed at a temperature set point of 80 °C at an increased current range of 1 to 10 A.

6.3.1 Current Density vs Voltage at 80°C

Figure 6.5 shows the results for MEC current versus voltage at 80°C for each CEM between current set points of 1 A and 10 A. The temperature increase from 40°C to 80°C affects a voltage decrease for all membranes.

At 80°C, the voltage increases linearly with increasing current for the high selective (1.0 meq/g) membranes in the trialled current range of 1 A to 10 A. However, the voltage curve of the higher capacity membranes AGC SX-1831WN (1.25 meq/g) and AGC SX-1811WN (1.1 meq/g) show a decreasing rate of voltage increase relative to the increase in current above 5 A, giving the curves an 'S' shape.

As the current is increased to 5 A to 10 A, the voltage reduction benefit of the higher capacity membrane AGC SX-1831WN is more significant. At 5 A the AGC SX-1831WN voltage is 7% lower than the high selectivity membrane AGC SX-2301 WNY, this increases to 14% at 10 A.

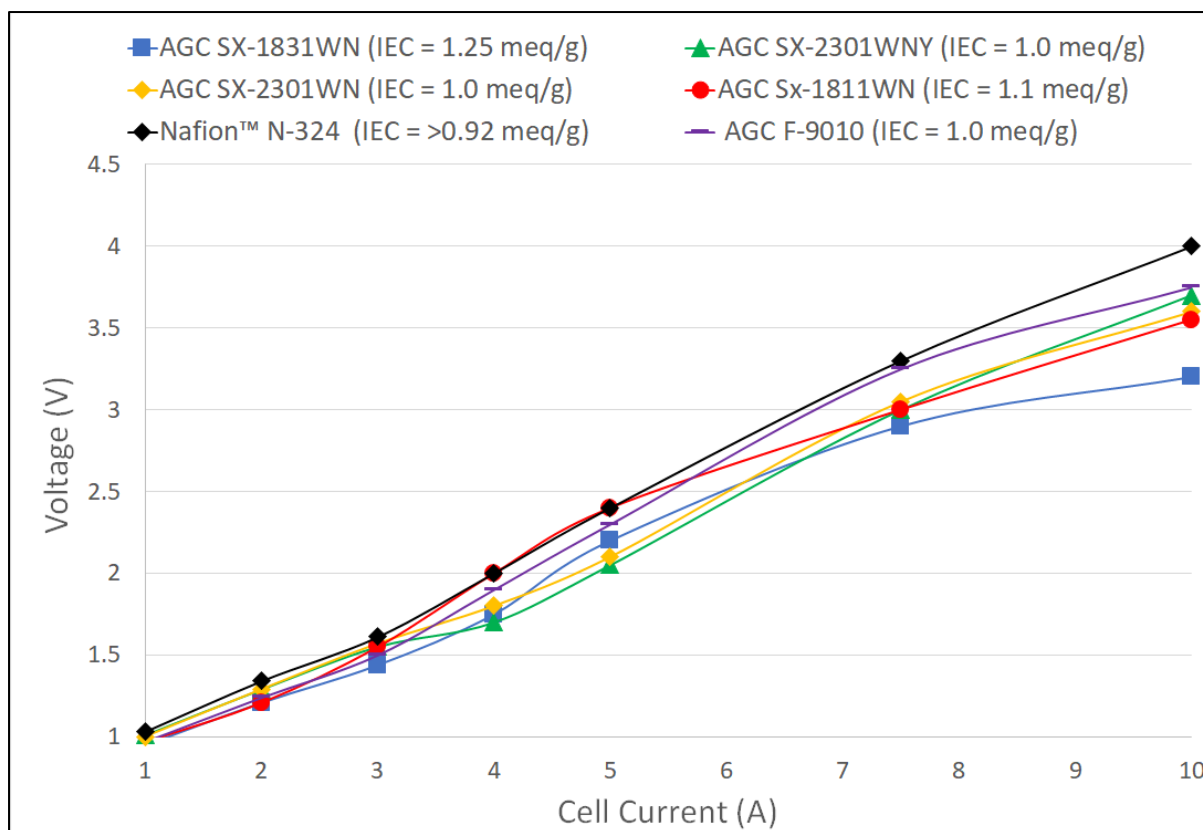


Figure 6.5 – Current (A) vs Voltage (V) – All Membranes at 80°C

6.3.2 Current Density vs Current Efficiency at 80°C

Figure 6.6 shows the results for MEC current versus current efficiency at 80°C for each CEM. The temperature increase from 40°C to 80°C affects a current efficiency decrease for all membranes.

At 80°C the high selectivity AGC SX-1831WN and AGC SX-1831WNY membranes display similar trend, with current efficiency decreasing as current is increased from 1 to 10 A. This observation is consistent with the concentration gradient moving in favour of the diffusion of ions from the cathode to the anode, increasing current leakage.

The Nafion N-324 and AGC-F-9010 membranes show a similar trend in current efficiency between 1 and 5A, remaining relatively stable in this range at 65% and 62% respectively. As current increased above 5 A to 10 A, the current efficiency of both membranes decreased to 53%.

In contrast, at 80°C the high capacity (1.25 meq/g) SX-1831WN membrane increased in current efficiency from 25% to 38% as applied current increased from 1 to 5 A. This indicates

that at the higher temperature of 80°C, current leakage is very significant with this low selectivity membrane. As current increases from 1 A to 5A, the electro potential gradient across the cell is increasing and appears to be the cause of the improvement in current efficiency. As current increases above 5 A the current efficiency of SX-18311WN starts to decrease, finishing at 34% at 10 A, consistent with the concentration gradient moving in favour of diffusion of ions from the cathode to the anode.

Overall, at 80°C at currents below 5 A, the AGC SX-2301WN membranes showed the best current efficiency. However as current density increased from 10 A, the current efficiency performance of each of the high-selectivity membranes was similar, between 52 and 54%.

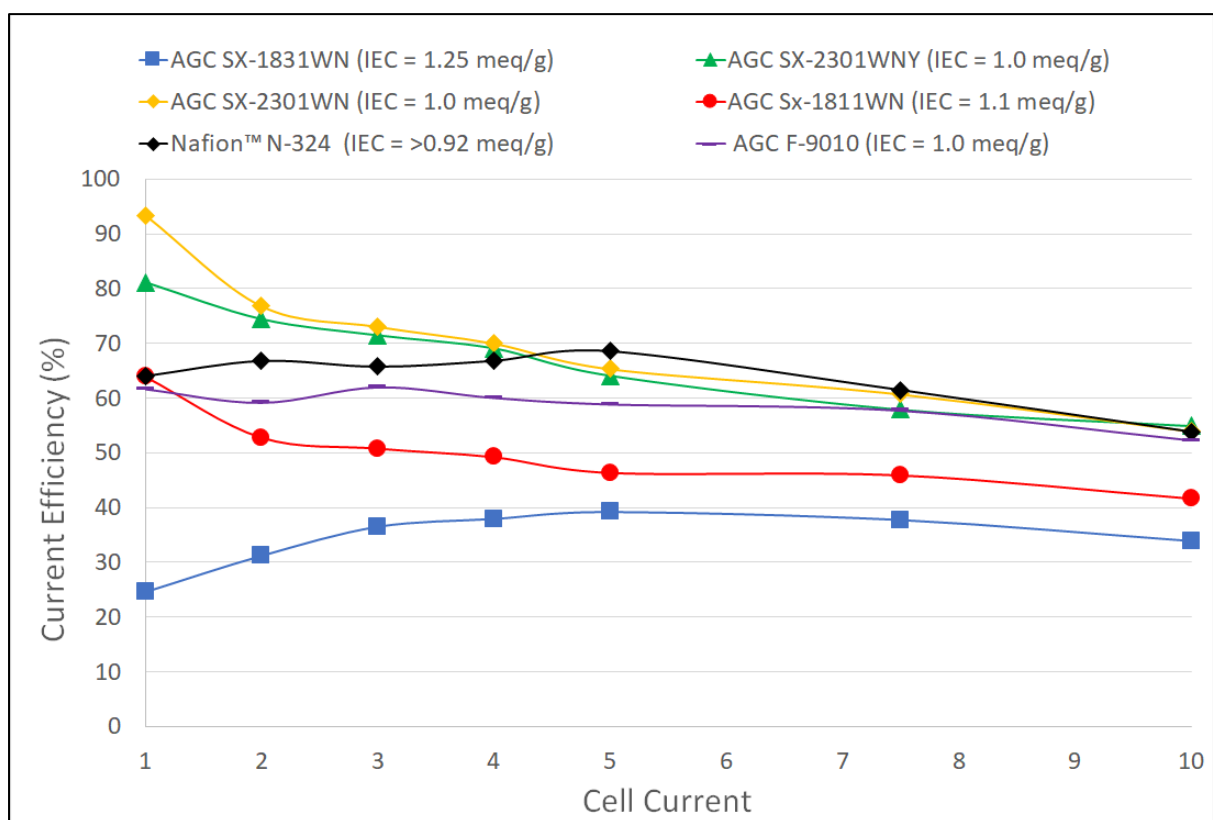


Figure 6.6 – Current (A) vs Current Efficiency (%) – All Membranes at 80°C

6.3.3 Current Density vs Specific Energy of NaOH Production at 80°C

Figure 6.7 shows the results for MEC current versus specific energy of NaOH production at 80°C for each CEM between the current range of 1 and 10 A. The temperature increase from 40°C to 80°C affects an overall specific energy decrease for all membranes, as the voltage decrease outweighs the minor loss in current efficiency.

Across the current range and at the specific set of process parameters, the membranes of high capacity AGC-SX1831WN (1.25 meq/g) showed consistently the highest specific energy. The benefit of higher capacity and lower voltage is consistently outweighed by the negative effect of current leakage.

The high selectivity (1.0 meq/g) membranes showed similar overall specific energy performance. The AGC SX-2301 WNY showed best overall specific energy performance across the current range, attributable to its lower voltage that can be linked to the membrane's zirconia coating improving the membrane surface exchange kinetics.

The medium capacity AGC-1811WN membrane displayed specific energy performance between the low and high selectivity membranes.

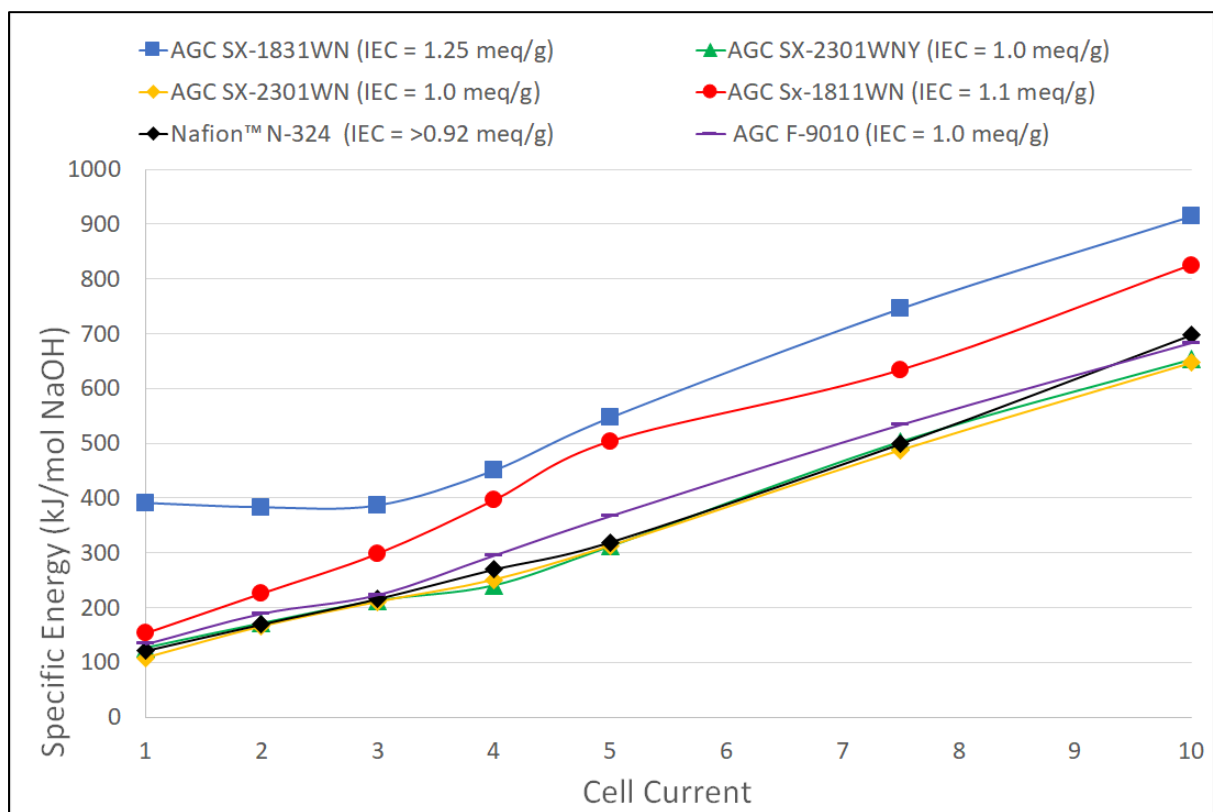


Figure 6.7 – Current (A) vs Specific Energy (kJ/mol NaOH) – All Membranes at 80°C

The AGC SX-2301 WNY is identified as having best overall specific energy performance at a current density of 1.39 kA/m² at 80°C and the other specified operating parameters.

6.3.4 Comparison of CEM Performance at 80°C and 1.39 kA/m²

The performance of each membrane at 80°C focussing on the current set point of 5 A, corresponding to a current density of 1.39 kA/m² are compared in Figure 6.8 below. The best performed membrane at this set of parameters was again the AGC SX-2301WNY membrane, which produced NaOH at a specific energy 312 kJ/mol NaOH.

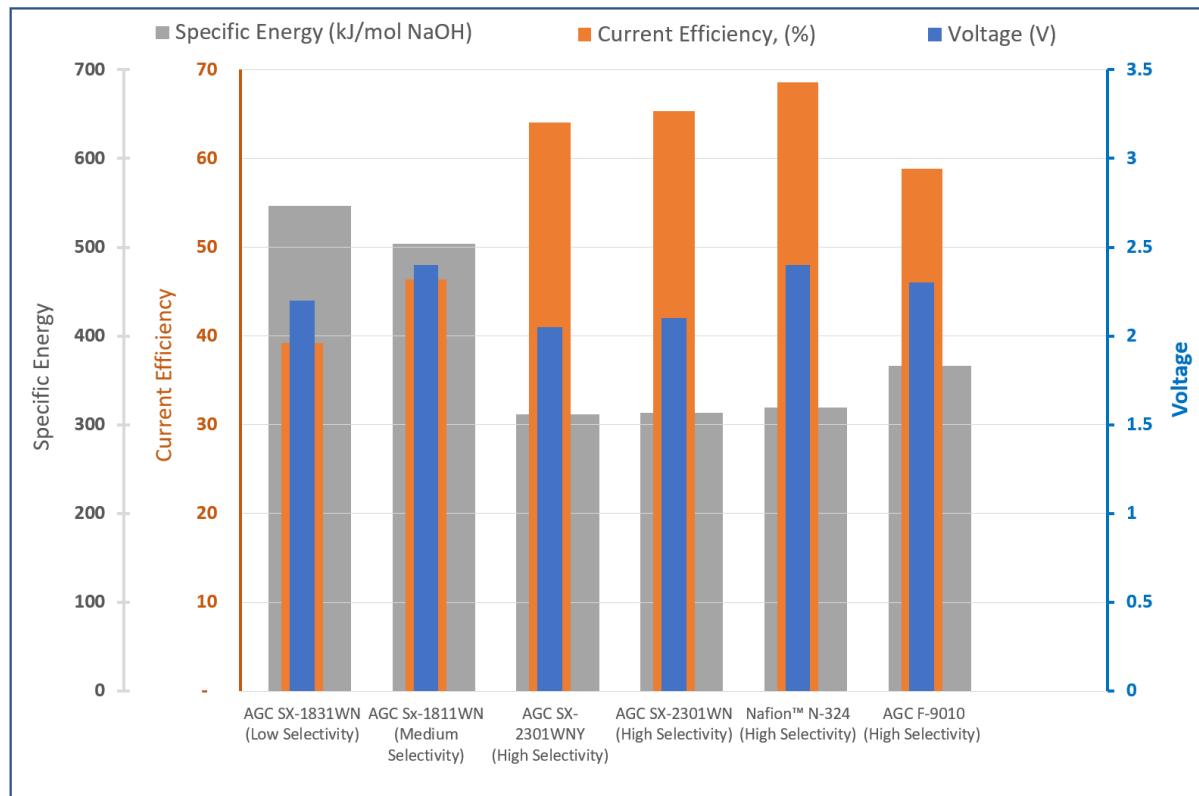


Figure 6.8: Comparison of CEM Performance at 80°C and 1.39 kA/m² (5 A)

Table 6.3 details the voltage, current efficiency, and specific energy performance of each membrane at 80°C and 1.39 kA/m², and gives the change in performance for each membrane affected by the increase in temperature from 40 to 80°C.

Table 6.3: Comparison of CEM Performance at 80°C and 1.39 kA/m² (5 A)

Membrane	Design IEC (meq/g)	Voltage (V)		NaOH Conc. (M)	Current Efficiency (%)		Specific Energy (kJ/mol NaOH)	
		At 80°C	Change from 40°C		At 80°C	Change from 40°C	At 80°C	Change from 40°C
AGC SX-1831WN (Low Selectivity)	1.25	2.2	-0.5	2.92	39%	-2%	546	-85
AGC Sx-1811WN (Medium Selectivity)	1.10	2.4	-0.4	3.00	46%	-3%	504	-49
AGC SX-2301WNY (High Selectivity)	1.0	2.1	-0.85	3.18	64%	-2%	312	-115
AGC SX-2301WN (High Selectivity)	1.0	2.1	-1	3.20	65%	-2%	313	-136
Nafion™ N-324 (High Selectivity)	> 0.95	2.4	-0.8	3.21	69%	3%	319	-128
AGC F-9010 (High Selectivity)	1.0	2.3	-0.9	3.12	60%	-6%	367	-95

In all cases, the increase in temperature from 40°C to 80°C affected a decrease in voltage. The voltage reduction was most significant with the high selectivity membranes, with the AGC SX-2301WN membrane decreasing from 3.1 V to 2.1 V. The change in voltage across the higher capacity membrane AGC SX-1831WN was less significant, decreasing from 2.7 to 2.2 V. With a constant current set point, the MEC voltage reflects energy required to overcome the resistance of the cell (R_{MEC}) and the energy required to perform the oxidation and reduction reactions at the anode and cathode. In the case of the high capacity (low resistance) SX-1831WN membrane, the contribution of the CEM resistance to voltage at 40°C was already reduced, so increasing temperature to 80°C did change MEC voltage as significantly as the high selectivity membranes.

In all cases the increase in temperature from 40°C to 80°C affected a small decrease in current efficiency, but this was outweighed by the decrease in MEC voltage, giving an overall reduction in specific energy. The overall impact in all cases of the temperature increase was a decrease in the specific energy required to produce NaOH.

The best performed membrane was the AGC SX-2301WNY, producing NaOH at a specific energy of 312 kJ/mol NaOH. This result will be used following comparisons to the conventional Kraft cycle.

6.3.5 Comparison of CEM Performance at 80°C at 2.78 kA/m²

Industrial IEMs produced by AGC Selemion LTD and DuPont with their Nafion membrane for NaOH production in the chloralkali industry are typically designed to operate at a range of 4 to 6 kA/m² (Selemion, 2019a). At 80°C, in each membrane trial, the current was increased to 10 A (2.78 kA/m²) to better reflect industrial application for comparison.

The solubility of some the constituents of Kraft Green liquor are lower than NaCl in the chlor-alkali process. In typical chloralkali processes, NaCl brine is fed to the electrolysis at concentrations close to saturation, above 300 g/L. In this experiment Green Liquor is fed at a lower concentration of 200 g/L, so it was warranted to reduce the current density in this application to 2.78 kA/m².

The performance of each membrane at 80°C at current set point of 10 A are compared in Figure 6.9 below. The best performed membrane at this set of parameters was the AGC SX-2301WN membrane, which produced NaOH at a specific energy 647 kJ/mol NaOH.

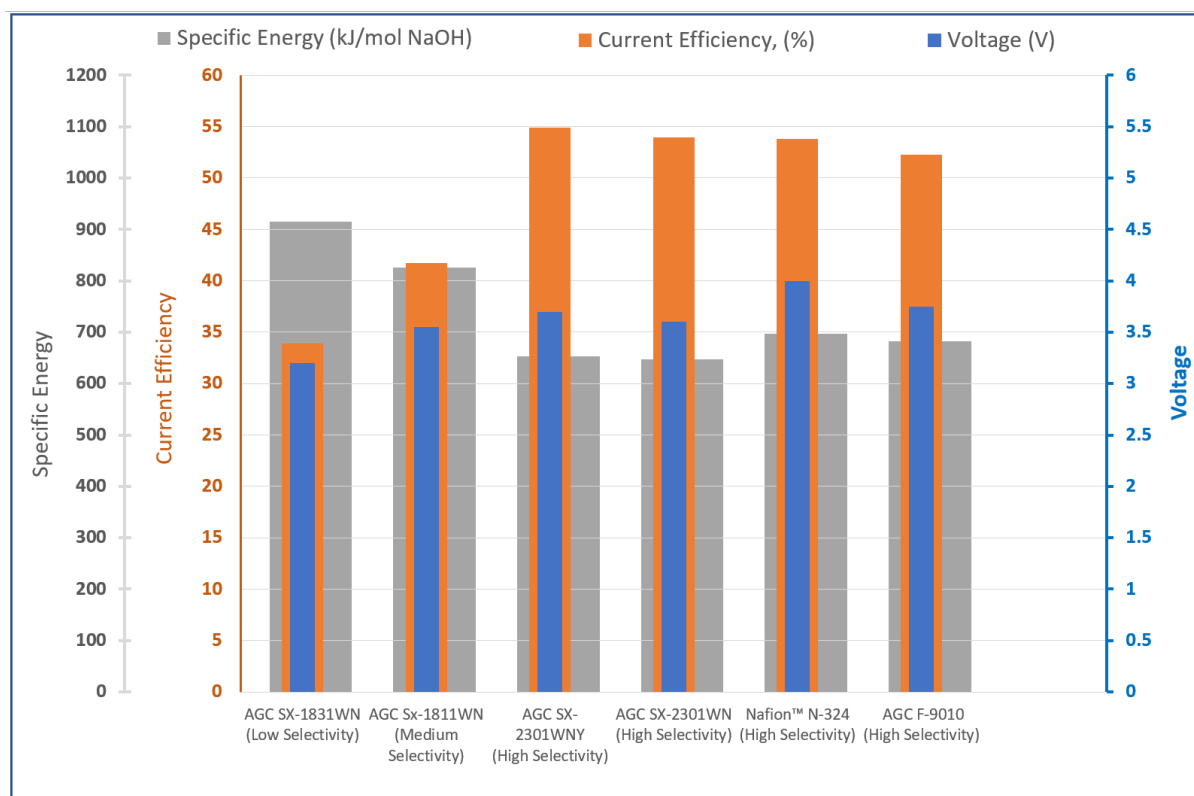


Figure 6.9: Comparison of CEM Performance at 80°C at 2.78 kA/m² (10 A)

The increase in current density from 1.39 to 2.78 kA/m² provides a response by increasing the voltage. Similarly, the increase in current density decreases the average concentration of ions

in the anode compartment and increases the average concentration of ions in the cathode compartment. This results in a shift in concentration gradient in favour of diffusion from the anode to the cathode and decrease in current efficiency.

The performance data for each membrane at 80°C and 2.78 kA/m² current density is given below in table 6.4.

Table 6.4 – Comparison of CEM Performance at 80°C and 2.78 kA/m² (10 A)

Membrane	Design IEC (meq/g)	Voltage (V)		NaOH Conc. (M)	Current Efficiency (%)		Specific Energy (kJ/mol NaOH)	
		At 10 A	Change from 5 A		At 10 A	Change from 5 A	At 10 A	Change from 5 A
AGC SX-1831WN (Low Selectivity)	1.25	3.2	+1.0	3.23	34%	-5.2%	914	368
AGC Sx-1811WN (Medium Selectivity)	1.10	3.55	+1.1	3.40	42%	-4.4%	825	300
AGC SX-2301WNY (High Selectivity)	1.0	3.7	+1.7	3.68	55%	-9.1%	653	341
AGC SX-2301WN (High Selectivity)	1.0	3.6	+1.5	3.66	54%	-11.3%	647	334
Nafion™ N-324 (High Selectivity)	> 0.95	4	+1.6	3.62	54%	-14.6%	697	378
AGC F-9010 (High Selectivity)	1.0	3.75	+1.5	3.60	53%	-6.8%	668	315

At the increased current density of 2.78 kA/m², the current efficiency of the group of high selectivity membranes is very similar, between 53% and 55%.

The AGC SX-2301WNY and SX-2301WN high selectivity membranes produced the lowest overall specific energy of 653 and 647 kJ/mol NaOH respectively. They matched the current efficiency performance of industrial chloralkali membranes, Nafion N-324 and AGC F-9010, but at a lower overall MEC voltage.

At 80°C and 2.78 kA/m², the AGC SX-2301WNY and SX-2301WN membranes showed similar voltage, indicating that the effect of the zirconia coating at higher temperature and current density is less.

The Nafion N-324 and AGC F-9010 both designed for NaOH production in the chlor-alkali industry performed similarly at 2.78 kA/m², with specific energies of 668 kJ/mol and 697 kJ/mol NaOH, respectively.

6.4 Best Membrane Performance with Optimal Process Parameters

A variety of six different membranes provide by AGC Selemion and Dupont Nafion provided an opportunity to understand the importance of ion exchange membrane selectivity characteristics on the performance of the MEC Green Liquor recovery. The cationic exchange membranes trialled were:

- AGC Selemion SX-1831WN: Low Selectivity (IEC = 1.25 meq/g)
- AGC Selemion SX-1811WN: Medium Selectivity (IEC = 1.1 meq/g)
- AGC Selemion SX-2301WN: High Selectivity (IEC = 1.0 meq/g)
- AGC Selemion SX-2301WN(Y): High Selectivity with zirconia coating (IEC = 1.0 meq/g)
- AGC Selemion F-9010: High Selectivity CEM for chloralkali industry (IEC = 1.0 meq/g)
- Dupont Nafion™ N-32: High Selectivity CEM for chloralkali industry (IEC = 1.0 meq/g)

The six membranes were evaluated using the established set of operation parameters:

- Green Liquor Flow Rate: 350 mL/hr
- Green Liquor Feed Concentration: 200 g/L
- Anode feed Flow Rate: 175 mL/hr
- Anode feed concentration: 100 g NaOH/L

At a temperature of 40°C, it was confirmed that the MEC with high selectivity membranes produced NaOH at a lower specific energy than membranes of low selectivity. Whilst the MEC with high-capacity membranes like the AGC SX 1831WN show low resistance, the decrease in current efficiency outweighed any voltage reduction benefit. The best performed membrane at 40°C at a current density of 1.39 kA/m² was the AGC Selemion SX-2301WNY, producing an NaOH product of 3.21M at a specific energy of 426 kJ/mol NaOH.

Each membrane was also trialled at 80°C to evaluate whether temperature had a greater effect on either high or low resistance membranes. Every membrane exhibited an improvement in specific energy performance with the increase in temperature. The increase in temperature affected a decrease in current efficiency with all membranes, however this was relatively small compared to a significant decrease in voltage. The decrease in voltage was most significant with the high selectivity membranes, resulting in a greater decrease in specific energy with the temperature increase from 40°C to 80°C. The best performed

membrane at 80°C at a current density of 1.39 kA/m² was again the AGC Selemion SX-2301WNY, producing an NaOH product of 3.12M at a specific energy of 312 kJ/mol NaOH.

At 80°C the MEC current density was increased to 2.78 kA/m² to better reflect a membrane current density found in industrial applications, where the cost of membrane area must be balanced against energy costs. Every membrane exhibited an increase in specific energy reflecting the increase in voltage required to drive the passage of ions and a decrease in current efficiency. The increase current from 1.39 to 2.78 kA/m² affected an increase of 300 to 350 kJ/mol NaOH for all membranes. The best performed membrane at 80°C at a current density of 2.78 kA/m² was the AGC Selemion SX-2301WN, producing an NaOH product of 3.66 M at a specific energy of 647 kJ/mol NaOH.

6.5 Final Evaluation of MEC NaOH Production Metrics vs Kraft Reausticisation

The analysis presented in this chapter establishes the key metrics of MEC performance that are used for comparison to the conventional Kraft reausticisation process. The best membrane specific energy performance is identified at each the three sets of parameter settings in Table 6.5.

The key metrics of the conventional Kraft process were established in the Chapter 2 literature review and are summarised in Table 6.6 below.

Table 6.5 – Membrane Performance at Optimal Parameter Settings

	Parameter Settings 1	Parameter Settings 2	Parameter Settings 3
Temperature (°C)	40	80	80
Current Density (kA/m ²)	1.39	1.39	2.78
Best Performed Membrane	AGC SX-2301WNY (High Selectivity)	AGC SX-2301WNY (High Selectivity)	AGC SX-2301WN (High Selectivity)
Voltage (V)	2.9	2.05	3.6
NaOH Concentration (mol/L)	3.21	3.18	3.66
Current Efficiency (%)	66	64	54
Specific Energy (kJ/mol NaOH)	426	312	647

Table 6.6 – Summary of Key Metrics of Conventional Kraft Caustic Recovery

Metric 1: NaOH Concentration Requirement	
Minimum required	60 g NaOH/L (1.5 M)
Maximum required	90 g NaOH/L (2.25 M)
Metric 2: Specific Energy Requirements – Thermal Energy Lime Kiln	
NaOH Production	8.0 MJ/kg NaOH Produced (320 kJ/mol NaOH)
Metric 3: Greenhouse Gas Emissions – Lime Kiln (kg CO₂/kg NaOH)	
Based on Diesel Fuel	0.49 kg CO ₂ /kg NaOH
Based on Gasoline Fuel	0.51 kg CO ₂ /kg NaOH
Based on Natural Gas Fuel	0.28 kg CO ₂ /kg NaOH

6.5.1 Metrics 1: NaOH Concentration Required (2.15 M NaOH)

The MEC can easily produce NaOH solution in concentrations exceeding that required by the Kraft pulping cycle, which can benefit the Kraft cycle by presenting opportunity to decrease storage, transfer, and heating systems. This is evident from the chapter 4 single solute experiments with recirculating cathode product using 100 g Na₂CO₃ feed to the MEC which showed that a 3.5. M NaOH product can be produced using the test MEC cell.

With a Green Liquor flowrate of 350 mL/hr and concentration of 200 g/L at 80°C, AGC SX-2301WN membrane, the MEC produced a 3.18 M concentration at 1.39 kA/m², and a 3.66 M concentration at 2.78 kA/m². This proved that the MEC could achieve the required NaOH concentration with Green Liquor feed also.

6.5.2 Metrics 2: Specific Energy of MEC

As specific energy increases with current density, a balance must be chosen between membrane area and energy requirement. In the chloralkali industry, current densities of around 4.0 kA/m² are typical, however given that Green Liquor is a mixture of solutes of different solubilities, a lower current density is warranted. The results of configurations 2 and 3 are taken forward for comparison with the conventional lime recausticisation metrics.

At 1.39 kA/m² (configuration 2) the MEC produced NaOH at a specific energy of 312 kJ/mol, which is less than the conventional lime recausticisation fuel requirement of 320 kJ/mol.

However, at 2.78 kA/m^2 (configuration 3), the MEC produced NaOH at a specific energy of 647 kA/m^2 , which is greater than the conventional process.

6.5.3 Metric 3: Greenhouse Gas (GHG) Emissions

The MEC NaOH recovery process can be driven by electrical energy sourced from renewables that release relatively low levels of Greenhouse Gases (GHG). This is an advantage over the conventional Kraft recausticisation process that must use fossil fuels to burn Ca_2CO_3 to produce CaO. The GHG emissions of the Kraft Lime kiln were established in chapter 2 and are summarised in Table 6.5 above.

An electrolysis process powered by renewable energy regenerating Kraft Green liquor offers an opportunity to reduce overall plant greenhouse gas emissions. Referring to the optimal membrane configurations in Table 6.5, in configuration 2 and 3 the specific energy of the MEC was 312 and 647 kJ/mol NaOH respectively.

The US-based National Renewable Laboratory (NREL) estimates that solar power produces lifetime emissions of 40g CO_2 equivalent per kilowatt-hour (NREL, 2012). (Pehl et al., 2017) estimated the average lifetime emissions of solar power to be even less at 3.5 – 11.5g CO_2 equivalent per kilowatt hour. Average fossil fuel CO_2 emission intensity of global electricity supply is currently 504g CO_2 equivalent per kilowatt hour (Pehl et al., 2017).

Based on the lifetime emissions calculation by NREL, 40g CO_2 per kWh, the potential emissions per kilogram NaOH of an electrolysis process could be close to 0.083 kg CO_2 per kg NaOH produced in configuration 2.

Figure 6.10 below shows a graph comparing the calculated CO_2 emissions from the fossil fuel required to heat a conventional lime kiln to the electrical energy required to potentially drive an electrolysis process.

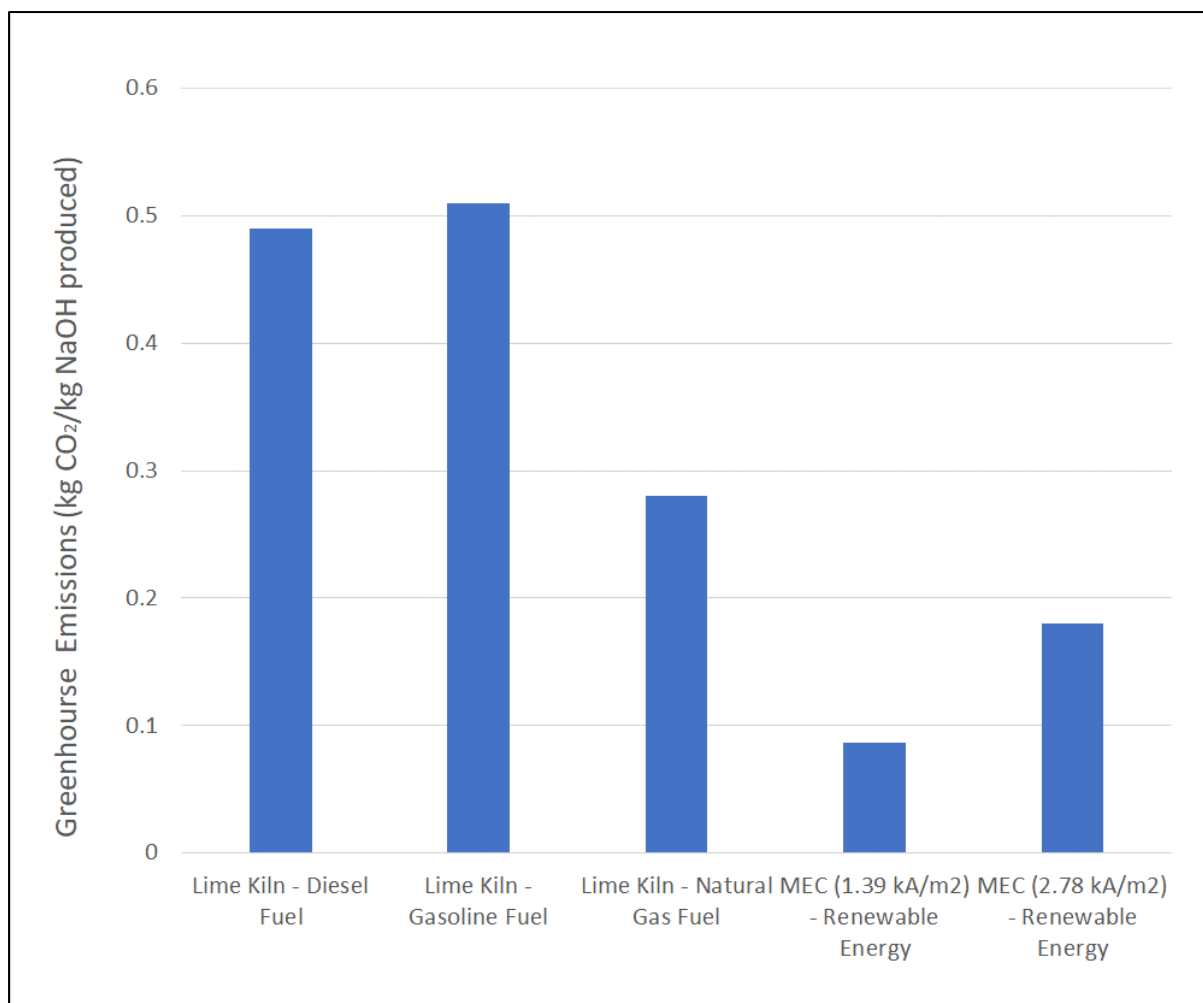


Figure 6.10 Comparison of Calculated Carbon Emissions

Conventional Lime Kiln Fossil Fuel Emissions versus Photovoltaic Cell Powered Electrolysis Membrane Cell. (Energy requirement for membrane electrolysis cell based on Trial 8 (5amps)

6.6 Summary of Outcomes

Experimentation presented in Chapter 6 showed that high selectivity membranes produce NaOH at a lower overall specific energy than low selectivity/high-capacity membranes. With the optimal process parameters identified in Chapter 5, the increased current efficiency offered by high selectivity membranes, outweighed the voltage reduction benefit of high-capacity membranes.

The MEC produced NaOH at lower specific energy at 80°C with all membranes trialled, than at 40°C. The benefit of reduced voltage at 80°C, outweighed the minor reduction in current efficiencies observed. The benefit of 80°C over 40°C was most significant with high selectivity membranes.

The best performed membrane in this set of experiments was the AGC Selemion SX-2301WNY membrane. With this membrane and a 200 g/L Green Liquor feed of 375 mL/hr, at 80°C and a current density of 1.39 kA/m², the MEC produced an NaOH concentration of 3.18 M at a specific energy of 312 kJ/mol.

The conventional Kraft recaustization process uses fossil fuels to burn lime used to regenerate Na₂CO₃ to NaOH, requiring a thermal energy of 320 kJ/mol NaOH produced. At a current density of 1.39 kA/m², the MEC can produce NaOH at a lower specific energy of 312 kJ/mol NaOH. At a current density of 2.78 kA/m² this increases to 647 kJ/mol NaOH.

The key benefit of the MEC recovery process is its ability to be powered by renewable energy. Powered by photovoltaics, the MEC can produce NaOH with reduced GHG emissions. At 1.39 kA/m², the GHG emissions are calculated to be 0.09 kg CO₂/kg NaOH produced and at 2.78 kA/m², the result is 0.18 kg CO₂/kg NaOH produced. This shows that there is strong merit in the MEC on an environmental basis.

Chapter 7 Discussion, Conclusions and Recommendations

Development of ion exchange membranes (IEM) integrated with electro chemistry have been adopted by diverse industries and used in a variety of applications that include desalination, acid and alkali recovery, chloralkali production and the manufacture of valuable salts. IEM technology can be extended beyond current applications into the Kraft paper making process where it has the potential to improve resource recovery of key chemical compounds essential to maintain consistent and reliable pulping performance. This improved resource recovery promises to:

- Improve pulping performance efficiency,
- Improve production efficiency,
- Reduce energy consumption, and
- Significantly reduce associated greenhouse gas (GHG) emissions.

The Kraft cycle recovers the weak alkali Na_2CO_3 contained in Green Liquor and converts it into a stronger alkali NaOH solution, whilst retaining Na_2S . In the conventional process, hydroxide is returned to the process by the addition of hydrated lime ($\text{Ca}(\text{OH})_2$), which reacts with Na_2CO_3 to form NaOH and a lime mud, CaCO_3 , which is separated by settling. Lime mud (CaCO_3) that is separated from the regenerated liquor is burned in a lime kiln to form quicklime, CaO , for it to be used again.

The key energy and environmental metrics of the conventional Kraft caustic recovery process were developed from literature, chemistry, mass, and energy balance and were the basis for comparison to alternative IEM technologies. In summary the benchmarks of the conventional Kraft Reausticisation Process developed were:

- NaOH production concentration required: 60 - 90g/L (1.5 to 2.25 M)
- Specific (thermal) energy requirement: 7.5 MJ/kg NaOH (300 kJ/mol NaOH)
- GHG Emissions (using diesel fuel): 0.49 kg CO_2 /kg NaOH Produced
- Na_2CO_3 to NaOH conversion: 75 to 85%
- Na_2S losses: 1 – 2% of Na_2S losses through lime kiln
- Other emissions: 20% of plant total reduced sulphur emissions.

7.1 The Outcome

The overall research objective was to determine whether IEM technologies have the potential to replace conventional NaOH recovery operations using lime in the Kraft pulping process. Understanding the fate of important chemical compounds, such as Na_2S , using membrane electrolysis cell (MEC) enables the membrane technology to be directly compared to the conventional NaOH recovery operation using lime.

NaOH recovery from a synthesised Kraft Green liquor was successfully performed using an MEC of CEM area of 6cm x 6cm, in a “zero gap” arrangement with iridium oxide coated expanded titanium mesh anode and woven nickel mesh cathode membrane supports. Optimised MEC process parameters were developed through initial experimentation:

- Current density (1.39 kA/m²),
- Green Liquor feed flowrate (350 mL/hr)
- Green Liquor feed concentration (200 g/L), and
- Feed temperature (80°C)

Using the optimised process parameters and AGC SX-2301WNY high selectivity CEM a NaOH solution of 3.2 M was produced with a cathode feed 2.5 M at 175 mL/hr at a specific energy of 312 kJ/mol NaOH produced and a current efficiency of 64%.

An MEC system that can be electrically powered by renewable energy will emit 0.09 kg CO₂/kg NaOH produced compared to 0.49 kg CO₂/kg NaOH produced under the currently employed using conventional processes. This represents a GHG reduction of 82% compared to the conventional lime recausticisation process.

Operating with the same process parameters but at higher current density (2.78 kA/m²), closer to normal IEM specifications, a NaOH solution of 3.63 M (145g/L) was produced at a specific energy of 647 kJ/mol NaOH, current efficiency of 54% and 0.18 kg CO₂/kg NaOH produced.

Analysis of the remaining hydroxide and carbonate in the Green Liquor stream leaving the MEC confirmed the oxidation of Na_2CO_3 at the MEC anode, proving the MEC system achieves the objective of the rejection of the Na_2CO_3 deadload from the Kraft cycle. The production of

a pure NaOH solution at the cathode that can be returned to the Kraft pulping cycle represents an elimination of Na₂CO₃ deadload.

At a current density of 1.39 kA/m² and identified optimal operating parameters, the MEC IEM technology successfully converted the Na₂CO₃ in Kraft Green Liquor to a pure NaOH solution concentration 3.2 M, eliminating Na₂CO₃ deadload, whilst releasing less GHG emissions than the conventional Kraft recausticisation process. However, analysis of the Green Liquor discharge confirmed the oxidation of Na₂S along the pathway of Na₂S to S to Na₂SO₃ to Na₂SO₄. An adjunct process will be required to separate the Na₂S from the Green Liquor before the MEC system or regenerated it from the weaker alkali salts, Na₂SO₃ and Na₂SO₄, for MEC to replace the conventional recausticisation process.

The results of this research are summarised in Table 7.1 relative to the key metrics of the conventional Kraft recausticisation process.

Table 7.1 – Comparison of Key Metrics: Recaustricisation vs IEM System

Metric	Conventional Process Recaustricisation	IEM System Membrane Electrolysis Cell	Change in performance
1. NaOH Concentration (mol/L)	2.25	3.2	42% higher concentration
2. Specific Energy Requirement (kJ/mol NaOH)	320	312	2% reduction
3. GHG Emissions (CO ₂ /kg NaOH)	0.49	0.08	82% reduction
4. Deadload Reduction - Na ₂ CO ₃ in NaOH Product - Na ₂ CO ₃ reduction in feed	20% 75 – 85%	0% Up to 100%	100% reduction 18% improvement
5. Na ₂ S Retention	1 to 2% lost in Lime kiln	Na ₂ S is oxidised at MEC anode along pathway: Na ₂ S to S to Na ₂ SO ₃ to Na ₂ SO ₄	More than 99% of sulphur Green Liquor the MEC leaves in the anode discharge, but in the form of Na ₂ SO ₃ and Na ₂ SO ₄ .
6. Other emissions	Lime kiln 20% of overall process TRS emissions because of fuel requirement and entrained sulphur in lime mud.	Fossil fuel eliminated from Kraft Cycle	100% reduction in fossil fuel sourced TRS emissions

7.2 Summary of Thesis and Findings

Establishing the chemistry and the key energy and environmental metrics of the conventional Kraft caustic recovery process was used to establish the operating metrics that could be used to compare the conventional recaustization against that offered by IEM and electro chemistry. These operating metrics established and developed from literature, chemistry, mass, and energy balance and were the basis for comparison to alternative IEM technologies that are reported in Table 7.1.

The IEM processes of diffusion dialysis (DD), electrodialysis (ED), electrodialysis metathesis (EDM) and membrane electrolysis (MEC) were evaluated in the context of Kraft Green Liquor recovery. DD and ED were not suitable as they are designed for purification and desalination functions and not alkali production, which is necessary for the conversion of Na_2CO_3 to NaOH. EDM in the form of an acid-alkali bipolar electrodialysis (BPED) arrangement can produce a NaOH product, however it would also produce unwanted side reactions involving the conversion of Na_2S to H_2S in an acidic discharge stream.

MEC was chosen over EDM as it is an established technique for NaOH production in the chloralkali industry and with a Green Liquor feed. The MEC technique oxidises the unwanted deadload carbonate (CO_3^{2-}) at the anode that removes it from the Green Liquor as $\text{CO}_2(\text{g})$, whilst producing hydroxide at the cathode. Potential side reactions were identified that were associated with Na_2S at the MEC anode, however these indicated the conversion to more neutral salts of S, Na_2SO_3 and Na_2SO_4 , which may be recovered, rather than highly undesirable H_2S produced in the case of EDM.

Developing the MEC apparatus and the testing methods used across the range of experiments identified design objectives that needed attention, this included hydraulic design and MEC membrane supports.

Using an IEM integrated with electrochemical principles established that gas production rate at the anode and the cathode needs to be considered in the design of the apparatus. Effective removal of the gas phase was essential to promote an unrestricted flow path to maximise NaOH recovery. The MEC discharge hydraulics were modified during design to allow the free discharge of any gas produced at the anode and cathode, to ensure an unrestricted flow path was provided and that any accumulation of gas within the MEC compartments is prevented.

Initial testing of the bench scale IEM apparatus was performed using a single solute 100 g Na₂CO₃/L solution evaluating the merit of conductive membrane supports, extending the electrodes to the membrane surface in a “zero gap” configuration, and then without membrane supports in an “open channel” configuration. The results confirmed that the “zero gap’ arrangement improved the specific energy performance and stability of the MEC, and supports were then incorporated into the MEC design used in all Green Liquor experiments. The type and configuration of the metal mesh membrane supports may be an important factor to enhance MEC performance and requires further examination.

The ability of MEC to convert Na₂CO₃ in Green Liquor was established by evaluating the effect of key process parameters on the performance of the MEC. A testing regime using a synthesised Green Liquor solution was undertaken to identify the impact of various settings and configurations that enabled selection of optimum settings. Table 7.2 below summarises the variables and selections made.

Table 7.2 – Comparison of Key Metrics: Recausticisation vs IEM System

MEC Variable	Range Tested	Optimum Selected	Comment
Current Density (kA/m ²)	0.28 – 1.39	1.39	The specific energy of NaOH production increases with current density, following Ohm’s law. A sensible current density must be chosen to balance membrane area and power consumption. 1.39 kA/m ² produced NaOH at a specific energy of 312 kJ/mol NaOH, which is comparable to the conventional Kraft recausticisation metric.
Green Liquor Concentration (g/L)	100 - 200	200	Anode concentration directly affects CEM Na ⁺ ion concentration gradient. Feed concentration must be maximised to increase current efficiency and reduce MEC specific energy.
Green Liquor Feed Flow (mL/hr)	175 - 350	350	Green liquor feed flow improves the supply of Na ⁺ relative to current density, improving concentration gradient, but not as significantly as feed concentration. Feed flow should be maximised relative to the hydraulics of the MEC anode compartment, without causing a pressure differential across the membrane that may drive transport of solvent across the membrane.
NaOH feed/product concentration (g NaOH/L)	0 - 100	100	As NaOH concentration increases, CEM concentration gradient becomes negative, promoting current leakage and increased specific energy of NaOH production. The Kraft pulping process requires a NaOH concentration of up to 90 g/L. Any concentration above this offers opportunity for overall Kraft process efficiencies in the form of reduced size of storage, transfer, and heating requirements. A feed concentration of 100 g NaOH/L was chosen to simulate a recirculated NaOH product. This was proven an acceptable assumption in Chapter 4 where NaOH was recirculated to a concentration above 140 g/L.
MEC Feed Temperature (°C)	40 - 80	80	The solubility and mobility of ions in solution increases with temperature. With a favourable CEM concentration gradient increased temperature enhances MEC current efficiency, decreases resistance and specific energy performance. With a negative concentration gradient, increased temperature decreases current efficiency beyond any resistance reduction benefit, decreasing overall specific energy performance. The optimum temperature of 80°C is suitable because of the chosen Green Liquor feed concentration and flow, which infers a positive concentration gradient. Kraft Green liquor is typically in the range of 80 - 90°C.

The impact of the MEC on the Green Liquor discharge was evaluated where Green Liquor feed flow and concentration was lowest relative to the current applied across the MEC. Analysis of the MEC anode liquid discharge showed the concentration of Na^+ ions and carbonate (CO_3^{2-}) diminishing linearly with applied current density, confirming that the MEC achieved the elimination of Na_2CO_3 deadload.

The MEC discharge showed some precipitation, analysis of which showed the presence of an elemental sulphur, $\text{S}_{(s)}$, and Na_2SO_3 , both of which are a result of the oxidation of Na_2S at the anode. The measured change in S concentration between the MEC anode feed and discharge was negligible, indicated the amount of S lost to precipitate is also minor. This result strongly indicated that at the MEC anode Na_2S is transforming to the neutral salts of Na_2SO_3 and Na_2SO_4 . It can be concluded that MEC retains the sulphur in the Green Liquor but does not retain it in the form of Na_2S required by the Kraft pulping process. For MEC to be a viable substitute to the conventional recausticisation process, Na_2S needs to be isolated from the Green Liquor prior to the MEC, or reduction process needs to come after the MEC to convert the Na_2SO_3 and Na_2SO_4 back to Na_2S .

Hydrogen production, which is a potentially valuable by-product of the MEC recovery process was measured in all experiments. Unlike NaOH production, the molar production rate of hydrogen gas was shown to not be significantly affected by the changes in MEC temperature, Green Liquor flow rate, concentration or NaOH concentration. Hydrogen production followed increases in applied current linearly in agreement with Faraday's law at all tested process parameter set points.

MEC operation using a variety of commercially available IEM membranes from AGC Selemion and Dupont Nafion of high and low selectivity enabled a direct performance comparison. Benchmarking the performance of various membranes under identical operating conditions provided an opportunity to identify membranes with superior performance that could then be directly compared to operational metrics associated with the current NaOH recovery process employed in the Kraft pulping process.

At the optimised process parameters identified, the benefits that high selectivity CEMs offered in the form of better current efficiencies, outweighed any voltage reduction given by CEMs of lower selectivity, meaning high selectivity CEMs produced NaOH at a lower specific energy requirement (kJ/mol NaOH). This result reflected the effect of a relatively high NaOH

feed concentration (2.5 M) at the cathode, relative to the concentration of Na⁺ ions (4.1 M) in the 200 g/L Green Liquor feed. With increasing current density, the concentration gradient of Na⁺ ions can become negative, so a high resistance membrane preventing the leakage of NaOH back towards the anode is very important.

At current density of 1.39 kA/m² and the optimum MEC process parameters identified, the AGC Selemion SX-2301 WNY CEM produced a NaOH concentration of 3.2 M at a specific energy of 312 kJ/mol NaOH. This compares to the approximately 320 kJ/mol NaOH of thermal energy required by the lime kiln in the conventional process. It also cannot be forgotten that NaOH produced in the conventional process also contains a 20% deadload of unconverted Na₂CO₃, while the MEC NaOH product is essentially a pure NaOH solution. The retention of Na₂CO₃ deadload in the Kraft cycle requires more dilution water, requiring greater storage volumes, larger transfer systems and increased heating energy.

A current density of 2.78 kA/m² at the same optimum MEC process parameters was also presented to reflect a current density closer to that of typical commercial chloralkali MEC systems. With all process parameters kept constant, the resistance of the MEC cell is essentially unchanged, so a doubling in current density infers a doubling in electrode potential required to drive the passage of ions across the MEC, as per Ohm's law. Current efficiency was shown to decrease with increasing current density, due to increasing current leakage. The doubling of current density affected an increase in specific energy requirement of slightly more than double, to 647 kJ/mol NaOH. An MEC system for the regeneration of Kraft Green liquor will need to balance energy costs and membrane costs, which could be managed by research into the production of more affordable membranes specifically designed for Kraft Green liquor recovery.

Based on the relatively high US-based National Renewable Laboratory (NREL) estimate that solar power produces lifetime emissions of 40g CO₂ equivalent per kilowatt-hour (NREL, 2012), a MEC NaOH recovery process powered by renewables was estimated to be up to 82% lower than conventional recovery processes. At a current density of 1.39 kA/m², AGC Selemion SX-2301 WNY CEM, and the identified optimal parameters the MEC will produce 0.09 kg CO₂/kg NaOH. At an increased current density of 2.78 kA/m² this increases to 0.180 kg CO₂/kg NaOH. This compares well against the lime kiln that emits 0.49 kg CO₂/kg NaOH based on a diesel oil thermal energy source. Kraft pulping mills can often be net electricity exporters where excess

energy generated by the Kraft reboiler is not required by the process. MEC Green Liquor recovery may be an even more attractive application in these circumstances.

7.3 Findings in Context of Current Research

There have been recent investigations into the conversion of Green Liquor into caustic solution using IEM processes including the Membrane Electrolysis Cell (MEC) and Electrodialysis with Bipolar Membranes (BPED). A MEC process with a cationic exchange membrane (CEM) was used to convert Na_2CO_3 in Kraft Green Liquor to NaOH by (Goel et al., 2021) and (Mandal et al., 2021), while (Eswaraswamy et al., 2022) used BPED process to convert the Na_2CO_3 in Green Liquor to NaOH. The results of this study in the context of their results are presented in Table 7.3 below. The research by (Goel et al., 2021), (Mandal et al., 2021), and (Eswaraswamy et al., 2022) focused on the conversion of Na_2CO_3 to NaOH and did not evaluate the impact on Na_2S in the Green Liquor discharge.

Table 7.3 – Comparison of Key Metrics: Recausticisation vs IEM System

Research	IEM Process	Current Density (kA/m ²)	Specific Energy (kJ/mol)	NaOH Produced (mol/L)
(Goel et al., 2021)	MEC	0.60	372	1.17
(Mandal et al., 2021)	MEC	0.60	454	2.35
(Eswaraswamy et al., 2022)	BPED	0.50	790	1.2
This research	MEC	1.39	312	3.22
	MEC	2.78	647	3.63

Using commercially available Nafion and AGC Selemion CEMs this research extended on the previous research by:

- Trialling the MEC at higher current densities closer to what is used in production systems using commercially available CEMs at 1.39 and 2.78 kA/m².
- By feeding a 2.5 M NaOH solution to the MEC cathode, to simulate the recirculation of a concentrated product, a higher NaOH concentration of 3.63 M was produced.
- The Green Liquor solution leaving the MEC was analysed to show that at the MEC anode Na_2S is oxidised, and with increasing current application the oxidation pathway is from Na_2S to S to Na_2SO_3 to Na_2SO_4 .

This research has shown that an MEC can convert Na_2CO_3 in Kraft Green Liquor to NaOH . At a current density of 1.39 kA/m^2 , a concentration of 3.2 M NaOH was produced at a specific energy of 312 kJ/mol NaOH , comparable to the specific thermal energy required by the Kraft process lime kiln, 320 kJ/mol NaOH .

MEC offers the benefit that it can be an electrically powered process by renewables, greatly decreasing the carbon footprint of the Kraft cycle. This could be even greater, as MEC can produce NaOH at higher concentration, with no residual Na_2CO_3 , eliminating Na_2CO_3 deadload in the Kraft cycle.

However, a Green Liquor feed to an MEC process will also oxidise Na_2S at the anode. The identified oxidation pathway is Na_2S to $\text{S}_{(s)}$ to Na_2SO_3 and Na_2SO_4 . Without an adjunct process upstream of the MEC, separating Na_2S from the Green Liquor, or converting Na_2SO_3 and Na_2SO_4 to Na_2S after the MEC, the MEC process cannot be directly substituted into the Kraft Cycle in place of the conventional recaustization process.

7.4 Limitations of the Research and Methods

This research was performed using a bench scale MEC apparatus of 36 cm^2 . Scaling this process up from a bench scale to a pilot scale to an industrial scale will affect performance results. Scaling up the MEC will involve larger membrane surface areas, higher flow rates, and larger MEC cell compartment volumes relative to compartment cross sectional area and length. The relationships between solution residence time, cross-sectional velocity, and concentration polarisation between the MEC inlets and outlets will unavoidably shift as the MEC is scaled up. Changes in average ion concentration in the MEC compartments will affect the resistance of those compartments and concentration gradient across the CEM, affecting MEC current efficiency and voltage.

A synthesised Green Liquor was used, based on average concentrations found in literature. Industrial Green liquors will generally contain very low concentrations of organic material carried over from the Kraft reboiler. Organic fouling was not considered as a particular problem given the strong alkalinity of Kraft Green liquor. In research by (Mandal et al., 2022) the MEC performance was compared with a synthetic Green liquor feed and an industrial sourced sample. In two separate trials, the specific energy using the industrial sample feed as 421 kJ/mol NaOH , compared to 400 kJ/mol NaOH using an equivalent synthetic feed. An

explanation for the differences in performance was potentially insoluble particles present in the industrial sample affecting CEM performance. The results presented by (Mandal et al., 2022) show approximately only a 5% change in specific energy between the synthetic and industrial Green Liquor experiments, illustrating that synthetic industrial liquor closely mirrors industrial Green Liquor performance.

7.5 Recommendations for Future Research

This research proved that Na_2CO_3 in Kraft Green Liquor can be converted to NaOH using the IEM technology of MEC. However, analysis of the Green Liquor solution leaving the MEC anode showed Na_2S is oxidised, and with increasing current application the oxidation pathway is from Na_2S to S to Na_2SO_3 to Na_2SO_4 . Na_2S is fundamental to the Kraft pulping process and without an adjunct process upstream of the MEC, separating Na_2S from the Green Liquor, or converting Na_2SO_3 and Na_2SO_4 to Na_2S after the MEC, the MEC process cannot be directly substituted into the Kraft Cycle in place of the conventional recaustization process.

There may be merit in using ED or EDM for the separation of Na_2CO_3 from Kraft Green liquor, from which the Na_2CO_3 could be sent to secondary process for conversion to NaOH, preventing the oxidation of the required Na_2S . Carbonate (CO_3^{2-}) has the lowest diffusion coefficient and mobility of the anions present in Kraft Green Liquor, which may offer a mechanism for separation using IEM process. Table 7.4 below gives the mobility of ions in Kraft Green Liquor.

Table 7.4: Anion Mobility in Aqueous Solutions – Diffusion Coefficient, D, Stokes Radius, r (Haynes, 2014-2015), (Luo et al., 2018)

Anion	Radius, r (nm)	Width of hydration shell, Δr (nm)	Number of water molecules in this shell, n	Diffusion coefficient, D, of the ion in dilute aqueous solution ($10^{-5} \text{ cm}^2 \text{ s}^{-1}$)
CO_3^{2-}	0.178	0.076	4	0.96
SO_4^{2-}	0.23	0.043	3.1	1.07
SO_3^{2-}	0.2	0.059	3.6	1.132
SH^-	0.207	0.031	1.7	1.731
S^{2-}	0.184	0.07	3.9	1.731
OH^-	0.133	0.079	2.7	5.27

Figure 7.1 shows an example of a possible repeating 2 cell ED process utilising alternating anionic (AEM) and cation (CEM) selective membranes. In this arrangement Green Liquor is fed to one cell and a NaOH stream is fed to the other. The hypothesis of the arrangement

shown in Figure 7.1 is that hydroxide ions (OH^-) and sulphide ions (S^{2-}) in the Green Liquor feed to the first cell with their higher mobility through solution will move preferentially across the AEM and sodium ions (Na^+) will move across the CEM to preserve electrical neutrality.

The feed to the second cell is NaOH to ensure a stable Na_2S solution is formed in the cell product (stream B). The proportion of Na_2CO_3 carbonate in the first cell discharge (Stream A) should be higher because CO_3^{2-} ion has lower mobility in solution and across the membrane.

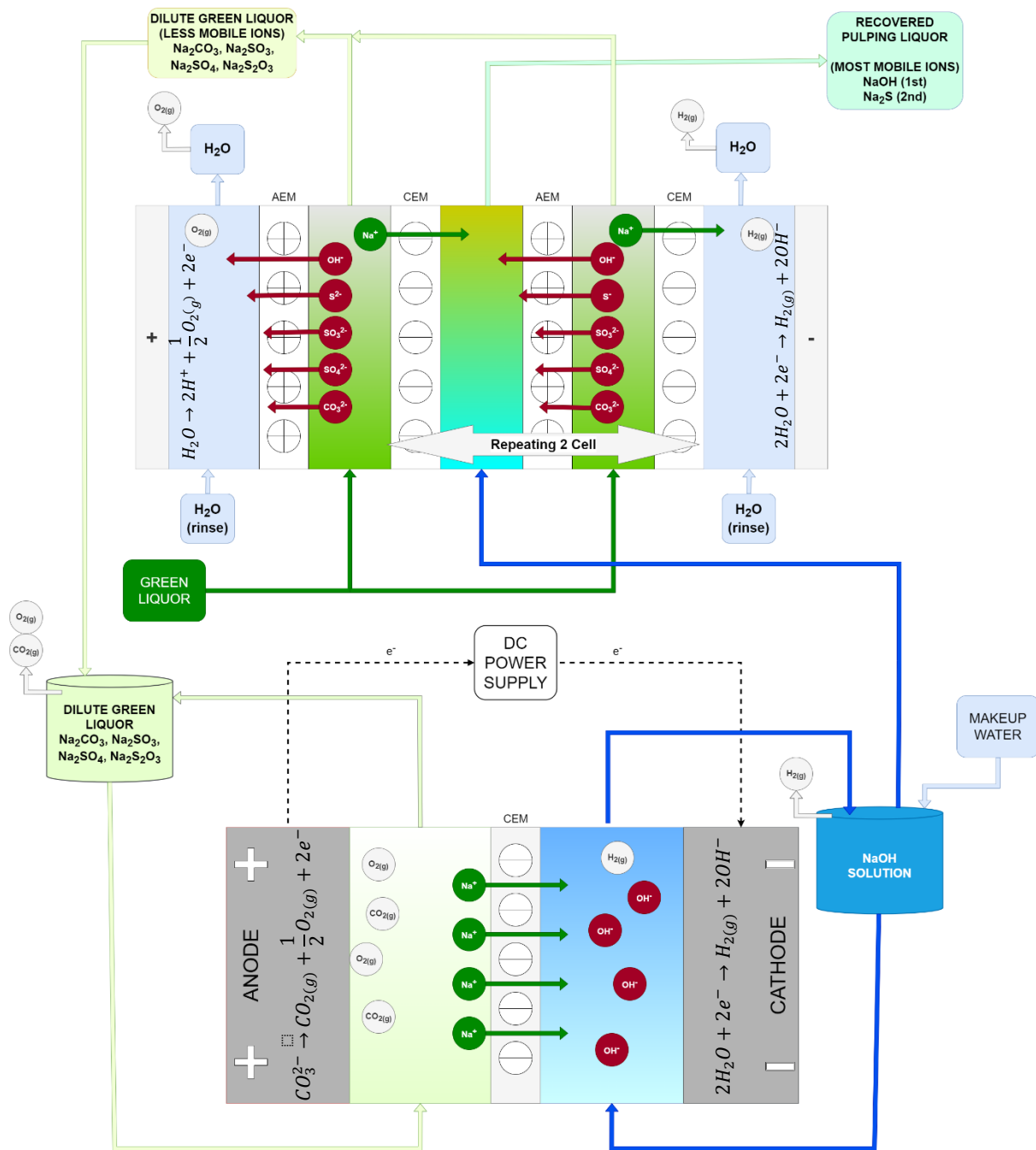


Figure 7.1 – Kraft Green Liquor Regeneration cycle with ED and MEC

The hypothesis of the system shown in Figure 7.1 is that the separated Na_2CO_3 solution leaving an electrodialysis process can be sent to a membrane electrolysis cell to be converted to NaOH and hydrogen gas (H_2).

Bibliography:

<._Camacho-2017-Optimization of electrodialysis 1.pdf>.

AFPA 2016. AFPA 2016 National Pulp & Paper Sustainability Report. *Australian Forest Productions Association*.

AMINVAZIRI, B. 2009. REDUCTION OF TRS EMISSIONS FROM LIME KILNS. *Graduate Department of Chemical Engineering and Applied Chemistry University of Toronto*.

AZGOMI, F. 2014. Impact of Liming Ratio on Lime Mud Settling and Filterability in the Kraft Recovery Process. *Graduate Department of Chemical Engineering and Applied Chemistry University of Toronto*.

BAYER, T., CUNNING, B. V., SELYANCHYN, R., DAIO, T., NISHIHARA, M., FUJIKAWA, S., SASAKI, K. & LYTH, S. M. 2016. Alkaline anion exchange membranes based on KOH-treated multilayer graphene oxide. *Journal of Membrane Science*, 508, 51-61.

BIERMANN, C. 1996a. *Handbook_of_Pulping_and_Papermaking*. 2nd Edition, Chapter 3.

BIERMANN, C. J. 1996b. *Handbook of Pulping and Papermaking*, 2E.

BUDIARTO, T., ESCHE, E., REPKE, J. U. & LEKSONO, E. 2017. Dynamic Model of Chloralkali Membrane Process. *Procedia Engineering*, 170, 473-481.

CAMACHO, L. M., FOX, J. A. & AJEDEGBA, J. O. 2017. Optimization of electrodialysis metathesis (EDM) desalination using factorial design methodology. *Desalination*, 403, 136-143.

CHANDRA, Y. 2004. ALKALINE PULPING: DEADLOAD REDUCTION STUDIES IN CHEMICAL RECOVERY SYSTEM. *School of Chemical & Biomolecular Engineering Georgia Institute of Technology*

DEAN, J. A. 1999. <Lange's Handbook of Chemistry, Fifteenth Edition.pdf>.

ELLIS, M. & JOHNSON, T. 2011. Liquor cycle optimisation at Australian Paper, Maryvale mill. *Annual Appita Conference*.

ENVIRONMENTAUSTRALIA 1998. Emission Estimation Technique Manual for Pulp and Paper Manufacturing.

EPA, U. 2018. METHOD 6010D Inductively Coupled Plasma - Optical Emission Spectrometry. *US EPA SW-846 Rev 5*.

ESWARASWAMY, B., MANDAL, P., GOEL, P., CHANDRA, A. & CHATTOPADHYAY, S. 2022. Intricacies of caustic production from industrial green liquor using bipolar membrane electrodialysis. *Journal of Environmental Chemical Engineering*, 10.

- FRANCEY, S., TRAN, H. & BERGLIN, N. 2011. Global survey on lime kiln operation, energy consumption, and alternative fuel usage. *TAPPI Journal*, 10, 19-26.
- GAUDREAU, C., MALMBERG, B., UPTON, B. & MINE, R. 2012. Life cycle greenhouse gases and non-renewable energy benefits of kraft black liquor recovery. *Biomass and Bioenergy*, 46, 683e692.
- GOEL, P., MANDAL, P., E, B., SHAHI, V. K. & CHATTOPADHYAY, S. 2021. Sulfonated poly (ether ether ketone) composite cation exchange membrane for NaOH production by electro-electrodialysis using agro-based paper mill green liquor. *Journal of Environmental Chemical Engineering*, 9.
- GONZÁLEZ SUÁREZ, V. M., GARCÍA-GONZALO, E., MAYO BAYÓN, R., GARCÍA NIETO, P. J. & ÁLVAREZ ANTÓN, J. C. 2018. Predictive model of gas consumption and air emissions of a lime kiln in a kraft process using the ABC/MARS-based technique. *The International Journal of Advanced Manufacturing Technology*.
- GRACE, T. M. & TRAN, H. 2009. The effect of dead load chemicals in the kraft pulping and recovery system. *Chemical Recovery*, 18-24.
- HAYNES, W. M. 2014-2015. *CRC Handbook of Chemistry and Physics 95th Edition*.
- HERRERO-GONZALEZ, M., DIAZ-GURIDI, P., DOMINGUEZ-RAMOS, A., IRABIEN, A. & IBAÑEZ, R. 2020. Highly concentrated HCl and NaOH from brines using electrodialysis with bipolar membranes. *Separation and Purification Technology*, 242.
- HNÁT, J., KODÝM, R., DENK, K., PAIDAR, M., ŽITKA, J. & BOUZEK, K. 2019. Design of a Zero-Gap Laboratory-Scale Polymer Electrolyte Membrane Alkaline Water Electrolysis Stack. *Chemie Ingenieur Technik*, 91, 821-832.
- HOLTZAPPLE, M. T. 2003. Kraft Process - LIGNIN. *Encyclopedia of Food Sciences and Nutrition (Second Edition)*.
- JOHNSON, M. E. A. T. 2011. Liquor cycle optimisation at Australian Paper, Maryvale mill. *65th Appita Annual Conference*.
- KEVLICH, N. S., SHOFNER, M. L. & NAIR, S. 2017. Membranes for Kraft black liquor concentration and chemical recovery: Current progress, challenges, and opportunities. *Separation Science and Technology*, 52, 1070-1094.
- KIM, Y., WALKER, W. S. & LAWLER, D. F. 2012. Competitive separation of di- vs. mono-valent cations in electrodialysis: effects of the boundary layer properties. *Water Res*, 46, 2042-56.
- KISHIDA, M., HARATO, T., TOKORO, C. & OWADA, S. 2017. In situ remediation of bauxite residue by sulfuric acid leaching and bipolar-membrane electrodialysis. *Hydrometallurgy*, 170, 58-67.
- KREUE, K.-D. 2013. Ion Conducting Membranes for Fuel Cells and other Electrochemical Devices. *American Chemistry Society*, 361-380.

- KUMAR, P., BHARTI, R. P., KUMAR, V. & KUNDU, P. P. 2018. Polymer Electrolyte Membranes for Microbial Fuel Cells: Part A. Nafion-Based Membranes. *Progress and Recent Trends in Microbial Fuel Cells*.
- LINDEDAHL, K. 2008. Chemical Reaction in Kraft Pulping. <http://www.h2obyki.com/cooperation.html>.
- LIU, R., WU, L., PAN, J., JIANG, C. & XU, T. 2014. Diffusion dialysis membranes with semi-interpenetrating network for alkali recovery. *Journal of Membrane Science*, 451, 18-23.
- LIUA, G., LIU, Y., SHIB, H. & QIAN, Y. 2004. Application of inorganic membranes in the alkali recovery process. *Desalination*, 169, 193-205.
- LUNDQVIST, P. 2009. Mass and energy balances over the lime kiln in a kraft pulp mill. *Uppsala Universitet*.
- LUO, J., WU, C., WU, Y. & XU, T. 2013. Diffusion dialysis of hydrochloric acid with their salts: Effect of co-existence metal ions. *Separation and Purification Technology*, 118, 716-722.
- LUO, J., WU, C., XU, T. & WU, Y. 2011. Diffusion dialysis-concept, principle and applications. *Journal of Membrane Science*, 366, 1-16.
- LUO, T., ABDU, S. & WESSLING, M. 2018. Selectivity of ion exchange membranes: A review. *Journal of Membrane Science*, 555, 429-454.
- MANDAL, P., BHUVANESH, E., GOEL, P., SUJIT KUMAR, K. & CHATTOPADHYAY, S. 2021. Caustic recovery from green liquor of agro-based paper mills using electrolysis. *Separation and Purification Technology*, 262.
- MANDAL, P., GOEL, P., E, B., SHAHI, V. K. & CHATTOPADHYAY, S. 2022. Caustic production from industrial green liquor using alkali resistant composite cation exchange membrane. *Journal of Environmental Chemical Engineering*, 10.
- MATSUYAMA, A., YANO, S., TANINAKA, T., KINDAICHI, M., SONODA, I., TADA, A. & AKAGI, H. 2018. Chemical characteristics of dissolved mercury in the pore water of Minamata Bay sediments. *Marine Pollution Bulletin*, 129, 503-511.
- MINER, R. & UPTON, B. 2002. Methods for estimating greenhouse gas emissions from lime kilns at kraft pulp mills. *Energy*, 27, 729-738.
- NAFION 2017. Nafion N-324 Product Sheet P-07.
- NIKONENKO, V. V., PISMENSKAYA, N. D., BELOVA, E. I., SISTAT, P., HUGUET, P., POURCELLY, G. & LARCHET, C. 2010a. Intensive current transfer in membrane systems: modelling, mechanisms and application in electrodialysis. *Adv Colloid Interface Sci*, 160, 101-23.
- NIKONENKO, V. V., PISMENSKAYA, N. D., BELOVA, E. I., SISTAT, P., HUGUET, P., POURCELLY, G. & LARCHET, C. 2010b. Intensive current transfer in membrane systems: Modelling,

- mechanisms and application in electrodialysis. *Advances in Colloid and Interface Science*, 160, 101-123.
- NREL 2012. Life Cycle Greenhouse Gas Emissions from Solar Photovoltaics. *National Renewable Energy Laboratory*, 2.
- O'BRIEN, T. F., BOMMARAJU, T. V. & HINE, F. 2005. Handbook of Chlor-Alkali Technology.
- PARK, J. H., KANG, S. M., KWON, Y.-I., NAM, G. D., YUN, K. S., SONG, S.-J., YU, J. H. & JOO, J. H. 2020. Role of surface exchange kinetics in coated zirconia dual-phase membrane with high oxygen permeability. *Journal of Membrane Science*, 597.
- PEHL, M., ARVESEN, A., HUMPENÖDER, F., POPP, A., HERTWICH, E. G. & LUDERER, G. 2017. Understanding future emissions from low-carbon power systems by integration of life-cycle assessment and integrated energy modelling. *Nature Energy*, 2, 939-945.
- PHILLIP MURRAY, B. C., KATHLEEN FALLER, AND AMERICAN WATER WORKS ASSOCIATION 1995. Electrodialysis and Electrodialysis Reversal (M38) - INTRODUCTION.
- PYUN, S.-I. 2021. Thermodynamic aspects of energy conversion systems with focus on osmotic membrane and selectively permeable membrane (Donnan) systems including two applications of the Donnan potential. *ChemTexts*, 7.
- R. MINER A, B. U. 2001. Methods for estimating greenhouse gas emissions from lime kilns at kraft pulp mills. *Pergamon Energy*.
- RABBANI, M., DINCER, I. & NATERER, G. F. 2014. Experimental investigation of processing parameters and effects on chloralkali products in an electrolysis based chloralkali reactor. *Chemical Engineering and Processing: Process Intensification*, 82, 9-18.
- RAN, J., WU, L., HE, Y., YANG, Z., WANG, Y., JIANG, C., GE, L., BAKANGURA, E. & XU, T. 2017. Ion exchange membranes: New developments and applications. *Journal of Membrane Science*, 522, 267-291.
- ROSEMOUNT_ANALYTICAL 2010. Emerson Conductance Data for Commonly Used Chemicals December 2010.
- SADRZADEH, M. & MOHAMMADI, T. 2009. Treatment of sea water using electrodialysis: Current efficiency evaluation. *Desalination*, 249, 279-285.
- SATA, T. 2007a. Ion Exchange Membranes : Preparation, Characterization, Modification and Application - Chapter 1.
- SATA, T. 2007b. Ion Exchange Membranes : Preparation, Characterization, Modification and Application - Chapter 2.
- SATA, T. 2007c. Ion Exchange Membranes : Preparation, Characterization, Modification and Application - Chapter 3.

- SATA, T. 2007d. Ion Exchange Membranes : Preparation, Characterization, Modification and Application - Contents.
- SATO, T. 2000. Studies on anion exchange membranes having permselectivity for specific anions in electrodialysis — effect of hydrophilicity of anion exchange membranes on permselectivity of anions. *Journal of Membrane Science*, 167.
- SATURNINO, D. M. 2012. Modeling of Kraft Mill Chemical Balance. *Graduate Department of Chemical Engineering and Applied Chemistry University of Toronto*
- SELEMION, A. 2019a. Introduction of new Generation Membrane FLEMION F-9010.
- SELEMION, A. 2019b. Introduction_of_F-9010.
- SELEMION, A. 2020a. Forblue(TM) S-Series SX-2301 Data Sheet.
- SELEMION, A. 2020b. Sx-1811 Data Sheet.
- SELEMION, A. 2020c. Sx-1831_EN Data Sheet.
- SELEMION(AGC) 2018. SELEMION - Ion Exchange Membranes. <https://www.agec.co.jp/selemion/SELC.pdf>.
- SIMON, A., FUJIOKA, T., PRICE, W. E. & NGHIEM, L. D. 2014a. Sodium hydroxide production from sodium carbonate and bicarbonate solutions using membrane electrolysis: A feasibility study. *Separation and Purification Technology*, 127, 70-76.
- SIMON, A. R., FUJIOKA, T., PRICE, W. & NGHIEM, L. 2014b. Sodium hydroxide production from sodium carbonate and bicarbonate solutions using membrane electrolysis: A feasibility study. *Separation and Purification Technology*, 127, 70-76.
- SORIANO, A. N., AGAPITO, A. M., LAGUMBAY, L. J. L. I., CAPARANGA, A. R. & LI, M.-H. 2011. Diffusion coefficients of aqueous ionic liquid solutions at infinite dilution determined from electrolytic conductivity measurements. *Journal of the Taiwan Institute of Chemical Engineers*, 42, 258-264.
- SOUTAR, B. M. 2016. Kraft batch digester cooking optimisation. *Appita Journal*.
- TANAKA, Y. 2004. The effect of solution leakage in an ion-exchange membrane electrodialyzer on mass transport across a membrane pair. *Journal of Membrane Science*, 231, 13-24.
- THERMOFISCHER_SCIENTIFIC 2021. Phenom Pharos G2 Desktop FEG-SEM - Data Sheet. *ThermoFischer Scientific Product Data Sheet*.
- THOMAS M. GRACE, H. T. 2009. The effect of dead load chemicals in the kraft pulping and recovery system. *TAPPI*.
- TIANODE 2022. TiAnode Fabricators Pvt. Ltd Zero Gap Retrofit.

- TOM DAVIS, B. B. 2012. Zero discharge desalination technology: A new twist on conventional desalination techniques. *American Water Works Association*.
- TRAN, H. 2008. Lime Kiln Chemistry and Effects on Kiln Operations. *Pulp and Paper Centre and Department of Chemical Engineering and Applied Chemistry - University of Toronto*.
- TRAN, H. & PAPANGELAKIS, V. July 2013. Formation of pirssonite in green liquor handling systems. *TAPPI*, July 2013.
- TRAN, H. & VAKKILAINNEN, E. K. 2016. The Kraft Chemical Recovery Process. *Pulp & Paper Centre University of Toronto Toronto, Ontario, CANADA*.
- UNFAO 2016. Food and Agriculture Organisation of the United Nations - 2016-2021 Pulp and Paper Capacities. *Food and Agriculture Organisation of the United Nations*.
- WANG, K., XING, W., ZHONG, Z. & FAN, Y. 2013. Study on adsorption phenomenon of diffusion dialysis for acid recovery. *Separation and Purification Technology*, 110, 144-149.
- WEI, C., LI, X., DENG, Z., FAN, G., LI, M. & LI, C. 2010. Recovery of H₂SO₄ from an acid leach solution by diffusion dialysis. *J Hazard Mater*, 176, 226-30.
- WEI, Y., WANG, Y., ZHANG, X. & XU, T. 2013. Comparative study on regenerating sodium hydroxide from the spent caustic by bipolar membrane electrodialysis (BMED) and electro-electrodialysis (EED). *Separation and Purification Technology*, 118, 1-5.
- XU, T. 2005. Ion exchange membranes: State of their development and perspective. *Journal of Membrane Science*, 263, 1-29.
- YAN, H., XUE, S., WU, C., WU, Y. & XU, T. 2014. Separation of NaOH and NaAl(OH)₄ in alumina alkaline solution through diffusion dialysis and electrodialysis. *Journal of Membrane Science*, 469, 436-446.
- YE, W., HUANG, J., LIN, J., ZHANG, X., SHEN, J., LUIS, P. & VAN DER BRUGGEN, B. 2015. Environmental evaluation of bipolar membrane electrodialysis for NaOH production from wastewater: Conditioning NaOH as a CO₂ absorbent. *Separation and Purification Technology*, 144, 206-214.

Appendix A: Green Liquor Trials 1 to 16: Experimental Results

Varying four experimental parameters across two data points, required 16 experimental trials. Table A.1 below details the 16 trials and their respective operation settings for each trial. Each trial also includes five current setpoints, giving a total of 80 experimental data points. Trials 14 and 16 were repeated to confirm results and the anode discharge from these trials was evaluated to confirm the impact on Kraft Green Liquor leaving the MEC anode discharge.

Table A.1: Green Liquor Experimental List and Operation Settings

Experimental Trial Number	Feed Temperature (T) (°C)	Anode Feed Flow (AF) (mL/hr)	Anode Feed Concentration (AC) (g/L)	Cathode Feed Flow (mL/hr)	Cathode Feed Concentration (CC) (g NaOH/L)
1	40	175	200	175	0
2	80	175	200	175	0
3	40	350	200	175	0
4	80	350	200	175	0
5	40	175	200	175	100
6	80	175	200	175	100
7	40	350	200	175	100
8	80	350	200	175	100
9	40	175	100	175	0
10	80	175	100	175	0
11	40	350	100	175	0
12	80	350	100	175	0
13	40	175	100	175	100
14*	80	175	100	175	100
15	40	350	100	175	100
16*	80	350	100	175	100

*Trials 14 and 16 were repeated to confirm results. The anode discharge from these trials was evaluated to confirm impact on Kraft Green Liquor leaving MEC anode discharge.

The current efficiency, voltage and specific energy of NaOH production are shown in Figures A.1 to A.16.

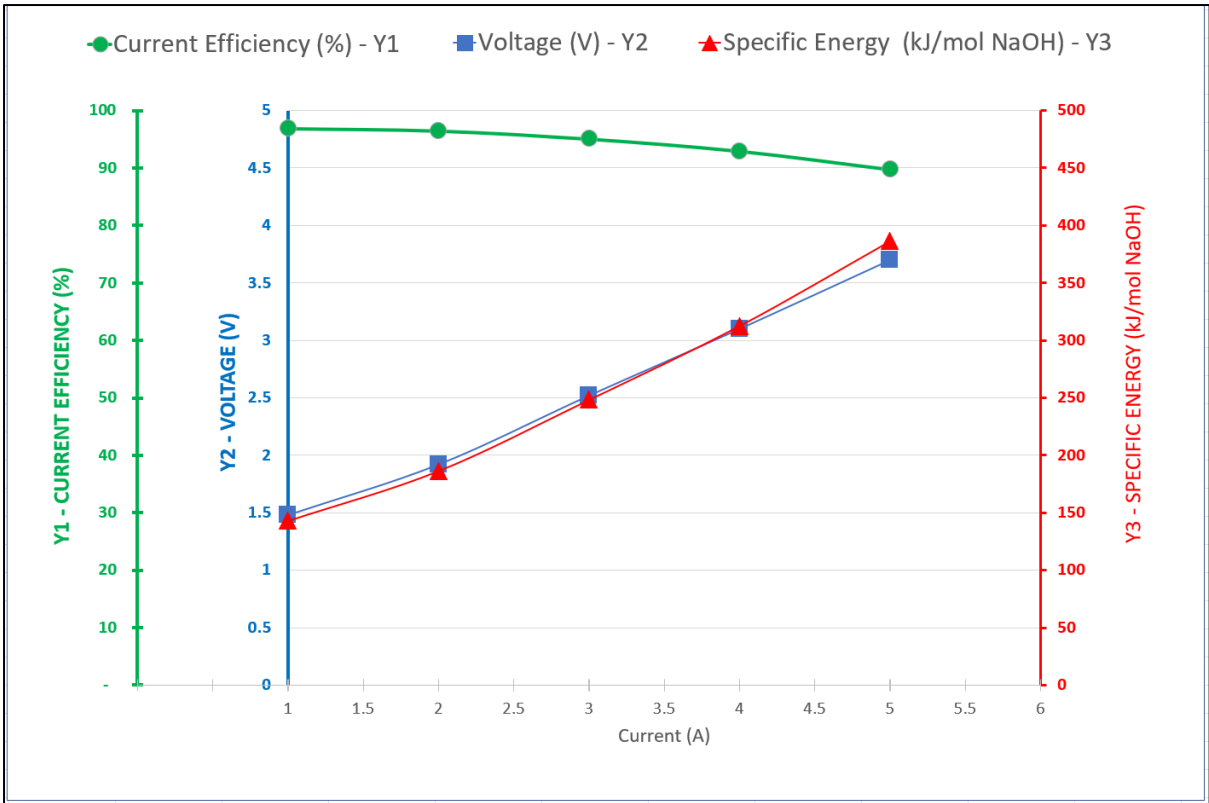


Figure A.1: Trial 1 (T = 40°C, AF = 175 mL/H, AC = 200 g/L, CC = 0 g NaOH/L)

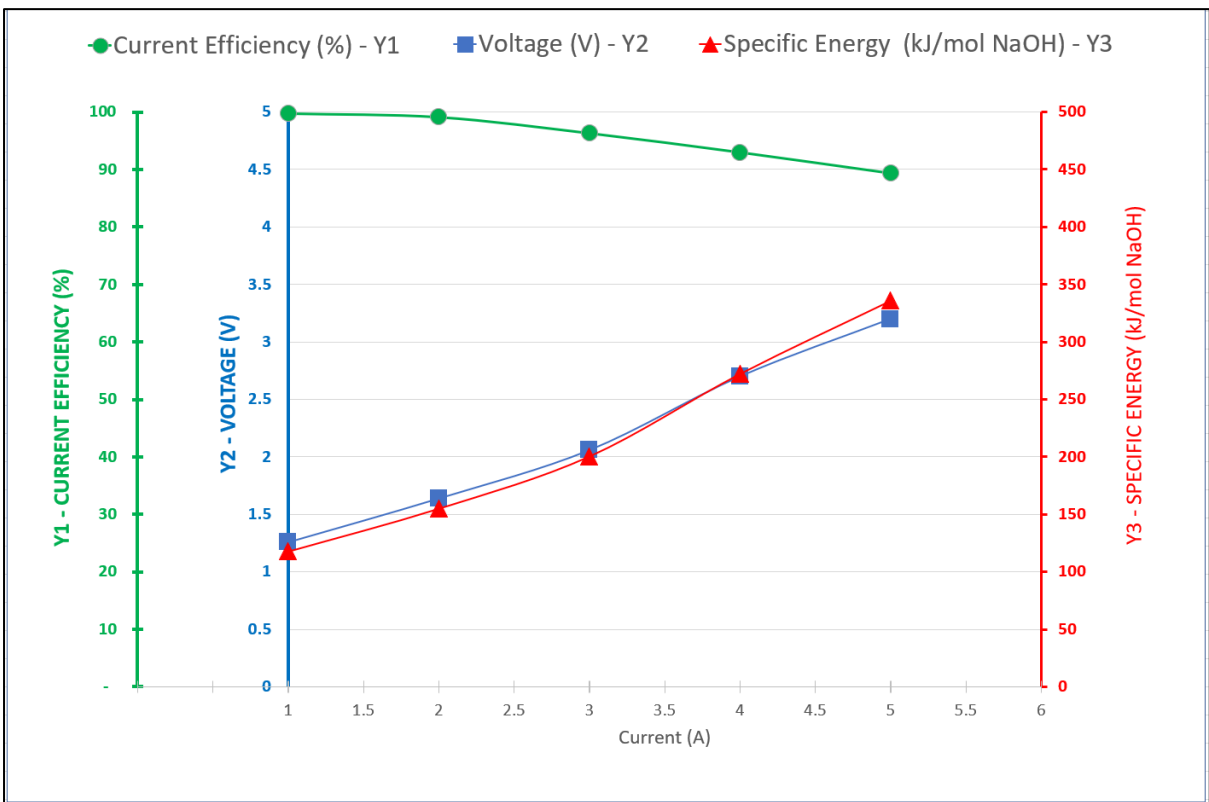


Figure A.2: Trial 2 (T = 80°C, AF = 175 mL/H, AC = 200 g/L, CC = 0 g NaOH/L)

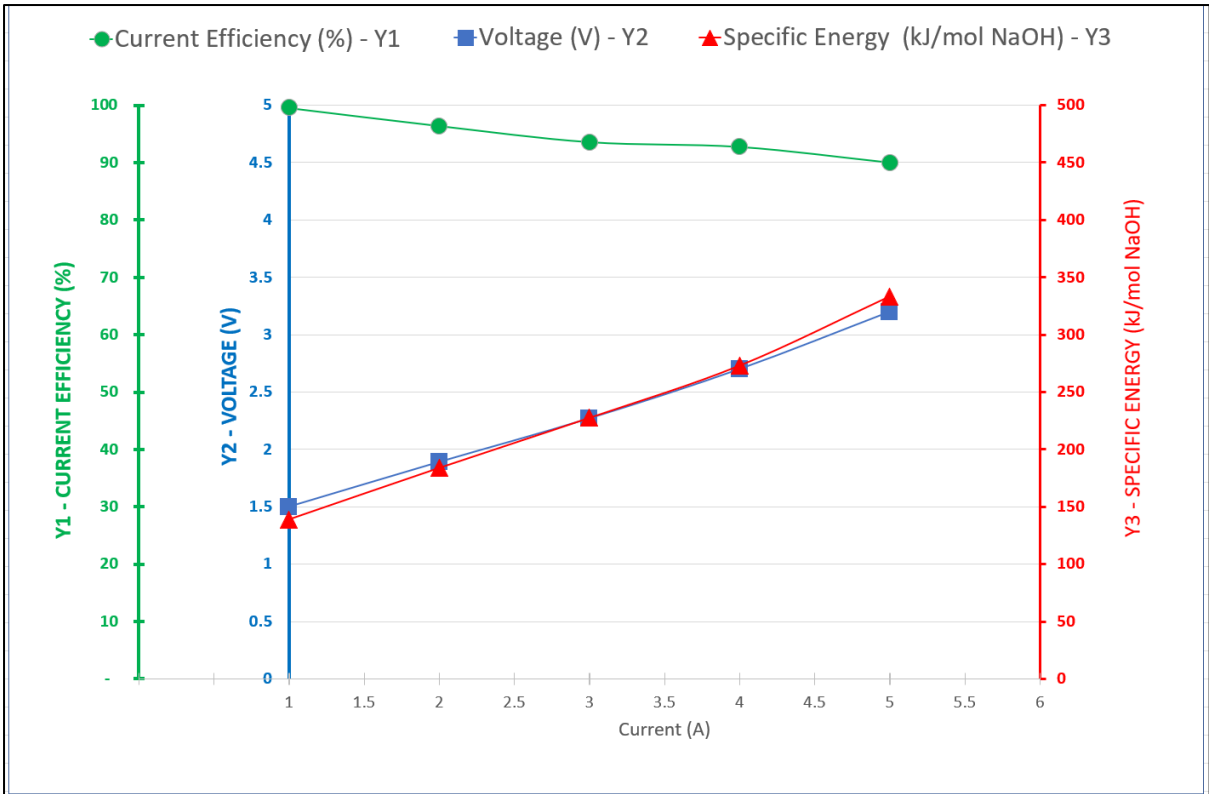


Figure A.3: Trial 3 (T = 40°C, AF = 350 mL/H, AC = 200 g/L, CC = 0 g NaOH/L)

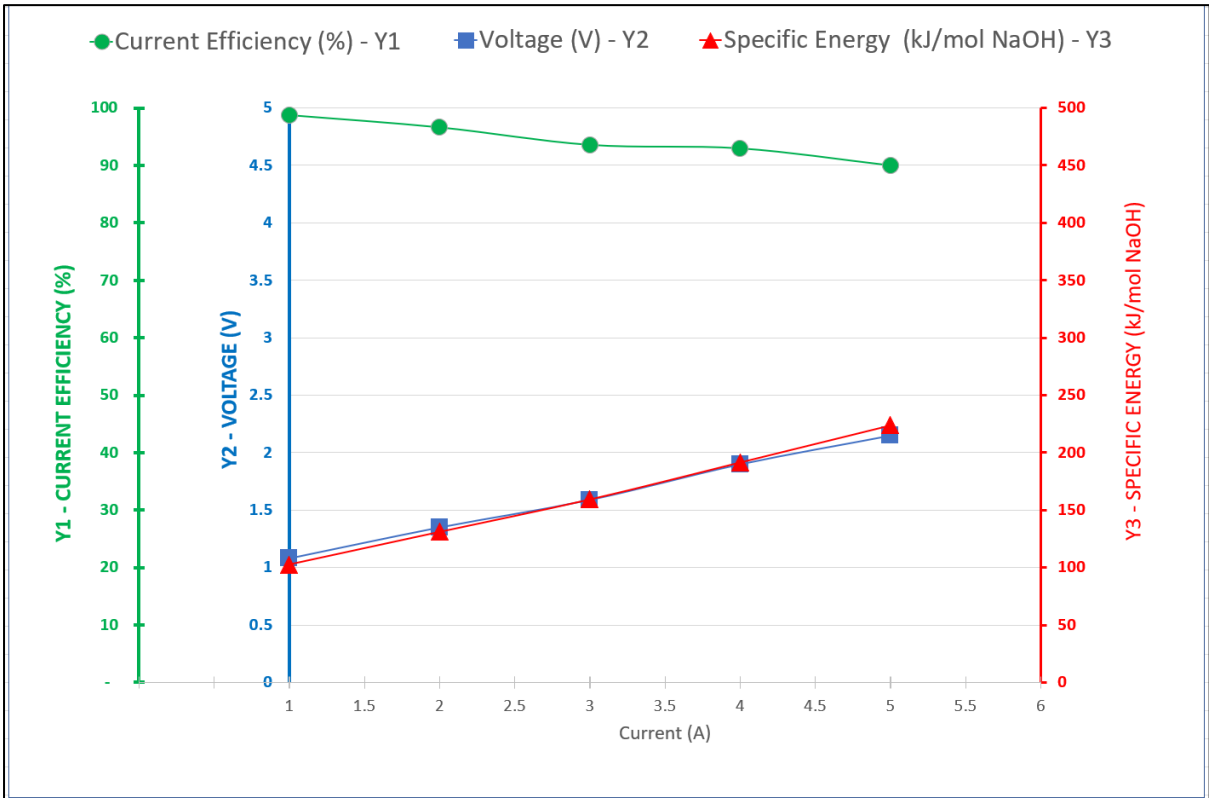


Figure A.4: Trial 4 (T = 80°C, AF = 350 mL/H, AC = 200 g/L, CC = 0 g NaOH/L)

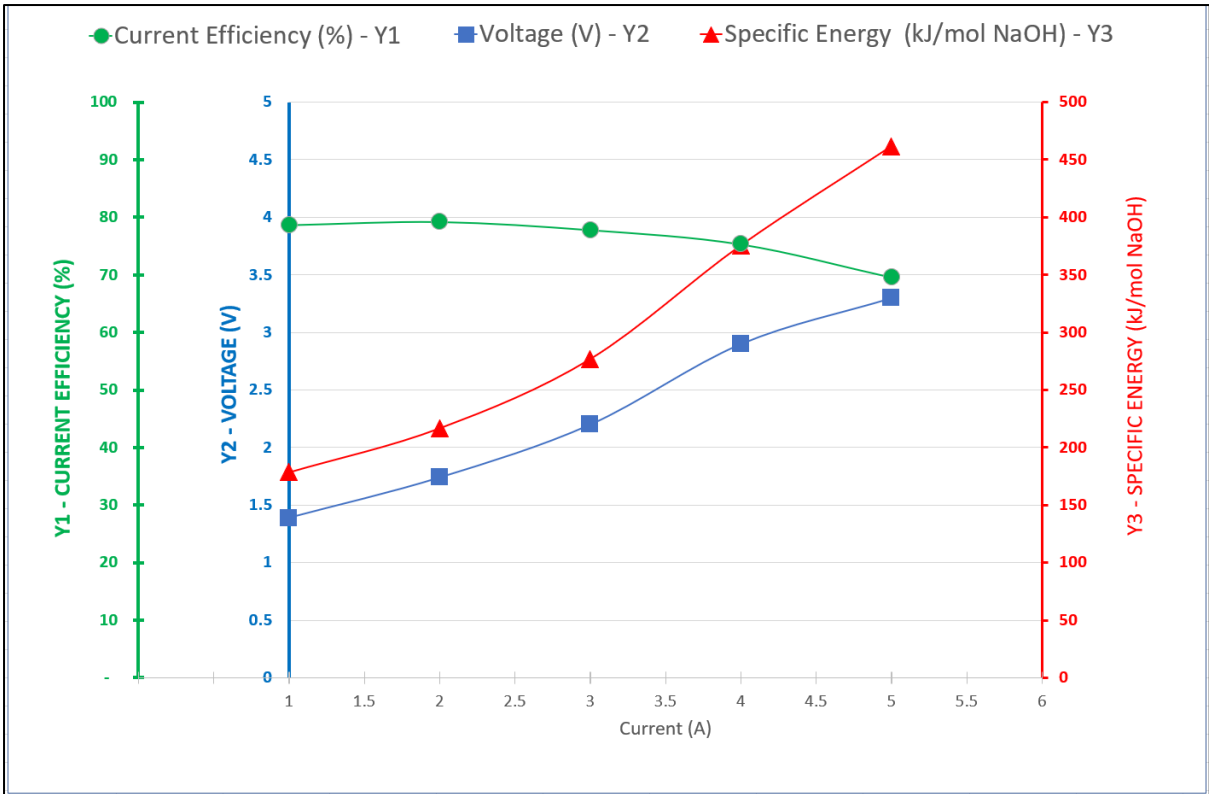


Figure A.5: Trial 5 (T = 40°C, AF = 175 mL/H, AC = 200 g/L, CC = 100 g NaOH/L)

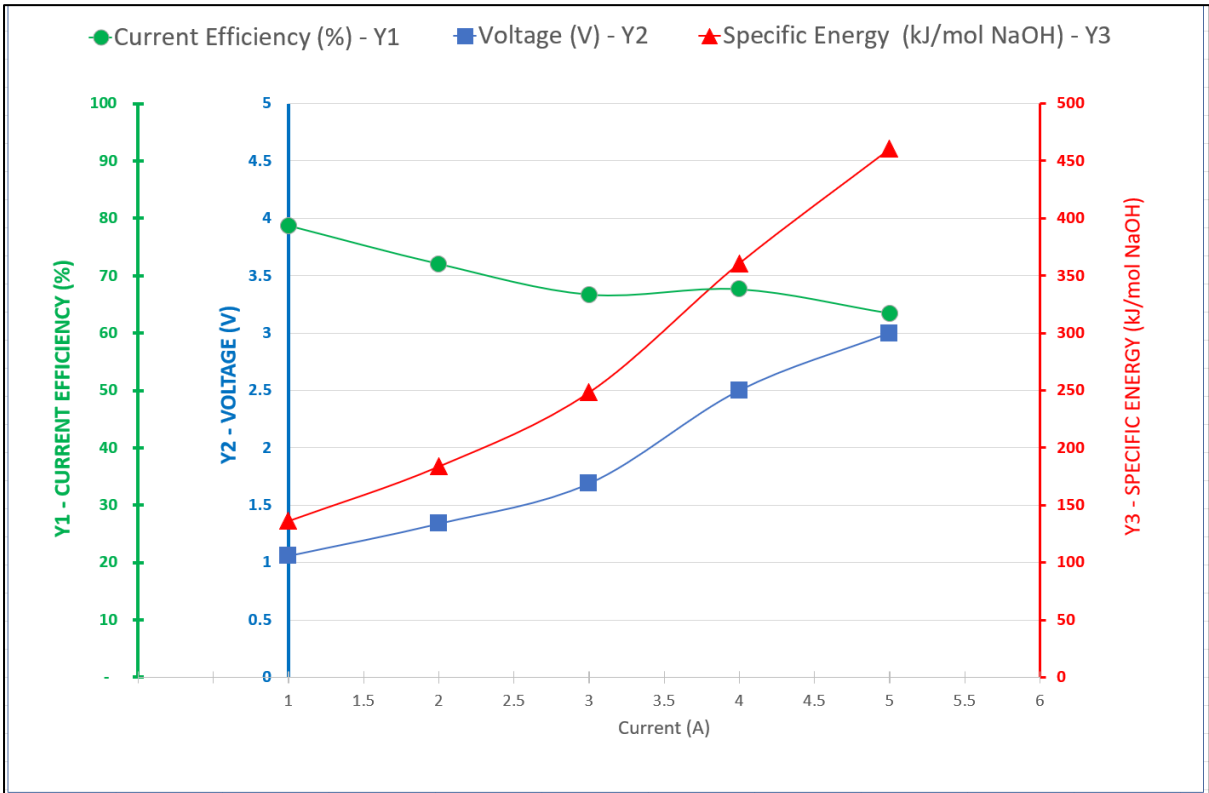


Figure A.6: Trial 6 (T = 80°C, AF = 175 mL/H, AC = 200 g/L, CC = 100 g NaOH/L)

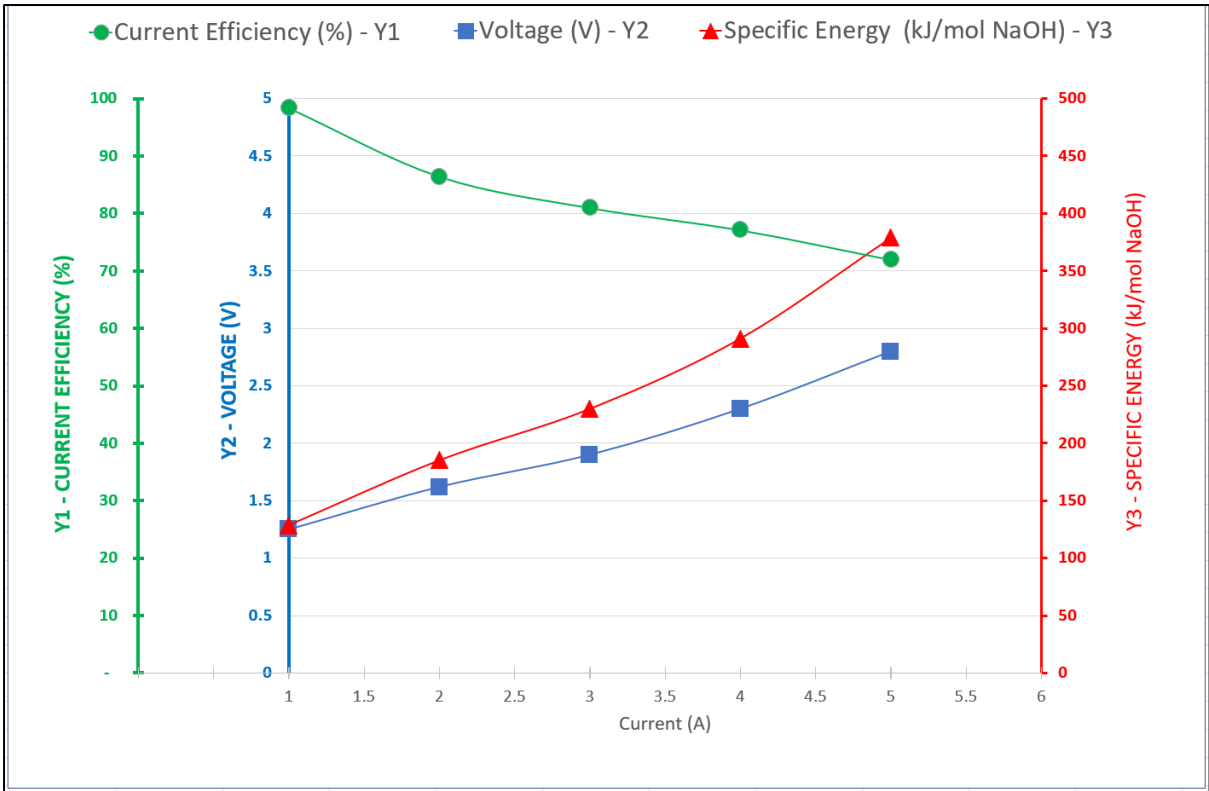


Figure A.7: Trial 7 (T = 40°C, AF = 350 mL/H, AC = 200 g/L, CC = 100 g NaOH/L)

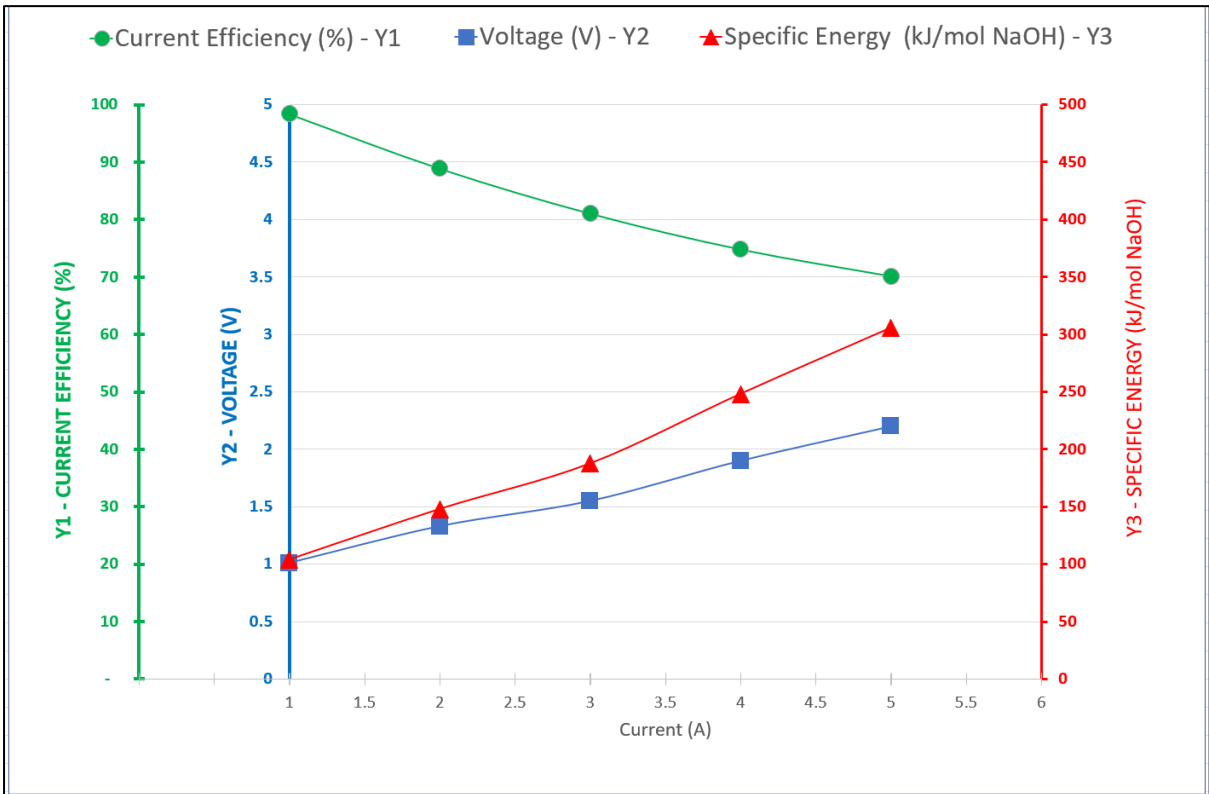


Figure A.8: Trial 8 (T = 80°C, AF = 350 mL/H, AC = 200 g/L, CC = 100 g NaOH/L)

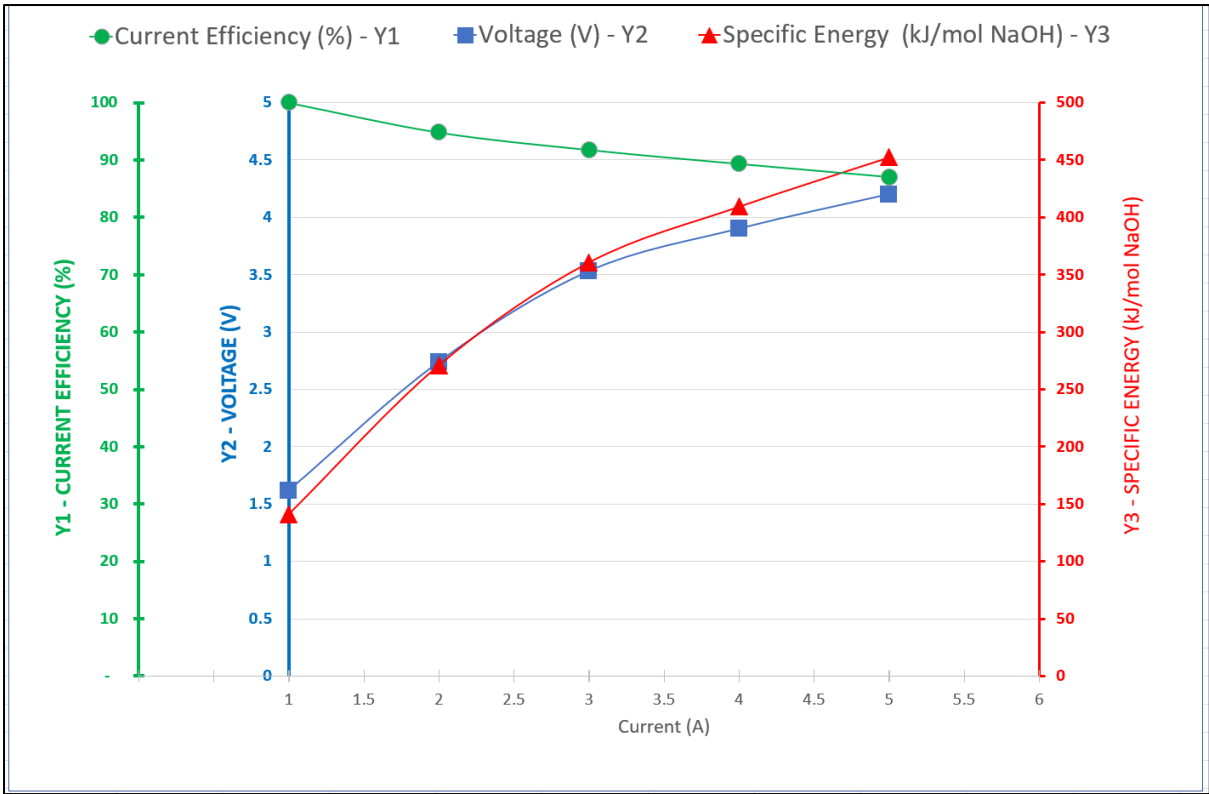


Figure A.9: Trial 9 (T = 40°C, AF = 175 mL/H, AC = 100 g/L, CC = 0 g NaOH/L)

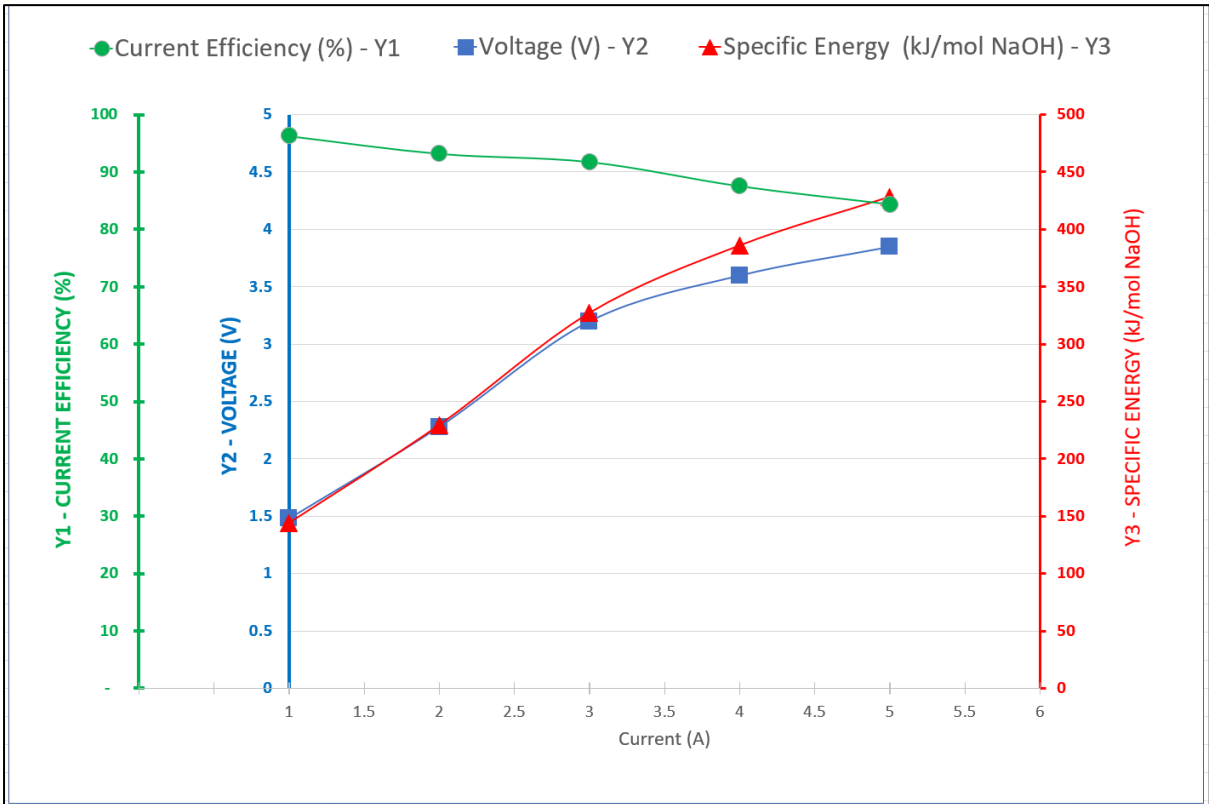


Figure A.10: Trial 10 (T = 80°C, AF = 175 mL/H, AC = 100 g/L, CC = 0 g NaOH/L)

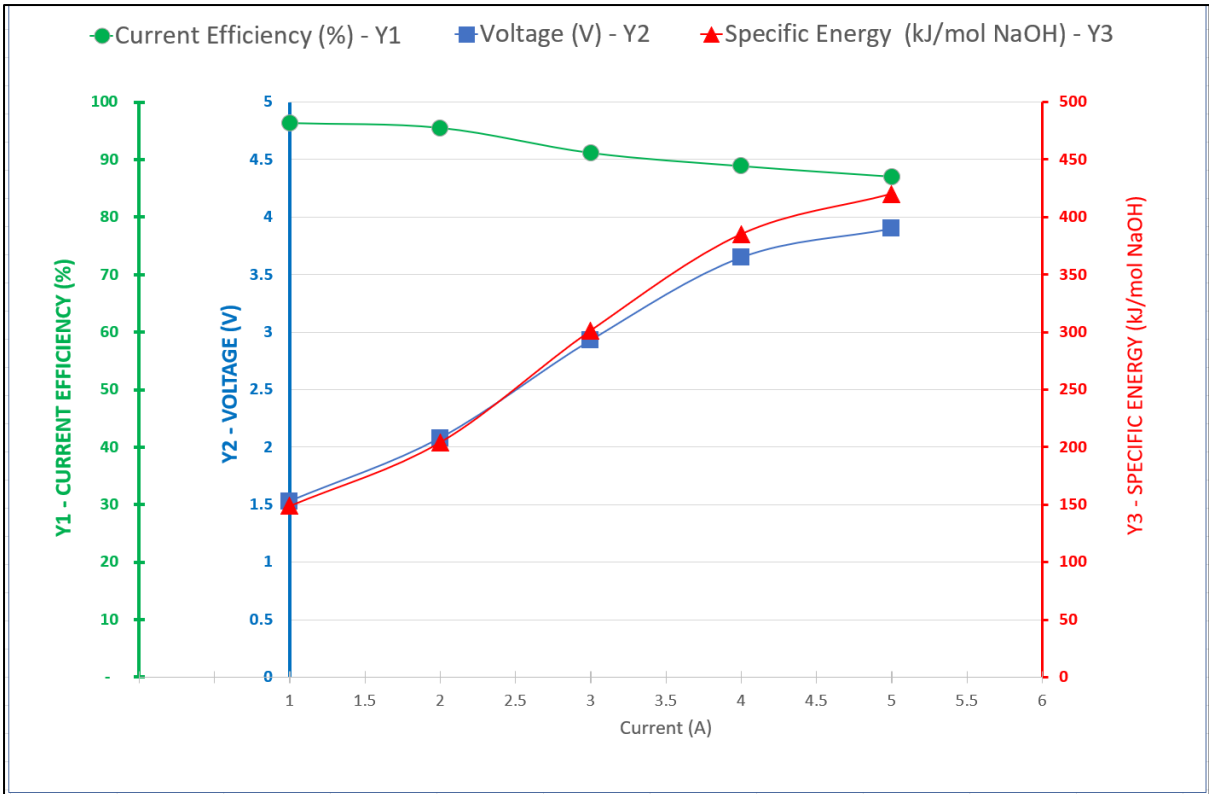


Figure A.11: Trial 11 (T = 40°C, AF = 350 mL/H, AC = 100 g/L, CC = 0 g NaOH/L)

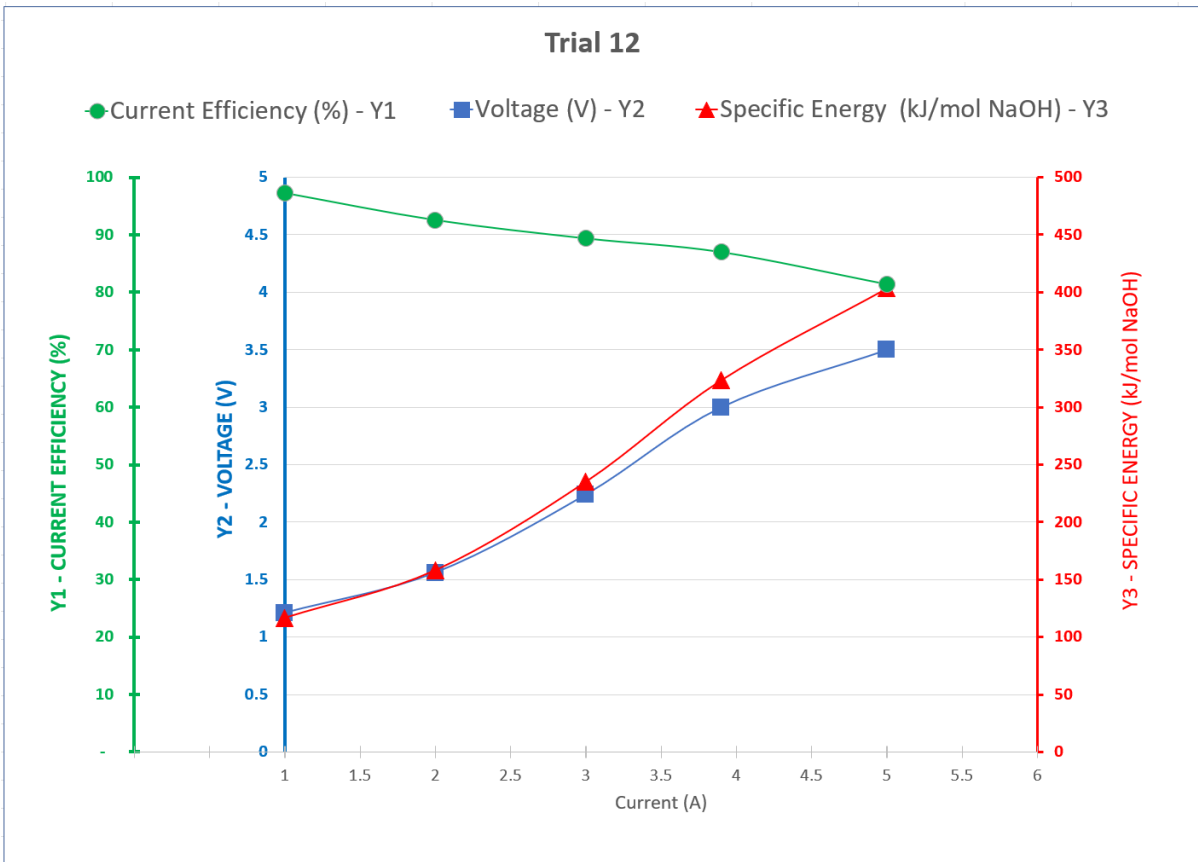


Figure A.12: Trial 12 (T = 80°C, AF = 350 mL/H, AC = 100 g/L, CC = 0 g NaOH/L)

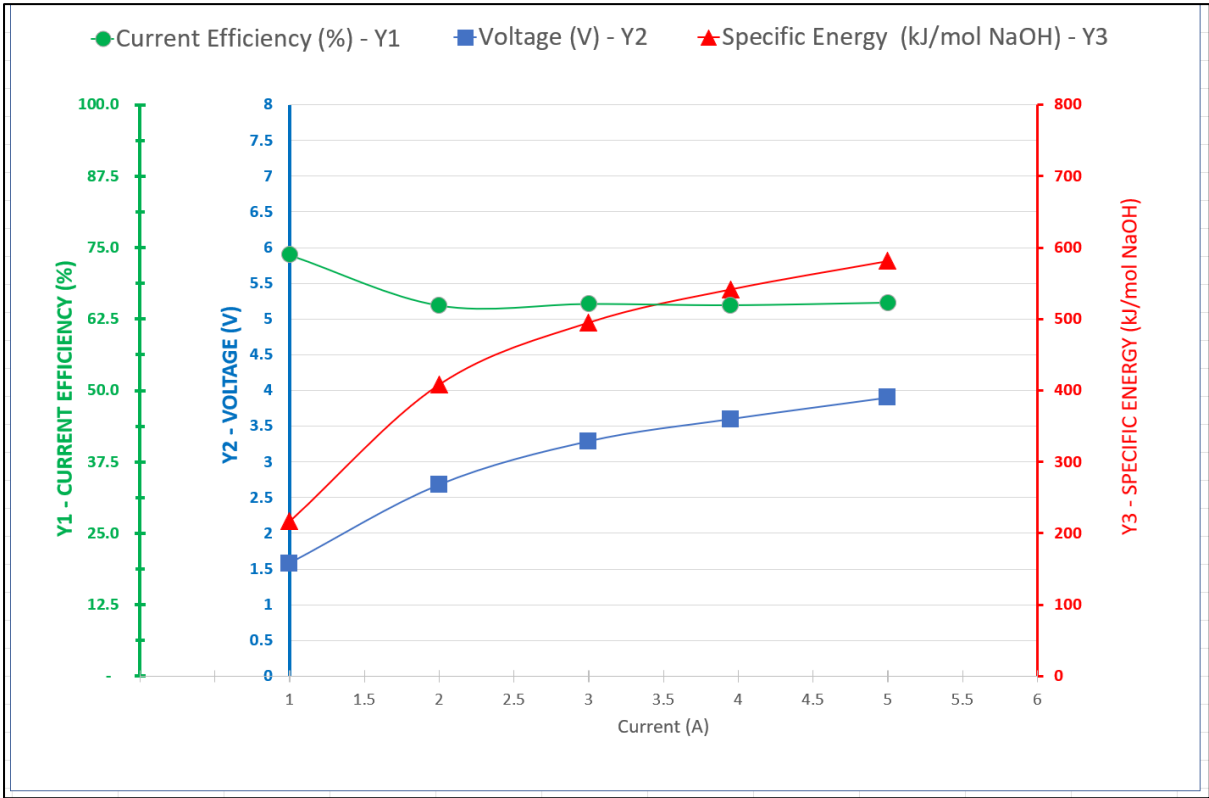


Figure A.13: Trial 13 (T = 40°C, AF = 175mL/H, AC = 100 g/L, CC = 100 g NaOH/L)

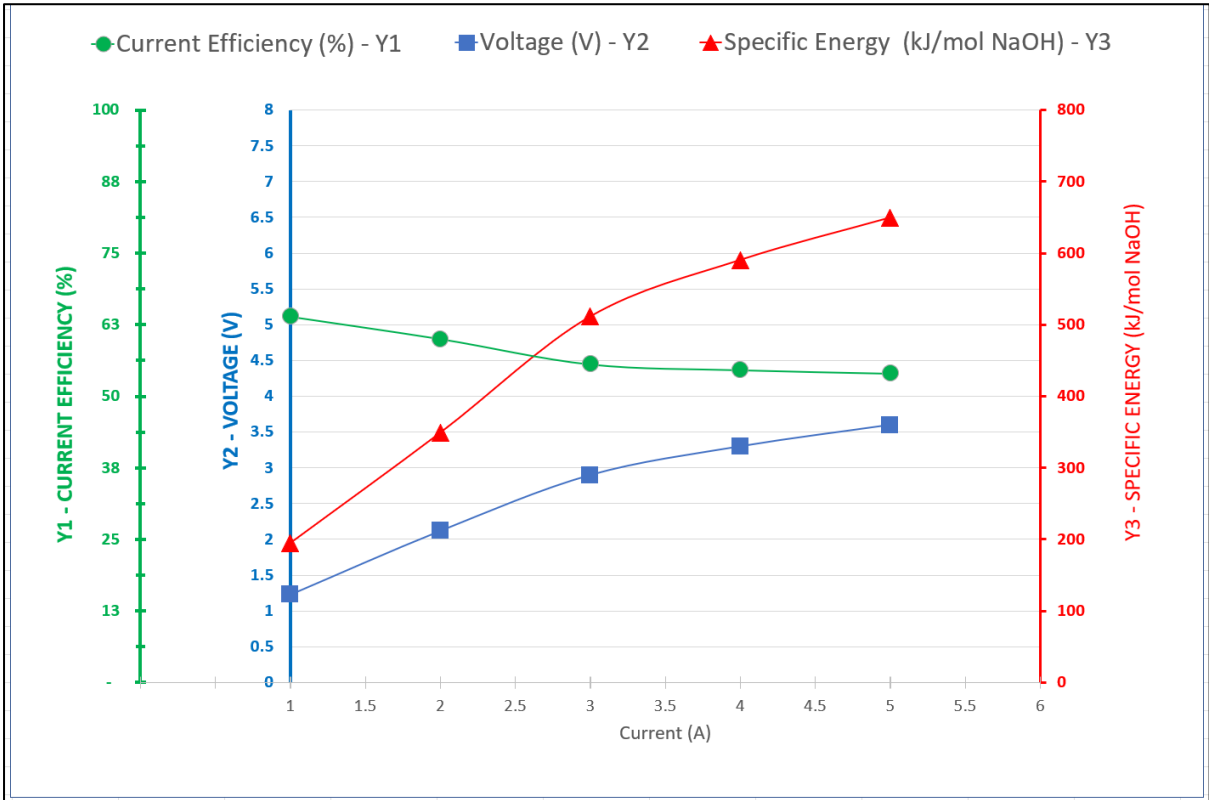


Figure A.14: Trial 14 (T = 80°C, AF = 175mL/H, AC = 100 g/L, CC = 100 g NaOH/L)

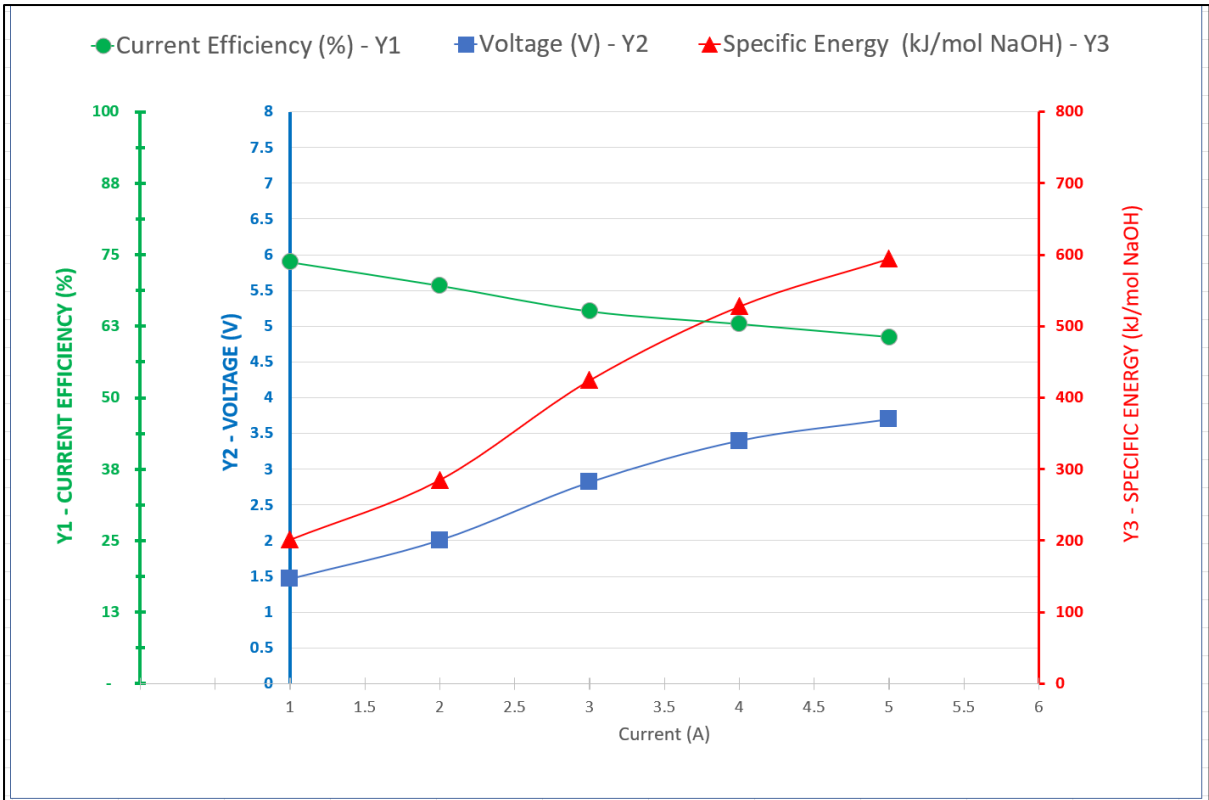


Figure A.15: Trial 15 (T = 40°C, AF = 350mL/H, AC = 100 g/L, CC = 100 g NaOH/L)

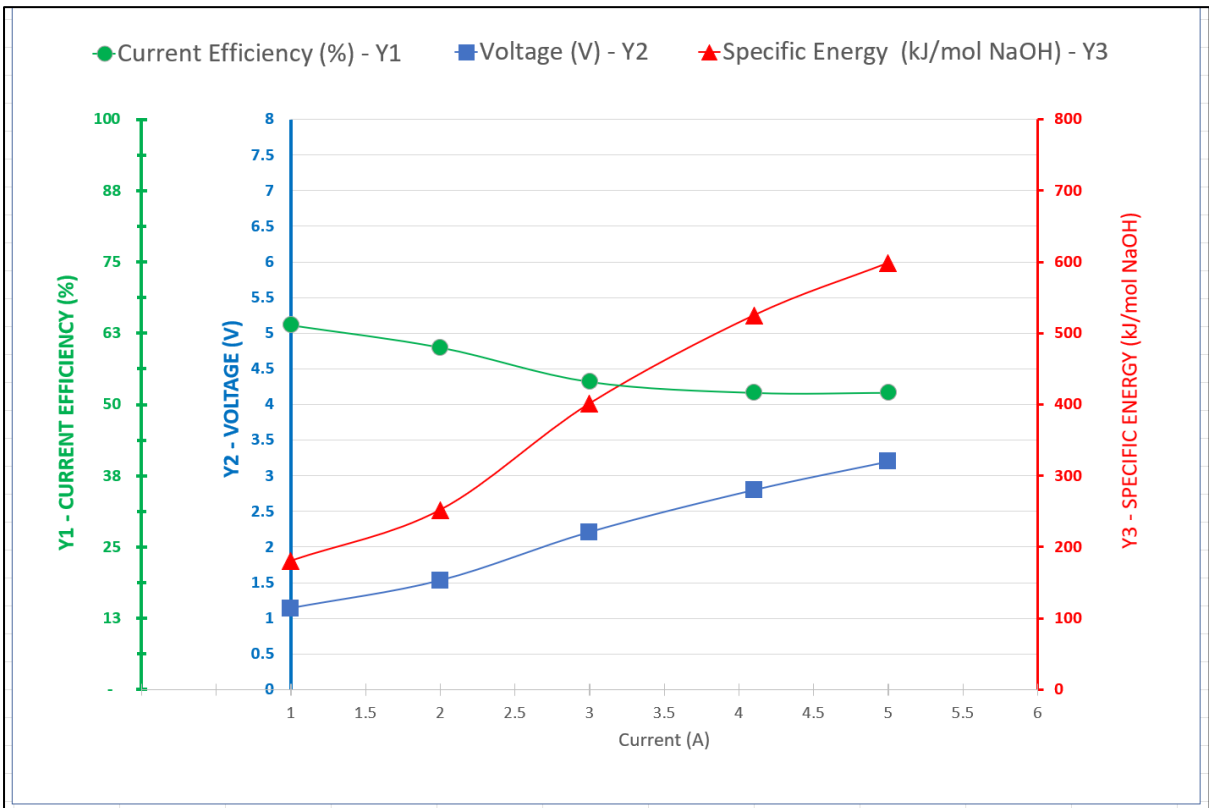


Figure A.16: Trial 16 (T = 80°C, AF = 350mL/H, AC = 100 g/L, CC = 100 g NaOH/L)

Appendix B: Trial 16 Repeated – Titration and ICP-OES results

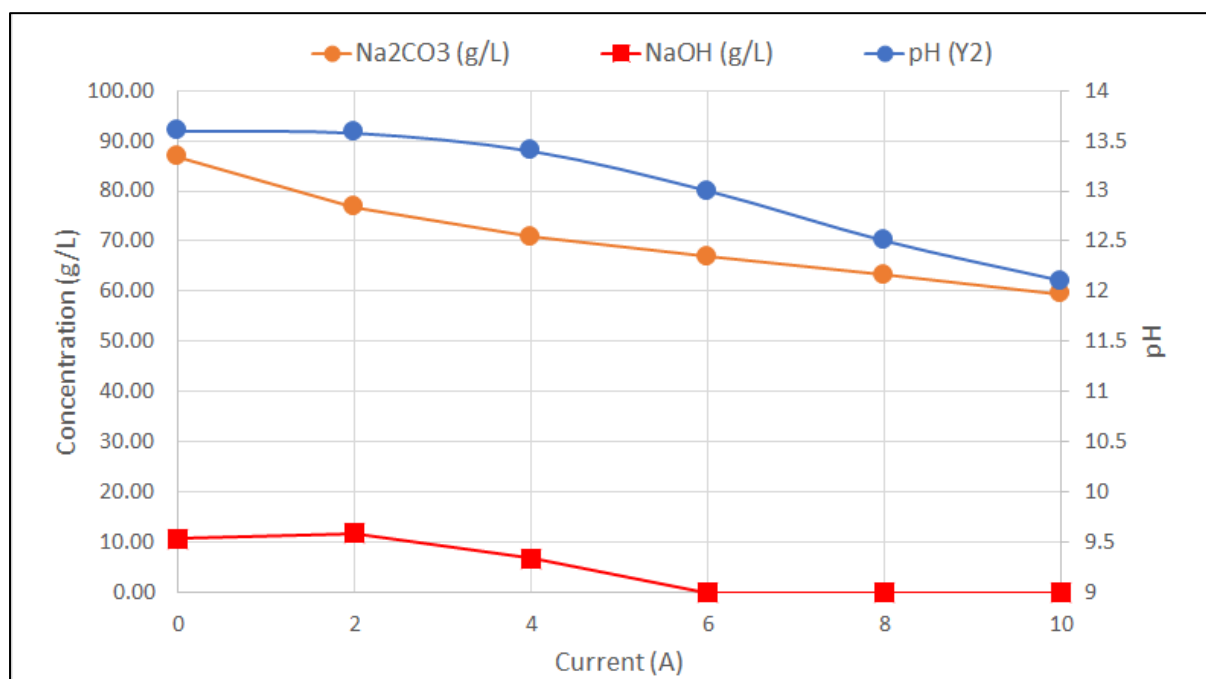


Figure B.1: Trial 16 Repeated – Titration and ICP-OES results

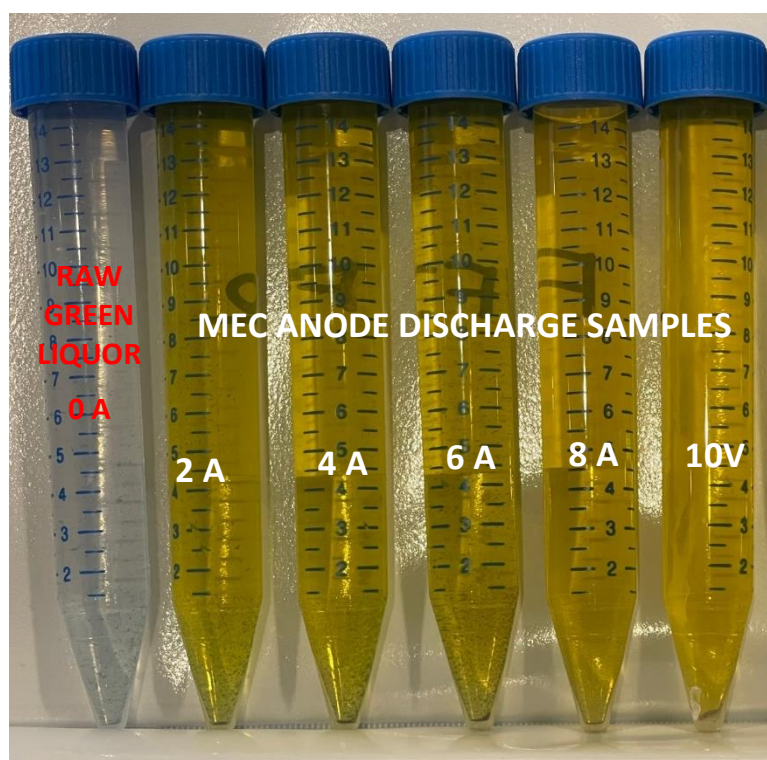


Figure B2: Trial 16 (Repeated):

Top: MEC Anode Discharge Residual NaOH and Na₂CO₃.

Bottom: Photo of Samples taken: Raw Green Liquor, 2 A, 4 A, 6 A, 8 A and 10 A)

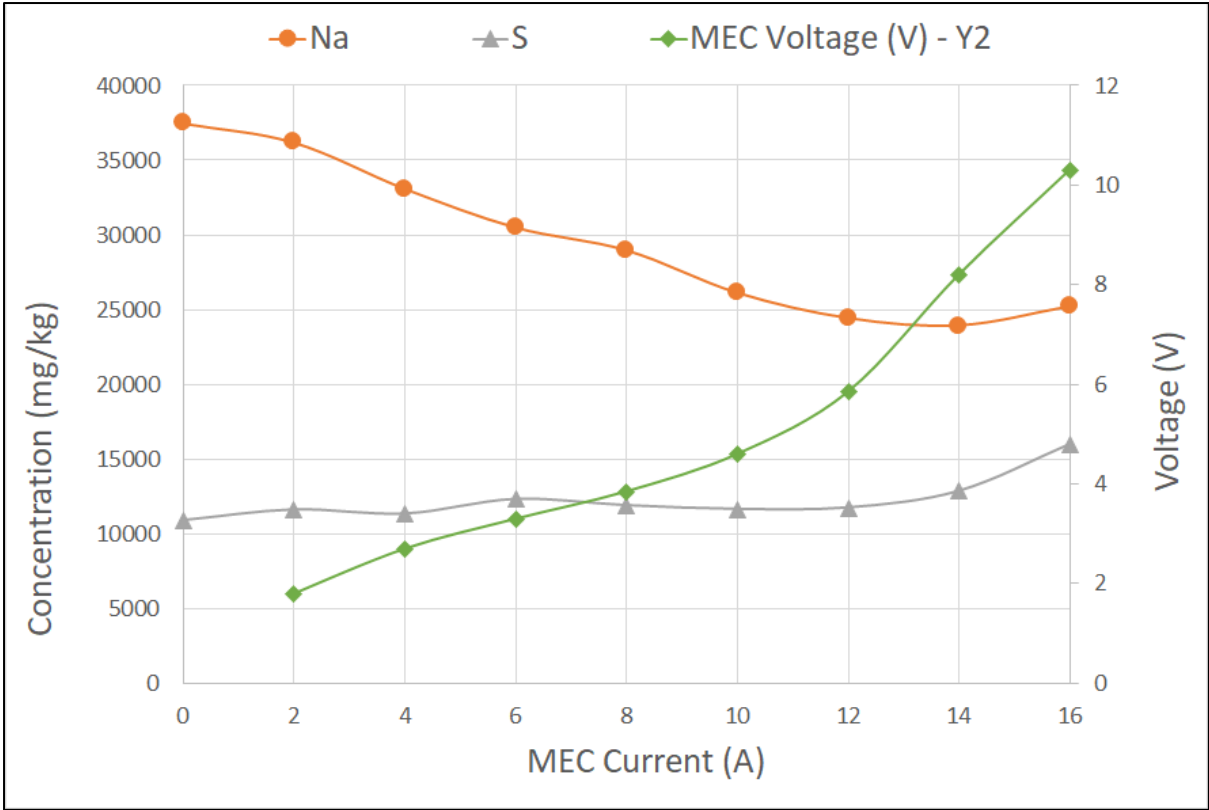


Figure B3: MEC Anode Discharge Trial 16 – Liquid Phase Analysis by ICP-OES

Appendix C: Summary of Na₂CO₃ Pre-Trial Integrity Testing Results

Table C.1 below summarises the results of Na₂CO₃ membrane integrity test performed on the electrolysis cell before each trial. The results confirm good repeatability of results before each trial, with minor voltage differences mostly related to slight differences in temperature ($\pm 5^{\circ}\text{C}$) at experimental start up.

Table C.1: Standard Schedule for each Trial

Trial	Voltage	Current Efficiency	Hydrogen (mol/hr)
Trial 1	3.6	93%	0.061
Trial 2	3.6	92%	0.059
Trial 3	3.6	94%	0.061
Trial 4	3.6	92%	0.063
Trial 5	3.55	94%	0.061
Trial 6	3.5	93%	0.062
Trial 7	3.45	93%	0.062
Trial 8	3.45	94%	0.061
Trial 9	3.54	93%	0.063
Trial 10	3.5	94%	0.061
Trial 11	3.55	92%	0.061
Trial 12	3.5	92%	0.061
Trial 13	3.5	92%	0.061
Trial 14	3.45	93%	0.061
Trial 15	3.5	93%	0.060
Trial 16	3.5	93%	0.061
Average	3.5	93%	0.061
Standard Deviation	1%	1%	1%